

# NOVEL ORGANOTYPIC MODELLING FOR THE STUDY OF PERIODONTAL INFECTIONS

---

**Dissertation\***

**zur**

**Erlangung der naturwissenschaftlichen Doktorwürde  
(Dr. sc. nat.)  
vorgelegt der**

**Mathematisch-naturwissenschaftlichen Fakultät**

**der**

**Universität Zürich**

**von**

Kai Bao (BEng, MSc)

**von/aus**

V.R. China

**Promotionskomitee**

Prof. Dr. Leo Eberl (Vorsitz)

PD Dr. Nagihan Bostanci (Leitung der Dissertation)

Prof. Dr. Georgios N Belibasakis (Co-Leitung der Dissertation)

Prof. Dr. Jakob Pernthaler

Prof. Dr. Annelies Zinkernagel

Zürich, 2015

## CONTENTS

SUMMARY .....	3
ZUSAMMENFASSUNG .....	8
Introduction .....	14
1. Periodontal disease .....	14
1.1 Background .....	14
1.2 Histopathology of periodontal diseases .....	15
1.3 Clinical and microbiological diagnosis and therapy .....	16
2. Microbiology of periodontal disease .....	18
2.1 Biofilms: composition and complexity .....	18
2.2 Theories on the microbial etiology of periodontal disease .....	21
2.3 <i>Porphyromonas gingivalis</i> .....	23
2.4 <i>Aggregatibacter actinomycetemcomitans</i> .....	26
3. Host–bacteria interaction.....	28
3.1 Structure and function of periodontium .....	28
3.2 Immunological components of the periodontium .....	30
3.3 Host–bacteria interaction to the inflammation.....	33
4. Periodontal infection models.....	34
Aims .....	39
Methodology .....	41
1. Bacterial strains .....	41
2. Multispecies subgingival biofilm model .....	41
3. Biofilm harvesting and quantification by qRT-PCR and FISH.....	43
4. Establishment, cultivation, and characterization of cell lines .....	43



5. Generation and characterization of organotypic gingival tissue in a perfusion bioreactor .....	45
6. Host-biofilm interaction model in a perfusion bioreactor .....	46
7. Proteomic identification and characterization by LC-MS/MS .....	46
Results and discussion.....	49
Role of <i>P. gingivalis</i> gingipains in multispecies biofilm formation (Paper 1) .....	49
Quantitative proteomics reveal distinct protein regulations caused by <i>Aggregatibacter actinomycetemcomitans</i> within subgingival biofilms (Paper 2) .....	50
Establishment and characterization of immortalized gingival epithelial and fibroblast cell lines for the development of organotypic cultures (Paper 3) .....	52
Establishment of an oral infection model resembling the periodontal pocket in a perfusion bioreactor system (Paper 4) .....	53
Proteomic profiling of host-biofilm interactions in an oral infection model resembling the periodontal pocket (Paper 5, in revision) .....	55
Conclusions and future work.....	58
Acknowledgements .....	60
References .....	62
Papers .....	86
Paper 1 .....	87
Paper 2 .....	96
Paper 3 .....	114
Paper 4 .....	125
Paper 5 .....	136
Curriculum Vitae .....	154

## SUMMARY

Periodontal diseases are inflammatory, infectious diseases triggered by the accumulation of oral microbes on the tooth surface in the form of biofilms that cause destruction of the tooth-supporting (periodontal) structures. It is the primary cause of adult tooth loss. The interaction between biofilm and host tissue is crucial for the development of periodontal disease, thus making treatment difficult. Biofilms, a dense structure of matrix-embedded oral bacteria forming on the tooth surface, result in increased resistance against antimicrobials and greater host immune defenses of their constituent microorganisms. They are a dynamic ecosystem in which each species may not only regulate their own functions but also that of their neighboring species. The periodontal tissues are the first ones to be affected by the established oral biofilm and represent the site of initial inflammatory host response against oral microbes. Therefore, understanding the underlying mechanisms of interactions between oral biofilm and periodontal tissue is of fundamental importance for effective treatment of these diseases.

However, available study models have several limitations. *In vitro* experimental models at present are too simplified to adequately study the pathogenic mechanisms of periodontal infections. Animal models are useful tools to address mechanistic questions. But they cannot fully reflect the human condition because differences in oral microflora and tissue structure. Human experiments can only address questions focusing on the early or progressed stages of the disease and also require several important ethical considerations.

To gain deeper insight into the mechanisms underlying periodontal infections, the primary aim of this thesis was to develop a novel organotypic 3D *in vitro* infection model that may circumvent some of the previously mentioned limitations. The major individual aims of this PhD thesis were as follows: 1) a better understanding of the role of specific virulence factors in the structure and function of a subgingival biofilm model, illustrated by the comparison of gingipains (cysteine proteinases) of *Porphyromonas gingivalis*; 2) to evaluate whether this subgingival biofilm model is amenable to additional species, illustrated by the incorporation of *Aggregatibacter actinomycetemcomitans*, and to monitor the proteomic changes that occur in the biofilm during this process; 3) to construct and characterize immortalized gingival epithelial and fibroblast cell lines that can be further utilized in 3D cultures; 4) to develop a 3D organotypic tissue-biofilm interaction model in a dynamic microenvironment; and 5) to characterize the global proteomic events taking place in this experimental periodontal infection model.

The biofilm model used in this thesis is based on a previously developed *in vitro* 10-species model with a typical composition of subgingival biofilms consisting of *Prevotella intermedia*, *Campylobacter rectus*, *Veillonella dispar*, *Fusobacterium nucleatum*, *Streptococcus oralis*, *Treponema denticola*, *Actinomyces oris*, *Streptococcus anginosus*, *Tannerella forsythia*, and *P. gingivalis*. The relative role of the gingipain virulence factors of *P. gingivalis* was studied by the incorporation of an Arg-gingipain or a Lys-gingipain *P. gingivalis* mutant into the biofilm. On comparing the biofilms with either the wild-type or one of these two gingipain-deficient

strains, it was evident that the numbers of *T. forsythia* were reduced in the absence of Lys-gingipain. However, in the absence of the Arg-gingipain, spatial rearrangements in the clustering of *T. denticola* were observed.

*Aggregatibacter actinomycetemcomitans*, an oral species associated with aggressive forms of periodontal infection, was introduced successfully into the biofilm resulting in an 11-species final model. This was characterized by means of proteomic evaluation and used in the subsequent host-biofilm interaction studies. Within the biofilm structure, this bacterium aggregated in dense clumps but did not significantly change the cell numbers of other species. Using label-free quantification, a total of 483 proteins were found to be regulated compare to the original 10-species biofilm, most of which belonged to *Campylobacter rectus* and *Streptococcus anginosus*. All the proteins from *Prevotella intermedia* were up-regulated, while almost all the proteins from *P. gingivalis*, *S. anginosus* and *C. rectus* were down-regulated. Therefore, while the presence of *A. actinomycetemcomitans* did not affect bacterial numbers, it caused changes in the protein expression of other species in the biofilm.

To establish stable immortalized cell lines, primary gingival epithelial and fibroblast cells were transfected with E6 and E7 human papillomavirus oncoprotein. Expansion of the primary cells was impaired at an early stage, while the immortalized cell lines continued expanding for more than 30 passages. When cultured in a 3D conformation, the morphological features and expression of cell type-specific markers of immortalized cells were more similar to *in vivo* human gingival tissues than monolayer cultures, confirming

that these cell lines can be used for generating a standard organotypic model.

An organotypic *in vitro* infection model was then generated using the established biofilm and immortalized cell lines. The model consisted of two tissues of human gingiva, namely gingival epithelium and gingival connective tissue (collagen sponge + fibroblasts + monocytes). This tissue was utilized to establish an *in vitro* infection model by co-culture with the 11-species subgingival biofilm in a perfusion bioreactor. Histology and scanning electronic microscopy revealed an epithelial layer on the surface of the collagen sponge, underlined by fibroblastic and monocytic cells that were aligned within the sponge mass. This fine epithelial layering was disrupted when co-cultured with the biofilm, and more monocytic cells were also recruited. Multiplex immunoassaying revealed that the production of inflammatory markers interleukin (IL)-1 $\beta$ , IL-2, IL-4, and tumor necrosis factor (TNF)- $\alpha$  were up-regulated, indicating the induction of immune responses in this organotypic tissue by the biofilm. Bacterial quantification of the biofilm also indicated a potential antimicrobial effect of this tissue.

In the last part of the thesis, this established periodontal infection model was further evaluated by characterizing the global proteome regulations using liquid chromatography-tandem mass spectrometry. A total of 896 and 3363 proteins were identified in the secreted culture supernatants and biofilm lysates, respectively. The regulatory trends of these proteins were further calculated through spectral counting, and bioinformatic analysis showed that secreted human proteins were related to antigen presentation, stress responses, and apoptosis. The regulated bacterial proteins were

associated primarily with cytokinesis, GTP binding, and GTPase activity.

Taken together, this thesis achieved structural and proteomic characterization of a host–bacteria interaction model consisting of an organotypic gingival tissue and a subgingival biofilm in a perfusion bioreactor. This is one of the most complex *in vitro* periodontal infection models available until date and may recapitulate the early events that occur *in vivo* in a periodontal pocket. Thus, this *in vitro* model has the potential to substitute experimental animal models and to provide an accurate laboratory platform for the investigation of mechanisms of periodontal pathogenesis and evaluation of anti-inflammatory and anti-microbial agents prior to application in clinical trials.

## ZUSAMMENFASSUNG

Parodontale Erkrankungen sind entzündliche Infektionskrankheiten, die durch das Festsetzen oraler Bakterien auf der Zahnoberfläche in Form von Biofilmen ausgelöst werden. Sie verursachen die Zerstörung des (parodontalen) Zahnhaltegewebes und sie sind die Hauptgründe für den Zahnverlust bei Erwachsenen. Die Wechselwirkung zwischen Biofilmen und Wirtsgewebe ist entscheidend für die Entwicklung von Parodontitis, was ihre Behandlung zu einer herausfordernden Aufgabe macht. Der Biofilm besteht aus einer dichten Struktur von in der Matrix eingebetteten oralen Mikroorganismen, welcher sich auf der Zahnoberfläche bildet. Dieser Biofilm führt zu erhöhter Resistenz gegenüber antimikrobiellen Substanzen und schwächt die Wirtsabwehr gegen die im Biofilm enthaltenen Mikroorganismen. Außerdem bilden Biofilme ein dynamisches System, in welchem jede Spezies nicht nur ihre eigenen Funktionen regulieren können, sondern auch die ihrer benachbarten Spezies. Die parodontalen Gewebe sind die ersten, die mit dem entstehenden Biofilm in Berührung kommen und sie stellen den Ort der ursprünglichen Wirtsantwort und Entzündung gegen die oralen Mikroorganismen dar. Daher ist das Verstehen der Wechselwirkungen zwischen oralen Biofilmen und parodontalen Geweben und der ihnen zugrunde liegenden Mechanismen von grundlegender Bedeutung für eine wirksame Behandlung solcher Erkrankungen.

Allerdings sind Modelle zur Studie von Parodontalerkrankungen

nur begrenzt verfügbar. Gegenwärtige in-vitro-Versuchsmodelle sind zu vereinfacht, um die pathogenen Mechanismen der parodontalen Infektionen ausreichend erforschen zu können. Bei Tiermodellen ergeben sich methodologische Einschränkungen, da die Wirtsantworten auf parodontale Infektionen zwischen Menschen und Tieren sehr unterschiedlich sind und es ausserdem erhebliche Unterschiede in der Zusammensetzung der oralen Mikrobiota verschiedener Spezies gibt. Versuche an Menschen könnten nur Fragen zu frühen oder bereits fortgeschrittenen Stadien der Krankheit ansprechen, zudem stellen sich dabei auch einige wichtige ethische Erwägungen.

Um tiefere Einblicke in die Mechanismen der parodontalen Infektionen zu gewinnen, war das primäre Ziel dieser Arbeit, ein organotypisches 3D-in vitro-Infektionsmodell zu entwickeln, welches einige der oben genannten Einschränkungen umgehen kann. Die wichtigsten während dieser Doktorarbeit angestrebten Ziele waren: 1) ein besseres Verständnis der Rolle der spezifischen Virulenzfaktoren in Bezug auf Struktur und Funktion im subgingivalen Biofilm-Modell zu schaffen, veranschaulicht durch den Vergleich von *Porphyromonas gingivalis* Gingipains (Cysteinproteinasen); 2) zu beurteilen, ob dieses subgingivale Biofilm-Modell für zusätzliche Spezies anwendbar ist, dargestellt durch die Inkorporation von *Aggregatibacter actinomycetemcomitans* und das Untersuchen der proteomischen Veränderungen im Biofilm während dieses Vorgangs; 3) die Bildung und Charakterisierung immortalisierter gingivaler Epithel- und



Fibroblastenzelllinien, die in 3D-Kulturen weiter genutzt werden können; 4) die Entwicklung eines experimentellen 3D-organotypischen Modells zur Untersuchung von Interaktionen zwischen Biofilmen und Geweben in einer dynamischen Mikroumgebung und 5) die globalen proteomischen Ereignisse in diesem experimentellen Parodontitis-Infektionsmodell zu charakterisieren.

Das Biofilm-Modell, das in dieser Arbeit verwendet wurde, basiert auf einem zuvor entwickelten *in vitro* 10-Spezies-Modell mit einer für subgingivale Biofilme typischen Zusammensetzung aus *Prevotella intermedia*, *Campylobacter rectus*, *Veillonella dispar*, *Fusobacterium nucleatum*, *Streptococcus oralis*, *Treponema denticola*, *Actinomyces oris*, *Streptococcus anginosus*, *Tannerella forsythia* und *P. gingivalis*. Die Rolle der Gingipain-Virulenzfaktoren wurde durch die Inkorporation einer Arg-Gingipain oder einer Lys-Gingipain Mutante von *P. gingivalis* im Biofilm untersucht. Der Vergleich der Biofilme, die entweder den Wildtyp oder eine der beiden Gingipain-defizienten Stämme enthielten, zeigten, dass die Anzahl von *T. forsythia* in Abwesenheit von Lys-Gingipain reduziert worden war, während in Abwesenheit von Arg-Gingipain räumliche Umlagerungen im Clustering von *T. denticola* beobachtet werden konnten.

*Aggregatibacter actinomycetemcomitans*, eine orale Bakterienart mit aggressiven Formen parodontaler Infektionen, konnte erfolgreich in den Biofilm eingeführt werden, woraus schlussendlich das 11-Spezies-

Modell resultierte. Dieses wurde mittels Proteomik-Auswertung charakterisiert und in den nachfolgenden Studien über Wechselwirkungen zwischen Wirtszellen und Biofilm eingesetzt. Im Biofilm aggregierte dieses Bakterium zwar zu dichten Klumpen, aber es veränderte die Zellzahlen der anderen Spezies nicht signifikant. Im Vergleich zum 10-Spezies-Biofilm wurden im 11-Spezies-Modell mittels markierungsfreier Quantifizierung insgesamt 483 regulierte Proteine gefunden. Die meisten dieser regulierten Proteine gehörten zu *Campylobacter rectus* und *Streptococcus anginosus*. Interessanterweise wurden alle Proteine von *P. gingivalis* herunterreguliert, während alle Proteine von *Prevotella intermedia* hochreguliert wurden. Während die Anwesenheit von *A. actinomycetemcomitans* also keinen Einfluss auf die Bakterienzahlen im Biofilm hatte, beeinflusste es die Protein-Expression anderer Spezies.

Für die Herstellung stabiler immortalisierter Zelllinien wurden primäre gingivale Epithelzellen und Fibroblasten mit humanen Papillomavirus-Onkoproteinen E6- und E7 transfiziert. Die Expansion der Primärzellen wurde in einem frühen Stadium beeinträchtigt, während die immortalisierten Zelllinien über mehr als 30 Passagen expandierten. Wenn immortalisierte Zellen in einer 3D-Konformation gezüchtet wurden, zeigten sie, im Gegensatz zu Monolayer-Kulturen, ähnliche morphologische Merkmale und Expression der Zelltyp-spezifischen Marker wie in in vivo humanem gingivalem Gewebe, was bestätigte, dass diese Zelllinien zur Herstellung eines Standard-organotypischen Modells

verwendet werden konnten.

Mit Hilfe des etablierten Biofilms und den immortalisierten Zelllinien wurde dann ein organotypisches in vitro-Infektionsmodell generiert. Das Modell bestand aus zwei konstituierenden Geweben humaner Gingiva, nämlich Gingivaepithel und gingivalem Bindegewebe (Kollagenschwamm + Fibroblasten + Monozyten). Durch Ko-Kultivierung dieses Gewebes mit dem 11-Spezies subgingivalen Biofilm in einem Perfusionsbioreaktor entstand das in vitro Infektionsmodell. Histologische und Rasterelektronenmikroskop-Analysen zeigten eine Epithelschicht auf der Oberfläche des Kollagenschwamms, darunter Fibroblasten und Monozyten, welche innerhalb der Masse des Kollagenschwamms verbunden waren. Durch Ko-Kultivierung mit Biofilm wurde diese feine Epithelschicht zerstört, währenddem mehr Monozyten rekrutiert wurden. Multiplex-Immunoassay-Analysen ergaben, dass die Produktion von Entzündungsmarkern, einschließlich Interleukin (IL) -1 $\beta$ , IL-2, IL-4 und Tumor-Nekrose-Faktor- $\alpha$ , hochreguliert war, was auf die Induktion der Immunantwort durch den Biofilm in diesem organotypischen Gewebe schließen lässt. Die bakterielle Quantifizierung des Biofilms weist auch auf eine potentielle antimikrobielle Wirkung dieses Gewebes hin.

Im letzten Teil der Doktorarbeit wurde dieses etablierte parodontale Infektionsmodell weiter untersucht durch Charakterisierung der globalen Proteom-Regulation mittels Flüssig-Chromatographie-

Tandem-Massenspektrometrie. Insgesamt wurden 896 und 3363-Proteinen in den sezernierten Kulturüberständen bzw. Biofilm-Lysaten identifiziert. Die Regulations-Trends dieser Proteine wurden weiter durch „spectral counting“ berechnet. Bioinformatische Analysen zeigten, dass diese regulierten humanen sekretorischen Proteine in Verbindung mit Antigenpräsentation, Stressreaktionen und Apoptose stehen. Das regulierte Bakterienprotein war vor allem mit Zytokinese, GTP-Bindung und GTPase-Aktivität assoziiert.

Insgesamt wurde in dieser Arbeit die Herstellung eines Wirt-Bakterien-Interaktionsmodells bestehend aus einem organotypischen Zahnfleischgewebe und einem subgingivalen Biofilm in einem Perfusionsbioreaktor erreicht sowie dessen strukturelle und proteomische Charakterisierung durchgeführt. Dies ist zur Zeit eines der komplexesten parodontalen in vitro Infektions-Modelle und könnte die frühen Ereignisse, die in vivo in einer Zahnfleischtasche ablaufen, wiedergeben. Somit hat dieses in-vitro-Modell das Potenzial, Tierversuchsmodelle zu ersetzen, und es stellt eine präzise Labor-Plattform zur Untersuchung von parodontalen Pathogenese-Mechanismen sowie zur präklinischen Evaluierung von entzündungshemmenden und antimikrobiellen Stoffen dar.

## **Introduction**

### **1. Periodontal disease**

#### **1.1 Background**

Periodontal diseases, also known as periodontal infections, are a cluster of inflammatory diseases of the oral cavity that cause destruction of the tooth-supporting tissues (periodontium). A complex interplay of microbial, genetic, and environmental factors (such as smoking) is responsible for triggering this disease. The early stage of periodontal infection can cause gingival edema and inflammation, manifesting as “gingivitis.” If left untreated, the inflammation may destroy the periodontal connective tissues and underlying alveolar bone, manifesting as “periodontitis” (Ohlrich et al., 2009). It is estimated that around 50% of the adult population is suffering from periodontal diseases (Albandar, 2011), and 15% of these patients may exhibit severe destructive symptoms and lose their teeth (Brown and Loe, 1993). Records on periodontal infections from approximately 2700–2600 BC in China (Dentino et al., 2013) and fossil evidence from 3 million year old hominid showed that these diseases have threatened our teeth since the dawn of civilization (Forshaw, 2009). According to the U.S. Department of Health and Human services, at least 5 billion US dollars are spent on treatment of periodontal disease each year (Bonito et al., 2004). Apart from being the primary reason for human adult tooth loss (Ong, 1998), significant associations between periodontal infections and systemic diseases such as diabetes mellitus or cardiovascular

diseases have also been reported (Belibasakis and Bostanci, 2014; Kebschull et al., 2010).

## **1.2 Histopathology of periodontal diseases**

Although individual forms of periodontal disease may vary in terms of etiology, progression, or response to treatment, they share basic pathological mechanisms, histopathological appearance, ultrastructural features, and tissue destruction. This suggests a common chain of events underlying different periodontal diseases. According to Page & Schroeder (Page and Schroeder, 1976), the development of periodontal infections can be roughly divided into four stages: initial lesion, early lesion, established lesion, and advanced lesion (Ohlrich et al., 2009). During the initial lesion, large numbers of polymorphonuclear leukocytes (PMNs) are recruited, and there is an increase in gingival crevicular fluid (GCF). The start of the early lesion (second stage) is characterized by infiltration of matured leukocytes. Meanwhile, the accumulation of lymphocytes and further increasing GCF flow are also observed. With the progression of periodontal infections, recruited immune cells shift from primarily PMNs to macrophages and lymphocytes. This is when periodontal infection progresses into an established lesion (third stage), characterized by predominant number of plasma cells (activated B-cells). Another characteristic feature of this established lesion is collagen degradation. It has been reported that 60%–70% of collagen within the inflammation zone is degraded at this stage (Page and Schroeder, 1976). In the advanced lesion (fourth stage), many destructive clinical symptoms such

as periodontal pocket formation and destruction of the alveolar bone that supports the tooth are observed. The first three non-destructive stages of this disease are classified as gingivitis, while progression to an advanced lesion is defined as periodontitis. Gingivitis is reversible once the causative factors are controlled (Syed and Loesche, 1978). However, destruction of the bone in the periodontitis stage is almost permanent. Because the symptoms can be rather mild, most patients fail to recognize periodontal infection at the stage of gingivitis.

### **1.3 Clinical and microbiological diagnosis and therapy**

The clinical diagnosis of periodontal diseases depends on the changes in gingival tissue color and volume, increased periodontal pocket depth, and bleeding upon gentle provocation with a periodontal probe (Holtfreter et al., 2012; Lindhe and Nyman, 1975; Mariotti, 1999). Some putative microbial pathogens, such as *A. actinomycetemcomitans*, *P. gingivalis*, *T. forsythia* (previously *Bacteroides forsythus*), *T. denticola*, *P. intermedia*, *F. nucleatum*, *C. rectus*, *Streptococcus intermedius*, present in dental biofilms are highly associated with periodontal disease and are therefore also considered as potential indicators of the disease (Lovegrove, 2004; Socransky et al., 1998). However, any of these “pathogens” alone should not be considered as sole markers as these diseases are opportunistic polymicrobial infections (Teles et al., 2013) and may result from a complex polymicrobial synergy and dysbiosis between the biofilm and the host response (Hajishengallis and

Lamont, 2012; Lamont and Hajishengallis, 2015). The enzymatic activity of bacteria in biofilms once held good promise for the early diagnosis of this disease. A synthetic compound BANA [n-benzoyl-dl-arginine- $\beta$ -naphthylamide (PerioScan™)] was developed to detect proteolytic enzymes produced by *T. denticola*, *P. gingivalis*, and *T. forsythia*, which are believed to be associated with adult periodontitis (Bretz et al., 1993). Methods that evaluate the levels of periodontal pathogen-specific immunoglobulins in serum were also used to identify potential periodontal infection (Papapanou et al., 2001). In recent years, newly developed non-invasive periodontal diagnostic methods consider cytokine changes in GCF or saliva as markers for periodontal infections. Several studies have reported that GCF obtained from periodontitis patients exhibit higher concentrations of IL-1 $\beta$  (Navarro-Sanchez et al., 2007; Shaddox et al., 2011), IL-2 (Shaddox et al., 2011), IL-6 (Duarte et al., 2007; Kardesler et al., 2011), and TNF- $\alpha$  (Navarro-Sanchez et al., 2007). Other researchers found elevated expression levels of IL-1 $\beta$  (Gursoy et al., 2009; Miller et al., 2006), IL-6 (Aurer et al., 1999; Gursoy et al., 2009), TNF- $\alpha$  (Gursoy et al., 2009), and MMP-8 (Miller et al., 2006) in saliva collected from periodontal patients.

Clinically, periodontal therapies focus on professional and personal plaque removal, with the optional use of antiseptics or the occasional support by antibiotics. In general, standard periodontal treatments have good effects in terms of removing the biofilm causative factor and reducing inflammation. This results in improved clinical periodontal measurements and subsequent restoration of health. However, this outcome can persist only if patients



maintain personal oral hygiene and ensure continuous elimination of risk factors (Pihlstrom et al., 2005).

## **2. Microbiology of periodontal disease**

### **2.1 Biofilms: composition and complexity**

Periodontal infections are initiated by the accumulation of tooth-adherent oral microflora in the form of biofilms (Hajishengallis and Lamont, 2012). Biofilms (also known as dental plaque) consist of multispecies bacterial communities, which are embedded in a dense polymeric matrix. They attach to the tooth surface and neighboring host periodontal tissues (Socransky and Haffajee, 2005). Researchers have observed oral biofilms since the very beginning of microbiology. In 1683, the report sent by Antony van Leeuwenhoek to the Royal Society about “a few living animalcules” from his teeth, believed to be the first observation of live bacteria from human beings, was actually a description of a scarp from an oral biofilm. After more than 300 years since this first report, modern technologies such as electron microscopy, confocal laser scanning microscopy (CLSM), and quantitative real time polymerase chain reactions (qRT-PCR), allowed us to study other aspects of the oral biofilm. For example, one can now identify different species and their locations in a multiple-species biofilm by combining CLSM with fluorescence *in situ* hybridization (FISH) (Zijnga et al., 2010; Zuger et al., 2007). With electron microscopy, one can observe the shape and surface of the biofilm and therefore, record interspecies contacts and changes between

bacteria (Zhu et al., 2013). Sequencing of 16S rRNA genes allows the detection of more bacteria, particularly those that cannot be cultivated. At present, at least 1000 species have been found in the oral cavity (Dewhirst et al., 2010; Jenkinson and Lamont, 2005; Kuramitsu et al., 2007; Rosan and Lamont, 2000), with more species expected to be identified with improving technologies such as high-through next generation sequencing (Aas et al., 2005; Kumar et al., 2003; Wade, 2013; Zaura et al., 2009).

One of the difficulties of investigating the functions of oral biofilms is the high diversity of its constituent species. The oral microbiome has been shown to be the second-most complex after the colon microbiome in terms of species diversity. The oral biofilms are classified into supragingival or subgingival, based on their location in relation to the gingival margin. This thesis primarily focuses on the subgingival biofilm due to its closely documented association with periodontal infections (Socransky and Haffajee, 2005). Approximately 500 different species can potentially reside in a subgingival biofilm (Hajishengallis and Lamont, 2012; Paster et al., 2001) and form complex relationships with one another. It is known that not all of these bacteria can directly attach to the tooth surface, implying that late colonizers require the formation of a mature oral biofilm with species that first need to colonize on the tooth surfaces. In an *in vivo* situation, early colonizers generate optimal microenvironments and sometimes become the foundation for later colonizing species (Kuramitsu et al., 2007). Examination of the co-aggregation relationships between oral microbes is a good way to understand the organizational relationships of a biofilm (Kolenbrander et al., 2006).

However, in addition to direct attachment between bacteria, a number of other factors are involved in biofilm formation. For example, BspA protein from *Tannerella forsythia* favors co-aggregation with *F. nucleatum* and the growth of a dual-species biofilm (Sharma et al., 2005). Moreover, lysine-gingipain from *P. gingivalis* regulates the growth of *T. forsythia* in a 10-species biofilm (Bao et al., 2014), whereas its arginine gingipain promotes the growth of a dual-species biofilm with *T. denticola* (Zhu et al., 2013). Thus, it can be concluded that interspecies bacterial aggregation is only a part of the mechanisms that govern biofilm formation and that bacterial growth represents another important factor in this respect.

Living in the form of a biofilm, oral bacteria build physical contact with each other, interact on the metabolic level, and exhibit signal-mediated communication with other biofilm members (Kolenbrander et al., 2006; Wright et al., 2013). For example, *A. actinomycetemcomitans* utilizes lactate from streptococci as an energy source (Brown and Whiteley, 2007; Ramsey et al., 2011). *Porphyromonas gingivalis* produces isobutyric acid, which stimulates the growth of *T. denticola*, whereas *T. denticola* produces succinic acid that enhances the growth of *P. gingivalis* (Grenier, 1992). Furthermore, Autoinducer-2 (AI-2), an important quorum-sensing signal molecule present in many Gram-negative bacteria (Miller and Bassler, 2001), is expressed by many different oral microbial species including *streptococci spp.* *A. actinomycetemcomitans*, *F. nucleatum*, *P. gingivalis*, and *P. intermedia* (Fong et al., 2001; Frias et al., 2001; Shao and Demuth, 2010). AI-2 is a highly conserved molecule that enables interspecies communication in a multispecies

biofilm (Schauder et al., 2001; Shao and Demuth, 2010). AI-2 can also be treated as an energy source. *Actinomyces oris* uses AI-2 produced by *S. oralis* as an essential nutrition source (Rickard et al., 2006). However, although some bacteria act as synergistic neighbors to others (Ramsey et al., 2011), others may show antagonistic properties. For example, the expression of *fimA* from *P. gingivalis* is inhibited by arginine deiminase from *streptococci spp* and thus abrogates the colonization of *P. gingivalis* (Lin et al., 2008). Moreover, biofilm formation of *Candida albicans* is disturbed by *A. actinomycetemcomitans* through AI-2 expression (Bachtar et al., 2014). Besides, other non-bacterial factors such as nutrient availability, pH, toxic metabolites, shear forces, and host conditions contribute to the modeling of the structure and activities of an oral biofilm (Jenkinson, 2011). Only after elucidating the role of these factors in biofilm physiology can researchers possibly understand the shift of health-related biofilms to disease-related biofilms (Berezow and Darveau, 2011).

## **2.2 Theories on the microbial etiology of periodontal disease**

The oral cavity is an open environment where the gingiva is consistently challenged by bacteria. Commensal biofilms may benefit oral health by positively boosting a minimal immune response in the gingiva (Jenkinson and Lamont, 2005). However, when shifting to a more pathogenic composition, the biofilm may eventually trigger periodontal infection (Darveau, 2010; Sbordone and Bortolaia, 2003). Unlike some infectious diseases, periodontal

infections are not triggered by single species. In the 1920s, researchers doubted the primary role of bacteria in periodontal infections (Belding and Belding, 1933) due to failure in finding specific pathogenic microorganisms in the oral biofilm. It was not until the late 1950s when interest in the oral biofilm was raised again that researchers realized that the accumulation of subgingival biofilm was the non-specific cause of the disease (Schultz-Haudt et al., 1954). These observations led researchers to notice the importance of microbial shifts in periodontitis (Socransky, 1977), which then became the foundation of the theory that specific plaque may cause the disease (Loesche, 1992). Based on the studies of Socransky et al. (Socransky et al., 1998), periodontal microbial communities were sorted into different color-coded systems based on their community ordination and association with disease severity. *P. gingivalis*, *T. denticola*, and *T. forsythia* were grouped as “red complex,” a group most likely to trigger the disease due to their strong association with it. With respect to shifts in the biofilm community, it is now the predominant school of thought that enrichment of the pathogenic bacteria is driven by environmental factors (Marsh, 2006). Thus, the action of low abundance “keystone” pathogenic bacteria (Hajishengallis et al., 2011) may shape the dysbiotic microbiota that cause periodontal infections (Hajishengallis and Lamont, 2012).

## **2.3 *Porphyromonas gingivalis***

### **2.3.1 Characteristics of *P. gingivalis***

*P. gingivalis* is a Gram-negative, anaerobic, black-pigmented rod commonly found in the subgingival biofilm of patients with periodontitis (Boutaga et al., 2007). This species draws a lot of attention in periodontal research due to its association with the severity of periodontal infection (Boutaga et al., 2007; Yang et al., 2004). Since the early study of periodontal infections, *P. gingivalis* was considered as one of the main pathogens that cause this disease (Holt et al., 1988). In his color-complex coded system, Socransky considered *P. gingivalis* as one of the three bacteria belonging to the “red complex” a group displaying the closest relationship to chronic periodontal disease (Socransky et al., 1998). The survival strategy of *P. gingivalis* focuses on avoiding the immune response rather than fighting against it, which may end up in establishing chronic inflammation. It is known that *P. gingivalis* is able to invade human epithelial cells (Tribble et al., 2006) without triggering apoptosis or necrosis (Nakhjiri et al., 2001). Instead, it regulates human toll-like receptors (TLR)-4 through an atypical lipopolysaccharide (Coats et al., 2009), perturbs the cross-talk between C5a receptor and TLR signaling to prevent dysbiosis caused by bacterial clearance (Maekawa et al., 2014), and inhibits the production of pro-inflammatory chemokines (Bostanci et al., 2007a; Bostanci et al., 2013; Hamed et al., 2009; Hasegawa et al., 2008). These findings are contrary to the dogma that biofilms trigger the inflammation associated with periodontal infection and leave an ambiguous

understanding of the contribution of *P. gingivalis* to the disease. Recently, Hajishengallis et al. demonstrated that this species could increase the virulence of the overall biofilm community even when present at low levels. Therefore, it is considered as a “keystone” species, the kind that is crucial for shifting the biofilm composition but does not need to exist in large proportions (Hajishengallis et al., 2011). Other reports have shown that *P. gingivalis* co-aggregates with *T. denticola* (Abe et al., 2004; Ito et al., 2010; Yamada et al., 2005), regulates growth (Bao et al., 2014), and controls the aggregation (Ito et al., 2010; Yamada et al., 2005) of other species, all of which support the “keystone” traits of *P. gingivalis*. In conclusion, even if the role of this species in biofilm may seem paradoxical, *P. gingivalis* certainly plays a prominent part in orchestrating inflammatory responses in the periodontal tissues (Hajishengallis and Lamont, 2014).

### **2.3.2 Virulence factors of *P. gingivalis***

*Porphyromonas gingivalis* expresses numerous virulence factors including lipopolysaccharide (LPS), capsular polysaccharide (CPS), fimbriae, and its cysteine proteases, namely gingipains (Bostanci and Belibasakis, 2012; Curtis et al., 2001). LPS of the *P. gingivalis* has been reported to stimulate bone resorption in experimental animals (Chiang et al., 1999; Nishida et al., 2001); CPS is known to induce systemic IgG responses (Sims et al., 2001); and fimbriae facilitate the adherence of *P. gingivalis* to other species (Yamada et al., 2005) or host cells (Amano et al., 2004). However, this thesis mainly focuses on the functions of gingipains of *P. gingivalis*.

### 2.3.3 Gingipains

Gingipains, including arginine-specific proteinases A and B (RgpA and RgpB) and lysine-specific proteinase (Kgp) (Aduse-Opoku et al., 2000; Curtis et al., 2001), are potent cysteine proteases that are responsible for 85% of the proteolytic activity and 99% of trypsin-like amidolytic activities of *P. gingivalis* (Curtis et al., 2001; Potempa et al., 1997). The initial translation product of RgpA is a polyprotein composed of 1706 amino acids, including a 227 amino acid propeptide domain, 492 amino acid catalytic domain, 543 amino acid adhesin/hemagglutinin domain, and 444 amino acids C-terminal extension, whereas RgpB consists of 736 amino acids and lacks the major adhesin/hemagglutinin domain (Curtis et al., 2001). The arginine-specific proteinase can form in the 1) hetero-dimeric or multimeric form of RgpA composed of catalytic chain non-covalently associated with adhesin and Kgp enzyme (Rangarajan et al., 1997), 2) monomeric RgpA and RgpB in soluble form (Chen et al., 1992), or 3) monomeric forms in membrane associated form (Slakeski et al., 1998). Arg-gingipains cleave only protein/peptide substrates with Arg in the P1 position (Chen et al., 1992). The initial translation product of Kgp varies in size between 1723 and 1732 amino acids, depending on the strain (Curtis et al., 2001). Kgp cleaves peptides with Lys in the P1 position but can be blocked if Lys or Arg occupy the residue at P2 (Abe et al., 1998).



In a closed environment such as the periodontal pocket, the main carbon and nitrogen resources for *P. gingivalis* come from the host (Milner et al., 1996), which largely relies on the proteolytic activity of its gingipains. Accordingly, *P. gingivalis* gingipain deficient strains require longer doubling time than normal (Grenier et al., 2003). Moreover, unlike other Gram-negative bacteria, *P. gingivalis* does not produce siderophore to sequester and transport iron (Olczak et al., 2005). Therefore, gingipains also play a crucial role in the uptake of iron in *P. gingivalis* by taking in hemoglobin, heme protein, and ferritin from the host tissues (Bramanti and Holt, 1991; Gao et al., 2010; Sroka et al., 2001). They are also important in the formation or regulation of oral biofilms. Arg-gingipains were shown to affect the co-aggregation between *P. gingivalis* and *T. denticola* (Ito et al., 2010; Yamada et al., 2005; Zhu et al., 2013) and regulate the structure of *T. denticola* aggregates in the 10 species biofilm (Bao et al., 2014). Lysine gingipains have been found to regulate the growth of *T. forsythia* in a 10 species biofilm (Bao et al., 2014). Both gingipains have also been found to regulate the co-aggregation of *P. gingivalis* with *P. intermedia*, *F. nucleatum*, *Actinomyces naeslundii*, and *Actinomyces viscosus* (Abe et al., 2004; Kamaguch et al., 2001).

## **2.4 *Aggregatibacter actinomycetemcomitans***

*A. actinomycetemcomitans* is a small, non-motile, facultative anaerobic, Gram-negative coccobacillus. This “*Bacterium actinomycetem comitans*” was first isolated from the actinomycotic lesion (Klinger, 1912) and was

previously classified as *Actinobacillus actinomycetemcomitans* (Topley and Wilson, 1929) and later as *Haemophilus actinomycetemcomitans* (Potts et al., 1985). *A. actinomycetemcomitans*, particularly the JP2 clone used in this thesis, is strongly associated with aggressive forms of periodontitis among young individuals (Haubek et al., 2008) and multiple non-oral infections (van Winkelhoff and Slots, 1999). JP2 is a strain that exhibits high production of leukotoxin (LtxA) and differs from other species by a 530-bp deletion in the promoter region of the *LtxA* gene, which is believed to enhance its expressions (Hayashida et al., 2002). Many reports have demonstrated that *A. actinomycetemcomitans* is able to invade the cell, escape from immune defenses (Handfield et al., 2005; Lepine et al., 1998; Morimoto et al., 1999; Takayama et al., 2003), and activate various innate immune pathways (Belibasakis and Johansson, 2012; Takayama et al., 2003). Armed with many virulence factors such as LtxA, cytolethal distending toxin (CDT), and cytotoxin-associated genes E (CagE), *A. actinomycetemcomitans* is highly resistant to host immune cells such as PMNs, T-lymphocytes, and macrophages (Henderson et al., 2010).

*A. actinomycetemcomitans* is also reported to regulate its neighboring microbial cells in an oral biofilm. Similar to other Gram-negative bacteria, AI-2 receptors were found in *A. actinomycetemcomitans* (Shao et al., 2007), indicating a quorum-sensing regulatory mechanism across species within the oral biofilm. Moreover, *A. actinomycetemcomitans* utilizes lactate from streptococci as an energy source (Brown and Whiteley, 2007; Ramsey et al., 2011), which not only benefits its own growth but also enables change in pH

of the biofilm environment by reducing lactate. *A. actinomycetemcomitans* co-cultures with other species such as *P. gingivalis* (Periasamy and Kolenbrander, 2009b), *Granulicatella spp.* (Karched et al., 2015a), and *F. nucleatum* (Periasamy and Kolenbrander, 2009a) and form dual-species biofilms. Although both are related to periodontal infection, *A. actinomycetemcomitans* and *P. gingivalis* show antagonistic effects on each other's growth. A competitive advantage of *P. gingivalis* has been displayed over *A. actinomycetemcomitans* (Takasaki et al., 2013). In a 6-species biofilm including *P. gingivalis* and *A. actinomycetemcomitans*, this advantage was also indicated by decreasing the cell number of *A. actinomycetemcomitans* and increasing numbers of *P. gingivalis* through biofilm cultivation (Karched et al., 2015b).

### **3. Host–bacteria interaction**

#### **3.1 Structure and function of periodontium**

The periodontium [including the gingiva (or “gums”), periodontal ligament, root cementum, and alveolar bone] is the set of tissues that surround and support the tooth. Similar to most mucosal structures, the gingiva consists of a surface epithelial layer and fibrous connective tissue (lamina propria) underneath (Schroeder and Listgarten, 1997). The gingival epithelium is a stratified squamous one and acts as a physical barrier against infection (Kobayashi et al., 1976). The epithelial layer itself is also involved in immune responses through its enzyme-rich lysosomes and by allowing and regulating

trafficking of immune cells to the site of infection (Ohlrich et al., 2009; Segulier et al., 2000). The gingival epithelium can be divided into three functional compartments: gingival, sulcular, and junctional epithelium. In addition to their morphological differences, keratin expressions are variable between these three compartments (Bragulla and Homberger, 2009; Hsieh et al., 2010). The junctional epithelium plays a crucial role in maintaining a healthy periodontium and consists of flatten cobblestone-like epithelial cells lying parallel to the tooth surface and sealing the periodontal tissues from the oral environment (Nanci and Bosshardt, 2006). In addition, junctional epithelium has 2%–5% of its total surface occupied by intercellular spaces (Schroeder and Munzel-Pedrazzoli, 1970), creating a unique semi-permeable passage that allows GCF and immune cells to pass through (Schroeder, 1970; 1973). This tissue is crucial for the establishment of periodontal disease (Bosshardt and Lang, 2005), because it is exposed to the biofilm and cannot be inversely generated once the periodontal lesion has been established (Nanci and Bosshardt, 2006).

Gingival connective tissue is a fibrous tissue that lies underneath the gingival epithelium. It consists mainly of collagen and fibroblasts but allows inflammatory cells to infiltrate through a dense capillary and post-capillary venule network in inflammatory and clinically healthy circumstances (Nanci and Bosshardt, 2006). In addition to providing physical support to the epithelium, the connective tissue produces growth factors for epithelial survival and growth through its fibroblasts (Costea et al., 2006; Locke et al.,

2008). Moreover, fibroblasts themselves participate in innate immune responses against bacteria (Lekic et al., 1997; Locke et al., 2008).

The crevice between the tooth and surrounding gingival tissue is called the gingival sulcus. It is constantly washed by GCF due to the microbial challenge and subsequent immune response. A healthy sulcular depth is <3 mm. However, when periodontal infection occurs, the sulcular depth increases along with other clinical changes such as bleeding and apical migration of the attached epithelium. The gingival sulcus in this stage is classified as a gingival pocket or periodontal pocket, depending on the type of periodontal disease. Its depth is an important clinical parameter in the diagnosis of periodontal disease (Holtfreter et al., 2012; Lindhe and Nyman, 1975; Mariotti, 1999).

### **3.2 Immunological components of the periodontium**

In response to the biofilm, the host tissue secretes numerous small compounds of the immune system (e.g., antibodies, cytokines, and prostaglandins) at the site of infection and recruits immune cells (e.g., PMNs, monocytes/macrophages, T-cells, and B-cells) (Ohlrich et al., 2009) to defend against the developing infection. In response to a bacterial antigen, the innate immune response, mainly through phagocytic cells such as PMNs and macrophages, forms the first line of defense. PMNs are the main immune cell type recruited in the early stages of periodontal infection (Tonetti et al., 2012). These cells migrate to the inflammatory area following an increase in the

chemotactic cytokine IL-8 concentration (Ebersole, 2003) and execute their bactericidal functions through neutrophil extracellular traps (NETs), phagocytosis, or oxidative burst (Nussbaum and Shapira, 2011). The effects of PMN on the control of bacterial infection are proven in PMN-deficient patients (Weston et al., 1991) as well as neutropenia animals (Verzeletti et al., 2007). However, in addition to their protective role against pathogenic bacteria, PMNs trigger the destruction of connective tissues by producing molecules that amplify inflammation, such as triggering receptor expressed on myeloid cells 1 (TREM-1) (Bostanci et al., 2013); degrading enzymes such as matrix metalloproteinases (MMPs); and cytotoxic substances such as reactive oxygen species (Nussbaum and Shapira, 2011; Ryder, 2010). PMNs also induce osteoclastic bone resorption through the membrane bound receptor activator of nuclear factor kappa-B ligand (RANKL) (Chakravarti et al., 2009). In addition to their roles in periodontal infection, the tissue-destructive capacity of PMNs is documented in several chronic inflammatory diseases (Caielli et al., 2012).

Macrophages, another important scavenger in early inflamed periodontal lesions, are specialized phagocytes differentiated from monocytes. After they have been stimulated by microbe-associated molecular patterns (MAMPs) such as LPS, monocytes express high levels of toll-like receptor-4 (TLR-4) and cluster of differentiation 14 (CD14) (Sabroe et al., 2002). The monocytes have been reported to express higher levels of cytokines in periodontal patients compared to periodontally healthy individuals (Fokkema et al., 2003). Pro-inflammatory cytokines, particularly IL-1 and TNF- $\alpha$ , are

potent inducers of connective tissue degrading enzymes such as MMPs as well as bone resorption pathways such as RANKL-OPG (Belibasakis and Bostanci, 2012; Graves et al., 2001). Both IL-1 and TNF- $\alpha$  are increased drastically in the GCF of patients with periodontitis (Giannopoulou et al., 2003).

Plasma cells and lymphocytes become the dominant immune cells in the tissue during the course of periodontal infection (Kinane et al., 2008). Lymphocytes include B cells, T cells, and natural killer T cells (NK T cells). Plasmas cells/ B cells are important for producing immunoglobulins (Igs) that guide adaptive immune cells by specifically binding to the antigen. T cells are considered to play an important role in the progress and control of inflammation during periodontal infection. T helper 1 (Th1) and T helper 2 (Th2) are important subsets of T cells in periodontal disease, and their ratios are regulated by the cytokine profile in the tissue (Berglundh et al., 2002). T helper 17 (Th17) cells are newly discovered T helper cells that are characterized by IL-17 expression and are also reported to be involved in the periodontal infection (Steinman, 2007). Th1 and Th17 induce autoimmunity in the host tissues during periodontal infection and are therefore potential drug targets (Gaffen and Hajishengallis, 2008). Because these three types of Th cells develop from the same T-cell precursor, T cells are considered to exhibit plasticity in the presence of a diverse cytokine milieu (e.g., Th1, Th2, and Th17 polarization is induced by IL-12, prostaglandin E<sub>2</sub>, and IL-1, respectively) (Bluestone et al., 2009). Another distinct subset of T cells, T regulatory cells (Tregs), control the immune responses and maintain

peripheral tolerance (Thompson and Powrie, 2004), while NK T-cells recognize and eliminate bacteria directly or through other immune cells (Mattner et al., 2005). The regulation of cytokines or chemokines in gingival tissues is a complex process that involves secretion by many cells of the immune system (Bostanci et al., 2007a; Bostanci et al., 2007b; Bostanci et al., 2011; Hamed et al., 2009) and structural tissue cells (Belibasakis et al., 2005; Belibasakis and Guggenheim, 2011). In the context of periodontal infection, Th1 cells express RANKL and may induce periodontal bone resorption (Han et al., 2007) that can be mediated by Th2 cells (Ohlrich et al., 2009). Interestingly, despite the autoimmune-related response of Th17 cells, they have also been reported to display a protective role against bone resorption (AlShwaimi et al., 2013).

### **3.3 Host–bacteria interaction to the inflammation**

In the oral environment, gingival tissues are constantly challenged by the biofilm. Periodontal inflammation in the gingival tissue is initiated when the host–bacteria balance is disturbed (Page and Kornman, 1997). Immune responses most likely contribute to the prevention of bacterial spread into deeper periodontal tissues, but total elimination, which is the ultimate goal of the immune system, cannot be reached as long as biofilms persist on the tooth surfaces. The permeability of the epithelium not only allows immune cells to emigrate towards the biofilm but also allows microorganisms from the biofilm to invade the underlying tissues (Sandro et al., 1994). Putative periodontal



pathogens such as *P. gingivalis*, *A. actinomycetemcomitans*, and *F. nucleatum* attach to the surface or invade the host cells (Bostanci et al., 2007a; Bostanci and Belibasakis, 2012; Han et al., 2000; Handfield et al., 2005; Morimoto et al., 1999; Pierce et al., 2009; Weiss et al., 2000). Periodontal pathogens or their virulence factors alone can stimulate cytokine production by the cells of the periodontium (Madianos et al., 2005). Despite these indications that bacteria may enhance the inflammatory response of the tissues, there is also evidence to suggest that some species act against each other to reduce the level of inflammation and survive (Gaffen and Hajishengallis, 2008). In this manner, the pathology of periodontal infection is masked by the complex relationship between the host tissues and oral microbiota.

#### **4. Periodontal infection models**

Although different models have been established to understand the mechanisms of periodontal infections, they are all limited to a certain extent. In the 1970s, Syed and Loesche proved that gingivitis could be induced by biofilm that has accumulated due to absence of oral hygiene (Syed and Loesche, 1978). Experimental gingivitis is a useful model to study the initiation of periodontal infections, with recent application of proteomics in studying the development of inflammation (Bostanci et al., 2012). However, due to ethical considerations, human experiments cannot proceed till the tissue destructive lesion appears and thus can only answer questions regarding initiation of the early inflammatory stages of the disease. Additionally, the

microbial profile is highly diverse in each individual, which increases the complexity of the study (Paster et al., 2001).

Animal models, including oral gavage model, ligature-induced periodontitis model, chamber model, and abscess model are the other available choices for the study of periodontal diseases (Hajishengallis et al., 2015b). In the oral gavage model, periodontal infections are induced by bacterial inoculation in the animal (Baker et al., 2000). The ligature-induced models involve the placement of a silk ligature around the posterior teeth to accumulate bacteria and, therefore, induce inflammation (Abe and Hajishengallis, 2013). Consequently, these models are the most common *in vivo* models for the study of inflammation and bone resorption as they are capable of inducing late stage periodontal infection (Daep et al., 2011; Orth et al., 2011; Settem et al., 2012). The chamber and abscess models, on the other hand, are developed mainly to study the effects of specific microbiota on periodontal infections. In the chamber model, the lumen of a subcutaneously implanted titanium coil chamber is used to inject bacteria to allow subcutaneous quantification of the recruited inflammatory cells (Graves et al., 2008). In the abscess model, bacteria are injected into the dorsum, and their impact is scored according to the histopathological characteristics of the abscess (Singh et al., 2011). Similar to humans, animals have a highly complicated immune system. Use of various genetically engineered mouse models provides studies with a unique platform for studying host responses. One may argue that the oral microbial composition in animal models differs from that of humans. Nevertheless, experimental mouse models are meant to

target specific aspects of the disease to be studied and should not be considered as absolute substitutes for the study of human disease (Hajishengallis et al., 2015a). Although non-human primates may reduce such issues (McMahon et al., 1990), they raise other issues such as tight ethical restrictions and high financial costs.

Another important option for studying periodontal infection is the use of *in vitro* models. In single species studies, putative periodontal pathogens such as *P. gingivalis* and *A. actinomycetemcomitans* can be introduced in the cell cultures to understand the effects of certain bacteria on host responses (Belibasakis et al., 2011b; Bostanci et al., 2009; Hamed et al., 2009). However, 3D organotypic cell culture systems may express the histological features of the *in vivo* oral or gingival mucosa more accurately than 2D monolayer cultures. Therefore, models that use multi-layered epithelium were created and subsequently became increasingly popular (Schaller et al., 2006). Support of the epithelial multilayers by underlying connective tissue fibroblasts is important to allow the epithelium to exhibit features and behavior closer to their natural state in primary tissue (Karring et al., 1975; Mussig et al., 2009). Moreover, fibroblasts themselves also contribute to the local innate immunity, and their presence is important in a multi-tissue culture model (Belibasakis et al., 2014). Therefore, 3D oral gingival models reconstituted by epithelial cells and fibroblasts (Bragulla and Homberger, 2009; Chai et al., 2010; Choe et al., 2006; Dongari-Bagtzoglou and Kashleva, 2006; Igarashi et al., 2003; Mussig et al., 2009) have been widely accepted ever since Tomakidi et al. developed the first one in 1997 (Tomakidi et al.,

1997). These complex models are based on oral epithelium cultured on top of an oral fibroblast-containing collagen gel or human de-epithelialized dermis at an air-to-liquid interface and remarkably broaden our understanding of bacteria-host relationships in periodontal infection (Dabija-Wolter et al., 2012; Diaz et al., 2012; Paino et al., 2012; Pollanen et al., 2012). However, the complexity of biofilm cannot be represented by the single bacterial challenge most often used in such studies. Therefore, utilizing a multi-species biofilm has also been considered in periodontal infection models to allow better understanding of tissue biofilm interactions (Belibasakis et al., 2013b; Thurnheer et al., 2014). Obviously, no one *in vitro* or *in vivo* model is able to reproduce the complexity of human periodontal infection and address all aspects of the disease. Nevertheless, specific aspects can be productively investigated by using the most upfront bioengineering tools.

Moreover, the earlier 3D models have been generated mainly by static seeding conditions, whereas bioreactor-based systems could offer a better control over cell culture parameters such as enhanced diffusion of oxygen and nutrients inside the cell-seeded scaffold, therefore leading to a standardized and reproducible production process. In particular, perfusion bioreactors for cell seeding and continuous culturing may lead to a uniform cell distribution and better growth/survival (Papadimitropoulos et al., 2013; Wendt et al., 2006). In addition, the generated flow in the dynamic culture system may mimic naturally occurring oral fluid flows such as saliva and GCF and may therefore provide mechanical stimulation such as shear stress to the cells. In a given periodontal pocket, subgingival biofilms are estimated to be present in

2% oxygen and are exposed to the shear forces of saliva and gingival exudate at a flow rate of 0.4–2.0 ml/min (Loesche et al., 1983).

Bioreactor-based models have been successfully used for modeling many other mucosal diseases such as lung infections (Carterson et al., 2005), intestinal diseases (Timmins et al., 2007; Voisard et al., 2003), and colon diseases (McCoy and O'Brien, 2010; Yeatts and Fisher, 2011). Such a system is missing in the field of periodontal infections. There is a great need for the development and exploitation of novel *in vitro* experimental models enabling the concomitant study of biofilms and host tissue. These could provide a better understanding of different aspects of periodontal infections, including relationships of different bacteria within the biofilm, behavior of biofilms in the presence of host tissue, and effect of biofilms on the host tissue. Such approaches could be also used in therapeutics as the first step to development and validation of periodontal infection-targeted medications.

## Aims

The principal aim of this PhD thesis was to develop a standardized organotypic tissue-biofilm interaction model that is capable of recapitulating *in vitro* the early events taking place during the establishment of periodontal infection. The more specific aims, which are realized in each of the individual papers of the thesis, are as follows:

- 1: To understand the role of individual virulence factors in subgingival biofilm formation and structure. This was evaluated by using two mutant strains of *P. gingivalis* that lacked the expression of a gingipain as a model organism.
- 2: To evaluate if a standard subgingival biofilm model is amenable to the incorporation of additional species, using *A. actinomycetemcomitans* as a newly introduced organism. This evaluation aimed primarily at the study of proteomic changes that take place in the biofilm as a whole unit following the incorporation of *A. actinomycetemcomitans*.
- 3: To establish immortalized gingival epithelial and fibroblast cell lines that can be utilized either in monocultures or in multi-layered cultures for the development of host-biofilm interaction experimental models.
- 4: To generate an *in vitro* experimental model in a dynamic microenvironment that recapitulates key biological events in early periodontal infection. This involved a gingival epithelial-fibroblast-monocyte organotypic co-culture on collagen sponges, challenged by a subgingival biofilm, all performed in a dynamic perfusion bioreactor system.

5: To characterize the global proteomic events taking place in the established organotypic tissue-biofilm interaction model of periodontal infection. This was performed by using high-throughput quantitative proteomic technology.

## Methodology

In this thesis, different methods were used to establish a standardized organotypic tissue-biofilm interaction model and to characterize its features. The general descriptions and theoretical principles of the methods used within the thesis are given in this chapter, while the more detailed methodology is described in each individual paper of the thesis.

### 1. Bacterial strains

A total of 13 strains, including 2 mutants of *P. gingivalis* W50, were used in this study. These were *A. actinomycetemcomitans* JP2 (OMZ 295), *P. intermedia* ATCC 25611 T (OMZ278), *C. rectus* (OMZ 398), *Veillonella dispar* ATCC 17748 T (OMZ 493), *F. nucleatum subsp. nucleatum* (OMZ 598), *S. oralis* SK248 (OMZ 607), *T. denticola* ATCC 35405 T (OMZ 661), *A. oris* (OMZ 745), *S. anginosus* ATCC 9895 (OMZ 871), *T. forsythia* (OMZ 1047), *P. gingivalis* W50 (OMZ 308), *P. gingivalis*, K1A (OMZ 1126) and *P. gingivalis* E8 (OMZ 1127). The *P. gingivalis* K1A (OMZ 1126) and *P. gingivalis* (OMZ 1127) are genetically modified strains of *P. gingivalis* W50, with a deletion of Lysine-gingipain (kgp) and Arginine gingipain (rgpA and rgpB) genes, respectively.

### 2. Multispecies subgingival biofilm model

Earlier studies have used single species in planktonic form or in biofilm. However, the oral biofilm is a multi-species dynamic system, and its



complexity cannot be reflected by any single species cannot. Besides, most bacteria that are considered as “pathogens” are late colonizers and may be unable to attach to the tooth surface directly. Thus, in a biofilm, earlier colonizing bacteria optimize the environment for such late colonizing bacteria. Compared to the single species biofilm models, multispecies models are morphologically and physiologically closer to the *in vivo* oral biofilm.

The *in vitro* dental biofilm model described here is a more advanced version of the well accepted “subgingival biofilm model” developed at the Section of Oral Microbiology and Immunology and also known as the “Zürich” biofilm model (Ammann et al., 2012; Ammann et al., 2013a; Ammann et al., 2013b; Belibasakis et al., 2013a; Belibasakis et al., 2014; Guggenheim et al., 2009). This model included in its composition typical early, intermediate, and late colonizers, which are detailed in the previous section. In brief, the biofilms are grown on hydroxyapatite discs following the addition of 200 µl of bacterial cell suspensions containing equal densities and volumes of each strain. A volume of 1.6 ml of growth medium (consisting principally of 60% saliva, 10% human serum, 30% modified fluid universal medium) is added to this suspension and incubated anaerobically for 64 h to achieve biofilm formation. During this period, the hydroxyapatite discs containing the growing biofilms on their surface are periodically dip-washed in physiological saline to mimic the shear forces of saliva in the oral cavity.

In paper 1, by comparing the 10 species biofilms with the wild-type or the gingipain mutated *P. gingivalis* strains, we estimated the role of the gingipains in the structure and function of the biofilm. Paper 2 focuses on the

role of *A. actinomycetemcomitans* in the whole biofilm, indicated by the difference between 10-species biofilm and the same biofilm with additional bacterium.

### **3. Biofilm harvesting and quantification by qRT-PCR and FISH**

For the evaluation of bacterial composition of the biofilm, quantitative real-time PCR (qRT-PCR) and fluorescence *in situ* hybridization (FISH) were used. By relying on species-specific target sequences, qRT-PCR may more precisely quantify different species compared to colony forming unit (CFU) measurement, albeit CFU may more accurately define the number of living bacterial cells in the biofilm (Ammann et al., 2013b). The FISH method labels different species with matched fluorescent 16S rRNA oligonucleotide probes. With the help of confocal laser scanning microscopy (CLSM), FISH can easily identify the specific species within the biofilm (Thurnheer et al., 2001; Thurnheer et al., 2014).

### **4. Establishment, cultivation, and characterization of cell lines**

One of the challenges in establishing a standardized, reproducible cell culture model is that primary cells have a short life span, last for few passages, and therefore do not provide sufficient cell numbers, not to mention the genetic differences between individual donors (Pi et al., 2007; Sacks, 1996). In the context of gingival tissues, gingival epithelial cells can only replicate for a few passages, and although gingival fibroblasts can replicate for more

passages, these traits are not sufficient to establish a reproducible model. Transfection with oncogenes E6 and E7 from high-risk human papillomavirus type 16 (HPV-16) is an efficient and reproducible way of producing immortalized cell lines (Dimri et al., 2005). This method has been used on other non-gingival epithelial or fibroblast cells (Dimri et al., 2005; Illeperuma et al., 2012; Oda et al., 1996). Therefore, in this thesis, immortalized epithelial and fibroblast cell lines were established from primary human gingival epithelial keratinocytes (HGEK) and gingival fibroblasts (GF) by inducing E6 and E7 oncoproteins from HPV-16, conducted in collaboration with the Department of Virology, University of Cologne, Germany. The various cytokeratin (CK) expression patterns have been used as molecular indicators for different regions of the oral epithelium (Bragulla and Homberger, 2009; Hsieh et al., 2010). These CKs, including early epithelial markers CK19 (cornified stratified epithelial markers CK10 and CK16) were used to characterize the immortalized cells developed in this thesis using qRT-PCR.

MonoMac 6, a monocytic cell line established from the peripheral blood of a patient with monoclastic leukemia (Ziegler-Heitbrock et al., 1988), was also used in this model. It is the only human cell line that constitutively expresses the phenotypic and functional characteristics of mature monocytes and has therefore been used in earlier periodontal infection models (Bostanci et al., 2007a; Bostanci et al., 2007b; Hamed et al., 2009).

## **5. Generation and characterization of organotypic gingival tissue in a perfusion bioreactor**

Our *in vitro* organotypic gingival tissue model consists of the gingival epithelial continuous cell line, the GF continuous cell line developed in this study on a collagen scaffold, the MonoMac6 cell line, and the “subgingival” biofilm. All these elements were brought in a dynamic flow system regulated by a U-tube perfusion bioreactor (Bao et al., 2015b). The pump of the bioreactor regulates the flow rate of the contained suspensions and reverses the flow when the injected fluid amount in the column reaches a set volume. With appropriate cell type and optimized growth medium, the scaffold that supports the cells growth is the most essential element to establish a proper 3D model. Collagen is one of the most widely used textures due to its similarities with natural connective tissue (Moharamzadeh et al., 2007), though collagen gels that are used in most 3D static gingival models are unable to be penetrated by immune cells. The collagen sponge, made of porcine collagen type 1, used in Paper 4 of this thesis shows biologically favorable properties for the growth of epithelial cells, is strong enough for the bioreactor shear forces, has the porous structure that acts as a flow-through channel for the monocytes, is easier to handle than traditional collagen gels, and may induce collagen synthesis by the cells more efficiently than a collagen gel (Berthod et al., 1993).

## **6. Host-biofilm interaction model in a perfusion bioreactor**

To mimic the inflammation processes in periodontal infection, the 11-species biofilm developed in Paper 2 was placed on the surface of collagen sponge to challenge the *in vitro* organotypic gingival tissue model detailed in the previous section. To mimic the distance between the tooth surface and the gingival tissue in real life, a small plastic ring was positioned on top of the organotypic layer just prior to placement of the biofilm-carrying discs (Belibasakis et al., 2014; Bostanci et al., 2015). These co-cultures were performed in the absence of antibiotics/antifungals to permit the survival of biofilm bacteria. In addition, during co-culture experiments, the atmospheric conditions were adjusted to 2% O<sub>2</sub>. A 24 h co-culture, collagen scaffolds, biofilm-containing discs, and culture medium were collected for various analyses. Masson's trichrome staining and scanning electron microscopy were employed to study the cell distributions and organotypic tissue structure developed on the collagen sponges. A multiplex immunoassay was used to measure the levels of different cytokines in the secreted supernatant of the biofilm-challenged organotypic cultures.

## **7. Proteomic identification and characterization by LC-MS/MS**

The modern liquid chromatography-tandem mass spectrometry (LC-MS/MS) is a powerful tool that can identify and quantify thousands of proteins from complex biological samples in a single run (Hebert et al., 2014; Hendrickson et al., 2014; Lundberg et al., 2014; Shen et al., 2014). In this thesis, LC-

MS/MS has been used to understand the effects of *A. actinomycetemcomitans* on the biofilm (Paper 2) and to monitor the interactions between the organotypic host tissue and the biofilm (Paper 5).

Our present understanding of biofilm behavior is mainly based on the growth characteristics of the biofilm, reflected by the individual bacterial cell numbers and bacterial localization (Amano et al., 2004; Ammann et al., 2012; Bao et al., 2014; Guggenheim et al., 2004). However, some reports have shown more in-depth regulatory trends in biofilms and uncovered molecular networks with LC-MS/MS (Hendrickson et al., 2012; Hendrickson et al., 2014; Maeda et al., 2015; Trindade et al., 2014; Zainal-Abidin et al., 2012). By using a label-free quantitative proteomics platform, we compared the identified biofilm lysate composition (“lysomes”) of biofilm with or without *A. actinomycetemcomitans* to understand the effects of this species on the whole biofilm.

It is long known that the gingival epithelium secretes different proteins in response to the biofilm challenge, even before the appearance of clinical signs, which may be considered as biomarkers of the disrupted epithelial barrier (Ohlrich et al., 2009). However, a bigger picture of this process could only be studied in the whole range of regulated proteins. In Paper 5 of this thesis, we not only identified the proteins but also studied their abundance using a spectral counting method (Bao et al., 2015a). The host proteomic profile was identified in the secreted culture supernatant (“secretome”), and further analysis was performed on Metacore (an online bioinformatics database) to pursue protein pathways that were specifically affected in the

presence of the biofilm. The bacterial proteomic profile was mainly identified in the biofilm lysates, along with numerous potentially secreted bacterial proteins in the supernatant.

## Results and discussion

### Role of *P. gingivalis* gingipains in multispecies biofilm formation (Paper 1)

A quantitative evaluation of bacterial numbers in the biofilms revealed that the lack of gingipain expression did not affect the growth of *P. gingivalis* or any other species, with the exception of *T. forsythia*, which was significantly reduced in the absence of the Lys-gingipain. In terms of biofilm structure, CLSM showed that the wild-type *P. gingivalis* strain formed aggregates within its own species. *T. forsythia* was often scattered close to *P. gingivalis*. The association between *P. gingivalis* Lys-gingipain deficient strain and *T. forsythia* was less obvious. *Treponema denticola* formed aggregates or clusters in the presence of the wild-type *P. gingivalis* as well as when the Lys-gingipain deficient strain was used. However, in the presence of the Arg-gingipain deficient strain, *Treponema denticola* lost this cluster-like conformation and was distributed in a more threaded structure.

Gingipains are crucial for the co-aggregation of *P. gingivalis* or its co-adhesion with other species such as *T. denticola* (Abe et al., 2004; Ito et al., 2010; Yamada et al., 2005), as was evident in this study by the formation of dense circular clumps of *T. denticola* dependent on the expression of Arg-gingipain by *P. gingivalis*. In support of this, a similar multi-species biofilm showed that *P. gingivalis* and *T. denticola* tend to co-colonize gingival epithelial tissue (Thurnheer et al., 2014), whereas in a dual *P. gingivalis* - *T. denticola* biofilm, it was demonstrated that gingipains contributed to their interaction (Zhu et al., 2013). The communities of *T. forsythia* were also



frequently co-localized with those of *P. gingivalis* without impinging onto one another. This pattern was not noticeable when the Lys-gingipain deficient *P. gingivalis* was used, which was also marked by a reduction in *T. forsythia* numbers, suggesting that this gingipain is an important factor for the growth of *T. forsythia* in biofilms. The close association of *T. denticola* and *T. forsythia* with *P. gingivalis* communities in the biofilm suggest a metabolic or quorum-sensing relationship (Hojo et al., 2009) regulated by its gingipains.

**Quantitative proteomics reveal distinct protein regulations caused by *Aggregatibacter actinomycetemcomitans* within subgingival biofilms (Paper 2)**

A quantitative evaluation of bacterial numbers in the biofilm containing *A. actinomycetemcomitans* indicated that this bacterium did not affect the numeric composition of the other 10-biofilm species. However, the protein compositions of both biofilms were altered in the presence or absence of *A. actinomycetemcomitans*. The LC-MS/MS analysis identified a total of 3225 and 3352 proteins from the biofilm lysates in the presence and absence of *A. actinomycetemcomitans*, respectively. A label-free quantification of the identified proteins revealed that 483 of them (excluding those of *A. actinomycetemcomitans*) were regulated in a species-based trend. All quantified proteins of *P. intermedia* were up-regulated in the biofilm when *A. actinomycetemcomitans* was present, while most quantified proteins of *C. rectus*, *S. anginosus*, and *P. gingivalis* were down-regulated. As oral biofilms are polymicrobial and dynamic (Hajishengallis, 2014; Socransky and

Haffajee, 2005), the proteomic profiles of the bacterial species are expressed differently than in their planktonic state (Zijnge et al., 2010). It therefore makes more sense to consider the nature/function of expressed proteins, rather than the number of each bacterial species in a biofilm. GO pathway analysis of the regulated proteins indicated that their function was responsible primarily for control of the metabolic rate, ferric iron binding, and 5S RNA binding capacities.

In the closed environment of the periodontal pocket, subgingival bacteria can utilize alternative iron-acquiring mechanisms to digest the host iron-containing proteins. As such, *A. actinomycetemcomitans* binds to lactoferrin and hemoglobin (Rhodes et al., 2007; Zainal-Abidin et al., 2012), *T. denticola* expresses outer membrane protein HbpA with hemin binding ability (Rhodes et al., 2007; Xu et al., 2001), and *P. gingivalis* employs specific outer membrane receptors, proteases, and lipoproteins for iron (Hajishengallis and Lamont, 2014; Olczak et al., 2005; Xu et al., 2001). The overall changes of ferric iron-binding protein by *A. actinomycetemcomitans* may also affect the overall virulence of the biofilm. The enriched 5S RNA binding may be explained by the increased protein transport and fatty acid biosynthetic processes, also observed in the up-regulated biological process category. In the presence of *A. actinomycetemcomitans* in the biofilm, metabolic processes such as tricarboxylic acid cycle, fructose 1,6-bisphosphate metabolism, carbohydrate metabolism, glycolytic process, and galactose metabolism were also regulated. This may not be surprising, because *A. actinomycetemcomitans* can utilize lactate from streptococci as an energy source (Brown and Whiteley,

2007; Hendrickson et al., 2012; Ramsey et al., 2011), and many glucose transport pathways in this bacterium can also be inhibited as a consequence of using lactate as a carbon source (Brown and Whiteley, 2007; Hendrickson et al., 2012).

### **Establishment and characterization of immortalized gingival epithelial and fibroblast cell lines for the development of organotypic cultures (Paper 3)**

Primary human GEK and GF were induced by E6 and E7 oncoproteins of human papillomavirus, resulting in stable expression levels throughout many passages which confirmed successful immortalization. The primary cells ceased to proliferate in the early stages, while immortalized cell lines expanded for more than 30 passages. The established HGEK-16 cell line had the characteristic ‘cobblestone’ appearance of gingival epithelial cells, while the established GFB-16 cell line exhibited spindle-shape morphology as their primary counterparts. These established immortalized cell lines were used to construct a 3D multilayer organotypic culture in collagen gel and showed a histological structure similar to the gingiva *in vivo*. The qRT-PCR showed that the immortalized cell lines expressed all the cell type specific markers in the primary cell cultures. When cultivated in a 3D conformation, these expression levels were closer to human gingival tissue than to monolayer cultures.

A drawback of utilizing immortalized cell lines in organotypic cultures is that these cells may show carcinoma-like invasion patterns into the underlying connective tissues, particularly in the presence of fibroblast collagen matrix (Costea et al., 2006). The HGEK-16 cell line showed no such invasive trend into the fibroblast/collagen matrix when both cell lines were used to concomitantly construct an organotypic tissue. The abundant expression of CK19, a marker of early stratified epithelial differentiation (Groger et al., 2008), and the low expression of CK10 and CK16, largely expressed in cornifying stratified epithelia (Coulombe and Omary, 2002), suggested that the HGEK-16 mimicks the phenotype of junctional epithelial cells (Mackenzie and Gao, 1993). Hence, these newly generated cell lines have the potential to be useful tools for studying the physiology and pathobiology of gingival tissue *in vitro*.

#### **Establishment of an oral infection model resembling the periodontal pocket in a perfusion bioreactor system (Paper 4)**

The previously established immortalized epithelial and fibroblast cell lines were cultivated along with the Mono Mac 6 cell lines on collagen sponge to construct an organotypic model in a U-tube perfusion bioreactor. The 11-species “subgingival” biofilm generated in Paper 2 was incorporated into this system to challenge the organotypic tissue. Scanning electron microscopy and histology identified an epithelial-like layer on the surface of the collagen sponge, which was further disrupted in co-culture by biofilm over 24 h. Underlying the epithelial layer, GF growth was revealed in the mass of the

collagen sponge, with increasing number of recruited monocytic cells in the presence of the biofilm. By quantifying the bacterial numbers in the biofilm, it was confirmed that *C. rectus*, *A. oris*, *S. anginosus*, *V. dispar*, and *P. gingivalis* were suppressed in co-culture with the organotypic tissue. Multiplex immunoassay analysis revealed that cytokines IL-1 $\beta$ , IL-2, IL-4, and TNF- $\alpha$  level was significantly up-regulated in response to the biofilm, which also indicated a potential antimicrobial effect triggered by the tissue.

Earlier approaches have been applied to create such an epithelial structure *in vitro*. The gingival epithelium is supported by the gingival connective tissue (Schroeder and Listgarten, 1997), which is imperative for the proper reconstruction of organotypic gingiva and epithelial survival and growth (Costea et al., 2006; Locke et al., 2008). Earlier oral/gingival mucosa models combining epithelial and gingival tissue included impermeable collagen gels as scaffolds (Choe et al., 2006; Dongari-Bagtzoglou and Kashleva, 2006; Igarashi et al., 2003; Rouabhia and Deslauriers, 2002; Tomakidi et al., 1997; Tomakidi et al., 1998), which may have impeded the incorporation of immune cells due to lack of a continuous flow. The collagen sponge used in this study creates appropriate spaces for the flow of the monocytic (and potentially other immune) cells, while allowing gingival fibroblast growth and epithelial cell attachment. This property in itself is an advancement on previous models. The 11-species subgingival biofilm used to challenge this organotypic tissue *in vitro* is also superior to models using single bacterial species on epithelial-fibroblast co-cultures (Dabija-Wolter et al., 2012; Paino et al., 2012; Pollanen et al., 2012), or subgingival biofilms on

static co-culture with gingival fibroblasts (Belibasakis et al., 2014), or gingival epithelial cultures (Belibasakis et al., 2013b; Guggenheim et al., 2009; Thurnheer et al., 2014). In addition, the micro-environmental conditions created by the perfusion bioreactor were regulated to mimic the *in vivo* periodontal pocket environment, set at 2% oxygen and exposed to the shear forces of GCF flow rate of 0.4–2.0 ml/min. (Loesche et al., 1983) Survival of both the organotypic tissue and the bacterial biofilm under these conditions prove that they are able to co-exist in an interactive relationship. The reduction in the numbers of some bacterial species denotes the antimicrobial capacity of the tissue, capable of controlling bacterial colonization. The elevated levels of several cytokines in response to the biofilms are also in line with clinical studies showing that patients with periodontitis exhibit higher GCF concentrations of these cytokines (Duarte et al., 2007; Kardesler et al., 2011; Navarro-Sanchez et al., 2007; Shaddox et al., 2011). Hence, this novel model shows compatible histopathological, microbiological, and immunological features to a periodontal pocket *in vivo*.

#### **Proteomic profiling of host-biofilm interactions in an oral infection model resembling the periodontal pocket (Paper 5, in revision)**

The global proteome of the collected supernatant and biofilm samples from Paper 4 was analyzed using LC-MS/MS. A total of 896 and 3363 proteins were found in supernatants and biofilm lysates, respectively. Most of the regulated secreted human proteins were related to processes of cytoskeletal rearrangement, stress responses, apoptosis, and antigen presentation. In terms

of bacterial proteins, most of the regulated secreted proteins were derived from cytoplasmic domain, while the up-regulated intracellular proteins were associated primarily with cytokinesis.

The lower number of host proteins detected in the presence of biofilm supports the notion that biofilm challenge can dampen the host responses to favor microbial survival and establishment in the tissue (Hajishengallis and Lambris, 2011). This is consistent with previous reports studying the secretome or individual cytokines secreted in response to biofilms (Belibasakis et al., 2013b; Bostanci et al., 2015). The content of the secreted supernatant collected from the bioreactor system contains protein similarities to the GCF *in vivo*, particularly with regards to ones associated with immune responses such as annexin A1, calgranulin B, and cathepsin G (Bostanci et al., 2010). The morphological disruption of the epithelial surfaces of this organotypic tissue observed in response to biofilms was backed-up by the proteomic analysis of this study. It revealed that cytoskeletal remodeling, keratinisation, and deregulation of protein unfolding were among the most affected process networks. Disruption of epithelial integrity could also be explained by regulation of lamins, which are components of the inner nuclear member, with a role in nuclear assembly, chromatin organization, and apoptosis (Okinaga et al., 2007). Considering that lamins are mainly found in cytoplasm, their increased presence in the bioreactor supernatant probably originates from lysed epithelial cells, which could also be interpreted as cell death. The epithelium can also mediate the innate immune responses by antigen presentation to T-helper cells (Ohlrich et al., 2009). Indeed, in

response to the biofilms, the MHC class I antigen processing and presentation molecules were also regulated. IL-13 signaling was also one of the most affected process networks, in line with its roles in inflammation such as the induction of MMPs (Van Dyken and Locksley, 2013).

Secreted bacterial proteins from the biofilms may regulate host tissue functions in a manner that is detrimental to the pathogenesis of periodontal disease (Belibasakis and Guggenheim, 2011; Belibasakis et al., 2011a). In the present model, the number of identified secreted bacterial proteins was less than half of the number of human proteins. *F. nucleatum* expressed more than half of these regulated bacterial proteins, and their numbers were enhanced in the presence of the tissue. Because *F. nucleatum* plays an important role in connecting early to late colonizers in the biofilm (Kolenbrander et al., 2006) and can invade oral epithelial (Han et al., 2000) and fibroblastic cells (Dabija-Wolter et al., 2009); it may have a mechanistic advantage in surviving the host challenge, while maintaining a relatively stable bacterial number.

The most commonly up-regulated molecular function category of bacterial proteins in the presence of the organotypic tissue was nucleotide binding, consistent with the most commonly up-regulated biological processes which were translation and protein folding.



## Conclusions and future work

The first part of this thesis revealed that the *in vitro* “subgingival” biofilm model used here was very amenable to changes in bacterial additions or virulence factor expressions. These changes impacted the structure and function of the biofilms. For instance, *P. gingivalis* gingipains affected the numeric levels of *T. forsythia* and the localization of *T. denticola*. The addition of *A. actinomycetemcomitans* to the biofilm did not affect the numeric composition of the other biofilm species but instead altered the abundance of their protein content. Therefore, the present study revealed that the virulence properties of the subgingival biofilm as a whole entity may be regulated by *A. actinomycetemcomitans*.

Immortalized cell lines ensure the maintenance of long-term experimentations by increasing the stability of cell behavior. Two immortalized cell lines were established using primary human gingival epithelial cells and fibroblasts which, when cultured in 3D conformation, developed histological similarities and expressed CKs in levels close to *in vivo* gingival tissue. Therefore, these newly established immortalized cell lines can be a standard cell source for generating 3D static models as well as organotypic tissue models.

The gingival organotypic model developed using these cell lines in a perfusion bioreactor that controls the physical parameters (e.g., shear forces, temperature, O<sub>2</sub> level) resembles the periodontal tissue and the periodontal pocket environment, in particular, when co-cultured with a subgingival biofilm. Because the disruption of the epithelial layer was evident,

accompanied by higher influx of monocytes within the tissue mass and elevated secretion of pro-inflammatory cytokines, it was concluded that this model may mimic the early stages of periodontal infection. Hence, this dynamic model could be used for further applications in the study of the pathogenesis, prevention, and treatment of periodontal diseases, and simultaneously reduce the need for *in vivo* experimental animal models.

Proteomic characterization of this organotypic host-biofilm interaction allowed for simultaneous screening of all events that take place following biofilm challenge and is paramount in understanding the initiation processes of periodontal disease. Clearly, changes such as cytoskeletal rearrangement, enhanced stress responses, apoptosis, and antigen presentation occurred in the organotypic tissue, all denoting and confirming the initial steps of periodontal tissue pathology.

This thesis demonstrated that the generated organotypic model is appropriate for the study of relationships between host and biofilm-associated pathogens. In the future, this model can be technically advanced by incorporating other immune cells of relevance to periodontal infections (e.g., PMNs and lymphocytes). Furthermore, longitudinal and interventional experiments can also be performed to monitor the protein regulations over time and evaluate the efficacy of different treatment modalities on the inhibition of tissue pathology.

## **Acknowledgements**

Firstly, I express my sincere gratitude to PD Dr Nagihan Bostanci, who was the supervisor of my PhD study and related researches, for her patience, motivation, and immense knowledge. Her guidance helped me in all the time of everyday lab work, publications, and writing of this thesis. I could not have imagined having a better advisor and mentor for my PhD study. I would also to express my special appreciation to my co-supervisor, Prof Dr Georgios N Belibasakis, for his enormous experience and knowledge for the oral biology field. Prof George's advices on both research and writing have been priceless.

I would like to thank Prof Dr Leo Eberl, for being my responsible faculty member and for his helps with the administrative part during the entire PhD study.

Besides my supervisors and faculty member, I would like to thank the rest of my thesis committee: Prof Dr Jakob Pernthaler, and Prof Dr Annelies Zinkernagel, for their insightful comments and encouraging advice.

I would also like to thank Dr Thomas Thurnheer and Mrs Christine Lämmli for their help on translate abstract into German, and Dr. Thurnheer's useful suggestions on the biofilm.

Many thanks to our lab technicians, Andy Meier, Elly Plattner, Helga Lüthi-Schaller and Verena Osterwalder for their assistance.

I would also like to thank my friend Dr Andrew Irvine and Enago ([www.enago.com](http://www.enago.com)) for the English language review.

Finally, thanks to my father Bao Wen and my mother Wu Xiaoying, back in China for their supporting and understanding during all these year. I also wish to remember and thank my grandparents and all other relatives.

## References

- Aas JA, Paster BJ, Stokes LN, Olsen I, Dewhirst FE (2005). Defining the normal bacterial flora of the oral cavity. *J Clin Microbiol* 43(11):5721-5732.
- Abe N, Kadowaki T, Okamoto K, Nakayama K, Ohishi M, Yamamoto K (1998). Biochemical and functional properties of lysine-specific cysteine proteinase (Lys-gingipain) as a virulence factor of *Porphyromonas gingivalis* in periodontal disease. *Journal of biochemistry* 123(2):305-312.
- Abe N, Baba A, Takii R, Nakayama K, Kamaguchi A, Shibata Y *et al.* (2004). Roles of Arg- and Lys-gingipains in coaggregation of *Porphyromonas gingivalis*: identification of its responsible molecules in translation products of *rgpA*, *kgp*, and *hagA* genes. *Biological chemistry* 385(11):1041-1047.
- Abe T, Hajishengallis G (2013). Optimization of the ligature-induced periodontitis model in mice. *Journal of immunological methods* 394(1-2):49-54.
- Aduse-Opoku J, Davies NN, Gallagher A, Hashim A, Evans HE, Rangarajan M *et al.* (2000). Generation of lys-gingipain protease activity in *Porphyromonas gingivalis* W50 is independent of Arg-gingipain protease activities. *Microbiology* 146 ( Pt 8)(1933-1940.
- Albandar JM (2011). Underestimation of periodontitis in NHANES surveys. *Journal of periodontology* 82(3):337-341.
- AlShwaimi E, Berggreen E, Furusho H, Rossall JC, Dobeck J, Yoganathan S *et al.* (2013). IL-17 receptor A signaling is protective in infection-stimulated periapical bone destruction. *Journal of immunology* 191(4):1785-1791.
- Amano A, Nakagawa I, Okahashi N, Hamada N (2004). Variations of *Porphyromonas gingivalis* fimbriae in relation to microbial pathogenesis. *Journal of periodontal research* 39(2):136-142.
- Ammann TW, Gmur R, Thurnheer T (2012). Advancement of the 10-species subgingival Zurich Biofilm model by examining different nutritional conditions and defining the structure of the in vitro biofilms. *BMC microbiology* 12(1):227.

Ammann TW, Belibasakis GN, Thurnheer T (2013a). Impact of early colonizers on in vitro subgingival biofilm formation. *PloS one* 8(12):e83090.

Ammann TW, Bostanci N, Belibasakis GN, Thurnheer T (2013b). Validation of a quantitative real-time PCR assay and comparison with fluorescence microscopy and selective agar plate counting for species-specific quantification of an in vitro subgingival biofilm model. *Journal of periodontal research* 48(4):517-526.

Aurer A, Aurer-Kozelj J, Stavljenic-Rukavina A, Kalenic S, Ivic-Kardum M, Haban V (1999). Inflammatory mediators in saliva of patients with rapidly progressive periodontitis during war stress induced incidence increase. *Collegium antropologicum* 23(1):117-124.

Bachtiar EW, Bachtiar BM, Jarosz LM, Amir LR, Sunarto H, Ganin H *et al.* (2014). AI-2 of *Aggregatibacter actinomycetemcomitans* inhibits *Candida albicans* biofilm formation. *Frontiers in cellular and infection microbiology* 4(94).

Baker PJ, Dixon M, Roopenian DC (2000). Genetic control of susceptibility to *Porphyromonas gingivalis*-induced alveolar bone loss in mice. *Infection and immunity* 68(10):5864-5868.

Bao K, Belibasakis GN, Thurnheer T, Aduse-Opoku J, Curtis MA, Bostanci N (2014). Role of *Porphyromonas gingivalis* gingipains in multi-species biofilm formation. *BMC microbiology* 14(1):258.

Bao K, Belibasakis GN, Selevsek N, Grossmann J, Bostanci N (2015a). Proteomic profiling of host-biofilm interactions in an oral infection model resembling the periodontal pocket. *Sci Rep* 5(15999).

Bao K, Papadimitropoulos A, Akgul B, Belibasakis GN, Bostanci N (2015b). Establishment of an oral infection model resembling the periodontal pocket in a perfusion bioreactor system. *Virulence*:0.

Belding LJ, Belding PH (1933). An evaluation of various theories treating on the etiology of periodontoclasia. *Dent Cosmos* 75(140-145).

Belibasakis GN, Johansson A, Wang Y, Chen C, Lagergard T, Kalfas S *et al.* (2005). Cytokine responses of human gingival fibroblasts to *Actinobacillus actinomycetemcomitans* cytolethal distending toxin. *Cytokine* 30(2):56-63.

Belibasakis GN, Guggenheim B (2011). Induction of prostaglandin E(2) and interleukin-6 in gingival fibroblasts by oral biofilms. *FEMS immunology and medical microbiology* 63(3):381-386.

Belibasakis GN, Meier A, Guggenheim B, Bostanci N (2011a). The RANKL-OPG system is differentially regulated by supragingival and subgingival biofilm supernatants. *Cytokine* 55(1):98-103.

Belibasakis GN, Reddi D, Bostanci N (2011b). Porphyromonas gingivalis induces RANKL in T-cells. *Inflammation* 34(2):133-138.

Belibasakis GN, Bostanci N (2012). The RANKL-OPG system in clinical periodontology. *Journal of clinical periodontology* 39(3):239-248.

Belibasakis GN, Johansson A (2012). Aggregatibacter actinomycetemcomitans targets NLRP3 and NLRP6 inflammasome expression in human mononuclear leukocytes. *Cytokine* 59(1):124-130.

Belibasakis GN, Guggenheim B, Bostanci N (2013a). Down-regulation of NLRP3 inflammasome in gingival fibroblasts by subgingival biofilms: involvement of Porphyromonas gingivalis. *Innate immunity* 19(1):3-9.

Belibasakis GN, Thurnheer T, Bostanci N (2013b). Interleukin-8 responses of multi-layer gingival epithelia to subgingival biofilms: role of the "red complex" species. *PloS one* 8(12):e81581.

Belibasakis GN, Bao K, Bostanci N (2014). Transcriptional profiling of human gingival fibroblasts in response to multi-species in vitro subgingival biofilms. *Molecular oral microbiology*.

Belibasakis GN, Bostanci N (2014). Inflammatory and bone remodeling responses to the cytolethal distending toxins. *Cells* 3(2):236-246.

Berezow AB, Darveau RP (2011). Microbial shift and periodontitis. *Periodontology 2000* 55(1):36-47.

Berglundh T, Liljenberg B, Lindhe J (2002). Some cytokine profiles of T-helper cells in lesions of advanced periodontitis. *Journal of clinical periodontology* 29(8):705-709.

Berthod F, Hayek D, Damour O, Collombel C (1993). Collagen synthesis by fibroblasts cultured within a collagen sponge. *Biomaterials* 14(10):749-754.

Bluestone JA, Mackay CR, O'Shea JJ, Stockinger B (2009). The functional plasticity of T cell subsets. *Nature reviews Immunology* 9(11):811-816.

Bonito AJ, Lohr KN, Lux L, Sutton S, Jackman A, Whitener L *et al.* (2004). Effectiveness of antimicrobial adjuncts to scaling and root-planing therapy for periodontitis. *Evidence report/technology assessment* 88):1-4.

Bosshardt DD, Lang NP (2005). The junctional epithelium: from health to disease. *J Dent Res* 84(1):9-20.

Bostanci N, Allaker R, Johansson U, Rangarajan M, Curtis MA, Hughes FJ *et al.* (2007a). Interleukin-1alpha stimulation in monocytes by periodontal bacteria: antagonistic effects of *Porphyromonas gingivalis*. *Oral microbiology and immunology* 22(1):52-60.

Bostanci N, Allaker RP, Belibasakis GN, Rangarajan M, Curtis MA, Hughes FJ *et al.* (2007b). *Porphyromonas gingivalis* antagonises *Campylobacter rectus* induced cytokine production by human monocytes. *Cytokine* 39(2):147-156.

Bostanci N, Reddi D, Rangarajan M, Curtis MA, Belibasakis GN (2009). *Porphyromonas gingivalis* stimulates TACE production by T cells. *Oral microbiology and immunology* 24(2):146-151.

Bostanci N, Heywood W, Mills K, Parkar M, Nibali L, Donos N (2010). Application of label-free absolute quantitative proteomics in human gingival crevicular fluid by LC/MS E (gingival exudatome). *Journal of proteome research* 9(5):2191-2199.

Bostanci N, Akgul B, Tsakanika V, Allaker RP, Hughes FJ, McKay IJ (2011). Effects of low-dose doxycycline on cytokine secretion in human monocytes stimulated with *Aggregatibacter actinomycetemcomitans*. *Cytokine* 56(3):656-661.

Bostanci N, Belibasakis GN (2012). *Porphyromonas gingivalis*: an invasive and evasive opportunistic oral pathogen. *FEMS microbiology letters* 333(1):1-9.



Bostanci N, Ramberg P, Wahlander A, Grossman J, Jonsson D, Barnes VM *et al.* (2012). Label-free quantitative proteomics reveals differentially regulated proteins in experimental gingivitis. *Journal of proteome research*.

Bostanci N, Thurnheer T, Aduse-Opoku J, Curtis MA, Zinkernagel AS, Belibasakis GN (2013). Porphyromonas gingivalis regulates TREM-1 in human polymorphonuclear neutrophils via its gingipains. *PloS one* 8(10):e75784.

Bostanci N, Bao K, Wahlander A, Grossmann J, Thurnheer T, Belibasakis GN (2015). Secretome of gingival epithelium in response to subgingival biofilms. *Molecular oral microbiology*.

Boutaga K, Savelkoul PH, Winkel EG, van Winkelhoff AJ (2007). Comparison of subgingival bacterial sampling with oral lavage for detection and quantification of periodontal pathogens by real-time polymerase chain reaction. *Journal of periodontology* 78(1):79-86.

Bragulla HH, Homberger DG (2009). Structure and functions of keratin proteins in simple, stratified, keratinized and cornified epithelia. *Journal of anatomy* 214(4):516-559.

Bramanti TE, Holt SC (1991). Roles of porphyrins and host iron transport proteins in regulation of growth of Porphyromonas gingivalis W50. *Journal of bacteriology* 173(22):7330-7339.

Bretz WA, Eklund SA, Radicchi R, Schork MA, Schork N, Schottenfeld D *et al.* (1993). The use of a rapid enzymatic assay in the field for the detection of infections associated with adult periodontitis. *Journal of public health dentistry* 53(4):235-240.

Brown LJ, Loe H (1993). Prevalence, extent, severity and progression of periodontal disease. *Periodontology 2000* 2(57-71).

Brown SA, Whiteley M (2007). A novel exclusion mechanism for carbon resource partitioning in Aggregatibacter actinomycetemcomitans. *Journal of bacteriology* 189(17):6407-6414.

Caielli S, Banchereau J, Pascual V (2012). Neutrophils come of age in chronic inflammation. *Current opinion in immunology* 24(6):671-677.

Carterson AJ, Honer zu Bentrup K, Ott CM, Clarke MS, Pierson DL, Vanderburg CR *et al.* (2005). A549 lung epithelial cells grown as three-dimensional aggregates: alternative tissue culture model for *Pseudomonas aeruginosa* pathogenesis. *Infection and immunity* 73(2):1129-1140.

Chai WL, Moharamzadeh K, Brook IM, Emanuelsson L, Palmquist A, van Noort R (2010). Development of a novel model for the investigation of implant-soft tissue interface. *Journal of periodontology* 81(8):1187-1195.

Chakravarti A, Raquil MA, Tessier P, Poubelle PE (2009). Surface RANKL of Toll-like receptor 4-stimulated human neutrophils activates osteoclastic bone resorption. *Blood* 114(8):1633-1644.

Chen Z, Potempa J, Polanowski A, Wikstrom M, Travis J (1992). Purification and characterization of a 50-kDa cysteine proteinase (gingipain) from *Porphyromonas gingivalis*. *The Journal of biological chemistry* 267(26):18896-18901.

Chiang CY, Kyritsis G, Graves DT, Amar S (1999). Interleukin-1 and tumor necrosis factor activities partially account for calvarial bone resorption induced by local injection of lipopolysaccharide. *Infection and immunity* 67(8):4231-4236.

Choe MM, Tomei AA, Swartz MA (2006). Physiological 3D tissue model of the airway wall and mucosa. *Nature protocols* 1(1):357-362.

Coats SR, Jones JW, Do CT, Braham PH, Bainbridge BW, To TT *et al.* (2009). Human Toll-like receptor 4 responses to *P. gingivalis* are regulated by lipid A 1- and 4'-phosphatase activities. *Cellular microbiology* 11(11):1587-1599.

Costea DE, Kulasekara K, Neppelberg E, Johannessen AC, Vintermyr OK (2006). Species-specific fibroblasts required for triggering invasiveness of partially transformed oral keratinocytes. *The American journal of pathology* 168(6):1889-1897.

Coulombe PA, Omary MB (2002). 'Hard' and 'soft' principles defining the structure, function and regulation of keratin intermediate filaments. *Current opinion in cell biology* 14(1):110-122.

Curtis MA, Aduse-Opoku J, Rangarajan M (2001). Cysteine proteases of *Porphyromonas gingivalis*. *Critical reviews in oral biology and medicine* :

*an official publication of the American Association of Oral Biologists*  
12(3):192-216.

Dabija-Wolter G, Cimpan MR, Costea DE, Johannessen AC, Sornes S, Neppelberg E *et al.* (2009). *Fusobacterium nucleatum* enters normal human oral fibroblasts in vitro. *Journal of periodontology* 80(7):1174-1183.

Dabija-Wolter G, Sapkota D, Cimpan MR, Neppelberg E, Bakken V, Costea DE (2012). Limited in-depth invasion of *Fusobacterium nucleatum* into in vitro reconstructed human gingiva. *Archives of oral biology* 57(4):344-351.

Daep CA, Novak EA, Lamont RJ, Demuth DR (2011). Structural dissection and in vivo effectiveness of a peptide inhibitor of *Porphyromonas gingivalis* adherence to *Streptococcus gordonii*. *Infection and immunity* 79(1):67-74.

Darveau RP (2010). Periodontitis: a polymicrobial disruption of host homeostasis. *Nature reviews Microbiology* 8(7):481-490.

Dentino A, Lee S, Mailhot J, Hefti AF (2013). Principles of periodontology. *Periodontology 2000* 61(1):16-53.

Dewhirst FE, Chen T, Izard J, Paster BJ, Tanner AC, Yu WH *et al.* (2010). The human oral microbiome. *Journal of bacteriology* 192(19):5002-5017.

Diaz PI, Xie Z, Sobue T, Thompson A, Biyikoglu B, Ricker A *et al.* (2012). Synergistic interaction between *Candida albicans* and commensal oral streptococci in a novel in vitro mucosal model. *Infection and immunity* 80(2):620-632.

Dimri G, Band H, Band V (2005). Mammary epithelial cell transformation: insights from cell culture and mouse models. *Breast cancer research : BCR* 7(4):171-179.

Dongari-Bagtzoglou A, Kashleva H (2006). Development of a highly reproducible three-dimensional organotypic model of the oral mucosa. *Nature protocols* 1(4):2012-2018.

Duarte PM, de Oliveira MC, Tambeli CH, Parada CA, Casati MZ, Nociti FH, Jr. (2007). Overexpression of interleukin-1beta and interleukin-6 may

play an important role in periodontal breakdown in type 2 diabetic patients. *Journal of periodontal research* 42(4):377-381.

Ebersole JL (2003). Humoral immune responses in gingival crevice fluid: local and systemic implications. *Periodontology* 2000 31(135-166.

Fokkema SJ, Loos BG, van der Velden U (2003). Monocyte-derived RANTES is intrinsically elevated in periodontal disease while MCP-1 levels are related to inflammation and are inversely correlated with IL-12 levels. *Clinical and experimental immunology* 131(3):477-483.

Fong KP, Chung WO, Lamont RJ, Demuth DR (2001). Intra- and interspecies regulation of gene expression by *Actinobacillus actinomycetemcomitans* LuxS. *Infection and immunity* 69(12):7625-7634.

Forshaw RJ (2009). Dental health and disease in ancient Egypt. *British dental journal* 206(8):421-424.

Frias J, Olle E, Alsina M (2001). Periodontal pathogens produce quorum sensing signal molecules. *Infection and immunity* 69(5):3431-3434.

Gaffen SL, Hajishengallis G (2008). A new inflammatory cytokine on the block: re-thinking periodontal disease and the Th1/Th2 paradigm in the context of Th17 cells and IL-17. *J Dent Res* 87(9):817-828.

Gao JL, Nguyen KA, Hunter N (2010). Characterization of a hemophore-like protein from *Porphyromonas gingivalis*. *The Journal of biological chemistry* 285(51):40028-40038.

Giannopoulou C, Kamma JJ, Mombelli A (2003). Effect of inflammation, smoking and stress on gingival crevicular fluid cytokine level. *Journal of clinical periodontology* 30(2):145-153.

Graves DT, Nooh N, Gillen T, Davey M, Patel S, Cottrell D *et al.* (2001). IL-1 plays a critical role in oral, but not dermal, wound healing. *Journal of immunology* 167(9):5316-5320.

Graves DT, Fine D, Teng YT, Van Dyke TE, Hajishengallis G (2008). The use of rodent models to investigate host-bacteria interactions related to periodontal diseases. *Journal of clinical periodontology* 35(2):89-105.

Grenier D (1992). Nutritional interactions between two suspected periodontopathogens, *Treponema denticola* and *Porphyromonas gingivalis*. *Infection and immunity* 60(12):5298-5301.

Grenier D, Roy S, Chandad F, Plamondon P, Yoshioka M, Nakayama K *et al.* (2003). Effect of inactivation of the Arg- and/or Lys-gingipain gene on selected virulence and physiological properties of *Porphyromonas gingivalis*. *Infection and immunity* 71(8):4742-4748.

Groger S, Michel J, Meyle J (2008). Establishment and characterization of immortalized human gingival keratinocyte cell lines. *Journal of periodontal research* 43(6):604-614.

Guggenheim B, Gander M, Koller MM (2004). A comprehensive system for washing, pre-disinfecting and sterilizing of dental and surgical instruments. *Oral health & preventive dentistry* 2(4):335-344.

Guggenheim B, Gmur R, Galicia JC, Stathopoulou PG, Benakanakere MR, Meier A *et al.* (2009). In vitro modeling of host-parasite interactions: the 'subgingival' biofilm challenge of primary human epithelial cells. *BMC microbiology* 9(280).

Gursoy UK, Kononen E, Uitto VJ, Pussinen PJ, Hyvarinen K, Suominen-Taipale L *et al.* (2009). Salivary interleukin-1 $\beta$  concentration and the presence of multiple pathogens in periodontitis. *Journal of clinical periodontology* 36(11):922-927.

Hajishengallis G, Lambris JD (2011). Microbial manipulation of receptor crosstalk in innate immunity. *Nature reviews Immunology* 11(3):187-200.

Hajishengallis G, Liang S, Payne MA, Hashim A, Jotwani R, Eskandari MA *et al.* (2011). Low-abundance biofilm species orchestrates inflammatory periodontal disease through the commensal microbiota and complement. *Cell host & microbe* 10(5):497-506.

Hajishengallis G, Lamont RJ (2012). Beyond the red complex and into more complexity: the polymicrobial synergy and dysbiosis (PSD) model of periodontal disease etiology. *Molecular oral microbiology* 27(6):409-419.

Hajishengallis G (2014). Immunomicrobial pathogenesis of periodontitis: keystones, pathobionts, and host response. *Trends in immunology* 35(1):3-11.

Hajishengallis G, Lamont RJ (2014). Breaking bad: manipulation of the host response by *Porphyromonas gingivalis*. *European journal of immunology* 44(2):328-338.

Hajishengallis G, Lamont RJ, Graves DT (2015a). The enduring importance of animal models in understanding periodontal disease. *Virulence* 6(3):229-235.

Hajishengallis G, Lamont RJ, Graves DT (2015b). The enduring importance of animal models in understanding periodontal disease. *Virulence*:0.

Hamed M, Belibasakis GN, Cruchley AT, Rangarajan M, Curtis MA, Bostanci N (2009). *Porphyromonas gingivalis* culture supernatants differentially regulate interleukin-1 $\beta$  and interleukin-18 in human monocytic cells. *Cytokine* 45(2):99-104.

Han X, Kawai T, Taubman MA (2007). Interference with immune-cell-mediated bone resorption in periodontal disease. *Periodontology 2000* 45(76-94).

Han YW, Shi W, Huang GT, Kinder Haake S, Park NH, Kuramitsu H *et al.* (2000). Interactions between periodontal bacteria and human oral epithelial cells: *Fusobacterium nucleatum* adheres to and invades epithelial cells. *Infection and immunity* 68(6):3140-3146.

Handfield M, Mans JJ, Zheng G, Lopez MC, Mao S, Progulske-Fox A *et al.* (2005). Distinct transcriptional profiles characterize oral epithelium-microbiota interactions. *Cellular microbiology* 7(6):811-823.

Hasegawa Y, Tribble GD, Baker HV, Mans JJ, Handfield M, Lamont RJ (2008). Role of *Porphyromonas gingivalis* SerB in gingival epithelial cell cytoskeletal remodeling and cytokine production. *Infection and immunity* 76(6):2420-2427.

Haubek D, Ennibi OK, Poulsen K, Vaeth M, Poulsen S, Kilian M (2008). Risk of aggressive periodontitis in adolescent carriers of the JP2 clone of *Aggregatibacter (Actinobacillus) actinomycetemcomitans* in Morocco: a prospective longitudinal cohort study. *Lancet* 371(9608):237-242.

Hayashida H, Poulsen K, Kilian M (2002). Differences in iron acquisition from human haemoglobin among strains of *Actinobacillus actinomycetemcomitans*. *Microbiology* 148(Pt 12):3993-4001.

Hebert AS, Richards AL, Bailey DJ, Ulbrich A, Coughlin EE, Westphall MS *et al.* (2014). The one hour yeast proteome. *Molecular & cellular proteomics : MCP* 13(1):339-347.

Henderson B, Ward JM, Ready D (2010). *Aggregatibacter* (*Actinobacillus*) *actinomycetemcomitans*: a triple A\* periodontopathogen? *Periodontology* 2000 54(1):78-105.

Hendrickson EL, Wang T, Dickinson BC, Whitmore SE, Wright CJ, Lamont RJ *et al.* (2012). Proteomics of *Streptococcus gordonii* within a model developing oral microbial community. *BMC microbiology* 12(211).

Hendrickson EL, Wang T, Beck DA, Dickinson BC, Wright CJ, R JL *et al.* (2014). Proteomics of *Fusobacterium nucleatum* within a model developing oral microbial community. *MicrobiologyOpen* 3(5):729-751.

Hojo K, Nagaoka S, Ohshima T, Maeda N (2009). Bacterial interactions in dental biofilm development. *J Dent Res* 88(11):982-990.

Holt SC, Ebersole J, Felton J, Brunsvold M, Kornman KS (1988). Implantation of *Bacteroides gingivalis* in nonhuman primates initiates progression of periodontitis. *Science* 239(4835):55-57.

Holtfreter B, Alte D, Schwahn C, Desvarieux M, Kocher T (2012). Effects of different manual periodontal probes on periodontal measurements. *Journal of clinical periodontology* 39(11):1032-1041.

Hsieh PC, Jin YT, Chang CW, Huang CC, Liao SC, Yuan K (2010). Elastin in oral connective tissue modulates the keratinization of overlying epithelium. *Journal of clinical periodontology* 37(8):705-711.

Igarashi M, Irwin CR, Locke M, Mackenzie IC (2003). Construction of large area organotypical cultures of oral mucosa and skin. *J Oral Pathol Med* 0904-2512 (Print)).

Illeperuma RP, Park YJ, Kim JM, Bae JY, Che ZM, Son HK *et al.* (2012). Immortalized gingival fibroblasts as a cytotoxicity test model for dental materials. *Journal of materials science Materials in medicine* 23(3):753-762.

Ito R, Ishihara K, Shoji M, Nakayama K, Okuda K (2010). Hemagglutinin/Adhesin domains of Porphyromonas gingivalis play key roles in coaggregation with Treponema denticola. *FEMS immunology and medical microbiology* 60(3):251-260.

Jenkinson HF, Lamont RJ (2005). Oral microbial communities in sickness and in health. *Trends in microbiology* 13(12):589-595.

Jenkinson HF (2011). Beyond the oral microbiome. *Environmental microbiology* 13(12):3077-3087.

Kamaguchi A, Nakayama K, Ohshima T, Watanabe T, Okamoto M, Baba H (2001). Coaggregation of Porphyromonas gingivalis and Prevotella intermedia. *Microbiology and immunology* 45(9):649-656.

Karched M, Bhardwaj RG, Asikainen SE (2015a). Coaggregation and biofilm growth of Granulicatella spp. with Fusobacterium nucleatum and Aggregatibacter actinomycetemcomitans. *BMC microbiology* 15(114).

Karched M, Bhardwaj RG, Inbamani A, Asikainen S (2015b). Quantitation of biofilm and planktonic life forms of coexisting periodontal species. *Anaerobe*.

Kardesler L, Buduneli N, Cetinkalp S, Lappin D, Kinane DF (2011). Gingival crevicular fluid IL-6, tPA, PAI-2, albumin levels following initial periodontal treatment in chronic periodontitis patients with or without type 2 diabetes. *Inflammation research : official journal of the European Histamine Research Society [et al]* 60(2):143-151.

Karring T, Lang NP, Loe H (1975). The role of gingival connective tissue in determining epithelial differentiation. *Journal of periodontal research* 10(1):1-11.

Kebschull M, Demmer RT, Papapanou PN (2010). "Gum bug, leave my heart alone!"--epidemiologic and mechanistic evidence linking periodontal infections and atherosclerosis. *J Dent Res* 89(9):879-902.

Kinane DF, Berglundh T, Lindhe J (2008). Pathogenesis of periodontitis. In: Clinical Periodontology and Implant Dentistry, 5th edition. J Lindhe, NP Lang and T Karring editors: Oxford: Blackwell.



Klinger R (1912). Untersuchungen über menschliche Aktinomykose. *Zentralbl Bakteriol* 62(191–200).

Kobayashi K, Rose GG, Mahan CJ (1976). Ultrastructure of the dento-epithelial junction. *Journal of periodontal research* 11(6):313-330.

Kolenbrander PE, Palmer RJ, Jr., Rickard AH, Jakubovics NS, Chalmers NI, Diaz PI (2006). Bacterial interactions and successions during plaque development. *Periodontology 2000* 42(47-79).

Kumar PS, Griffen AL, Barton JA, Paster BJ, Moeschberger ML, Leys EJ (2003). New bacterial species associated with chronic periodontitis. *J Dent Res* 82(5):338-344.

Kuramitsu HK, He X, Lux R, Anderson MH, Shi W (2007). Interspecies interactions within oral microbial communities. *Microbiology and molecular biology reviews : MMBR* 71(4):653-670.

Lamont RJ, Hajishengallis G (2015). Polymicrobial synergy and dysbiosis in inflammatory disease. *Trends in molecular medicine* 21(3):172-183.

Lekic PC, Pender N, McCulloch CAG (1997). Is Fibroblast Heterogeneity Relevant To the Health, Diseases, and Treatments of Periodontal Tissues? *Critical Reviews in Oral Biology & Medicine* 8(3):253-268.

Lepine G, Caudry S, DiRienzo JM, Ellen RP (1998). Epithelial cell invasion by *Actinobacillus actinomycetemcomitans* strains from restriction fragment-length polymorphism groups associated with juvenile periodontitis or carrier status. *Oral microbiology and immunology* 13(6):341-347.

Lin X, Lamont RJ, Wu J, Xie H (2008). Role of differential expression of streptococcal arginine deiminase in inhibition of fimA expression in *Porphyromonas gingivalis*. *Journal of bacteriology* 190(12):4367-4371.

Lindhe J, Nyman S (1975). The effect of plaque control and surgical pocket elimination on the establishment and maintenance of periodontal health. A longitudinal study of periodontal therapy in cases of advanced disease. *Journal of clinical periodontology* 2(2):67-79.

Locke M, Hyland PL, Irwin CR, Mackenzie IC (2008). Modulation of gingival epithelial phenotypes by interactions with regionally defined populations of fibroblasts. *Journal of periodontal research* 43(3):279-289.

Loesche WJ, Gusberti F, Mettraux G, Higgins T, Syed S (1983). Relationship between oxygen tension and subgingival bacterial flora in untreated human periodontal pockets. *Infection and immunity* 42(2):659-667.

Loesche WJ (1992). The specific plaque hypothesis and the antimicrobial treatment of periodontal disease. *Dental update* 19(2):68, 70-62, 74.

Lovegrove JM (2004). Dental plaque revisited: bacteria associated with periodontal disease. *Journal of the New Zealand Society of Periodontology* 87):7-21.

Lundberg KC, Fritz Y, Johnston A, Foster AM, Baliwag J, Gudjonsson JE *et al.* (2014). Proteomics of skin proteins in psoriasis: discovery and verification in a mouse model to confirmation in humans. *Molecular & cellular proteomics : MCP*.

Mackenzie IC, Gao Z (1993). Patterns of cytokeratin expression in the epithelia of inflamed human gingiva and periodontal pockets. *Journal of periodontal research* 28(1):49-59.

Madianos PN, Bobetsis YA, Kinane DF (2005). Generation of inflammatory stimuli: how bacteria set up inflammatory responses in the gingiva. *Journal of clinical periodontology* 32 Suppl 6(57-71).

Maeda K, Nagata H, Ojima M, Amano A (2015). Proteomic and Transcriptional Analysis of Interaction between Oral Microbiota Porphyromonas gingivalis and Streptococcus oralis. *Journal of proteome research* 14(1):82-94.

Maekawa T, Krauss JL, Abe T, Jotwani R, Triantafilou M, Triantafilou K *et al.* (2014). Porphyromonas gingivalis manipulates complement and TLR signaling to uncouple bacterial clearance from inflammation and promote dysbiosis. *Cell host & microbe* 15(6):768-778.

Mariotti A (1999). Dental plaque-induced gingival diseases. *Annals of periodontology / the American Academy of Periodontology* 4(1):7-19.

Marsh PD (2006). Dental diseases--are these examples of ecological catastrophes? *International journal of dental hygiene* 4 Suppl 1(3-10; discussion 50-12.

Mattner J, Debord KL, Ismail N, Goff RD, Cantu C, 3rd, Zhou D *et al.* (2005). Exogenous and endogenous glycolipid antigens activate NKT cells during microbial infections. *Nature* 434(7032):525-529.

McCoy RJ, O'Brien FJ (2010). Influence of shear stress in perfusion bioreactor cultures for the development of three-dimensional bone tissue constructs: a review. *Tissue engineering Part B, Reviews* 16(6):587-601.

McMahon KT, Wasfy MO, Yonushonis WP, Minah GE, Falkler WA, Jr. (1990). Comparative microbiological and immunological studies of subgingival dental plaque from man and baboons. *J Dent Res* 69(1):55-59.

Miller CS, King CP, Jr., Langub MC, Kryscio RJ, Thomas MV (2006). Salivary biomarkers of existing periodontal disease: a cross-sectional study. *Journal of the American Dental Association* 137(3):322-329.

Miller MB, Bassler BL (2001). Quorum sensing in bacteria. *Annual review of microbiology* 55(165-199).

Milner P, Batten JE, Curtis MA (1996). Development of a simple chemically defined medium for *Porphyromonas gingivalis*: requirement for alpha-ketoglutarate. *FEMS microbiology letters* 140(2-3):125-130.

Moharamzadeh K, Brook IM, Van Noort R, Scutt AM, Thornhill MH (2007). Tissue-engineered Oral Mucosa: a Review of the Scientific Literature. *Journal of Dental Research* 86(2):115-124.

Morimoto Y, Morimoto H, Murata T, Kobayashi S, Ohba T, Haneji T (1999). Extracts of *Actinobacillus actinomycetemcomitans* induce apoptotic cell death in human osteoblastic MG63 cells. *J Dent Res* 78(3):735-742.

Mussig E, Tomakidi P, Steinberg T (2009). Gingival fibroblasts established on microstructured model surfaces: their influence on epithelial morphogenesis and other tissue-specific cell functions in a co-cultured epithelium: an in-vitro model. *Journal of orofacial orthopedics = Fortschritte der Kieferorthopädie : Organ/official journal Deutsche Gesellschaft für Kieferorthopädie* 70(5):351-362.

Nakhjiri SF, Park Y, Yilmaz O, Chung WO, Watanabe K, El-Sabaeny A *et al.* (2001). Inhibition of epithelial cell apoptosis by *Porphyromonas gingivalis*. *FEMS microbiology letters* 200(2):145-149.

Nanci A, Bosshardt DD (2006). Structure of periodontal tissues in health and disease. *Periodontology 2000* 40(11-28).

Navarro-Sanchez AB, Faria-Almeida R, Bascones-Martinez A (2007). Effect of non-surgical periodontal therapy on clinical and immunological response and glycaemic control in type 2 diabetic patients with moderate periodontitis. *Journal of clinical periodontology* 34(10):835-843.

Nishida E, Hara Y, Kaneko T, Ikeda Y, Ukai T, Kato I (2001). Bone resorption and local interleukin-1alpha and interleukin-1beta synthesis induced by *Actinobacillus actinomycetemcomitans* and *Porphyromonas gingivalis* lipopolysaccharide. *Journal of periodontal research* 36(1):1-8.

Nussbaum G, Shapira L (2011). How has neutrophil research improved our understanding of periodontal pathogenesis? *Journal of clinical periodontology* 38 Suppl 11(49-59).

Oda D, Bigler L, Lee P, Blanton R (1996). HPV immortalization of human oral epithelial cells: a model for carcinogenesis. *Experimental cell research* 226(1):164-169.

Ohlrich EJ, Cullinan MP, Seymour GJ (2009). The immunopathogenesis of periodontal disease. *Australian dental journal* 54 Suppl 1(S2-10).

Okinaga T, Kasai H, Tsujisawa T, Nishihara T (2007). Role of caspases in cleavage of lamin A/C and PARP during apoptosis in macrophages infected with a periodontopathic bacterium. *J Med Microbiol* 56(Pt 10):1399-1404.

Olczak T, Simpson W, Liu X, Genco CA (2005). Iron and heme utilization in *Porphyromonas gingivalis*. *FEMS microbiology reviews* 29(1):119-144.

Ong G (1998). Periodontal disease and tooth loss. *International dental journal* 48(3 Suppl 1):233-238.

Orth RK, O'Brien-Simpson NM, Dashper SG, Reynolds EC (2011). Synergistic virulence of *Porphyromonas gingivalis* and *Treponema denticola* in a murine periodontitis model. *Molecular oral microbiology* 26(4):229-240.

Page RC, Schroeder HE (1976). Pathogenesis of inflammatory periodontal disease. A summary of current work. *Laboratory investigation; a journal of technical methods and pathology* 34(3):235-249.

Page RC, Kornman KS (1997). The pathogenesis of human periodontitis: an introduction. *Periodontology 2000* 14(9-11).

Paino A, Lohermaa E, Sormunen R, Tuominen H, Korhonen J, Pollanen MT *et al.* (2012). Interleukin-1beta is internalised by viable *Aggregatibacter actinomycetemcomitans* biofilm and locates to the outer edges of nucleoids. *Cytokine* 60(2):565-574.

Papadimitropoulos A, Riboldi SA, Tonnarelli B, Piccinini E, Woodruff MA, Hutmacher DW *et al.* (2013). A collagen network phase improves cell seeding of open-pore structure scaffolds under perfusion. *Journal of tissue engineering and regenerative medicine* 7(3):183-191.

Papapanou PN, Neiderud AM, Sandros J, Dahlen G (2001). Checkerboard assessments of serum antibodies to oral microbiota as surrogate markers of clinical periodontal status. *Journal of clinical periodontology* 28(1):103-106.

Paster BJ, Boches SK, Galvin JL, Ericson RE, Lau CN, Levanos VA *et al.* (2001). Bacterial diversity in human subgingival plaque. *Journal of bacteriology* 183(12):3770-3783.

Periasamy S, Kolenbrander PE (2009a). *Aggregatibacter actinomycetemcomitans* builds mutualistic biofilm communities with *Fusobacterium nucleatum* and *Veillonella* species in saliva. *Infection and immunity* 77(9):3542-3551.

Periasamy S, Kolenbrander PE (2009b). Mutualistic biofilm communities develop with *Porphyromonas gingivalis* and initial, early, and late colonizers of enamel. *Journal of bacteriology* 191(22):6804-6811.

Pi SH, Lee SK, Hwang YS, Choi MG, Lee SK, Kim EC (2007). Differential expression of periodontal ligament-specific markers and osteogenic differentiation in human papilloma virus 16-immortalized human gingival fibroblasts and periodontal ligament cells. *Journal of periodontal research* 42(2):104-113.

Pierce DL, Nishiyama S, Liang S, Wang M, Triantafilou M, Triantafilou K *et al.* (2009). Host adhesive activities and virulence of novel fimbrial proteins of *Porphyromonas gingivalis*. *Infection and immunity* 77(8):3294-3301.

Pihlstrom BL, Michalowicz BS, Johnson NW (2005). Periodontal diseases. *Lancet* 366(9499):1809-1820.

Pollanen MT, Gursoy UK, Kononen E, Uitto VJ (2012). *Fusobacterium nucleatum* biofilm induces epithelial migration in an organotypic model of dento-gingival junction. *Journal of periodontology* 83(10):1329-1335.

Potempa J, Pike R, Travis J (1997). Titration and mapping of the active site of cysteine proteinases from *Porphyromonas gingivalis* (gingipains) using peptidyl chloromethanes. *Biological chemistry* 378(3-4):223-230.

Potts TV, Zambon JJ, Genco RJ (1985). Reassignment of *Actinobacillus actinomycetemcomitans* to the genus *Haemophilus* as *Haemophilus actinomycetemcomitans* comb. nov. . *International journal of systematic bacteriology* 35(3):337-341.

Ramsey MM, Rumbaugh KP, Whiteley M (2011). Metabolite cross-feeding enhances virulence in a model polymicrobial infection. *PLoS pathogens* 7(3):e1002012.

Rangarajan M, Smith SJ, U S, Curtis MA (1997). Biochemical characterization of the arginine-specific proteases of *Porphyromonas gingivalis* W50 suggests a common precursor. *The Biochemical journal* 323 ( Pt 3):701-709.

Rhodes ER, Menke S, Shoemaker C, Tomaras AP, McGillivray G, Actis LA (2007). Iron acquisition in the dental pathogen *Actinobacillus actinomycetemcomitans*: what does it use as a source and how does it get this essential metal? *Biometals : an international journal on the role of metal ions in biology, biochemistry, and medicine* 20(3-4):365-377.

Rickard AH, Palmer RJ, Jr., Blehert DS, Campagna SR, Semmelhack MF, Eglund PG *et al.* (2006). Autoinducer 2: a concentration-dependent signal for mutualistic bacterial biofilm growth. *Molecular microbiology* 60(6):1446-1456.

Rosan B, Lamont RJ (2000). Dental plaque formation. *Microbes and infection / Institut Pasteur* 2(13):1599-1607.

Rouabhia M, Deslauriers N (2002). Production and characterization of an in vitro engineered human oral mucosa. *Biochemistry and Cell Biology* 80(2):189-195.

Ryder MI (2010). Comparison of neutrophil functions in aggressive and chronic periodontitis. *Periodontology 2000* 53(124-137).

Sabroe I, Jones EC, Usher LR, Whyte MK, Dower SK (2002). Toll-like receptor (TLR)2 and TLR4 in human peripheral blood granulocytes: a critical role for monocytes in leukocyte lipopolysaccharide responses. *Journal of immunology* 168(9):4701-4710.

Sacks PG (1996). Cell, tissue and organ culture as in vitro models to study the biology of squamous cell carcinomas of the head and neck. *Cancer metastasis reviews* 15(1):27-51.

Sandros J, Papapanou PN, Nannmark U, Dahlen G (1994). Porphyromonas gingivalis invades human pocket epithelium in vitro. *Journal of periodontal research* 29(1):62-69.

Sbordone L, Bortolaia C (2003). Oral microbial biofilms and plaque-related diseases: microbial communities and their role in the shift from oral health to disease. *Clinical oral investigations* 7(4):181-188.

Schaller M, Zakikhany K, Naglik JR, Weindl G, Hube B (2006). Models of oral and vaginal candidiasis based on in vitro reconstituted human epithelia. *Nature protocols* 1(6):2767-2773.

Schauder S, Shokat K, Surette MG, Bassler BL (2001). The LuxS family of bacterial autoinducers: biosynthesis of a novel quorum-sensing signal molecule. *Molecular microbiology* 41(2):463-476.

Schroeder HE (1970). Quantitative parameters of early human gingival inflammation. *Archives of oral biology* 15(5):383-400.

Schroeder HE, Munzel-Pedrazzoli S (1970). Morphometric analysis comparing junctional and oral epithelium of normal human gingiva. *Helvetica odontologica acta* 14(2):53-66.

Schroeder HE (1973). Transmigration and infiltration of leucocytes in human junctional epithelium. *Helvetica odontologica acta* 17(1):6-18.

Schroeder HE, Listgarten MA (1997). The gingival tissues: the architecture of periodontal protection. *Periodontology 2000* 13(91-120).

Schultz-Haudt S, Bruce MA, Bibby BG (1954). Bacterial factors in nonspecific gingivitis. *J Dent Res* 33(4):454-458.

Seguier S, Godeau G, Brousse N (2000). Immunohistological and morphometric analysis of intra-epithelial lymphocytes and Langerhans cells in healthy and diseased human gingival tissues. *Archives of oral biology* 45(6):441-452.

Settem RP, El-Hassan AT, Honma K, Stafford GP, Sharma A (2012). *Fusobacterium nucleatum* and *Tannerella forsythia* induce synergistic alveolar bone loss in a mouse periodontitis model. *Infection and immunity* 80(7):2436-2443.

Shaddox LM, Wiedey J, Calderon NL, Magnusson I, Bimstein E, Bidwell JA *et al.* (2011). Local inflammatory markers and systemic endotoxin in aggressive periodontitis. *J Dent Res* 90(9):1140-1144.

Shao H, James D, Lamont RJ, Demuth DR (2007). Differential interaction of *Aggregatibacter* (*Actinobacillus*) *actinomycetemcomitans* LsrB and RbsB proteins with autoinducer 2. *Journal of bacteriology* 189(15):5559-5565.

Shao H, Demuth DR (2010). Quorum sensing regulation of biofilm growth and gene expression by oral bacteria and periodontal pathogens. *Periodontology 2000* 52(1):53-67.

Sharma A, Inagaki S, Sigurdson W, Kuramitsu HK (2005). Synergy between *Tannerella forsythia* and *Fusobacterium nucleatum* in biofilm formation. *Oral microbiology and immunology* 20(1):39-42.

Shen Y, Zhang Y, Zou J, Meng J, Wang J (2014). Comparative proteomic study on Brassica hexaploid and its parents provides new insights into the effects of polyploidization. *Journal of proteomics* 112C(274-284).

Sims TJ, Schifferle RE, Ali RW, Skaug N, Page RC (2001). Immunoglobulin G response of periodontitis patients to *Porphyromonas gingivalis* capsular carbohydrate and lipopolysaccharide antigens. *Oral microbiology and immunology* 16(4):193-201.

Singh A, Wyant T, Anaya-Bergman C, Aduse-Opoku J, Brunner J, Laine ML *et al.* (2011). The capsule of *Porphyromonas gingivalis* leads to a reduction in the host inflammatory response, evasion of phagocytosis, and increase in virulence. *Infection and immunity* 79(11):4533-4542.



Slakeski N, Bhogal PS, O'Brien-Simpson NM, Reynolds EC (1998). Characterization of a second cell-associated Arg-specific cysteine proteinase of *Porphyromonas gingivalis* and identification of an adhesin-binding motif involved in association of the prtR and prtK proteinases and adhesins into large complexes. *Microbiology* 144 ( Pt 6)(1583-1592.

Socransky SS (1977). Microbiology of periodontal disease -- present status and future considerations. *Journal of periodontology* 48(9):497-504.

Socransky SS, Haffajee AD, Cugini MA, Smith C, Kent RL, Jr. (1998). Microbial complexes in subgingival plaque. *Journal of clinical periodontology* 25(2):134-144.

Socransky SS, Haffajee AD (2005). Periodontal microbial ecology. *Periodontology 2000* 38(135-187.

Sroka A, Sztukowska M, Potempa J, Travis J, Genco CA (2001). Degradation of host heme proteins by lysine- and arginine-specific cysteine proteinases (gingipains) of *Porphyromonas gingivalis*. *Journal of bacteriology* 183(19):5609-5616.

Steinman L (2007). A brief history of T(H)17, the first major revision in the T(H)1/T(H)2 hypothesis of T cell-mediated tissue damage. *Nature medicine* 13(2):139-145.

Syed SA, Loesche WJ (1978). Bacteriology of human experimental gingivitis: effect of plaque age. *Infection and immunity* 21(3):821-829.

Takasaki K, Fujise O, Miura M, Hamachi T, Maeda K (2013). *Porphyromonas gingivalis* displays a competitive advantage over *Aggregatibacter actinomycetemcomitans* in co-cultured biofilm. *Journal of periodontal research* 48(3):286-292.

Takayama A, Satoh A, Ngai T, Nishimura T, Ikawa K, Matsuyama T *et al.* (2003). Augmentation of *Actinobacillus actinomycetemcomitans* invasion of human oral epithelial cells and up-regulation of interleukin-8 production by saliva CD14. *Infection and immunity* 71(10):5598-5604.

Teles R, Teles F, Frias-Lopez J, Paster B, Haffajee A (2013). Lessons learned and unlearned in periodontal microbiology. *Periodontology 2000* 62(1):95-162.

Thompson C, Powrie F (2004). Regulatory T cells. *Current opinion in pharmacology* 4(4):408-414.

Thurnheer T, Gmur R, Giertsen E, Guggenheim B (2001). Automated fluorescent in situ hybridization for the specific detection and quantification of oral streptococci in dental plaque. *Journal of microbiological methods* 44(1):39-47.

Thurnheer T, Belibasakis GN, Bostanci N (2014). Colonisation of gingival epithelia by subgingival biofilms in vitro: Role of "red complex" bacteria. *Archives of oral biology* 59(9):977-986.

Timmins NE, Scherberich A, Fruh JA, Heberer M, Martin I, Jakob M (2007). Three-dimensional cell culture and tissue engineering in a T-CUP (tissue culture under perfusion). *Tissue engineering* 13(8):2021-2028.

Tomakidi P, Fusenig NE, Kohl A, Komposch G (1997). Histomorphological and biochemical differentiation capacity in organotypic co-cultures of primary gingival cells. *Journal of periodontal research* 32(4):388-400.

Tomakidi P, Breitzkreutz D, Fusenig NE, Zoller J, Kohl A, Komposch G (1998). Establishment of oral mucosa phenotype in vitro in correlation to epithelial anchorage. *Cell and tissue research* 292(2):355-366.

Tonetti M, Palmer R, Working Group 2 of the VEWoP (2012). Clinical research in implant dentistry: study design, reporting and outcome measurements: consensus report of Working Group 2 of the VIII European Workshop on Periodontology. *Journal of clinical periodontology* 39 Suppl 12(73-80).

Topley WWC, Wilson GS (1929). The Principles of Bacteriology and Immunity. *London: Edward Arnold*:1-587.

Tribble GD, Mao S, James CE, Lamont RJ (2006). A Porphyromonas gingivalis haloacid dehalogenase family phosphatase interacts with human phosphoproteins and is important for invasion. *Proceedings of the National Academy of Sciences of the United States of America* 103(29):11027-11032.

Trindade F, Oppenheim FG, Helmerhorst EJ, Amado F, Gomes PS, Vitorino R (2014). Uncovering the molecular networks in periodontitis. *Proteomics Clinical applications* 8(9-10):748-761.

Van Dyken SJ, Locksley RM (2013). Interleukin-4- and interleukin-13-mediated alternatively activated macrophages: roles in homeostasis and disease. *Annual review of immunology* 31(317-343).

van Winkelhoff AJ, Slots J (1999). Actinobacillus actinomycetemcomitans and Porphyromonas gingivalis in nonoral infections. *Periodontology 2000* 20(122-135).

Verzeletti GN, Gaio EJ, Rosing CK (2007). Effect of methotrexate on alveolar bone loss in experimental periodontitis in Wistar rats. *Acta odontologica Scandinavica* 65(6):348-351.

Voisard D, Meuwly F, Ruffieux PA, Baer G, Kadouri A (2003). Potential of cell retention techniques for large-scale high-density perfusion culture of suspended mammalian cells. *Biotechnology and bioengineering* 82(7):751-765.

Wade WG (2013). The oral microbiome in health and disease. *Pharmacological research : the official journal of the Italian Pharmacological Society* 69(1):137-143.

Weiss EI, Shanitzki B, Dotan M, Ganeshkumar N, Kolenbrander PE, Metzger Z (2000). Attachment of Fusobacterium nucleatum PK1594 to mammalian cells and its coaggregation with periodontopathogenic bacteria are mediated by the same galactose-binding adhesin. *Oral microbiology and immunology* 15(6):371-377.

Wendt D, Stroebel S, Jakob M, John GT, Martin I (2006). Uniform tissues engineered by seeding and culturing cells in 3D scaffolds under perfusion at defined oxygen tensions. *Biorheology* 43(3-4):481-488.

Weston B, Todd RF, 3rd, Axtell R, Balazovich K, Stewart J, Locey BJ *et al.* (1991). Severe congenital neutropenia: clinical effects and neutrophil function during treatment with granulocyte colony-stimulating factor. *The Journal of laboratory and clinical medicine* 117(4):282-290.

Wright CJ, Burns LH, Jack AA, Back CR, Dutton LC, Nobbs AH *et al.* (2013). Microbial interactions in building of communities. *Molecular oral microbiology* 28(2):83-101.

- Xu X, Holt SC, Kolodrubetz D (2001). Cloning and expression of two novel hemin binding protein genes from *Treponema denticola*. *Infection and immunity* 69(7):4465-4472.
- Yamada M, Ikegami A, Kuramitsu HK (2005). Synergistic biofilm formation by *Treponema denticola* and *Porphyromonas gingivalis*. *FEMS microbiology letters* 250(2):271-277.
- Yang HW, Huang YF, Chou MY (2004). Occurrence of *Porphyromonas gingivalis* and *Tannerella forsythensis* in periodontally diseased and healthy subjects. *Journal of periodontology* 75(8):1077-1083.
- Yeatts AB, Fisher JP (2011). Tubular perfusion system for the long-term dynamic culture of human mesenchymal stem cells. *Tissue engineering Part C, Methods* 17(3):337-348.
- Zainal-Abidin Z, Veith PD, Dashper SG, Zhu Y, Catmull DV, Chen YY *et al.* (2012). Differential proteomic analysis of a polymicrobial biofilm. *Journal of proteome research* 11(9):4449-4464.
- Zaura E, Keijser BJ, Huse SM, Crielaard W (2009). Defining the healthy "core microbiome" of oral microbial communities. *BMC microbiology* 9(259).
- Zhu Y, Dashper SG, Chen YY, Crawford S, Slakeski N, Reynolds EC (2013). *Porphyromonas gingivalis* and *Treponema denticola* synergistic polymicrobial biofilm development. *PloS one* 8(8):e71727.
- Ziegler-Heitbrock HW, Thiel E, Futterer A, Herzog V, Wirtz A, Riethmuller G (1988). Establishment of a human cell line (Mono Mac 6) with characteristics of mature monocytes. *International journal of cancer Journal international du cancer* 41(3):456-461.
- Zijnge V, van Leeuwen MB, Degener JE, Abbas F, Thurnheer T, Gmur R *et al.* (2010). Oral biofilm architecture on natural teeth. *PloS one* 5(2):e9321.
- Zuger J, Luthi-Schaller H, Gmur R (2007). Uncultivated *Tannerella* BU045 and BU063 are slim segmented filamentous rods of high prevalence but low abundance in inflammatory disease-associated dental plaques. *Microbiology* 153(Pt 11):3809-3816.

## **Papers**

The work of this thesis is comprised of following five publications:

### **Paper 1**

Bao K, Belibasakis GN, Thurnheer T, Aduse-Opoku J, Curtis MA, Bostanci N. Role of *Porphyromonas gingivais* gingipains in multi-species biofilm formation. *BMC Microbiology* 2014; 14: 258

### **Paper 2**

Bao K, Bostanci N, Selevsek N, Thurnheer T, Belibasakis GN. Quantitative proteomics reveal distinct protein regulations caused by *Aggregatibacter actinomycetemcomitans* within subgingival biofilms. *PLoS One* 2015; 10: 3: e0119222

### **Paper 3:**

Bao K, Akgül B, Bostanci N. Establishment and characterization of immortalized gingival epithelial and fibroblastic cell lines for development of organotypic cultures *Cells Tissues Organs* 2014; 199: 228-237

### **Paper 4**

Bao K, Papadimitropoulos A, Akgul B, Belibasakis GN, Bostanci N. Establishment of an oral infection model resembling the periodontal pocket in a perfusion bioreactor system. *Virulence* 2015; 6: 3: 265-273

### **Paper 5**

Bao K, Belibasakis GN, Selevsek N, Grossmann J, Bostanci N. Proteomic profiling of host-biofilm interactions in an oral infection model resembling the periodontal pocket. In revision 2015

# Paper 1

RESEARCH ARTICLE

Open Access

# Role of *Porphyromonas gingivalis* gingipains in multi-species biofilm formation

Kai Bao<sup>1</sup>, Georgios N Belibasakis<sup>2</sup>, Thomas Thurnheer<sup>2</sup>, Joseph Aduse-Opoku<sup>3</sup>, Michael A Curtis<sup>3</sup> and Nagihan Bostanci<sup>1\*</sup>

## Abstract

**Background:** Periodontal diseases are polymicrobial diseases that cause the inflammatory destruction of the tooth-supporting (periodontal) tissues. Their initiation is attributed to the formation of subgingival biofilms that stimulate a cascade of chronic inflammatory reactions by the affected tissue. The Gram-negative anaerobes *Porphyromonas gingivalis*, *Tannerella forsythia* and *Treponema denticola* are commonly found as part of the microbiota of subgingival biofilms, and they are associated with the occurrence and severity of the disease. *P. gingivalis* expresses several virulence factors that may support its survival, regulate its communication with other species in the biofilm, or modulate the inflammatory response of the colonized host tissue. The most prominent of these virulence factors are the gingipains, which are a set of cysteine proteinases (either Arg-specific or Lys-specific). The role of gingipains in the biofilm-forming capacity of *P. gingivalis* is barely investigated. Hence, this *in vitro* study employed a biofilm model consisting of 10 “subgingival” bacterial species, incorporating either a wild-type *P. gingivalis* strain or its derivative Lys-gingipain and Arg-gingipain isogenic mutants, in order to evaluate quantitative and qualitative changes in biofilm composition.

**Results:** Following 64 h of biofilm growth, the levels of all 10 species were quantified by fluorescence *in situ* hybridization or immunofluorescence. The wild-type and the two gingipain-deficient *P. gingivalis* strains exhibited similar growth in their corresponding biofilms. Among the remaining nine species, only the numbers of *T. forsythia* were significantly reduced, and only when the Lys-gingipain mutant was present in the biofilm. When evaluating the structure of the biofilm by confocal laser scanning microscopy, the most prominent observation was a shift in the spatial arrangement of *T. denticola*, in the presence of *P. gingivalis* Arg-gingipain mutant.

**Conclusions:** The gingipains of *P. gingivalis* may qualitatively and quantitatively affect composition of polymicrobial biofilms. The present experimental model reveals interdependency between the gingipains of *P. gingivalis* and *T. forsythia* or *T. denticola*.

**Keywords:** Biofilm, *Porphyromonas gingivalis*, Gingipains, *Tannerella forsythia*, *Treponema denticola*, Periodontal microorganisms, Periodontal disease, Fluorescence *in situ* hybridization, Immunofluorescence

## Background

Periodontal infections, or periodontal diseases, are a set of chronic inflammatory diseases that destroy the tooth-supporting (periodontal) tissues. They are caused by oral bacterial biofilms attaching on the tooth surface. They have the capacity to trigger a series of inflammatory responses, which may destroy the gingival tissue and the alveolar bone supporting the tooth, if they become

exacerbated [1,2]. With regards to its capacity as an ecological niche, the oral cavity can be colonized by more than 700 species [3] and approximately 500 of those can be present within the forming biofilms [4,5]. Among the biofilm-associated microbiota, earlier clinical epidemiological studies have demonstrated that three species in particular, also designated as the “red complex”, are more associated with periodontal disease than others. These are namely *Porphyromonas gingivalis*, *Tannerella forsythia*, and *Treponema denticola*. They are all Gram-negative anaerobes, with a high proteolytic activity [6]. Among these three, *P. gingivalis* holds a prominent role in

\* Correspondence: nagihan.bostanci@zzm.uzh.ch

<sup>1</sup>Oral Translational Research, Institute of Oral Biology, Center of Dental Medicine, University of Zürich, Plattenstrasse 11, 8032 Zürich, Switzerland  
Full list of author information is available at the end of the article



orchestrating the virulence of the biofilm and the consequent tissue inflammatory response, earning itself the characteristics of a “keystone” periodontal pathogen [7,8]. *P. gingivalis* expresses several virulence factors, including, fimbriae, LPS, and its cysteine proteases, namely gingipains [9]. These include the arginine-specific proteinases RgpA and RgpB, and the lysine-specific proteinase Kgp, which represent the majority of the cell-surface proteinases of *P. gingivalis* [10]. Clinical studies have demonstrated that periodontal infection associated with *P. gingivalis* can result in significantly elevated systemic antibody response to the gingipains [11,12].

When growing in a subgingival (below the gingival margin) biofilm under strict anaerobic conditions, *P. gingivalis* is highly dependent on its gingipains for utilizing free amino acids as a source of carbon and nitrogen [13]. Moreover, unlike other gram-negative bacteria, *P. gingivalis* does not produce siderophores to sequester and transport iron but its gingipains mediate the uptake of iron from hemoglobin, heme proteins, and ferritin [14,15]. Gingipains are also considered important in the capacity of *P. gingivalis* to evade host defences, by degrading antibacterial peptides, such as neutrophil-derived  $\alpha$ -defensins, complement factor, such as C3 and C4, T cell receptors, such as CD4 and CD8 [16]. Alternatively, *P. gingivalis* and its gingipains can subvert the host immune response by proactively manipulating host molecules, particularly of the complement [17,18]. For instance, *P. gingivalis* may perturb the cross-talk between C5a receptor and toll-like receptor signalling in order to prevent bacterial clearance and cause dysbiosis [19], eventually resulting in periodontal bone loss [20,21]. The construction and phenotypic analysis of isogenic protease mutants of *P. gingivalis* have confirmed putative functions for these proteolytic enzymes [22]. *In vivo* studies using the *P. gingivalis* mutant strains in animal models have reinforced the view that the gingipains can modulate the infection process [23-26]. *In vitro* studies have demonstrated an involvement of the gingipains in the regulation of inflammatory mediators from various host cells, including IL-1  $\alpha$ , IL-1 $\beta$ , IL-18 [27], receptor activator of NF- $\kappa$ B ligand (RANKL) [28-31], tumor necrosis factor- $\alpha$  converting enzyme (TACE) [32], protease-activated receptor (PAR)-2 [33], or soluble triggering receptor expressed on myeloid cells (sTREM)-1 [34].

Understanding how different organisms act within a given polymicrobial biofilm brings us closer to understanding the etiological mechanisms of periodontal disease [1]. That is because interactions among different bacterial cells can determine the structural characteristics, maturation and virulence of the biofilms [35-37]. These interactions can occur at several levels, including physical contact, metabolic exchange, and signal-mediated communications [38]. Additionally, species-specific virulence factors may regulate bacterial growth, hence altering the

conditions of the ecological niche for biofilm formation. In this respect, most studies involving gingipains have focused on *P. gingivalis* as a single species, which might overlook the bacterial interactions within a complex biofilm community. Therefore, the present study used a 10-species “subgingival” biofilm, aiming to investigate the role of gingipains on the growth and structure of the biofilm, by incorporating *P. gingivalis* gingipain-deficient strains.

## Results

### Quantitative evaluation of bacteria in the biofilm

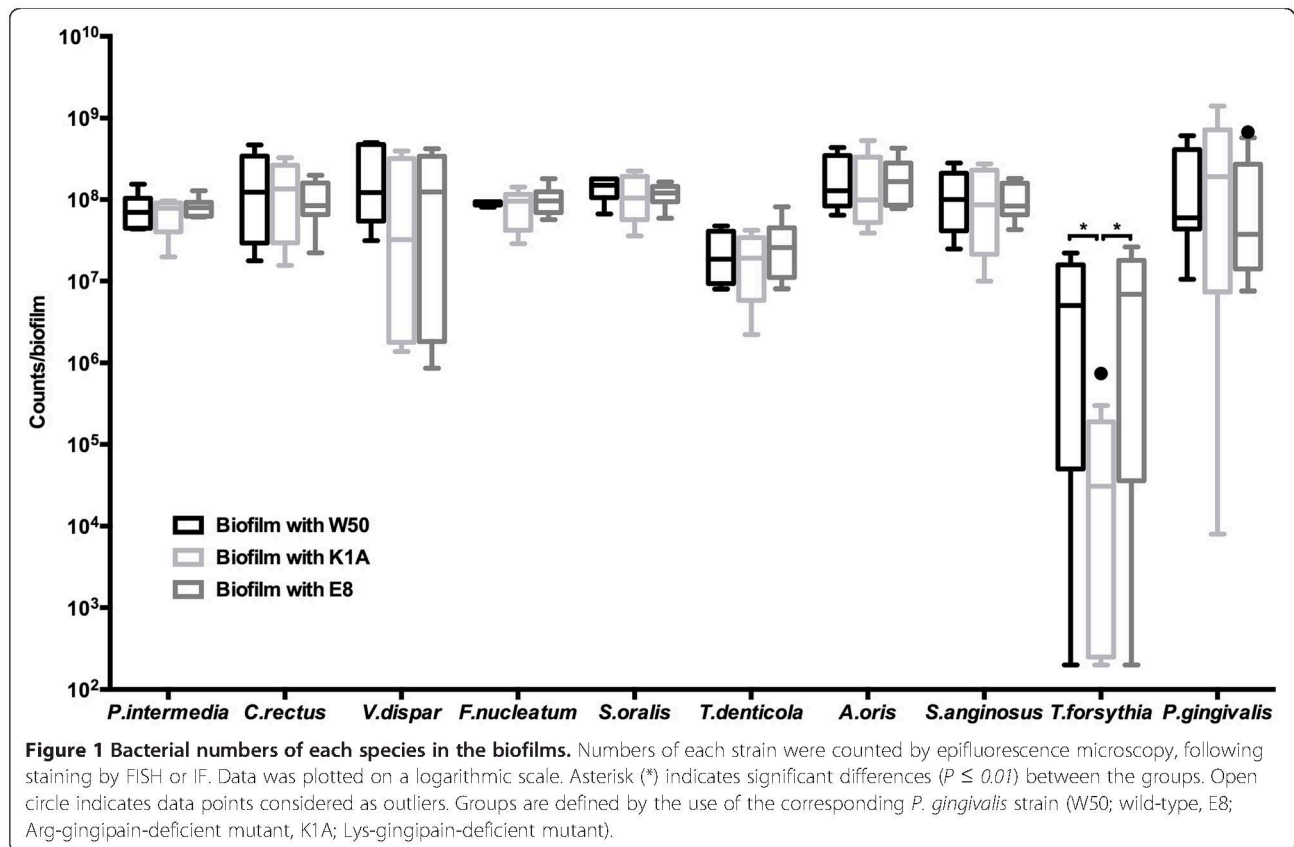
The numbers for each individual species within the different biofilm groups were quantified either by fluorescence *in situ* hybridization (FISH) or by immunofluorescence (IF). The growth of *P. gingivalis* was not affected depending on whether the wild-type or the gingipain-deficient strains were used. Statistically, compared to the wild-type strain, the *P. gingivalis* gingipain-deficient strains did not cause significant changes in the growth of the remaining nine-biofilm species in the biofilm, with the exception of *T. forsythia* (Figure 1). In particular, the presence of the Lys-gingipain deficient strain K1A caused a significant ( $P < 0.01$ ) reduction of *T. forsythia* cell numbers, compared to the wild-type W50, or the Arg-gingipain-deficient strain E8 (29.9-fold and 38.6-fold, respectively). However, no significant differences in *T. forsythia* numbers were observed between the wild-type W50 and the Arg-gingipain-deficient E8 biofilm groups.

### Qualitative evaluation of biofilm structure by confocal microscopy

Having identified that a dependency exists between the Lys-gingipain and the growth of *T. forsythia*, we further investigated the structure of the biofilm by means of confocal laser scanning microscopy (CLSM), and evaluated changes in the presence of the *P. gingivalis* gingipain-deficient strains. Firstly, the focus was placed on the structural association or localization between *P. gingivalis* and *T. forsythia*. Within the biofilm structure, *P. gingivalis* appeared in variable size aggregates or clusters of its own species, with no marked differences observed between the wild-type W50 and the gingipain-deficient strains (Figure 2). The distribution pattern of *T. forsythia* was in more scattered clusters, observed often in the immediate vicinity of *P. gingivalis* clusters, but not strongly intertwining each other (Figure 2). This pattern was observable irrespective of the use of *P. gingivalis* wild-type W50 or the Arg-gingipain deficient strain E8, whereas when the Lys-gingipain deficient strain K1A was included in the biofilm instead, this association was less obvious (Figure 2), presumably due of the low *T. forsythia* numbers.

It was of further interest to investigate the localization of *T. denticola* within the biofilm structure, as the third member of the “red complex” cluster. Interestingly,



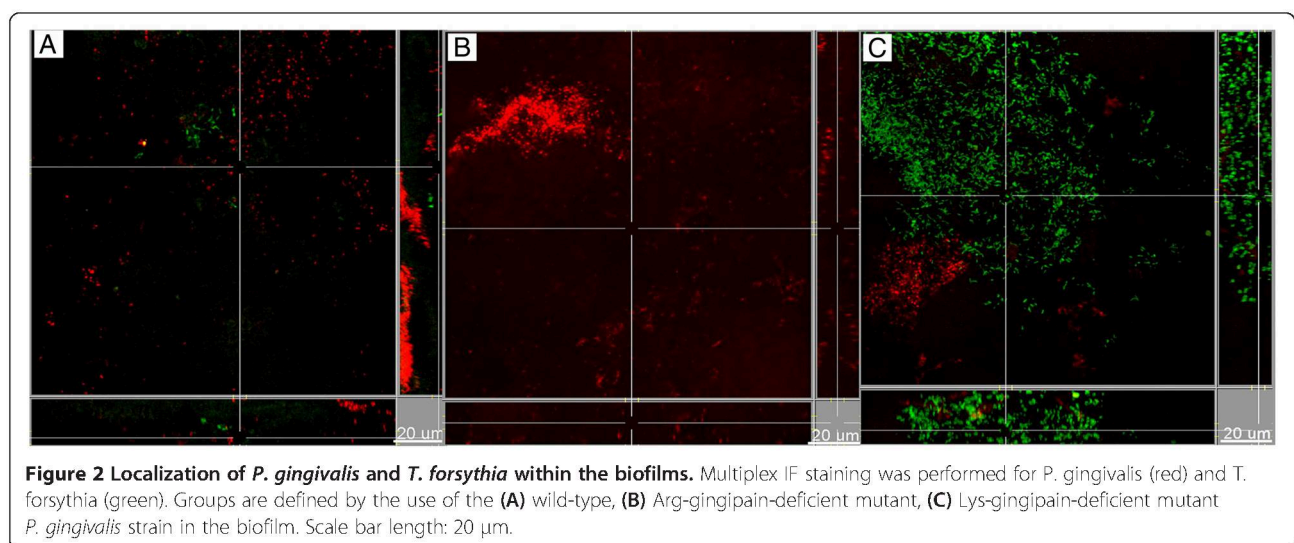


*T. denticola* formed aggregates or clusters in the presence of the *P. gingivalis* wild-type strain W50, as was the case also when the Lys-gingipain deficient strain K1A was used. However, in the presence of the Arg-gingipain deficient strain E8, *T. denticola* lost this “cluster-like” conformation in the biofilm, and acquired a more even and “thread-like” distribution (Figures 3 and 4). *Fusobacterium nucleatum* was also strongly present throughout the

biofilm and appeared to be evenly distributed among these *T. denticola* structures (Figure 4).

## Discussion

As it is well established that periodontal diseases are initiated by a mixed-species biofilm [39,40], *in vitro* biofilm models, may be more accurate in studying the causative factor of the disease, than single species in planktonic



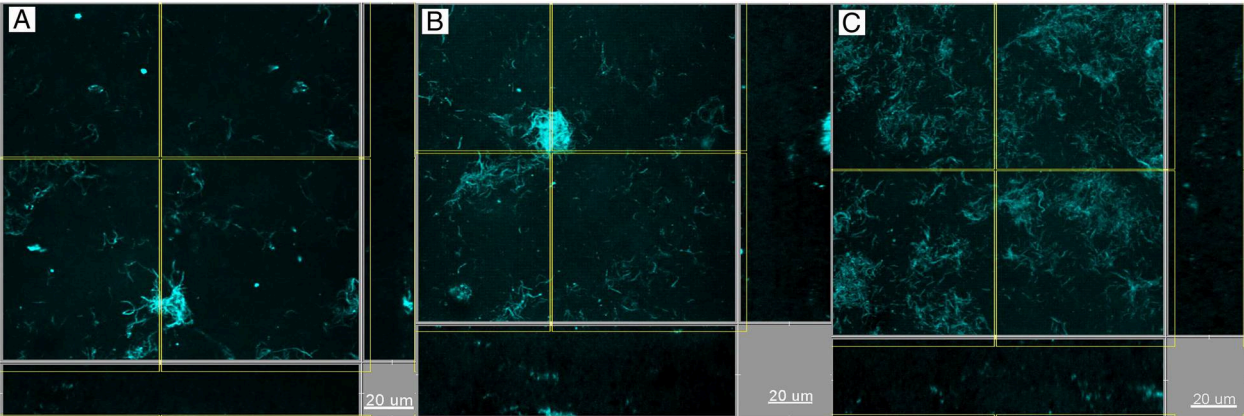


**Figure 3 Localization of *T. denticola* within the biofilms.** IF staining was performed for *T. denticola* (cyan). Groups are defined by the use of the (A) wild-type, (B) Arg-gingipain-deficient mutant, (C) Lys-gingipain-deficient mutant, *P. gingivalis* strain in the biofilm. Scale bar length: 20 μm.

form [37,41,42]. The present study investigated the involvement of *P. gingivalis* gingipains in the quantitative and qualitative composition of a polymicrobial biofilm consisting of 10 species that are frequently comprising part of the subgingival microbial flora. Among their many properties, gingipains are important for the growth of *P. gingivalis* and as transporters for iron [14]. While in planktonic culture *P. gingivalis* gingipain deficient strains require longer doubling times [43], their incorporation into a polymicrobial biofilm did not yield differences in numbers, compared

to the wild-type strain. Hence, the growth characteristics of *P. gingivalis* may differ depending on whether it grows in planktonic or biofilm state. When present in a biofilm, gingipains do not appear to be crucial for the growth of *P. gingivalis*, as shown here. Interestingly, among the remaining nine species in the biofilm, the only one whose growth was affected by the presence of gingipains was *T. forsythia*. In particular, the *P. gingivalis* Lys-gingipain deficient strain resulted in a strong reduction in *T. forsythia* numbers after 64 h of biofilm growth.

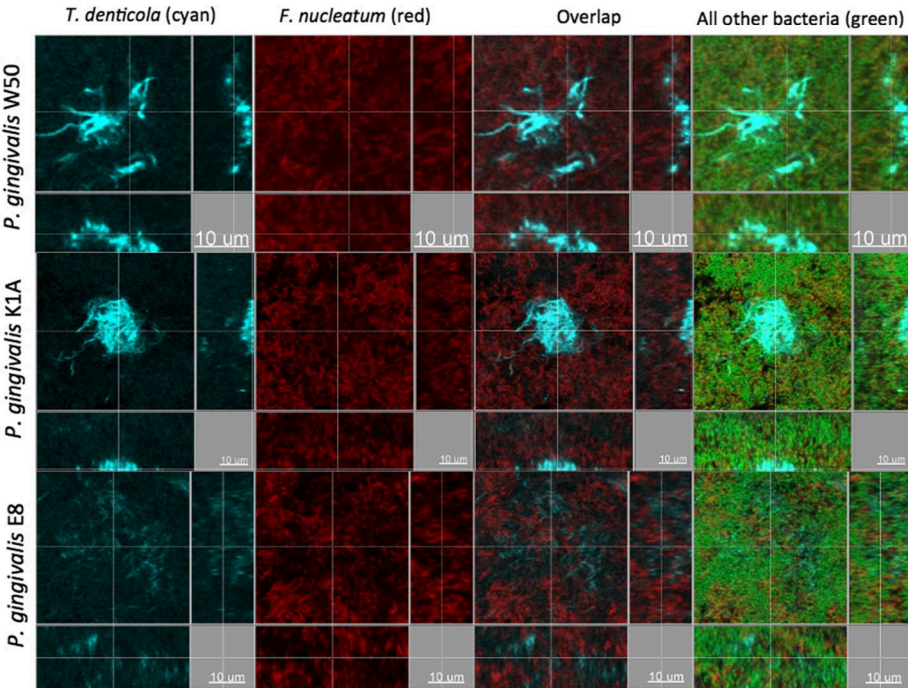


**Figure 4 Localization of *P. gingivalis*, *F. nucleatum* and *T. denticola* within the biofilms.** IF staining was performed for *T. denticola* (cyan), *F. nucleatum* (red) and YoPro-1 iodide & Sytox Green mixture for all other bacteria (green). Groups are defined by the use of the corresponding *P. gingivalis* strain (W50; wild-type, E8; Arg-gingipain-deficient mutant, K1A; Lys-gingipain-deficient mutant) in the biofilm. Scale bar length: 20 μm.



Reversely, this indicates that the Lys-gingipain produced by *P. gingivalis* has an additive effect on the growth of *T. forsythia* in the biofilm. This denotes a synergistic association between *T. forsythia* and *P. gingivalis* as mutual components of a polymicrobial community, which is mediated by the Lys-gingipain of the latter.

Previous studies have shown that gingipains are crucial for the co-aggregation of *P. gingivalis* or its co-adhesion with other species, such as *T. denticola* [44-46], or for the invasion of host cells [47]. Hence, the gingipains may not only affect the quantitative composition but also the structural conformation of the biofilm. For this reason, the biofilm architecture was also investigated by CLSM. *P. gingivalis* occurred in distinguishable and evenly distributed clusters within the biofilm regardless of whether it expressed a gingipain or not. The communities of *T. forsythia* within the biofilm exhibited similar patterns to those of *P. gingivalis*, and were frequently co-localized, yet without impinging onto each other. The proximal association of these two species' communities in biofilm may hint for an ecological relationship. This is also substantiated by the notable absence of *T. forsythia* clusters from the vicinity of the Lys-gingipain deficient *P. gingivalis*. Hence, this gingipain may be important for the growth of *T. forsythia* and its spatial interdependency to *P. gingivalis* within the biofilm. This observation could represent an example of the metabolic responses and bacterial quorum-sensing within the biofilm [48].

Another interesting observation of the present study is that of the structural re-arrangement of *T. denticola* in the biofilm, depending on the presence or absence of the Arg-gingipain. Earlier studies have shown that other species can interact with *P. gingivalis* in both planktonic suspensions and biofilms [46,49,50]. A recent study using the similar multi-species biofilm model as here demonstrated that *P. gingivalis* and *T. denticola* have the tendency to co-colonize gingival epithelial tissue [51]. In a dual *P. gingivalis* - *T. denticola* biofilm, it was also demonstrated that gingipains do contribute to their interaction [50]. In the present experimental model, *T. denticola* cells formed dense circular clumps with the wild-type *P. gingivalis* strain. However, in the presence of the *P. gingivalis* Arg-gingipain deficient strain, this conformation was lost and *T. denticola* cells were instead arranged in looser threaded structures, even though their numbers in the biofilm were not changed. This finding provides further evidence of the ecological association between *P. gingivalis* gingipains and the structural arrangement of *T. denticola* in the biofilm. It is difficult at this stage to interpret the biological meaning of this change in *T. denticola* structure. Of note, in a recent study using the similar biofilm model it was demonstrated that omission of streptococci from the biofilm resulted in numeric changes of *P. gingivalis*

and *P. intermedia*. The latter also lost its aggregated form and was arranged in filamentous long chains, resembling those of the missing streptococci [35].

## Conclusions

This study showed that the gingipains of *P. gingivalis* promote quantitative and qualitative shifts in the composition and structure of a multi-species biofilm. More specifically, the Lys-gingipain enhances the growth of *T. forsythia*, whereas the Arg-gingipain promotes the aggregation of *T. denticola* in the biofilm. These ecological interactions are interpreted as synergistic ones, and may support the survival and the virulence of the biofilm community as a whole.

## Methods

### *In vitro* biofilm formation

The method used to develop 10 species biofilm is a modification of a previous report of this model [52], with major changes described below. The following strains were used in this study: *Prevotella intermedia* ATCC 25611 T (OMZ 278), *Campylobacter rectus* (OMZ 398), *Veillonella dispar* ATCC 17748 T (OMZ 493), *Fusobacterium nucleatum subsp. nucleatum* (OMZ 598), *Streptococcus oralis* SK248 (OMZ 607), *T. denticola* ATCC 35405 T (OMZ 661), *Actinomyces oris* (OMZ 745), *Streptococcus anginosus* ATCC 9895 (OMZ 871), *T. forsythia* (OMZ 1047), *P. gingivalis* W50 (OMZ 308), *P. gingivalis* K1A (OMZ 1126) and *P. gingivalis* E8 (OMZ 1127). The latter two are genetically modified strains of *P. gingivalis* W50, with a deletion of Lysine-gingipain (*kgp*) and Arginine-gingipain (*rgpArgpB*) genes, respectively [22]. Each of the biofilm groups in this experimental design contains one of the three *P. gingivalis* strains and all other 9 species. For biofilm formation, 200 µl of bacterial cell suspension, containing equal volumes and densities (OD<sub>550</sub> = 1.0) of each strain were added onto pellicle-coated hydroxyapatite discs (diameter 5 mm), in 1.6 ml growth medium supplemented with 0.5% hemin, as described earlier [53]. The medium was renewed after 16 h and 24 h, during the total incubation time of 64 h. The discs were dip-washed three-times daily.

### Biofilm harvesting

After 64 h of incubation, the biofilm discs were ready to be harvested. For quantification of the bacterial numbers in the biofilm, the discs were vigorously vortexed for 2 min in 0.9%NaCl and then sonicated at 25 W in a Sonifier B-12 (Branson Sonic Power Company) for 5 sec. For confocal laser scanning microscopy (CLSM) of the biofilm structure, the discs were dip-washed and immediately fixed in 4% paraformaldehyde (Merck, Darmstadt, Germany) at 4°C for 1 h before being processed for fluorescence

*in situ* hybridization (FISH) or immunofluorescence (IF) analysis.

#### Quantification of bacteria by FISH and IF

The bacterial suspensions were diluted, fixed on the slides, stained and counted as described [54,55]. For FISH staining, slides were fixed at 4°C with 4% paraformaldehyde in PBS for 20 min and for IF staining they were fixed at room temperature with methanol for 2 min, before they were incubated with the antibodies at 37°C. FISH was used for the evaluation of *S. oralis*, *S. anginosus* and *V. dispar* (oligonucleotide probes listed in Table 1), while IF was used for the evaluation of *T. denticola*, *C. rectus*, *T. forsythia*, *P. gingivalis*, *P. intermedia*, *F. nucleatum* and *A. oris* (antibodies listed in Table 2).

For FISH, the fixed samples were first pre-hybridized, with hybridization buffer containing 0.9 M NaCl, 20 mM Tris/HCl (pH 7.5), 0.01%SDS, formamide (as indicated in Table 1) at 46°C, for 15 min. Following this step, hybridization was performed using specific oligonucleotide probes (Table 1) at the same temperature, for 3 h. Thereafter, the samples were incubated at 48°C with pre-warmed wash buffer containing 20 mM Tris/HCl (pH7.5), 5 mM EDTA, 0.01% SDS, and 40–159 mM NaCl for 30 min. For CLSM and image analysis, the samples were counterstained with a mixture of 3 µM YoPro-1 iodide (Invitrogen, Basel, Switzerland) and 15 µM Sytox Green (Invitrogen, Basel, Switzerland) then embedded with 10 µl Mowiol [55] with the biofilm surface facing towards the chamber slides. Prior to qualification, the samples were coated with mounting buffer consisting of 90% ultrapure glycerol and 10% 25 mg/g DABCO (Sigma-Aldrich, Buchs, Switzerland), on 24 well slides. Finally, the stained bacterial cells were visualized under an Olympus BX60 fluorescence microscope (Olympus Optical AG, Volketswil, Switzerland), at 100× magnification.

The box-plot data presented derives from four independent experiments each performed in triplicate biofilm cultures. The values were logarithmically transformed, and then inserted to Prism v.6 software (GraphPad, La Jolla California USA). The statistical differences between the groups were calculated by one-way ANOVA, using the Tukey's post-hoc test for multiple comparisons ( $P \leq 0.01$ ).

#### Confocal laser scanning microscopy and image analysis

For evaluation of the biofilm structure, CLSM was used for each one of the four independent experiments. The

**Table 2 Antibodies for IF**

Target	Antibody name	Isotype	Ref.
<i>C. rectus</i>	212WR2	mouse IgG3	[58]
<i>T. forsythia</i>	103BF1.1	mouse IgG2b	[59]
<i>P. gingivalis</i>	61BG1.3	mouse IgG1	[60]
<i>P. intermedia</i>	37BI6.1	rat IgG2b	[53]
<i>F. nucleatum</i>	305FN1.2	mouse IgM	[61]
<i>A. oris</i>	396AN1	mouse IgM	[61]
<i>T. denticola</i>	CD-1	Rabbit polyclonal antiserum	[41]

biofilm-containing discs stained by FISH or IF were visualized using a Leica SP-5 microscope at the Center of Microscopy and Image Analysis of the University of Zürich (ZMB), with a resonant scanner system (8000 Hz), a diode laser (405 nm excitation), an argon laser (458 nm/476 nm/488 nm/496 nm/514 nm excitation) and a helium neon laser (561 nm/594 nm/633 nm excitation). Filters were set to 500–540 nm, 570–630 nm, and 660–710 for detection of YoPro-1 iodide & Sytox Green mixture, Cy3 and Cy5, respectively. All images were captured using a 63× objective (glycerol immersion, NA 1.3). Stacked images were further processed using the Imaris™ 7.4.0 software (Bitplane, Zürich, Switzerland), in order to virtually reconstruct the biofilm structure.

#### Competing interests

The authors declare that they have no competing interests.

#### Authors' contribution

NB and GNB conceived the study. BK, GNB, TT, JAO, MAC and NB designed the study. JAO and MAC generated and provided the *Porphyromonas gingivalis* gingipain mutants. BK performed the experiments. BK and NB performed the data analysis. BK, GNB and NB wrote the paper. TT, JAO and MAC reviewed and approved the final version of the paper. All authors read and approved the final manuscript.

#### Acknowledgements

We thank the Centre of Microscopy and Image Analysis (ZMB) of the University of Zürich for their support with confocal microscopy. This study was supported by the authors' Institutes, the Forschungskredit Grant of the University of Zürich (NB), and the Medical Research Council UK grant MR/J011118/1 (MAC).

#### Author details

<sup>1</sup>Oral Translational Research, Institute of Oral Biology, Center of Dental Medicine, University of Zürich, Plattenstrasse 11, 8032 Zürich, Switzerland. <sup>2</sup>Oral Microbiology and Immunology, Institute of Oral Biology, Center of Dental Medicine, University of Zürich, Plattenstrasse 11, 8032 Zürich, Switzerland. <sup>3</sup>Barts and The London Institute of Dentistry, Queen Mary University of London, London E1 2 AD, UK.

Received: 24 June 2014 Accepted: 26 September 2014

Published online: 02 October 2014

#### References

1. Socransky SS, Haffajee AD: Periodontal microbial ecology. *Periodontol* 2000 2005, **38**:135–187.
2. Darveau RP: Periodontitis: a polymicrobial disruption of host homeostasis. *Nat Rev Microbiol* 2010, **8**(7):481–490.
3. Aas JA, Paster BJ, Stokes LN, Olsen I, Dewhirst FE: Defining the normal bacterial flora of the oral cavity. *J Clin Microbiol* 2005, **43**(11):5721–5732.

**Table 1 16S rRNA oligonucleotide probes for FISH**

Target	Probe name	FA	Sequence (5' → 3')	Ref.
<i>V. dispar</i>	VEI217	45%	AATCCCCCTCCTTCAGTGA	[55]
<i>S. oralis</i>	MIT447	25%	CACYCGTCTCTCTTACA	[56]
<i>S. anginosus</i>	Sang1203	45%	GGTACACCTTACCACAC	[57]

FA; Formamide concentration in the hybridization buffer.



4. Hajishengallis G, Lamont RJ: Beyond the red complex and into more complexity: the polymicrobial synergy and dysbiosis (PSD) model of periodontal disease etiology. *Mol Oral Microbiol* 2012, **27**(6):409–419.
5. Paster BJ, Boches SK, Galvin JL, Ericson RE, Lau CN, Levanos VA, Sahasrabudhe A, Dewhirst FE: Bacterial diversity in human subgingival plaque. *J Bacteriol* 2001, **183**(12):3770–3783.
6. Socarransky SS, Haffajee AD, Cugini MA, Smith C, Kent RL Jr: Microbial complexes in subgingival plaque. *J Clin Periodontol* 1998, **25**(2):134–144.
7. Hajishengallis G: Immune evasion strategies of *Porphyromonas gingivalis*. *J Oral Biosci* 2011, **53**(3):233–240.
8. Hajishengallis G, Darveau RP, Curtis MA: The keystone-pathogen hypothesis. *Nat Rev Microbiol* 2012, **10**(10):717–725.
9. Bostanci N, Belibasakis GN: *Porphyromonas gingivalis*: an invasive and evasive opportunistic oral pathogen. *FEMS Microbiol Lett* 2012, **333**(1):1–9.
10. Curtis MA, Aduse-Opoku J, Rangarajan M: Cysteine proteases of *Porphyromonas gingivalis*. *Crit Rev Oral Biol Med* 2001, **12**(3):192–216.
11. O'Brien-Simpson NM, Black CL, Bhogal PS, Cleal SM, Slakeski N, Higgins TJ, Reynolds EC: Serum immunoglobulin G (IgG) and IgG subclass responses to the RgpA-Kgp proteinase-adhesin complex of *Porphyromonas gingivalis* in adult periodontitis. *Infect Immun* 2000, **68**(5):2704–2712.
12. Gibson FC 3rd, Savelli J, Van Dyke TE, Genco CA: Gingipain-specific IgG in the sera of patients with periodontal disease is necessary for opsonophagocytosis of *Porphyromonas gingivalis*. *J Periodontol* 2005, **76**(10):1629–1636.
13. Milner P, Batten JE, Curtis MA: Development of a simple chemically defined medium for *Porphyromonas gingivalis*: requirement for alpha-ketoglutarate. *FEMS Microbiol Lett* 1996, **140**(2–3):125–130.
14. Sroka A, Szukowska M, Potempa J, Travis J, Genco CA: Degradation of host heme proteins by lysine- and arginine-specific cysteine proteinases (gingipains) of *Porphyromonas gingivalis*. *J Bacteriol* 2001, **183**(19):5609–5616.
15. Bramanti TE, Holt SC: Roles of porphyrins and host iron transport proteins in regulation of growth of *Porphyromonas gingivalis* W50. *J Bacteriol* 1991, **173**(22):7330–7339.
16. Bostanci N, Belibasakis GN: Doxycycline inhibits TREM-1 induction by *Porphyromonas gingivalis*. *FEMS Immunol Med Microbiol* 2012, **66**(1):37–44.
17. Hajishengallis G, Abe T, Maekawa T, Hajishengallis E, Lambris JD: Role of complement in host-microbe homeostasis of the periodontium. *Semin Immunol* 2013, **25**(1):65–72.
18. Hajishengallis G, Lambris JD: Complement and dysbiosis in periodontal disease. *Immunobiology* 2012, **217**(11):1111–1116.
19. Maekawa T, Krauss JL, Abe T, Jotwani R, Triantafyllou M, Triantafyllou K, Hashim A, Hoch S, Curtis MA, Nussbaum G, Lambris JD, Hajishengallis G: *Porphyromonas gingivalis* manipulates complement and TLR signaling to uncouple bacterial clearance from inflammation and promote dysbiosis. *Cell Host Microbe* 2014, **15**(6):768–778.
20. Liang S, Krauss JL, Domon H, McIntosh ML, Hosur KB, Qu H, Li F, Tzekou A, Lambris JD, Hajishengallis G: The C5a receptor impairs IL-12-dependent clearance of *Porphyromonas gingivalis* and is required for induction of periodontal bone loss. *J Immunol* 2011, **186**(2):869–877.
21. Abe T, Hosur KB, Hajishengallis E, Reis ES, Ricklin D, Lambris JD, Hajishengallis G: Local complement-targeted intervention in periodontitis: proof-of-concept using a C5a receptor (CD88) antagonist. *J Immunol* 2012, **189**(11):5442–5448.
22. Aduse-Opoku J, Davies NN, Gallagher A, Hashim A, Evans HE, Rangarajan M, Slaney JM, Curtis MA: Generation of lys-gingipain protease activity in *Porphyromonas gingivalis* W50 is independent of Arg-gingipain protease activities. *Microbiology* 2000, **146**(Pt 8):1933–1940.
23. Fletcher HM, Schenkein HA, Morgan RM, Bailey KA, Berry CR, Macrina FL: Virulence of a *Porphyromonas gingivalis* W83 mutant defective in the prtH gene. *Infect Immun* 1995, **63**(4):1521–1528.
24. Tokuda M, Karunakaran T, Duncan M, Hamada N, Kuramitsu H: Role of Arg-gingipain A in virulence of *Porphyromonas gingivalis*. *Infect Immun* 1998, **66**(3):1159–1166.
25. Kesavalu L, Holt SC, Ebersole JL: *Porphyromonas gingivalis* virulence in a murine lesion model: effects of immune alterations. *Microb Pathog* 1997, **23**(6):317–326.
26. O'Brien-Simpson NM, Paolini RA, Hoffmann B, Slakeski N, Dashper SG, Reynolds EC: Role of RgpA, RgpB, and Kgp proteinases in virulence of *Porphyromonas gingivalis* W50 in a murine lesion model. *Infect Immun* 2001, **69**(12):7527–7534.
27. Hamed M, Belibasakis GN, Cruchley AT, Rangarajan M, Curtis MA, Bostanci N: *Porphyromonas gingivalis* culture supernatants differentially regulate interleukin-1beta and interleukin-18 in human monocytic cells. *Cytokine* 2009, **45**(2):99–104.
28. Reddi D, Bostanci N, Hashim A, Aduse-Opoku J, Curtis MA, Hughes FJ, Belibasakis GN: *Porphyromonas gingivalis* regulates the RANKL-OPG system in bone marrow stromal cells. *Microbes Infect* 2008, **10**(14–15):1459–1468.
29. Reddi D, Brown SJ, Belibasakis GN: *Porphyromonas gingivalis* induces RANKL in bone marrow stromal cells: involvement of the p38 MAPK. *Microb Pathog* 2011, **51**(6):415–420.
30. Belibasakis GN, Bostanci N, Hashim A, Johansson A, Aduse-Opoku J, Curtis MA, Hughes FJ: Regulation of RANKL and OPG gene expression in human gingival fibroblasts and periodontal ligament cells by *Porphyromonas gingivalis*: a putative role of the Arg-gingipains. *Microb Pathog* 2007, **43**(1):46–53.
31. Bostanci N, Allaker R, Johansson U, Rangarajan M, Curtis MA, Hughes FJ, McKay IJ: Interleukin-1alpha stimulation in monocytes by periodontal bacteria: antagonistic effects of *Porphyromonas gingivalis*. *Oral Microbiol Immunol* 2007, **22**(1):52–60.
32. Bostanci N, Emingil G, Afacan B, Han B, Ilgenli T, Atilla G, Hughes FJ, Belibasakis GN: Tumor necrosis factor-alpha-converting enzyme (TACE) levels in periodontal diseases. *J Dent Res* 2008, **87**(3):273–277.
33. Belibasakis GN, Bostanci N, Reddi D: Regulation of protease-activated receptor-2 expression in gingival fibroblasts and Jurkat T cells by *Porphyromonas gingivalis*. *Cell Biol Int* 2010, **34**(3):287–292.
34. Bostanci N, Thurnheer T, Aduse-Opoku J, Curtis MA, Zinkernagel AS, Belibasakis GN: *Porphyromonas gingivalis* regulates TREM-1 in human polymorphonuclear neutrophils via its gingipains. *PLoS One* 2013, **8**(10):e75784.
35. Ammann TW, Belibasakis GN, Thurnheer T: Impact of early colonizers on in vitro subgingival biofilm formation. *PLoS One* 2013, **8**(12):e83090.
36. Belibasakis GN, Thurnheer T, Bostanci N: Interleukin-8 responses of multi-layer gingival epithelia to subgingival biofilms: role of the "red complex" species. *PLoS One* 2013, **8**(12):e81581.
37. Belibasakis GN, Guggenheim B, Bostanci N: Down-regulation of NLRP3 inflammasome in gingival fibroblasts by subgingival biofilms: involvement of *Porphyromonas gingivalis*. *Innate Immun* 2013, **19**(1):3–9.
38. Kolenbrander PE, Palmer RJ Jr, Rickard AH, Jakubovics NS, Chalmers NI, Diaz PI: Bacterial interactions and successions during plaque development. *Periodontol* 2000 2006, **42**:47–79.
39. Schultz-Haudt S, Bruce MA, Bibby BG: Bacterial factors in nonspecific gingivitis. *J Dent Res* 1954, **33**(4):454–458.
40. Maccdonald JB, Sutton RM, Knoll ML, Madlener EM, Grainger RM: The pathogenic components of an experimental fusospirochetal infection. *J Infect Dis* 1956, **98**(1):15–20.
41. Belibasakis GN, Thurnheer T: Validation of antibiotic efficacy on in vitro subgingival biofilms. *J Periodontol* 2014, **85**(2):343–348.
42. Ammann TW, Gmur R, Thurnheer T: Advancement of the 10-species subgingival Zurich Biofilm model by examining different nutritional conditions and defining the structure of the in vitro biofilms. *BMC Microbiol* 2012, **12**(1):227.
43. Grenier D, Roy S, Chandad F, Plamondon P, Yoshioka M, Nakayama K, Mayrand D: Effect of inactivation of the Arg- and/or Lys-gingipain gene on selected virulence and physiological properties of *Porphyromonas gingivalis*. *Infect Immun* 2003, **71**(8):4742–4748.
44. Ito R, Ishihara K, Shoji M, Nakayama K, Okuda K: Hemagglutinin/Adhesin domains of *Porphyromonas gingivalis* play key roles in coaggregation with *Treponema denticola*. *FEMS Immunol Med Microbiol* 2010, **60**(3):251–260.
45. Abe N, Baba A, Takii R, Nakayama K, Kamaguchi A, Shibata Y, Abiko Y, Okamoto K, Kadowaki T, Yamamoto K: Roles of Arg- and Lys-gingipains in coaggregation of *Porphyromonas gingivalis*: identification of its responsible molecules in translation products of rgpA, kgp, and hgaA genes. *Biol Chem* 2004, **385**(11):1041–1047.
46. Yamada M, Ikegami A, Kuramitsu HK: Synergistic biofilm formation by *Treponema denticola* and *Porphyromonas gingivalis*. *FEMS Microbiol Lett* 2005, **250**(2):271–277.
47. Andrian E, Grenier D, Rouabhi M: In vitro models of tissue penetration and destruction by *Porphyromonas gingivalis*. *Infect Immun* 2004, **72**(8):4689–4698.
48. Hojo K, Nagaoka S, Ohshima T, Maeda N: Bacterial interactions in dental biofilm development. *J Dent Res* 2009, **88**(11):982–990.
49. Kuramitsu HK, Chen W, Ikegami A: Biofilm formation by the periodontopathic bacteria *Treponema denticola* and *Porphyromonas gingivalis*. *J Periodontol* 2005, **76**(11 Suppl):2047–2051.

50. Zhu Y, Dashper SG, Chen YY, Crawford S, Slakeski N, Reynolds EC: *Porphyromonas gingivalis* and *Treponema denticola* synergistic polymicrobial biofilm development. *PLoS One* 2013, **8**(8):e71727.
51. Thurnheer T, Belibasakis GN, Bostanci N: Colonization of gingival epithelia by subgingival biofilms in vitro: role of "red complex" bacteria. *Arch Oral Biol* 2014, **59**(9):977–986.
52. Guggenheim B, Gmur R, Galicia JC, Stathopoulou PG, Benakanakere MR, Meier A, Thurnheer T, Kinane DF: In vitro modeling of host-parasite interactions: the 'subgingival' biofilm challenge of primary human epithelial cells. *BMC Microbiol* 2009, **9**:280.
53. Gmur R, Guggenheim B: Antigenic heterogeneity of *Bacteroides intermedius* as recognized by monoclonal antibodies. *Infect Immun* 1983, **42**(2):459–470.
54. Zuger J, Luthi-Schaller H, Gmur R: Uncultivated *Tannerella* BU045 and BU063 are slim segmented filamentous rods of high prevalence but low abundance in inflammatory disease-associated dental plaques. *Microbiology* 2007, **153**(Pt 11):3809–3816.
55. Thurnheer T, Gmur R, Guggenheim B: Multiplex FISH analysis of a six-species bacterial biofilm. *J Microbiol Methods* 2004, **56**(1):37–47.
56. Thurnheer T, Gmur R, Giertsens E, Guggenheim B: Automated fluorescent in situ hybridization for the specific detection and quantification of oral streptococci in dental plaque. *J Microbiol Methods* 2001, **44**(1):39–47.
57. Ammann TW, Bostanci N, Belibasakis GN, Thurnheer T: Validation of a quantitative real-time PCR assay and comparison with fluorescence microscopy and selective agar plate counting for species-specific quantification of an in vitro subgingival biofilm model. *J Periodontol Res* 2013, **48**(4):517–526.
58. Gmur R: *Value of New Serological Probes for the Study of Putative Periodontal Pathogens: A Survey after Five Years of Application*. Zurich: Dental Center of the University of Zurich; 1995:86.
59. Werner-Felmayer G, Guggenheim B, Gmur R: Production and characterization of monoclonal antibodies against *Bacteroides forsythus* and *Wolinella recta*. *J Dent Res* 1988, **67**(3):548–553.
60. Gmur R, Werner-Felmayer G, Guggenheim B: Production and characterization of monoclonal antibodies specific for *Bacteroides gingivalis*. *Oral Microbiol Immunol* 1988, **3**(4):181–186.
61. Thurnheer T, Guggenheim B, Gmur R: Characterization of monoclonal antibodies for rapid identification of *Actinomyces naeslundii* in clinical samples. *FEMS Microbiol Lett* 1997, **150**(2):255–262.

doi:10.1186/s12866-014-0258-7

Cite this article as: Bao et al.: Role of *Porphyromonas gingivalis* gingipains in multi-species biofilm formation. *BMC Microbiology* 2014 **14**:258.

**Submit your next manuscript to BioMed Central and take full advantage of:**

- Convenient online submission
- Thorough peer review
- No space constraints or color figure charges
- Immediate publication on acceptance
- Inclusion in PubMed, CAS, Scopus and Google Scholar
- Research which is freely available for redistribution

Submit your manuscript at  
www.biomedcentral.com/submit



# Paper 2



RESEARCH ARTICLE

# Quantitative Proteomics Reveal Distinct Protein Regulations Caused by *Aggregatibacter actinomycetemcomitans* within Subgingival Biofilms

Kai Bao<sup>1</sup>, Nagihan Bostanci<sup>1</sup>, Nathalie Selevsek<sup>2</sup>, Thomas Thurnheer<sup>3</sup>, Georgios N. Belibasakis<sup>3\*</sup>

**1** Oral Translational Research, Institute for Oral Biology, Center of Dental Medicine, University of Zurich, Zurich, Switzerland, **2** Functional Genomics Center Zurich, University of Zurich, Zurich, Switzerland, **3** Oral Microbiology and Immunology, Institute for Oral Biology, Center of Dental Medicine, University of Zurich, Zurich, Switzerland

\* [George.Belibasakis@zzm.uzh.ch](mailto:George.Belibasakis@zzm.uzh.ch)



## OPEN ACCESS

**Citation:** Bao K, Bostanci N, Selevsek N, Thurnheer T, Belibasakis GN (2015) Quantitative Proteomics Reveal Distinct Protein Regulations Caused by *Aggregatibacter actinomycetemcomitans* within Subgingival Biofilms. PLoS ONE 10(3): e0119222. doi:10.1371/journal.pone.0119222

**Academic Editor:** Özlem Yilmaz, University of Florida, UNITED STATES

**Received:** December 22, 2014

**Accepted:** January 26, 2015

**Published:** March 10, 2015

**Copyright:** © 2015 Bao et al. This is an open access article distributed under the terms of the [Creative Commons Attribution License](https://creativecommons.org/licenses/by/4.0/), which permits unrestricted use, distribution, and reproduction in any medium, provided the original author and source are credited.

**Data Availability Statement:** All relevant data are within the paper and its Supporting Information files.

**Funding:** The authors have no support or funding to report.

**Competing Interests:** The authors have declared that no competing interests exist.

## Abstract

Periodontitis is an infectious disease that causes the inflammatory destruction of the tooth-supporting (periodontal) tissues, caused by polymicrobial biofilm communities growing on the tooth surface. Aggressive periodontitis is strongly associated with the presence of *Aggregatibacter actinomycetemcomitans* in the subgingival biofilms. Nevertheless, whether and how *A. actinomycetemcomitans* orchestrates molecular changes within the biofilm is unclear. The aim of this work was to decipher the interactions between *A. actinomycetemcomitans* and other bacterial species in a multi-species biofilm using proteomic analysis. An *in vitro* 10-species “subgingival” biofilm model, or its derivative that included additionally *A. actinomycetemcomitans*, were anaerobically cultivated on hydroxyapatite discs for 64 h. When present, *A. actinomycetemcomitans* formed dense intra-species clumps within the biofilm mass, and did not affect the numbers of the other species in the biofilm. Liquid chromatography-tandem mass spectrometry was used to identify the proteomic content of the biofilm lysate. A total of 3225 and 3352 proteins were identified in the biofilm, in presence or absence of *A. actinomycetemcomitans*, respectively. Label-free quantitative proteomics revealed that 483 out of the 728 quantified bacterial proteins (excluding those of *A. actinomycetemcomitans*) were accordingly regulated. Interestingly, all quantified proteins from *Prevotella intermedia* were up-regulated, and most quantified proteins from *Campylobacter rectus*, *Streptococcus anginosus*, and *Porphyromonas gingivalis* were down-regulated in presence of *A. actinomycetemcomitans*. Enrichment of Gene Ontology pathway analysis showed that the regulated groups of proteins were responsible primarily for changes in the metabolic rate, the ferric iron-binding, and the 5S RNA binding capacities, on the universal biofilm level. While the presence of *A. actinomycetemcomitans* did not affect the numeric composition or absolute protein numbers of the other biofilm species, it caused qualitative changes in their overall protein expression profile. These molecular shifts within the biofilm



warrant further investigation on their potential impact on its virulence properties, and association with periodontal pathogenesis.

## Introduction

Oral biofilms play an important role in periodontal disease [1], a primary reason for human adult tooth loss [2]. With more than 700 species identified in the oral cavity [3], this biofilm presents a complex and dynamic ecosystem, whose growth is dictated by microenvironmental factors. As proof of concept, studies in murine models have demonstrated the multiple species biofilms display increased pathogenicity [4,5], reflecting the increased alveolar bone loss [6–8], which is the hallmark of periodontitis. Within a biofilm, the bacteria exert a significantly increased virulence and resistance to the host immune defences. Therefore, “traditional” experimental models that simply study single individual bacterial species might not be optimal to acknowledge the role of oral biofilms in periodontal diseases.

To understand the role of the oral biofilms in disease, it is necessary to unravel the relationships between their constituent species. Based on co-aggregation experiments, it is estimated that there can be numerous interactions between various microbial species of the human oral cavity [9]. Such aggregations reflect the formation of biofilms, both by defining the early colonizing events of the tooth surfaces, and generating optimal microenvironments for the later colonizing species [10]. Interestingly, in a multispecies biofilm model similar to the one employed in this study, it is shown that in the absence of the “early colonizing” species, the “late colonizing” species form different structures within the biofilm [11]. A number of experimental studies were also performed to investigate the detailed effects of virulence factors of one species to another, within a multi-species biofilm community. For example, BspA protein from *Tannerella forsythia* favours the co-aggregation with *Fusobacterium nucleatum* [12], whereas the lysine and arginine gingipains of *Porphyromonas gingivalis* regulated the growth of *T. forsythia* [13] and of *Treponema denticola* [13,14], respectively; *Aggregatibacter actinomycetemcomitans* utilizes L-lactate from *Streptococcus gordonii* as energy source [15]. However, not all relationships within biofilms are synergistic. For example, streptococcal arginine deiminase inhibits the expression of fimA from *Porphyromonas gingivalis* and thus abrogates colonization [16]; AI-2 of *A. actinomycetemcomitans* inhibits biofilm formation of *Candida albicans* [17]. Still, most of the models used to investigate inter-species associations involve pair-wise bacterial comparisons, and the obtained data might be an oversimplified version of the reality. Using multi-species biofilm models may be closer to the *in vivo* situation, and may allow for the extrapolation of biological data that is more clinically relevant. In recent years, a 10-species *in vitro* “subgingival” biofilm model has been established and optimized in order to address such issues [11,18–22]. In the present study, this model was evolved further to incorporate *A. actinomycetemcomitans*, a highly leukotoxic species that is strongly associated with aggressive forms of periodontitis occurring among young individuals [23]. The many virulence factors of *A. actinomycetemcomitans* identified are its putative “weapons” against the host immune armament, including polymorphonuclear leukocytes, T-lymphocytes and macrophages [24]. In a biofilm environment, these functions may not only be favouring *A. actinomycetemcomitans* itself, but might also support all other species in the biofilm in escaping the host immune system. Besides, this bacterium affects other species commonly found in subgingival biofilms, including *P. gingivalis* [25] and *F. nucleatum* [26]. As suggested by Hajishengallis et al [27,28], a keystone pathogen for periodontal infection might not actually be the dominant species within the biofilm,

but may induce changes in other constituent species. Deciphering the protein regulations across the biofilm could therefore be crucial in understanding the role of the individual species in the integrity and function of the biofilm. Yet, most studies have addressed the role of only one or a handful of proteins, rather than the overall protein profile in a biofilm.

Proteomics provide an important novel approach to extract detailed information of cellular regulatory mechanisms on the protein level at a large scale. With the utilization of mass spectrometry-based technologies, it is possible to identify and quantify thousands of proteins from complex biological samples in one run [29–32]. In a biofilm environment, this tool could not only support the identification of regulatory proteins, but also evaluate the trend of their regulation at a universal level. Based on the above considerations, a label-free quantitative proteomic approach was employed to quantify the protein expressions and cluster their functions, in an 11-species *in vitro* “subgingival” biofilm, or its 10-species variant lacking *A. actinomycetemcomitans*. Hence, by inference, the relative regulatory roles of *A. actinomycetemcomitans* in the biofilm were deduced.

## Results

### *Aggregatibacter actinomycetemcomitans* forms dense clusters without altering the composition of the other species alters in the biofilm

Upon completion formation after 64 h, the biofilms were either kept intact for the confocal laser scanning microscopy (CLSM) analysis or harvested in suspensions for further quantification. The numbers for each individual species within the 11-species biofilm with 10-species biofilm (with or without *A. actinomycetemcomitans*, respectively) were quantified using quantitative real-time polymerase chain reaction (qPCR) (Table 1). Interestingly, the t-tests indicated that there were no significant ( $P < 0.01$ ) differences in the numbers of each individual bacterial species within the biofilms, irrespective of the presence or absence of *A. actinomycetemcomitans*. To further study the localization of *A. actinomycetemcomitans* within the biofilm, the biofilm structure was investigated by CLSM (Fig. 1). It was demonstrated that *A. actinomycetemcomitans* formed dense clumps, or aggregates, with its own species.

**Table 1. Quantitative composition of the 11-species or 10-species biofilm after 64 h cultivation.**

Species	11-species biofilm		10-species biofilm	
	Mean <sup>1</sup>	SD	Mean <sup>1</sup>	SD
<i>A. actinomycetemcomitans</i>	3.76E+08	1.17E+08	-	-
<i>A. oris</i>	2.37E+08	3.99E+07	1.01E+08	4.10E+07
<i>F. nucleatum</i>	9.04E+09	5.11E+08	6.02E+09	3.20E+09
<i>C. rectus</i>	9.14E+08	9.36E+07	1.55E+09	8.07E+08
<i>P. gingivalis</i>	8.14E+07	2.40E+07	3.25E+08	3.44E+08
<i>P. intermedia</i>	5.58E+09	1.72E+09	1.22E+09	8.48E+08
<i>S. anginosus</i>	1.66E+09	4.45E+08	1.88E+09	1.28E+09
<i>S. oralis</i>	4.22E+09	4.19E+08	2.60E+09	1.35E+09
<i>T. denticola</i>	3.96E+07	1.03E+07	3.91E+07	2.73E+07
<i>T. forsythia</i>	5.64E+06	3.37E+06	3.71E+06	3.95E+06
<i>V. dispar</i>	8.20E+09	9.96E+08	3.64E+09	1.69E+09

1:Quantification was performed used qPCR for each species. The data is expressed as the bacterial mean counts  $\pm$  standard deviation (SD) from triplicate biofilm cultures. No statistical differences ( $P \leq 0.01$ ) of between the groups were found within the same species by student t-test.

doi:10.1371/journal.pone.0119222.t001



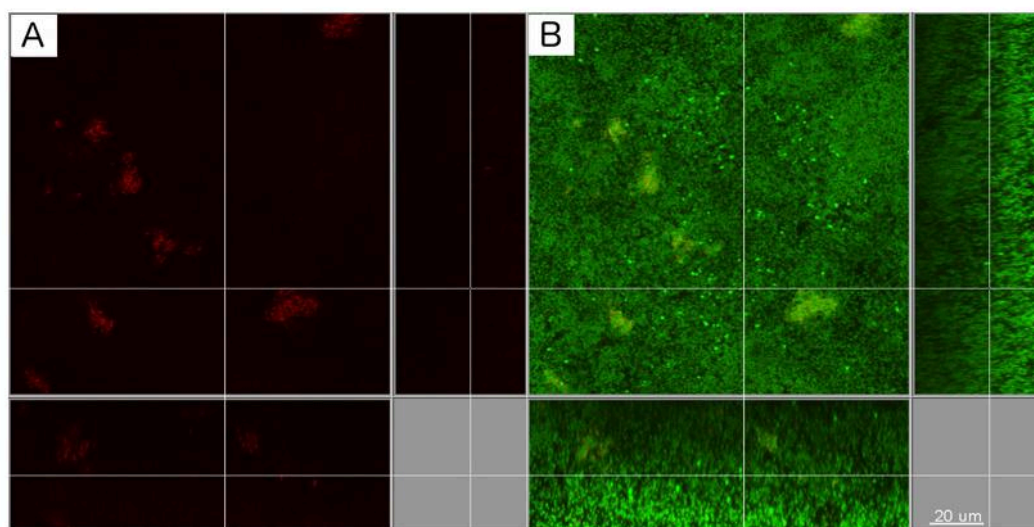


**Fig 1. Localization of *A. actinomycetemcomitans* within the biofilms.** (A) *A. actinomycetemcomitans* cells were stained by fluorescence *in situ* hybridization using Cy3-labelled 16 S rRNA oligonucleotide probe Act 639 (red), (B) *A. actinomycetemcomitans* cells (red) and rest of the biofilm cells was counter stained with a mixture of YoPro-1 iodide and Sytox Green (green). Scale bar length: 20  $\mu$ m.

doi:10.1371/journal.pone.0119222.g001

### *Aggregatibacter actinomycetemcomitans* causes shifts in the numbers of others species' detectable proteins in the biofilm

Total protein was extracted from biofilm suspensions for global proteomic characterization of the differences between the two forms of biofilms, each with biological triplicates. It was found that a total of 3225 and 3352 proteins (two or more peptides) were identified in the 11-species biofilm and the 10-species biofilm, respectively, with corresponding false discovery rates (FDR) of 1.5% and 1.3%. The protein detection overlaps (i.e. similar proteins detected) between these two biofilm groups is shown in Fig. 2. In brief, 80.29% of the identified proteins appeared in both biofilm groups. The species-specific taxonomy of the identified protein numbers are provided in Table 2, whereas S1 Table presents the detailed information of total unique peptide counts and the annotations for each identified protein. The greatest overlap of proteins between the two kinds of biofilm was from *Fusobacterium nucleatum* (832 proteins). Interestingly, no uniquely identified proteins were detected for *P. intermedia*, in the absence of *A. actinomycetemcomitans* from the biofilm, while in its presence 117 proteins were uniquely identified. Accordingly, 95 proteins of *P. gingivalis* were uniquely identified in the 10-species biofilm lacking *A. actinomycetemcomitans*, while only 3 were uniquely identified in its presence in the 11-species biofilm. Of note, less than 10 proteins were identified for *A. oris* and *T. forsythia*, and less than 30 proteins for *T. denticola* in either of the biofilms, indicating that these species may be underrepresented in the corresponding databases. It is less likely that the proteins are underrepresented in the biofilm, as *T. forsythia* is numerically present at high levels in both biofilms (Table 1).

### *Aggregatibacter actinomycetemcomitans* alters the protein abundance of other species present in the biofilm

Label free quantification was used to analyse protein expressions between 11-species biofilm and its 10-species variant, lacking *A. actinomycetemcomitans*). A true regulation was considered when there was more than 2-fold difference in the levels of a given protein between the

# 11 species biofilm 10 species biofilm

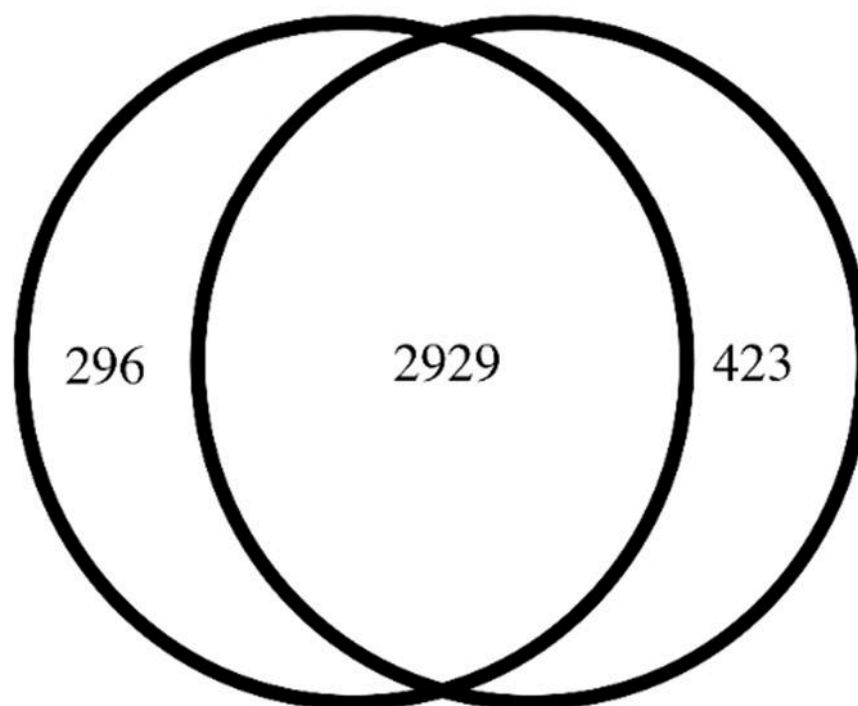


**Fig 2. Venn diagram of identified proteins and their overlapping groups between the 11-species and 10-species biofilm.** Protein numbers for each category were listed. Details of proteins in each group were listed in [S1 Table](#).

doi:10.1371/journal.pone.0119222.g002

two groups, with  $p < 0.05$ . Reproducibility between biological triplicates was evaluated using squared Pearson correlation coefficients ( $R^2$ ) of integrated peptide feature intensities. The  $R^2$  ranged between 0.95–0.96 in the 11 species biofilm group, and between 0.83–0.9 in the 10 species biofilm group, whereas this value was 0.84 between these two kinds of biofilm groups ([Fig. 3](#)).

**Table 2. Number of uniquely identified and overlapping proteins per species in two biofilm groups.**

Species	11-species	Overlap	10-species
<i>A. actinomycetemcomitans</i>	97	13	1
<i>A. oris</i>	1	5	3
<i>F. nucleatum</i>	5	256	105
<i>C. rectus</i>	22	832	43
<i>P. gingivalis</i>	3	43	95
<i>P. intermedia</i>	117	299	0
<i>S. anginosus</i>	2	268	98
<i>S. oralis</i>	4	417	26
<i>T. denticola</i>	2	4	1
<i>T. forsythia</i>	5	19	4
<i>V. dispar</i>	31	632	2
<i>H. sapiens</i>	7	141	45

doi:10.1371/journal.pone.0119222.t002

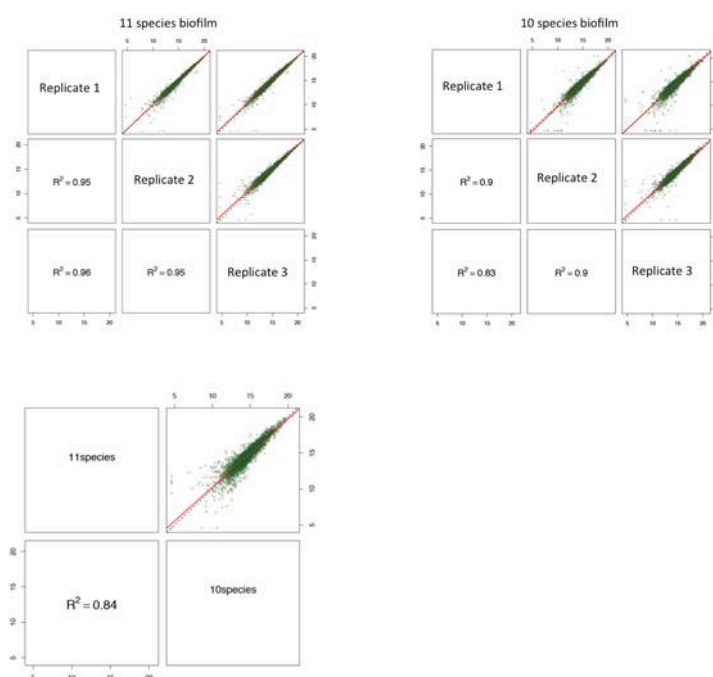


**Fig 3. Quality control of the label-free quantitation data.** Squared Pearson correlation coefficients ( $R^2$ ) of integrated peptide feature intensities are displayed for the comparisons within biological triplicates per biofilm group, and between the two biofilm groups. The linear regressions of the integrated peptide feature intensities of different conditions are indicated in red, whereas the dashed lines correspond to direct proportionality.

doi:10.1371/journal.pone.0119222.g003

A total of 790 proteins were identified, 278 of these were up-regulated in the 11-species biofilm compared with the 10-species biofilm, while 259 of these were down-regulated. The species-specific taxonomy of the numbers for identified proteins is provided in Table 3, whereas S2 Table presents the detailed information of the each corresponding protein. In brief, with the exception of *A. actinomycetemcomitans*, most of the up-regulated proteins in the 11-species

**Table 3. Number of label-free quantified proteins per species between two biofilm groups.**

Species	Up-regulated	Un-regulated	Down-regulated
<i>A. actinomycetemcomitans</i>	46	2	0
<i>A. oris</i>	0	0	1
<i>C. rectus</i>	0	67	84
<i>F. nucleatum</i>	5	25	9
<i>P. gingivalis</i>	1	2	53
<i>P. intermedia</i>	199	56	0
<i>S. anginosus</i>	0	33	96
<i>S. oralis</i>	5	4	3
<i>T. denticola</i>	2	0	0
<i>V. dispar</i>	19	58	6
<i>H. sapiens</i>	1	6	7

In comparing the 11-species versus the 10-species biofilm, the proteins are defined as up-regulated, un-regulated or down-regulated. A significant ( $p < 0.05$ ) difference of 2-fold in protein levels was defined as "regulation".

doi:10.1371/journal.pone.0119222.t003



biofilm belonged to *Prevotella intermedia* and *Veillonella dispar*, On the contrary, most down-regulated proteins belonged to *Porphyromonas gingivalis*, *Campylobacter rectus* and *Streptococcus anginosus*. Of note, no quantifiable proteins were available in the case of *T. forsythia*.

### *Aggregatibacter actinomycetemcomitans* causes distinctive changes in the functional ontology of quantified biofilm proteins

Following the label-free quantification, the functions of the regulated bacterial proteins were enriched according to Gene Ontology (GO) terms, with their redundant GO terms summarized and unified (Fig. 4). A total of 301, 148, and 90 GO terms for molecular function, biological process, and cellular component, respectively, were generated based upon the up-regulated

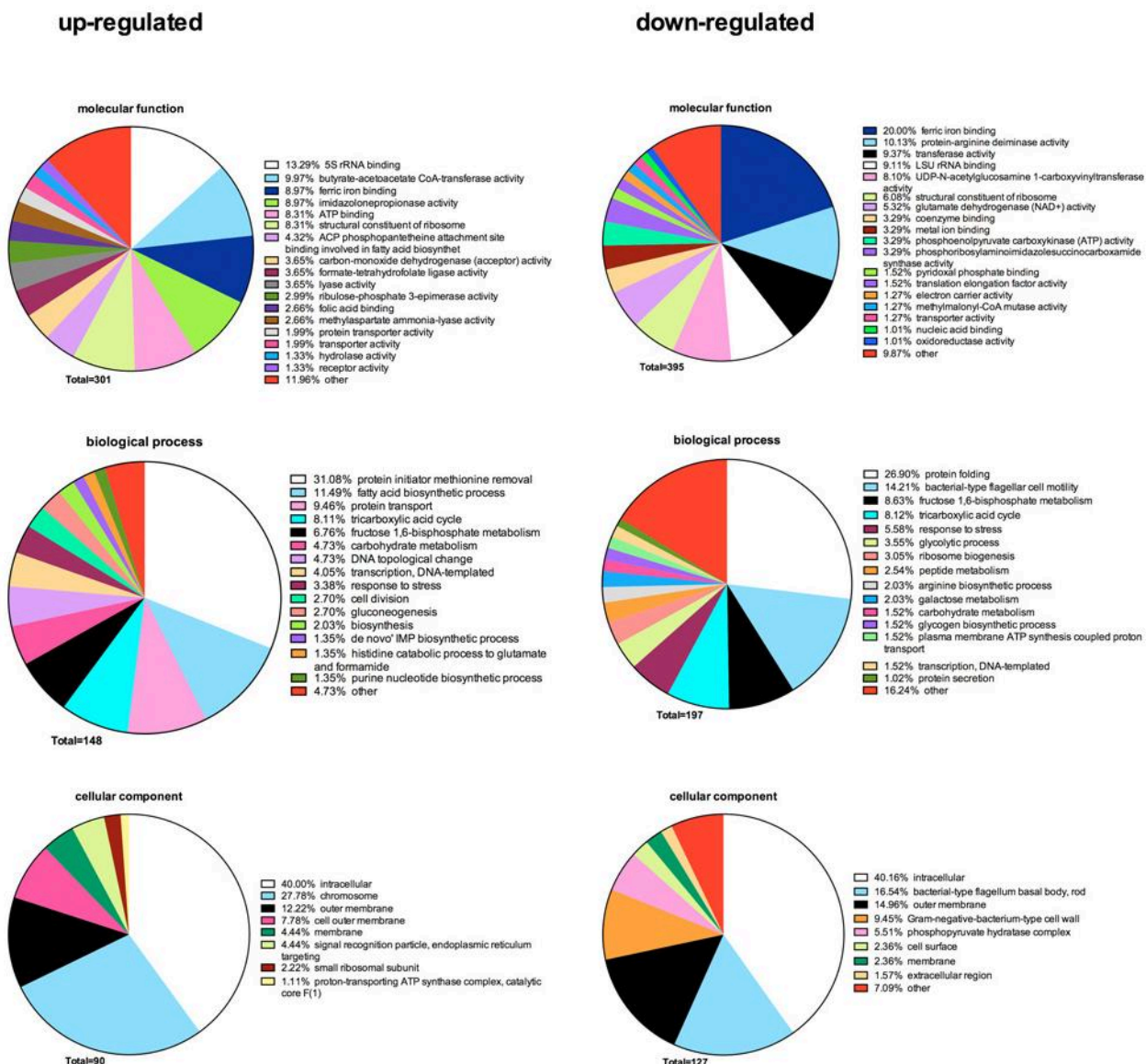


**Fig 4. Annotation of overall regulated bacterial protein functions by enrichment of Gene Ontology (GO) terms.** Based on the classifications of GO annotation, the overall bacterial functions were categorized into biological process, molecular function, and cellular component, and displayed in pie chart format. The numbers of GO terms for each of the three categories are shown, whereas the proportion of each specific subcategory is also provided. Subcategories with GO terms less than 1% are classified as "other".

doi:10.1371/journal.pone.0119222.g004

proteins between 11-species biofilms and 10-species biofilms. On the contrary, based upon the down-regulated proteins, a total of 395, 197, and 127 GO terms were generated accordingly. Among GO terms of molecular function, “5S rRNA binding” (13.29%) was the most common function in up-regulated proteins in the presence of *A. actinomycetemcomitans* (11-species biofilm), while for down-regulated proteins, the most common function was “ferric iron binding” (20.00%), followed by “protein-arginine deiminase activity” (10.13%). Among GO terms of biological process, the most common up-regulated proteins belonged to “protein initiator methionine removal” (31.08%), while the most common down-regulated ones belonged to “protein folding” (26.90%). Regarding their cellular localization, more than 50% of up- and down-regulated proteins accounted for the intracellular/membrane-associated fraction.

## Discussion

With the increasing numbers of identified bacteria in oral biofilms, there are increasing needs in understanding their individual or communal functions. Consequently, contemporary research in the field focuses on the study of oral biofilm communities as a whole unit [13,21,33], rather than on individual bacterial species. Hence, by using proteomic approaches, this study aimed at elucidating the particular effects of *A. actinomycetemcomitans* in a multi-species *in vitro* bacterial community.

An elevated number of *A. actinomycetemcomitans* is associated with the aggressive form of periodontal disease in a longitudinal manner [23]. Thus, it is rational to postulate that, given its high specificity to aggressive periodontitis, this species may play an important role in orchestrating its microbial counterparts within a complex subgingival biofilm community. To this extent, previous experiments showed that it could integrate into a 6-species *in vitro* oral biofilm without dramatically changing the proportions of the other bacteria [34]. This was also the case in the present 11-species “subgingival” biofilm in experimental model, as it did not significantly affect the numbers of the other species present.

Interestingly, however, trends of protein regulations within the biofilm were distinct between individual constituent species. In the presence of *A. actinomycetemcomitans*, all regulated proteins of *P. intermedia* were found to be up-regulated, while all the regulated proteins of *C. rectus* and *S. anginosus* were found to be down-regulated. In the case of *P. gingivalis*, the vast majority of the quantified proteins were reduced in the presence of *A. actinomycetemcomitans*. Accordingly, both identification and label-free quantification data in this work indicate that *A. actinomycetemcomitans* regulates protein expression of other species present in the biofilm, although it may not directly reflect changes in bacterial numbers. These findings are perhaps in line with a recent report showing whole cell proteomic interactions between *P. gingivalis* and *F. nucleatum*: despite the close proximity in absolute numbers, qualitative changes were observed in protein composition, including reductions in proteins associated with amino-acid fermentation, glycolysis, translation, and biosynthesis of lipopolysaccharide as well as cell wall [29].

Both *P. intermedia* and *P. gingivalis* are black-pigmented bacteroides. Yet, in the present study, *A. actinomycetemcomitans* appears to have a differential effect in their proteomic biofilm interactions, causing an increase of all detected proteins in *P. intermedia* and decrease in almost all proteins in *P. gingivalis*. This finding could be of clinical relevance, as both *P. intermedia* and *A. actinomycetemcomitans* display a significant association with periodontal tissue breakdown [35]. *P. gingivalis* and *A. actinomycetemcomitans* can be isolated from different hosts, despite that both bacteria strongly associate with periodontal disease [36,37], and can in fact trigger distinctive pathogenic pathways [38]. Still, *P. gingivalis* displays aggregation properties with *A. actinomycetemcomitans* [39], and shows a competitive advantage over [40], or a



mutualistic relationship with the latter [25]. Since aggregation between many bacteria used in our model are shown in dual species co-cultures [9], it is well possible that *A. actinomycetemcomitans* might not directly cause the differential regulation of proteins observed in the biofilm by its presence, but could rather work as a keystone bacterium that orchestrates the interaction between other constituted species. Such a role has already been described for and attributed to *P. gingivalis* [27,41,42].

As oral biofilms are polymicrobial and dynamic [1,43], both the genomic and proteomic profiles of the involved bacterial species are expressed differently from those in planktonic state [44]. Therefore, it makes more sense to consider the nature of expressed proteins, rather than numbers of each bacterial species in a biofilm. Interspecies signals should also be taken into count. For instance, autoinducer-2 (AI-2) produced by *S. oralis* is essential for the nutrition of *A. oris* [45], and AI-2 receptors were also found on *A. actinomycetemcomitans* [46]. To investigate the overall functions of the biofilm, the interpretation of all the regulated proteins should be evaluated as a whole rather than studied separately [47]. For this purpose, the protein profiles of the two forms of biofilm variants used in this study were pooled together in pursuing their regulated functions, including potential regulatory proteins for quorum sensing and mobile genetic elements. Different conjugative transposons are widespread in oral bacteria, including streptococci, *Veillonella* sp., *P. gingivalis*, *A. actinomycetemcomitans*, and *F. nucleatum* [48], and even horizontal gene transfer is common to oral biofilms [49]. Hence, the database used in this study contained all PubMed-retrieved protein information from each species, in order to avoid lost protein annotation. According to Uniprot, a universal protein resource with protein data created by combining the Swiss-Prot, TrEMBL and PIR-PSD databases, the final list of label-free quantified proteins comprised 96.4% of un-reviewed proteins, which are normally not accepted in most online functional annotation tools. Consequently, to give a general overview of the whole biofilm proteome in this case, we manually enriched all the GO terms for the label-free quantified proteins with Reduce + Visualize Gene Ontology (REVIGO) software, following the neighbour-joining method [50].

Based on the structured terminology of GO itself, all functions were divided into three separate ontologies: a) molecular function, b) biological process, and c) cell component. Only 3 out of 33 regulated GO molecular functions from label-free quantified proteins were enriched in both biofilms, which indicated that *A. actinomycetemcomitans* might have distinct effects on different molecular functions of the biofilm in general. Ferric iron binding, the most common down-regulated molecular function in the present *A. actinomycetemcomitans*-containing biofilm, was also as the fourth most common up-regulated molecular function, indicating a complex regulation among proteins of this category. Interestingly, regulation of ferric iron binding proteins has also been observed previously within a 3-species biofilm model [51]. This regulatory trend may not be surprising, as in the closed environment of the periodontal pocket, subgingival bacteria (including the ones used in this study) could utilize alternative, yet equally effective, iron-acquiring mechanisms in order to digest the host iron-containing proteins. For example, *A. actinomycetemcomitans* binds to lactoferrin and haemoglobin [52], *T. denticola* develops outer membrane protein HbpA with hemin binding ability [53], *P. gingivalis* employs specific outer membrane receptors, proteases, and lipoproteins for iron acquiring [54,55], and regulates the respective host cells responses [56]. Of note, gingipains, ferric iron binding proteases of *P. gingivalis*, including arginine-specific cysteine proteinase and lysine-specific cysteine proteinase, are also considered as virulence factors except for their hemin digestion ability [37]. Both gingipains were indeed found in Scaffold identification in the present study, with more peptides identified in the 10-species biofilm lacking *A. actinomycetemcomitans*. Hence, in the presence of this species, *P. gingivalis* gingipains may become more redundant for the entire biofilm community, as other factors of *A. actinomycetemcomitans* may also compensate for their



iron-acquisition functions. As such, leukotoxin, a virulence factor of *A. actinomycetemcomitans*, is not only regulated in the presence of iron, but may also be involved in ferric iron acquisition [57]. Consequently, the overall turmoil of ferric iron-binding protein regulation within the biofilm might also affect the overall virulence of the biofilm towards the host tissue.

Apart from its involvement in ferric iron-binding related proteins, the present findings show that *A. actinomycetemcomitans* regulated the metabolic rate within the biofilm. The most common up-regulated molecular function in the 11-species biofilm, compared to its 10-species variant, was that of 5S RNA binding. This enriched protein function of structural ribosomal constituents and the fact that more proteins were identified from the small ribosome subunit (in cell component category), could easily be interpreted as an increase of bacterial growth [58]; however, given the fact that although the biofilms are cultured under stable growth conditions [59] they do not display differences in bacterial numbers irrespective of the presence of *A. actinomycetemcomitans*, increased bacterial growth within the 11-species biofilm is an unlikely explanation for this observation. The increase of the ribosome content is rather explained by increased protein transport, fatty acid biosynthetic process, and protein initiator methionine removal, as also observed in the up-regulated biological process category. Indeed, around 3% more GO terms responsible for cell division were identified, but this might be counter-balanced by decreased ribosome biogenesis and protein folding processes.

An altered metabolic rate was observed in an earlier study in a 3-species biofilm model [29,60,61], a trend that was also shown in this experimental model. In the presence of *A. actinomycetemcomitans* in the biofilm, biological processes like tricarboxylic acid cycle, fructose 1,6-bisphosphate metabolism, and carbohydrate metabolism were enriched. By the present approach, it is not quite feasible to attribute these proteomic changes to one or another individual species, so at this stage they would have to be considered as a universal biofilm shift. Of note, fructose 1,6-bisphosphate metabolism and carbohydrate metabolism were 2 of the 5 biological processes shared between these two kinds of biofilm variants (i.e. with or without *A. actinomycetemcomitans*). These two GO entities, together with glycolytic process, galactose metabolism, and arginine biosynthetic process, were enriched in absence of *A. actinomycetemcomitans*, indicating a strong alternation in the metabolic pathways of the biofilm. This may not be surprising, as for example, *A. actinomycetemcomitans* may utilize lactate from streptococci as energy source [15,62]. On the other hand, many glucose transports in *A. actinomycetemcomitans* can also be inhibited, as consequence of using lactate as carbon source [62]. These inhibited processes include a phosphoenolpyruvate (PEP): carbohydrate phosphotransferase system (PTS) [62], a bacterial unique system for concomitant transport and phosphorylation of carbohydrates in many species [63,64]. Among all our identified proteins, 2, 4, 12, 7, and 1 PTS proteins were identified from *A. actinomycetemcomitans*, *F. nucleatum*, *S. anginosus*, *S. oralis*, *V. dispar*, respectively, while based on the label-free data, all the non-*A. actinomycetemcomitans* PST proteins were identified as *S. anginosus*-derived, with 1 un-regulated and 4 down-regulated proteins. Regulation of these proteins definitely affected the output of the related GO function categories. Apart from direct effects of the PST regulation, other driving forces of selecting different organisms as consequence of *A. actinomycetemcomitans* utilizing lactate from streptococci, including shifts in pH (as an effect of lactate digestion) [65] and regulating quorum sensing factor AI-2 by PTS [66], may also contribute in biofilm formation and growth. In the context of a multiple species biofilm, such as the one used in this study, all the interactions between species become very complex and intricate. Therefore, understanding these interactions as a whole unit is not only more biologically reliable, but also a more efficient way to start deciphering biologically meaningful explanations.

The cellular localization category analysis for the most up- or down- regulated proteins delivered fractions associated with the intracellular/membrane component, with more than half



of the identified GO terms falling into these categories. This indicated that *A. actinomycetemcomitans* could have a strong effect on mobilization of proteins in the bacterial cell compartments within the biofilm. Since by the present experimental approach we did not investigate the secreted protein fractions of the biofilm, it has not been possible to evaluate the overall turnover of extracellular proteins in the biofilm.

Elucidating the roles of specific bacterial species in a multiple species biofilm is a hard but eventually necessary task in understanding a biofilm as a community. The updated proteomic technologies provide powerful tools to understanding biofilms in a more detailed manner than earlier approaches [29,51,60,61]. Rather than identifying a panacea for the control of oral biofilms, the present study revealed shifts in the proteomic composition and functions within a complex *in vitro* biofilm environment, particularly focusing on the ecological pressures exerted by *A. actinomycetemcomitans* in the remainders of the bacterial community. On a further step, this type of analysis might be more meaningful if combined with a specific biological question (e.g whether ferric iron-binding-related functions are affected by *A. actinomycetemcomitans*), or in a co-culture system with host tissues, where one can more clearly predict the specific bacterial proteins in relation to their healthy or deleterious impact on the human host.

## Materials and Methods

### *In vitro* biofilm formation and harvesting

The 11-species biofilm used in this study included the following species: *Prevotella intermedia* ATCC 25611T (OMZ 278), *Aggregatibacter actinomycetemcomitans* JP2 (OMZ 295), *Campylobacter rectus* (OMZ 398), *Veillonella dispar* ATCC 17748T (OMZ 493), *Fusobacterium nucleatum subsp. nucleatum* (OMZ 598), *Streptococcus oralis* SK248 (OMZ 607), *Treponema denticola* ATCC 35405T (OMZ 661), *Actinomyces oris* (OMZ 745), *Streptococcus anginosus* ATCC 9895 (OMZ 871), *Tannerella forsythia* (OMZ 1047) and *Porphyromonas gingivalis* W50 (OMZ 308) was established. In parallel, the 10-species variant of this biofilm, lacking *A. actinomycetemcomitans* was also generated. The biofilms were grown in 24-well polystyrene cell culture plates on hydroxyapatite discs (diameter 13 mm). Briefly, 200  $\mu$ l of bacterial cell suspensions containing equal densities ( $OD_{550} = 1.0$ ) of each strain were mixed with 1.6 ml of growth medium consisting 60% saliva [67], 10% human serum, 30% modified fluid universal medium (mFUM) and 0.5% hemin to initiate biofilm formation. mFUM is a well-established tryptone-yeast-based broth medium designated as FUM [68] and modified by supplementing 67 mM Sørensen's buffer (final pH 7.2). After 16 h of incubation in anaerobic conditions, additional 40  $\mu$ l of *T. denticola* ( $OD_{550} = 1.0$ ) were added to each well. The discs were further incubated 48 h until the biofilm was ready to be harvested (i.e total 64 h). During this period, the hydroxyapatite discs on which the biofilms were grown were dip-washed in 0.9% w/v of NaCl at 16 h, 20 h, 24 h, 40 h, 44 h, 48 h and 64 h, with the medium replenished at 16 h and 40 h, respectively.

For image analysis, the discs were put in wells containing 4% paraformaldehyde for at least 60 min for the fixation of the biofilms. For further analyses the rest of the biofilms was collected by vigorous vortexing for 3 min with 1 ml 0.9% w/v of NaCl, and then sonicated at 25 W for 5 seconds to obtain fine suspensions. These were then stored at -20°C before being processed for further analysis.

### Confocal laser scanning microscopy and image analysis

The localization pattern of *A. actinomycetemcomitans* within the biofilm structure was evaluated by CLSM. Briefly, the biofilm-containing discs stained by fluorescence *in situ* hybridization (FISH) using the Cy3-labelled *A. actinomycetemcomitans* 16S rRNA oligonucleotide probe Act639 (sequence from 5' to 3': CTCCAGACCCCCAGTATG, formamide concentration: 40%,

NaCl concentration in wash buffer: 46mM) [34] and counter stained with YoPro-1 iodide and Sytox Green following the protocol described before [13]. A Leica SP-5 microscope (Center of Microscopy and Image Analysis of the University of Zürich), with a resonant scanner system (8000 Hz), an argon laser (458 nm/476 nm/488 nm/496 nm/514 nm excitation), and a helium neon laser (561 nm/594 nm/633 nm excitation) was used for visualization. Filters were set to 500–540 nm and to 570–630 nm, for the detection of green colour from YoPro-1 iodide & Sytox Green mixture and Cy3, respectively. All images were captured using a 63 × objective (glycerol immersion, NA 1.3). Stacked images were further processed using the Imaris 7.4.0 software (Bitplane), in order to virtually reconstruct the structure of the biofilm.

### Biofilm species quantification by quantitative real-time polymerase chain reaction (qPCR)

For individual species quantification in the biofilm, DNA was extracted from the bacterial suspensions using the GenElute bacterial genomic DNA kit (Sigma-Aldrich), as described before (Bao et al Virulence 2015). The qPCR assay was performed using SYBR Green PCR Master Mix (Life Technologies) in a StepOnePlus Real-Time PCR System (Applied Biosystems) with primers were designed using online NCBI/ Primer-BLAST tool (<http://www.ncbi.nlm.nih.gov/tools/primer-blast>), targeting the species-specific 16S rRNA gene (S3 Table). The numbers of each species were calculated on standard curves that were generated using extracted bacterial DNA of the corresponding planktonic cultures, and the theoretical genome weight of each organism from each strain according to the NCBI database as previous described [19].

### Protein extraction from biofilm pellet

The proteomic analysis was performed on the biofilm bacterial cell lysates from both biofilm variants, each represented in three biological triplicates. For this purpose, biofilm pellets were collected by centrifugation at 14,000 g for 15 min at room temperature, suspended with 30 µl of lysis buffer containing 4% w/v Sodium Dodecyl Sulfate (SDS), 0.1 mM dithiothreitol and 100 mM Tris-HCl pH 8.2, and incubated for 5 min at 95°C. High intensity focused ultrasound (UTR2000, Hielscher) was performed to lyse the bacterial pellets with 3 cycles of 3 min each, 0.5 cycle for intervals, and 65% ultrasonic amplitude. To avoid over-heating of the material, the samples were kept in an ice bath during the ultrasonic process and in wet ice for 3 min after each ultra-sonication cycle.

### Protein digestion and C18 clean up

After lysis, the protein concentrations from both biofilm variants, each represented by biological triplicates, were measured with Qubit Protein Assay Kit (Life Technologies). Then, 20 µg of extracted bacterial protein were subjected to ultrafiltration for filter device with relative molecular mass (Mr) cut-offs of 30,000 (30k filter) to efficiently retain proteins and allow removal of impurities following the similar protocol of Wisniewski et al [69] with minor modifications described below. Briefly, 200 µl of 8M urea in 100 mM Tris/HCl buffer (pH 8.2) were added and the samples were centrifuged at 14,000g for 20 min at 35°C. This step was repeated once. Then 100 µl of urea buffer with additional 0.05 M iodacetamide was added to the filters and centrifuged at 14,000 g for 20 min at 35°C. Filters were washed three times with 100 µl urea buffer and followed by two washes with 100 µl of 0.5 M NaCl at 14,000g for 17 min at 35°C. Proteins were digested in 120 µl of 0.05M Triethylammoniumbicarbonat (TEAB) using trypsin (Promega) at enzyme to protein ratio of 1:40 in wet-cell chamber overnight. The peptides were collected by centrifugation at 14,000g for 20 min. Digestion was stopped by adding trifluoroacetic acid (TFA) to a final concentration of 0.5% and diluted with 400ul 3% acetonitrile in 0.1% TFA



to optimal the binding volume. Peptide mixtures were desalted using reverse phase cartridges Finissterre SPE C18 (Wicom International AG) according to the following procedure: cartridge was wet with 1 ml of 100% methanol, washed with 1 ml 60% of acetonitrile (ACN) in 0.1% TFA, equilibrated with 2 ml of 3% ACN in 0.1% TFA, load-acidified digested, washed with 6 ml of 3% ACN in 0.1% TFA, and eluted with 0.5 ml of 60% ACN in 0.1% TFA. Peptides were dried using a vacuum centrifuge, resolubilized with 30  $\mu$ l 3% ACN in 0.1% formic acid, and frozen at  $-20^{\circ}\text{C}$ , until further use.

## LC-MS/MS analysis and database search

Tryptic peptides of obtained from the biofilm lysates were analyzed on a Q-Exact mass spectrometer (Thermo Fisher Scientific). Chromatographic separation of peptides was performed on an Easy nano-flow HPLC system (Thermo Fisher Scientific) coupled to a 15 cm fused silica emitter, 75  $\mu$ m diameter, packed with a ReproSil-Pur C18-AQ 120 A and 1.9  $\mu$ m resin (Dr. Maisch HPLC GmbH). Peptides were loaded on the column and separated with a linear gradient of acetonitrile/water, containing 0.1% formic acid, at a flow rate of 300 nl/min. A gradient from 2 to 35% acetonitrile in 120 minutes was used. Mass spectra were acquired in a data-dependent manner, with an automatic switch between MS and MS/MS using a top 12 method. MS spectra were acquired in the Orbitrap analyzer with a mass range of 300–1700  $m/z$ . Higher energy collisional dissociation (HCD) peptide fragments, acquired at 28 normalized collision energy, were analyzed at high resolution in the Orbitrap.

## Database search analysis and label-free quantification

Each file was searched with Mascot (version 2.4.1) against a database (containing 634157 sequence, 207,052,936 residues) consisting of *Homo sapiens* database (including isoforms) from Uniprot (release date 22 May 2014, containing 88,708 forward sequences and 88,708 reverse sequence as decoy), all protein lists the 11 bacterial species from NCBI database (release date 28 February 2014, containing 228,240 forward sequences and 228,240 reverse sequence as decoy), and a contaminates database with 261 sequences. The precursor ion tolerance was set to  $\pm 10$  ppm and a fragment-ion mass tolerance of  $\pm 0.05$  Da. For the search criteria, tryptic digests were allowed, up to 2 missed cleavages per peptide, carbamidomethylation (C) as a fixed modification on cysteine, and oxidation (M) as variable modification on methionine residues.

For the protein identification, the Mascot research results of the biofilms were imported into Scaffold (version Scaffold\_4.2.1, Proteome software) to validate MS/MS-based peptide and protein identifications with protein threshold: 3.0% FDR for protein threshold, 2 minimal peptides, and 1.0% FDR for peptide threshold.

For the label-free quantification, the Mascot search results were imported back to Progenesis LC—MS software (Nonlinear Dynamics) for feature detection, alignment, and quantification. The proteins identified by similar sets of peptides were grouped and only non-conflicting peptides with specific sequences for single proteins in the database were employed for protein quantification. All the exported files were further processed using Mascot, Scaffold, and imported back to Progenesis before loading the final protein reports to SafeQuant (v.1.0.1) for the statistical validation. The statistical significance of each ratio was given by its  $q$ -value ( $q < 0.05$  significance level), obtained by calculating modified  $t$ -statistic  $P$  values [70] and adjusting for multiple testing [71].

## Ontology analysis

The lists of regulated protein identifications (Uniprot IDs) from SafeQuant, with  $q$  values less than 0.05 and  $\log_2$  ratios more than 1 fold or less than -1 fold, were used to estimate the

differences of the presence of *A. actinomycetemcomitans* in the biofilm. Human proteins present in the experimental system (potentially deriving from the serum growth supplement or the pellicle) were excluded from further analyses. Only proteins of the relevant 11 bacterial species constituting the biofilms were imported into the Uniprot (release date 10 October 2014) to generate lists of Gene Ontology (GO) function using Retrieve/ID Mapping function. The similar GO terms generated from Uniprot were enriched by REVIGO (release date 13 October 2014) [72] with the medium allowing similarity of 0.7 to replace their original terms in the lists. Then, functions of the proteins were manually summarized in pie charts based on their GO terms. GO terms that less than one percentage were clustered into category “other”.

## Statistical evaluation

All data present in the experiment derives from triplicate biofilm cultures. For the bacterial determination by qPCR, the values were logarithmically transformed, and then inserted to Prism v.6 software (GraphPad, La Jolla California USA). The statistical differences ( $P \leq 0.01$ ) between the groups were calculated by student t-test.

## Supporting Information

**S1 Table. List of identified proteins from Scaffold.** Accession numbers, identified protein names, taxonomy, peptide count from each replicate, and overlap in different groups of identified proteins from 11-species biofilms or 10-species biofilms are presented in the table. The proteins were listed following the similarity between the proteins given by Scaffold. (XLSX)

**S2 Table. List of label-free quantified proteins from Progenesis.** Accession numbers, identified protein names, taxonomy, way of regulation,  $\log_2$  ration,  $q$ -value, and peptide used for quantification of identified proteins from 11-species biofilms or 10-species biofilms are presented in the table. Proteins with  $\log_2$  ratio more than 1-fold or less than 1-fold with  $q < 0.05$  were considered as regulated proteins. (XLSX)

**S3 Table. Primer sequences and related information.** (DOCX)

## Author Contributions

Conceived and designed the experiments: KB NB GNB. Performed the experiments: KB. Analyzed the data: KB NB NS TT GNB. Contributed reagents/materials/analysis tools: NS TT. Wrote the paper: KB NB GNB.

## References

1. Socransky SS, Haffajee AD (2005) Periodontal microbial ecology. *Periodontol* 2000 38: 135–187.
2. Darveau RP (2010) Periodontitis: a polymicrobial disruption of host homeostasis. *Nat Rev Microbiol* 8: 481–490. doi: [10.1038/nrmicro2337](https://doi.org/10.1038/nrmicro2337) PMID: [20514045](https://pubmed.ncbi.nlm.nih.gov/20514045/)
3. Aas JA, Paster BJ, Stokes LN, Olsen I, Dewhirst FE (2005) Defining the normal bacterial flora of the oral cavity. *J Clin Microbiol* 43: 5721–5732. PMID: [16272510](https://pubmed.ncbi.nlm.nih.gov/16272510/)
4. Kesavalu L, Sathishkumar S, Bakthavatchalu V, Matthews C, Dawson D, et al. (2007) Rat model of polymicrobial infection, immunity, and alveolar bone resorption in periodontal disease. *Infect Immun* 75: 1704–1712. PMID: [17210663](https://pubmed.ncbi.nlm.nih.gov/17210663/)
5. Hajishengallis G, Lamont RJ, Graves DT (2015) The enduring importance of animal models in understanding periodontal disease. *Virulence*: 0. PMID: [25574929](https://pubmed.ncbi.nlm.nih.gov/25574929/)



6. Daep CA, Novak EA, Lamont RJ, Demuth DR (2011) Structural dissection and in vivo effectiveness of a peptide inhibitor of *Porphyromonas gingivalis* adherence to *Streptococcus gordonii*. *Infect Immun* 79: 67–74. doi: [10.1128/IAI.00361-10](https://doi.org/10.1128/IAI.00361-10) PMID: [21041492](https://pubmed.ncbi.nlm.nih.gov/21041492/)
7. Orth RK, O'Brien-Simpson NM, Dashper SG, Reynolds EC (2011) Synergistic virulence of *Porphyromonas gingivalis* and *Treponema denticola* in a murine periodontitis model. *Mol Oral Microbiol* 26: 229–240. doi: [10.1111/j.2041-1014.2011.00612.x](https://doi.org/10.1111/j.2041-1014.2011.00612.x) PMID: [21729244](https://pubmed.ncbi.nlm.nih.gov/21729244/)
8. Settem RP, El-Hassan AT, Honma K, Stafford GP, Sharma A (2012) *Fusobacterium nucleatum* and *Tannerella forsythia* induce synergistic alveolar bone loss in a mouse periodontitis model. *Infect Immun* 80: 2436–2443. doi: [10.1128/IAI.06276-11](https://doi.org/10.1128/IAI.06276-11) PMID: [22547549](https://pubmed.ncbi.nlm.nih.gov/22547549/)
9. Kolenbrander PE, Palmer RJ Jr, Rickard AH, Jakubovics NS, Chalmers NI, et al. (2006) Bacterial interactions and successions during plaque development. *Periodontol* 2000 42: 47–79.
10. Kuramitsu HK, He X, Lux R, Anderson MH, Shi W (2007) Interspecies interactions within oral microbial communities. *Microbiol Mol Biol Rev* 71: 653–670. PMID: [18063722](https://pubmed.ncbi.nlm.nih.gov/18063722/)
11. Ammann TW, Belibasakis GN, Thurnheer T (2013) Impact of early colonizers on in vitro subgingival biofilm formation. *PLoS One* 8: e83090. doi: [10.1371/journal.pone.0083090](https://doi.org/10.1371/journal.pone.0083090) PMID: [24340084](https://pubmed.ncbi.nlm.nih.gov/24340084/)
12. Sharma A, Inagaki S, Sigurdson W, Kuramitsu HK (2005) Synergy between *Tannerella forsythia* and *Fusobacterium nucleatum* in biofilm formation. *Oral Microbiol Immunol* 20: 39–42. PMID: [15612944](https://pubmed.ncbi.nlm.nih.gov/15612944/)
13. Bao K, Belibasakis GN, Thurnheer T, Aduse-Opoku J, Curtis MA, et al. (2014) Role of *Porphyromonas gingivalis* gingipains in multi-species biofilm formation. *BMC Microbiol* 14: 258. doi: [10.1186/s12866-014-0258-7](https://doi.org/10.1186/s12866-014-0258-7) PMID: [25270662](https://pubmed.ncbi.nlm.nih.gov/25270662/)
14. Zhu Y, Dashper SG, Chen YY, Crawford S, Slakeski N, et al. (2013) *Porphyromonas gingivalis* and *Treponema denticola* synergistic polymicrobial biofilm development. *PLoS One* 8: e71727. doi: [10.1371/journal.pone.0071727](https://doi.org/10.1371/journal.pone.0071727) PMID: [23990979](https://pubmed.ncbi.nlm.nih.gov/23990979/)
15. Ramsey MM, Rumbaugh KP, Whiteley M (2011) Metabolite cross-feeding enhances virulence in a model polymicrobial infection. *PLoS Pathog* 7: e1002012. doi: [10.1371/journal.ppat.1002012](https://doi.org/10.1371/journal.ppat.1002012) PMID: [21483753](https://pubmed.ncbi.nlm.nih.gov/21483753/)
16. Lin X, Lamont RJ, Wu J, Xie H (2008) Role of differential expression of streptococcal arginine diiminase in inhibition of fimA expression in *Porphyromonas gingivalis*. *J Bacteriol* 190: 4367–4371. doi: [10.1128/JB.01898-07](https://doi.org/10.1128/JB.01898-07) PMID: [18408031](https://pubmed.ncbi.nlm.nih.gov/18408031/)
17. Bachtar EW, Bachtar BM, Jarosz LM, Amir LR, Sunarto H, et al. (2014) AI-2 of *Aggregatibacter actinomycetemcomitans* inhibits *Candida albicans* biofilm formation. *Front Cell Infect Microbiol* 4: 94. doi: [10.3389/fcimb.2014.00094](https://doi.org/10.3389/fcimb.2014.00094) PMID: [25101248](https://pubmed.ncbi.nlm.nih.gov/25101248/)
18. Ammann TW, Gmur R, Thurnheer T (2012) Advancement of the 10-species subgingival Zurich Biofilm model by examining different nutritional conditions and defining the structure of the in vitro biofilms. *BMC Microbiol* 12: 227. doi: [10.1186/1471-2180-12-227](https://doi.org/10.1186/1471-2180-12-227) PMID: [23040057](https://pubmed.ncbi.nlm.nih.gov/23040057/)
19. Ammann TW, Bostanci N, Belibasakis GN, Thurnheer T (2013) Validation of a quantitative real-time PCR assay and comparison with fluorescence microscopy and selective agar plate counting for species-specific quantification of an in vitro subgingival biofilm model. *J Periodontol Res* 48: 517–526. doi: [10.1111/jre.12034](https://doi.org/10.1111/jre.12034) PMID: [23278531](https://pubmed.ncbi.nlm.nih.gov/23278531/)
20. Belibasakis GN, Thurnheer T, Bostanci N (2013) Interleukin-8 responses of multi-layer gingival epithelia to subgingival biofilms: role of the “red complex” species. *PLoS One* 8: e81581. doi: [10.1371/journal.pone.0081581](https://doi.org/10.1371/journal.pone.0081581) PMID: [24339946](https://pubmed.ncbi.nlm.nih.gov/24339946/)
21. Belibasakis GN, Bao K, Bostanci N (2014) Transcriptional profiling of human gingival fibroblasts in response to multi-species in vitro subgingival biofilms. *Mol Oral Microbiol*. doi: [10.1111/omi.12053](https://doi.org/10.1111/omi.12053) PMID: [24758474](https://pubmed.ncbi.nlm.nih.gov/24758474/)
22. Belibasakis GN, Ozturk VO, Emingil G, Bostanci N (2014) Soluble triggering receptor expressed on myeloid cells 1 (sTREM-1) in gingival crevicular fluid: association with clinical and microbiologic parameters. *J Periodontol* 85: 204–210. doi: [10.1902/jop.2013.130144](https://doi.org/10.1902/jop.2013.130144) PMID: [23659423](https://pubmed.ncbi.nlm.nih.gov/23659423/)
23. Haubek D, Ennibi OK, Poulsen K, Vaeth M, Poulsen S, et al. (2008) Risk of aggressive periodontitis in adolescent carriers of the JP2 clone of *Aggregatibacter (Actinobacillus) actinomycetemcomitans* in Morocco: a prospective longitudinal cohort study. *Lancet* 371: 237–242. doi: [10.1016/S0140-6736\(08\)60135-X](https://doi.org/10.1016/S0140-6736(08)60135-X) PMID: [18207019](https://pubmed.ncbi.nlm.nih.gov/18207019/)
24. Henderson B, Ward JM, Ready D (2010) *Aggregatibacter (Actinobacillus) actinomycetemcomitans*: a triple A\* periodontopathogen? *Periodontol* 2000 54: 78–105.
25. Periasamy S, Kolenbrander PE (2009) Mutualistic biofilm communities develop with *Porphyromonas gingivalis* and initial, early, and late colonizers of enamel. *J Bacteriol* 191: 6804–6811. doi: [10.1128/JB.01006-09](https://doi.org/10.1128/JB.01006-09) PMID: [19749049](https://pubmed.ncbi.nlm.nih.gov/19749049/)



26. Periasamy S, Kolenbrander PE (2009) *Aggregatibacter actinomycetemcomitans* builds mutualistic biofilm communities with *Fusobacterium nucleatum* and *Veillonella* species in saliva. *Infect Immun* 77: 3542–3551. doi: [10.1128/IAI.00345-09](https://doi.org/10.1128/IAI.00345-09) PMID: [19564387](https://pubmed.ncbi.nlm.nih.gov/19564387/)
27. Hajishengallis G, Darveau RP, Curtis MA (2012) The keystone-pathogen hypothesis. *Nat Rev Microbiol* 10: 717–725. doi: [10.1038/nrmicro2873](https://doi.org/10.1038/nrmicro2873) PMID: [22941505](https://pubmed.ncbi.nlm.nih.gov/22941505/)
28. Lamont RJ, Hajishengallis G (2014) Polymicrobial synergy and dysbiosis in inflammatory disease. *Trends Mol Med*.
29. Hendrickson EL, Wang T, Beck DA, Dickinson BC, Wright CJ, et al. (2014) Proteomics of *Fusobacterium nucleatum* within a model developing oral microbial community. *Microbiologyopen* 3: 729–751. doi: [10.1002/mbo3.204](https://doi.org/10.1002/mbo3.204) PMID: [25155235](https://pubmed.ncbi.nlm.nih.gov/25155235/)
30. Hebert AS, Richards AL, Bailey DJ, Ulbrich A, Coughlin EE, et al. (2014) The one hour yeast proteome. *Mol Cell Proteomics* 13: 339–347. doi: [10.1074/mcp.M113.034769](https://doi.org/10.1074/mcp.M113.034769) PMID: [24143002](https://pubmed.ncbi.nlm.nih.gov/24143002/)
31. Lundberg KC, Fritz Y, Johnston A, Foster AM, Baliwag J, et al. (2014) Proteomics of skin proteins in psoriasis: discovery and verification in a mouse model to confirmation in humans. *Mol Cell Proteomics*.
32. Shen Y, Zhang Y, Zou J, Meng J, Wang J (2014) Comparative proteomic study on *Brassica hexaploid* and its parents provides new insights into the effects of polyploidization. *J Proteomics* 112C: 274–284. doi: [10.1016/j.jprot.2014.07.021](https://doi.org/10.1016/j.jprot.2014.07.021) PMID: [25123350](https://pubmed.ncbi.nlm.nih.gov/25123350/)
33. Bostanci N, Meier A, Guggenheim B, Belibasakis GN (2011) Regulation of NLRP3 and AIM2 inflammatory gene expression levels in gingival fibroblasts by oral biofilms. *Cell Immunol* 270: 88–93. doi: [10.1016/j.cellimm.2011.04.002](https://doi.org/10.1016/j.cellimm.2011.04.002) PMID: [21550598](https://pubmed.ncbi.nlm.nih.gov/21550598/)
34. Thumheer T, Belibasakis GN (2014) Integration of non-oral bacteria into in vitro oral biofilms. *Virulence* 5: 1–10. PMID: [25483866](https://pubmed.ncbi.nlm.nih.gov/25483866/)
35. Dahlen G, Claesson R, Aberg CH, Haubek D, Johansson A, et al. (2014) Subgingival bacteria in Ghanaian adolescents with or without progression of attachment loss. *J Oral Microbiol* 6.
36. Raja M, Ummer F, Dhivakar CP (2014) *Aggregatibacter actinomycetemcomitans*—a tooth killer? *J Clin Diagn Res* 8: ZE13–16. doi: [10.7860/JCDR/2014/9845.4766](https://doi.org/10.7860/JCDR/2014/9845.4766) PMID: [25302290](https://pubmed.ncbi.nlm.nih.gov/25302290/)
37. Bostanci N, Belibasakis GN (2012) *Porphyromonas gingivalis*: an invasive and evasive opportunistic oral pathogen. *FEMS Microbiol Lett* 333: 1–9. doi: [10.1111/j.1574-6968.2012.02579.x](https://doi.org/10.1111/j.1574-6968.2012.02579.x) PMID: [22530835](https://pubmed.ncbi.nlm.nih.gov/22530835/)
38. Tsaousoglou P, Nietzsche S, Cachovan G, Sculean A, Eick S (2014) Antibacterial activity of moxifloxacin on bacteria associated with periodontitis within a biofilm. *J Med Microbiol* 63: 284–292. doi: [10.1099/jmm.0.065441-0](https://doi.org/10.1099/jmm.0.065441-0) PMID: [24217128](https://pubmed.ncbi.nlm.nih.gov/24217128/)
39. Haraguchi A, Miura M, Fujise O, Hamachi T, Nishimura F (2014) *Porphyromonas gingivalis* gingipain is involved in the detachment and aggregation of *Aggregatibacter actinomycetemcomitans* biofilm. *Mol Oral Microbiol* 29: 131–143. doi: [10.1111/omi.12051](https://doi.org/10.1111/omi.12051) PMID: [24661327](https://pubmed.ncbi.nlm.nih.gov/24661327/)
40. Takasaki K, Fujise O, Miura M, Hamachi T, Maeda K (2013) *Porphyromonas gingivalis* displays a competitive advantage over *Aggregatibacter actinomycetemcomitans* in co-cultured biofilm. *J Periodontal Res* 48: 286–292. doi: [10.1111/jre.12006](https://doi.org/10.1111/jre.12006) PMID: [23033940](https://pubmed.ncbi.nlm.nih.gov/23033940/)
41. Darveau RP, Hajishengallis G, Curtis MA (2012) *Porphyromonas gingivalis* as a potential community activist for disease. *J Dent Res* 91: 816–820. doi: [10.1177/0022034512453589](https://doi.org/10.1177/0022034512453589) PMID: [22772362](https://pubmed.ncbi.nlm.nih.gov/22772362/)
42. Hajishengallis G (2014) Immunomicrobial pathogenesis of periodontitis: keystones, pathobionts, and host response. *Trends Immunol* 35: 3–11. doi: [10.1016/j.it.2013.09.001](https://doi.org/10.1016/j.it.2013.09.001) PMID: [24269668](https://pubmed.ncbi.nlm.nih.gov/24269668/)
43. Zijnga V, van Leeuwen MB, Degener JE, Abbas F, Thumheer T, et al. (2010) Oral biofilm architecture on natural teeth. *PLoS One* 5: e9321. doi: [10.1371/journal.pone.0009321](https://doi.org/10.1371/journal.pone.0009321) PMID: [20195365](https://pubmed.ncbi.nlm.nih.gov/20195365/)
44. Hall-Stoodley L, Costerton JW, Stoodley P (2004) Bacterial biofilms: from the natural environment to infectious diseases. *Nat Rev Microbiol* 2: 95–108. PMID: [15040259](https://pubmed.ncbi.nlm.nih.gov/15040259/)
45. Rickard AH, Palmer RJ DS Jr., Campagna SR, Semmelhack MF, et al. (2006) Autoinducer 2: a concentration-dependent signal for mutualistic bacterial biofilm growth. *Mol Microbiol* 60: 1446–1456. PMID: [16796680](https://pubmed.ncbi.nlm.nih.gov/16796680/)
46. Shao H, James D, Lamont RJ, Demuth DR (2007) Differential interaction of *Aggregatibacter (Actinobacillus) actinomycetemcomitans* LsrB and RbsB proteins with autoinducer 2. *J Bacteriol* 189: 5559–5565. PMID: [17526716](https://pubmed.ncbi.nlm.nih.gov/17526716/)
47. Hajishengallis G, Lamont RJ (2012) Beyond the red complex and into more complexity: the polymicrobial synergy and dysbiosis (PSD) model of periodontal disease etiology. *Mol Oral Microbiol* 27: 409–419. doi: [10.1111/j.2041-1014.2012.00663.x](https://doi.org/10.1111/j.2041-1014.2012.00663.x) PMID: [23134607](https://pubmed.ncbi.nlm.nih.gov/23134607/)
48. Mahajan A, Singh B, Kashyap D, Kumar A, Mahajan P (2013) Interspecies communication and periodontal disease. *ScientificWorldJournal* 2013: 765434. doi: [10.1155/2013/765434](https://doi.org/10.1155/2013/765434) PMID: [24396307](https://pubmed.ncbi.nlm.nih.gov/24396307/)



49. Roberts AP, Mullany P (2006) Genetic basis of horizontal gene transfer among oral bacteria. *Periodontol* 2000 42: 36–46.
50. Saitou N, Nei M (1987) The neighbor-joining method: a new method for reconstructing phylogenetic trees. *Mol Biol Evol* 4: 406–425. PMID: [3447015](#)
51. Zainal-Abidin Z, Veith PD, Dashper SG, Zhu Y, Catmull DV, et al. (2012) Differential proteomic analysis of a polymicrobial biofilm. *J Proteome Res* 11: 4449–4464. doi: [10.1021/pr300201c](#) PMID: [22808953](#)
52. Rhodes ER, Menke S, Shoemaker C, Tomaras AP, McGillivray G, et al. (2007) Iron acquisition in the dental pathogen *Actinobacillus actinomycetemcomitans*: what does it use as a source and how does it get this essential metal? *Biomaterials* 20: 365–377. PMID: [17206384](#)
53. Xu X, Holt SC, Kolodrubetz D (2001) Cloning and expression of two novel hemin binding protein genes from *Treponema denticola*. *Infect Immun* 69: 4465–4472. PMID: [11401987](#)
54. Olczak T, Simpson W, Liu X, Genco CA (2005) Iron and heme utilization in *Porphyromonas gingivalis*. *FEMS Microbiol Rev* 29: 119–144. PMID: [15652979](#)
55. Hajishengallis G, Lamont RJ (2014) Breaking bad: manipulation of the host response by *Porphyromonas gingivalis*. *Eur J Immunol* 44: 328–338. doi: [10.1002/eji.201344202](#) PMID: [24338806](#)
56. Reddi D, Belibasakis GN (2012) Transcriptional profiling of bone marrow stromal cells in response to *Porphyromonas gingivalis* secreted products. *PLoS One* 7: e43899. doi: [10.1371/journal.pone.0043899](#) PMID: [22937121](#)
57. Kachlany SC (2010) *Aggregatibacter actinomycetemcomitans* leukotoxin: from threat to therapy. *J Dent Res* 89: 561–570. doi: [10.1177/0022034510363682](#) PMID: [20200418](#)
58. Nomura M, Gourse R, Baughman G (1984) Regulation of the synthesis of ribosomes and ribosomal components. *Annu Rev Biochem* 53: 75–117. PMID: [6206783](#)
59. Guggenheim B, Gmur R, Galicia JC, Stathopoulou PG, Benakanakere MR, et al. (2009) In vitro modeling of host-parasite interactions: the 'subgingival' biofilm challenge of primary human epithelial cells. *BMC Microbiol* 9: 280. doi: [10.1186/1471-2180-9-280](#) PMID: [20043840](#)
60. Hendrickson EL, Xia Q, Wang T, Lamont RJ, Hackett M (2009) Pathway analysis for intracellular *Porphyromonas gingivalis* using a strain ATCC 33277 specific database. *BMC Microbiol* 9: 185. doi: [10.1186/1471-2180-9-185](#) PMID: [19723305](#)
61. Hendrickson EL, Wang T, Dickinson BC, Whitmore SE, Wright CJ, et al. (2012) Proteomics of *Streptococcus gordonii* within a model developing oral microbial community. *BMC Microbiol* 12: 211. doi: [10.1186/1471-2180-12-211](#) PMID: [22989070](#)
62. Brown SA, Whiteley M (2007) A novel exclusion mechanism for carbon resource partitioning in *Aggregatibacter actinomycetemcomitans*. *J Bacteriol* 189: 6407–6414. PMID: [17586632](#)
63. Deutscher J, Francke C, Postma PW (2006) How phosphotransferase system-related protein phosphorylation regulates carbohydrate metabolism in bacteria. *Microbiol Mol Biol Rev* 70: 939–1031. PMID: [17158705](#)
64. Comas I, Gonzalez-Candelas F, Zuniga M (2008) Unraveling the evolutionary history of the phospho-transfer chain of the phosphoenolpyruvate:phosphotransferase system through phylogenetic analyses and genome context. *BMC Evol Biol* 8: 147. doi: [10.1186/1471-2148-8-147](#) PMID: [18485189](#)
65. Bradshaw DJ, Marsh PD (1998) Analysis of pH-driven disruption of oral microbial communities in vitro. *Caries Res* 32: 456–462. PMID: [9745120](#)
66. Pereira CS, Santos AJ, Bejerano-Sagie M, Correia PB, Marques JC, et al. (2012) Phosphoenolpyruvate phosphotransferase system regulates detection and processing of the quorum sensing signal autoinducer-2. *Mol Microbiol* 84: 93–104. doi: [10.1111/j.1365-2958.2012.08010.x](#) PMID: [22384939](#)
67. Guggenheim B, Giertsen E, Schubach P, Shapiro S (2001) Validation of an in vitro Biofilm Model of Supragingival Plaque. *Journal of Dental Research* 80: 363–370. PMID: [11269730](#)
68. Gmur R, Guggenheim B (1983) Antigenic heterogeneity of *Bacteroides intermedius* as recognized by monoclonal antibodies. *Infect Immun* 42: 459–470. PMID: [6196291](#)
69. Wisniewski JR, Zougman A, Nagaraj N, Mann M (2009) Universal sample preparation method for proteome analysis. *Nat Methods* 6: 359–362. doi: [10.1038/nmeth.1322](#) PMID: [19377485](#)
70. Smyth GK (2004) Linear models and empirical bayes methods for assessing differential expression in microarray experiments. *Stat Appl Genet Mol Biol* 3: Article3. PMID: [16646809](#)
71. Benjamini Y, Hochberg Y (1995) Controlling the false discovery rate: a practical and powerful approach to multiple testing. *Journal of the Royal Statistical Society Series B* 57: 289–300.
72. Supek F, Bosnjak M, Skunca N, Smuc T (2011) REVIGO summarizes and visualizes long lists of gene ontology terms. *PLoS One* 6: e21800. doi: [10.1371/journal.pone.0021800](#) PMID: [21789182](#)



# Paper 3

# Establishment and Characterization of Immortalized Gingival Epithelial and Fibroblastic Cell Lines for the Development of Organotypic Cultures

Kai Bao<sup>a</sup> Baki Akguel<sup>b</sup> Nagihan Bostanci<sup>a</sup>

<sup>a</sup>Oral Translational Research Unit, Institute of Oral Biology, Center of Dental Medicine, University of Zurich, Zurich, Switzerland; <sup>b</sup>Institute of Virology, University of Cologne, Cologne, Germany

## Key Words

Gingival epithelium · Gingival fibroblasts · Human papillomavirus type 16 · Organotypic tissue

## Abstract

In vitro studies using 3D co-cultures of gingival cells can resemble their in vivo counterparts much better than 2D models that typically only utilize monolayer cultures with short-living primary cells. However, the use of 3D gingival models is still limited through lack of appropriate cell lines. We aimed to establish immortalized cell line models of primary human gingival epithelium keratinocytes (HGEK) and gingival fibroblasts (GFB). Immortalized cell lines (HGEK-16 and GFB-16) were induced by E6 and E7 oncoproteins of human papillomavirus. In addition, 3D multilayered organotypic cultures were formed by embedding GFB-16 cells within a collagen (Col) matrix and seeding of HGEK-16 cells on the upper surfaces. Cell growth was analyzed in both immortalized cell lines and their parental primary cells. The expression levels of cell type-specific markers, i.e. cytokeratin (CK) 10, CK13, CK16, CK18, CK19 for HGEK-16 and Col I and Col II for GFB-16, were evaluated by quantitative real-time polymerase chain reaction (qRT-PCR). Expansion of the primary cultures was impeded at early passages, while the transformed immortalized cell lines could be expanded for more than 30 passages.

In 3D cultures, immortalized HGEK formed a multilayer of epithelial cells. qRT-PCR showed that cell-specific marker expression in the 3D cultures was qualitatively and quantitatively closer to that in human gingival tissue than to monolayer cultures. These results indicate that immortalized gingival fibroblastic and epithelial cell lines can successfully form organotypic multilayered cultures and, therefore, may be useful tools for studying gingival tissue in vitro.

© 2014 S. Karger AG, Basel

## Introduction

Gingival tissue comprises the superficial oral epithelium and underlying connective tissue. These tissues are the first locations to be affected by biofilms as well as the initiation sites for inflammatory processes. They are therefore recognized as the places for the initiation of periodontal diseases, a widespread group of destructive oral infection-driven inflammatory diseases that affect 48.2% of the USA population aged  $\geq 30$  years [Albandar, 2011].

Based on structural and functional differences, gingival epithelial tissue has been classified as junctional epithelium, oral sulcular epithelium and oral gingival epithelium. Oral junctional epithelium connects the tooth to the sub-



epithelial connective tissue and sulcular epithelium lines the lateral wall of the gingival sulcus. Besides its supporting functions, the permeability of the epithelium allows emigration of granulocytes to the biofilm surface but also enables microorganisms to migrate from the biofilm [Sandro et al., 1994], which is believed to play an important role during the process of periodontal infection. In the clinic, the appearance of a periodontal pocket, an abnormal depth of the gingival sulcus, is considered to be an indicator for periodontal infection. Interestingly, disappearance of the junctional epithelium and ulceration of sulcular epithelium during the formation of the periodontal pocket has been observed [Nanci and Bosshardt, 2006], which means that gingiva is not able to form tight connections after the disease. Therefore, it is of importance to understand how healthy non-keratinized sulcular and junctional epithelium is breached by the oral biofilms; what changes occur to these structures during disease processes, and if the molecular mechanisms of the pristine status recover after clinical improvements [Belibasakis et al., 2011]. In progressive periodontal diseases presenting with ulcerated epithelium, the gingival connective tissue (mainly fibroblasts) is directly exposed to the bacterial biofilm. As connective tissue also influences the formation of gingival epithelia [Karring et al., 1975; Smola et al., 1998], concomitant studies using both epithelial and connective tissue are crucial for understanding the pathogenesis of periodontal diseases [MacNeil, 2007].

In vitro studies on gingival tissue have mainly employed monolayer cultures. Due to the lack of normal differentiation, gingival cells grown under these conditions are deficient in differentiation-dependent cell polarization and cell-cell contacts [Radyuk et al., 2003]. Thus, organotypic cell culture models that mimic the morphological and functional features of their in vivo counterparts are highly anticipated despite their methodological complexity. One of the main methodological problems of establishing such 3D cultures is that primary cells have short life spans, as they only replicate for a few passages and therefore do not provide sufficient cell numbers for further use in organotypic cultures [Sacks, 1996; Pi et al., 2007]. To overcome this problem, previous work has made use of the E6/E7 oncoproteins from human papillomavirus type 16 (HPV16-E6/E7) to immortalize epithelial cells [Yeh et al., 2013].

In the present study, we used primary human gingival epithelial keratinocytes (HGEK) and human gingival fibroblasts (GFB). Our primary aim was to immortalize them through the expression of oncogene HPV16-E6/E7. In addition, we aimed to establish a standardized organo-

typic gingival tissue model mimicking an oral junctional epithelial interface in vitro, using both immortalized gingival epithelial cells and gingival connective tissue. The characteristics of the established epithelia and fibroblasts in a 2D monolayer and organotypic culture were determined by histology and cell differentiation through quantification of cytokeratin (CK) and collagen (Col) expression using quantitative real-time polymerase chain reaction (qRT-PCR).

## Materials and Methods

### Primary Cultures

GFBs were collected from clinically healthy gingiva as previously described [Belibasakis et al., 2005] and HGEK were extracted following a published protocol [Guggenheim et al., 2009]. Ethical approval was granted from the Ethical Committee of the Dental Institute Board (StV Nr. 08/14). The study was conducted according to the guidelines of the Declaration of Helsinki. Written and informed consent was obtained from each patient before enrolment in the study. HGEKs were cultivated and passaged in defined keratinocyte serum-free medium (Gibco), supplemented with 100 U/ml penicillin (Sigma, St. Louis, Mo., USA), 100 µg/ml streptomycin (Sigma), 2 mM L-glutamine (Sigma) and 0.25 µg/ml Fungizone (Sigma). GFBs were cultivated and passaged in Dulbecco's modified Eagle's medium (DMEM):nutrient mixture F-12 (DMEM/F-12) media (Sigma) supplemented with 1.2 g/ml of sodium bicarbonate (Sigma), 10% FCS (Sigma), 100 U/ml penicillin, 100 µg/ml streptomycin, 2 mM L-glutamine and 0.05 µg/ml Fungizone. Cell cultures were incubated at 37°C in a humidified atmosphere of 5% CO<sub>2</sub> in air. The medium was changed every 2 days. When the primary cell cultures reached confluence, cells were dissociated with trypsin/EDTA solution (Gibco, Life Technologies) just before transferring for experiments. Cell numbers were determined under light microscopy using a hemocytometer. Population doubling was calculated as log<sub>2</sub> (cell number at subculture/cell number plated) for growth kinetics determination.

### Immortalization and Maintenance of Cultures

For immortalization, gingival cells were retrovirally transduced with virus coding either for pLXSN empty vector control (pLXSN) or HPV16-E6E7 (pLXSN-HPV16-E6E7) as described previously [Akgul et al., 2010]. Briefly, primary cells were seeded at a cell density of  $2 \times 10^5$  cells/cm<sup>2</sup> in 6-cm dishes. Retroviral supernatants were mixed with an equal volume of DMEM in the presence of 5 µg/ml of hexadimethrine bromide (Polybrene; Sigma) and added to the keratinocytes. Spin infection was made by centrifugation at 300 g for 1 h; the cells were then washed with PBS and cultured in corresponding fresh medium. After 2 days, cells were selected with G418 (Sigma-Aldrich; 100 µg/ml for keratinocytes and 500 µg/ml for fibroblasts) for 7 days after which only infected cells survived. The use of pooled stable cell populations minimizes possible variations due to randomness of the viral integration site in the cellular chromosomes. Established HGEK-16 or GFB-16 cells were seeded at 3,333 cells/cm<sup>2</sup> and incubated at 37°C in a humidified atmosphere of 5% CO<sub>2</sub> in air for passaging. HGEK-16 cells were culti-



**Table 1.** List of primers used to check cell-specific marker expression at mRNA level

Name	Sequence: (5' to 3')	Size	Tm, °C
CK10 forward primer	CTGACTGAAGAGCTGGCCTA	20	62.3
CK10 reverse primer	TTCCACATTACATCACCAG	20	62.1
CK13 forward primer	ATGCTGCTGGACATCAAGAC	20	63.0
CK13 reverse primer	TGGTAACAGAGGTGCTACGG	20	62.7
CK14 forward primer	TGCGATCCAGAGGAGAACTG	20	65.6
CK14 reverse primer	CAGGAGATGATTGGCAGCGT	20	67.6
CK16 forward primer	GCCAATCCTATTCTTCCCGC	20	66.6
CK16 reverse primer	GGGAGATAGCTGGGAACTG	20	64.8
CK18 forward primer	ATCTTGGTGATGCCTTGGAC	20	63.9
CK18 reverse primer	CCTGCTTCTGCTGGCTTAAT	20	63.3
CK19 forward primer	GACATGCGAAGCCAATATGA	20	63.6
CK19 reverse primer	TCAGTAACCTCGGACCTGCT	20	63.8
GAPDH forward primer	CAGCCTCCCCTTCGCTCTC	20	72.8
GAPDH reverse primer	CCAGGCGCCCAATACGACCA	20	74.2
HPV-16 E6 forward primer	TGTTTCAGGACCCACAGGA	19	64.4
HPV-16 E6 reverse primer	TTGTTTGACAGCTCTGTGCAT	20	64.7
HPV-16 E7 forward primer	CTGTTATGAGCAATTAATGACAGC	25	62.5
HPV-16 E7 reverse primer	CCAGCTGGACCATCTATTTCA	21	63.9
Col I forward primer	AAGATGGACTCAACGGTCTC	20	60.7
Col I reverse primer	CAGGAAGCTGAAGTCGAAAC	20	61.6
Col II forward primer	ACATCACCTACCACTGCAAG	20	60.2
Col II reverse primer	TACGTGAACCTGCTATTGCC	20	62.6

Tm = Melting temperature.

vated in defined keratinocyte serum-free medium supplemented with 100 µg/ml G418. GFB-16 cells were cultivated in DF12 medium supplemented with 250 µg/ml G418.

#### Construction of a 3D Organotypic Gingiva Model

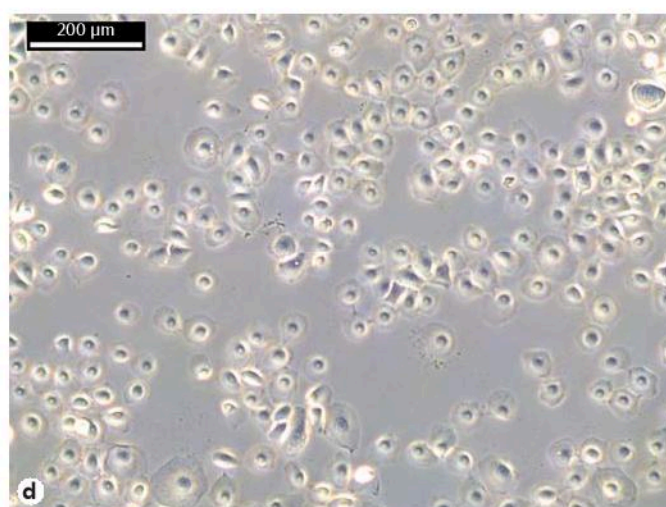
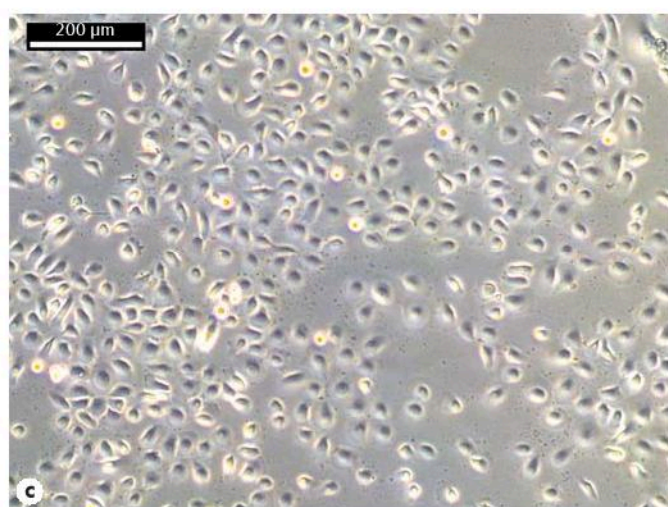
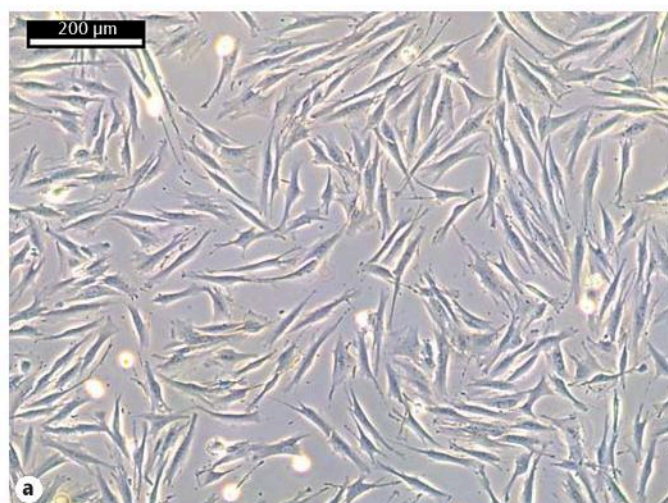
The method used to develop a 3D organotypic gingival model is a modification of previously reported models [Dongari-Bagtzoglou and Kashleva, 2006] with major changes described below. Briefly, the 3D organotypic gingiva models were constructed inside 13-mm-diameter Millicell cell culture inserts (Millipore) in 12-well plates. Collagen mixtures were composed of DMEM (Sigma), 10% FCS, 2 mM L-glutamine, 0.22 mg/ml sodium bicarbonate, 0.20 mM HEPES and 2.5 mg/ml rat tail Col I; 0.2 ml of this Col mixture were poured into each insert and allowed to gelify a the sterile hood to form acellular layers. Col matrix (0.5 ml) containing  $7.5 \times 10^5$  GFB-16 cells were later gelled above the acellular layers. The medium used to grow fibroblasts was then added to cover each gel for incubation at 37°C in a humidified atmosphere with 5% CO<sub>2</sub> until the Col contracted (normally takes 1 or 2 days). The medium was then removed and the gels were plated with  $1 \times 10^6$  HGEK-16 cells. The HGEK-16 cells were allowed to attach for 2 days in a mixture of HGEK-16 and GFB-16 growth medium at a ratio of 1:1 supplemented with 10 µg/ml of epithelial growth factors. Then, inserts were placed onto sterile cotton to expose the gels to the air but being still in contact with the medium. The medium used for this air-liquid interface was DMEM (4.5 mg/ml glucose) and Ham's F-12 mixed at ratio of 3:1 with 5 µg/ml insulin, 0.4 µg/ml hydrocortisone,  $2 \times 10^{-11}$  M 3,3',5-triiodo-L-thyronine,  $1.8 \times$

$10^{-4}$  M adenine, 5 µg/ml transferrin,  $10^{-10}$  M cholera toxin, 2 mM L-glutamine, 100 U/ml penicillin, 100 µg/ml streptomycin, 0.05 µg/ml Fungizone, 100 µg/ml G418 antibiotic and 5% FBS. Cultures were maintained in air-liquid interface for 14 days with the medium changed every 2 days.

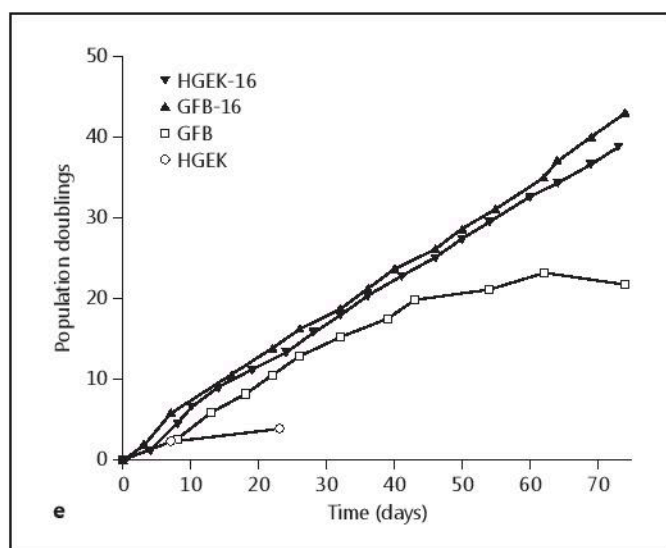
#### RNA Extraction and cDNA Synthesis

For RNA extraction from monolayer cultures, cells were dissociated with 1× trypsin/EDTA and collected by centrifugation. Organotypic cultures were first washed with PBS, then resuspended in 600 µl RLT buffer (Qiagen, Basel, Switzerland) and disintegrated at 25,000 rpm in a Mini-Beadbeater-1 disrupter (BioSpec) with ice cooling between cycles and collected by centrifugation at 3,700 rpm for 1 min at 4°C. The supernatants were aliquoted into a clean tube and placed on ice for later usage. The pellets were resuspended in 590 µl RNase-free water and incubated with 20 µl proteinase K solution at 55°C for 5 min. Mixtures were then centrifuged at 10,000 rpm for 3 min at 4°C and supernatants were combined with previous ones on ice for RNA extraction. Cell lysates from all strains were kept and extracted using the RNeasy Mini Kits (Qiagen) following the instructions of the manufacturer. Clinically healthy gingiva for RNA extraction was obtained as previously described [Bostanci et al., 2009]. Briefly, gingival tissue biopsies, including both epithelium and connective tissue, were obtained from periodontally healthy subjects (n = 3) during tooth extractions for orthodontic reasons or crown-lengthening procedures. The gingival tissue biopsies were immersed in RNA stabilization reagent (RNA Later; Ambion, Foster City, Calif., USA) and





**Fig. 1.** Cell morphologies and growth kinetics. Phase-contrast microphotography for primary human GFB (a), immortalized GFB-16 (b), primary HGEK (c) and immortalized HGEK-16 (d) at passages 2, 13, 2 and 16, respectively. Growth kinetics of HGEK-16, GFB-16, HGEK and GFB (e); cells were grown in culture, and doubling times were assessed using a hemacytometer. Data are presented to day 74 until GFB cells became senescent. Each dot on the curve represents the day of subculture of the cell line. Passages 2, 6, 8 and 7 are presented for HGEK, GFB, HGEK-16 and GFB-16, respectively.





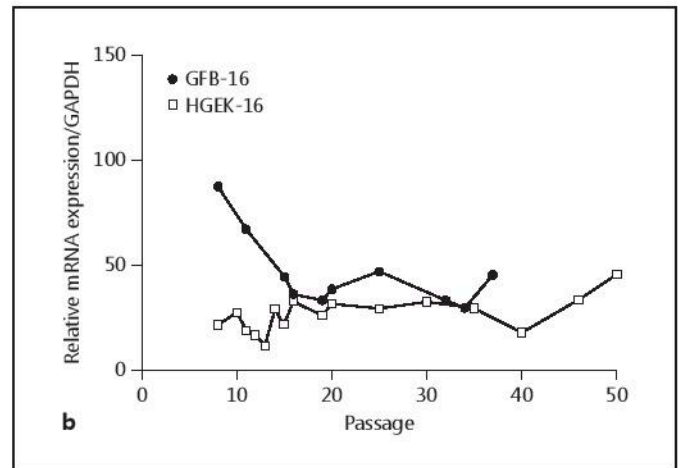
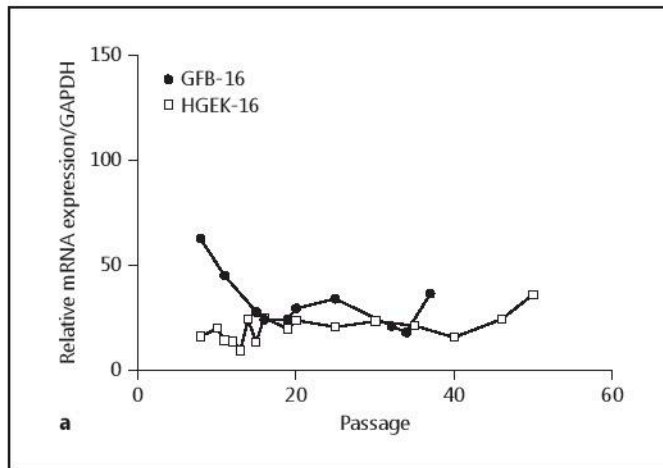


**Fig. 2.** HPV16-E6/E7 expression of the immortalized cell lines at different passages. mRNA expression levels of HPV16-E6 (a) and -E7 (b) were normalized with a housekeeping gene (GAPDH).

then frozen at  $-80^{\circ}\text{C}$ . Total RNA was extracted using the AllPrep Kit (Qiagen). Moloney murine leukemia virus reverse transcriptase (Promega) was used to synthesize cDNA according to the manufacturer's instruction.

#### qRT-PCR

For the characterization of gene expression in both 2D and 3D cultures, CK10, CK13, CK14, CK16, CK18, CK19, Col I and Col II were amplified using StepOnePlus™ real-time PCR systems (Applied Biosystems) following the standard instructions of the manufacturer and data were analyzed by the software provided. Oligonucleotide primer sequences are listed in table 1. Glyceraldehyde-3-phosphate dehydrogenase (GAPDH) was used as an endogenous RNA control in the samples (housekeeping gene). The SYBR Green PCR Master Mix (Applied Biosystems) was used for amplification reactions.

#### 3D Model Treatments for Immunohistology

Samples were rinsed twice with PBS for 5 min and then transferred into 3% paraformaldehyde supplemented with 2% sucrose/PBS fixation medium for 2 h. The samples were rinsed thrice with PBS, 20 min each; dehydrated by immersion in 15% sucrose/PBS for 2 h at room temperature, and then left in 30% sucrose/PBS overnight at  $4^{\circ}\text{C}$ . The next day, samples were placed in 5 ml of 5% (w/w) porcine-derived gelatin (Sigma) solution supplemented with 5% (w/w) sucrose that was prewarmed to  $45^{\circ}\text{C}$  in the models. The whole models were transferred in a cool 2-methylbutane (isopentane) and dry ice bath at around  $-40^{\circ}\text{C}$  until they were frozen. Specimens were stored at  $-80^{\circ}\text{C}$  and sectioned at  $8\text{-}\mu\text{m}$  thickness using a HYRAX C 50 cryostat (Zeiss, Jena, Germany).

#### Histological Staining and Image Composition

Cryosection slides at  $-80^{\circ}\text{C}$  were dried at room temperature for 0.5–2 h and then fixed in acetone ( $4^{\circ}\text{C}$ ) for 15 min. After washing thrice with PBS, the specimens were blocked with 1% BSA/PBS for 10 min. The specimens were then incubated with  $4\text{ }\mu\text{g/ml}$  mouse monoclonal keratin 14 Ab-1 (Clone LL002; Neomarker) or

$4\text{ }\mu\text{g/ml}$  keratin 16 Ab-1 (Clone LL025; Neomarker) at  $4^{\circ}\text{C}$  overnight. After removal of the primary antibody, the Alexa Fluor® 488 goat anti-mouse IgG (H+L) antibody was applied to the samples and incubated for 45 min at room temperature. DAPI was later applied on the samples as a counterstain.

#### Statistical Evaluation

The results of qRT-PCR analysis for the expression levels of different transcripts in each sample were calculated by the comparative Ct method ( $2^{-\Delta\text{Ct}}$  formula) after normalization to endogenous control GAPDH (i. e.  $\Delta\text{Ct} = \text{Ct}_{\text{target gene}} - \text{Ct}_{\text{GAPDH}}$ ). All data are expressed as means  $\pm$  SD for all of the determinations. Significance was calculated from log values of  $\Delta\text{Ct}$  between different conditions. Unpaired t tests were used to test the differences between immortalized cell lines with their parent primary cells. Multiple comparison tests following one-way ANOVA were used to test the differences between 3D organotypic gingiva models, clinical samples and 2D monolayer cultures.

## Results

### Characterization of Immortalized Human Gingival Epithelial and Fibroblastic Cell Lines in 2D Monolayer Cultures

#### Immortalized Cell Lines Show Cell Morphologies and Growth Kinetics Similar to Their Parental Cells in Monolayer Cultures

Primary HGEK and GFB exhibited distinct morphologies under the light microscope (fig. 1). Keratinocytes exhibited characteristic epithelial cobblestone morphologies (fig. 1c, d), while fibroblasts exhibited typical spindle-shaped fibroblast morphologies (fig. 1a, b). HPV16 immortalized clones of both keratinocytes and fibroblasts

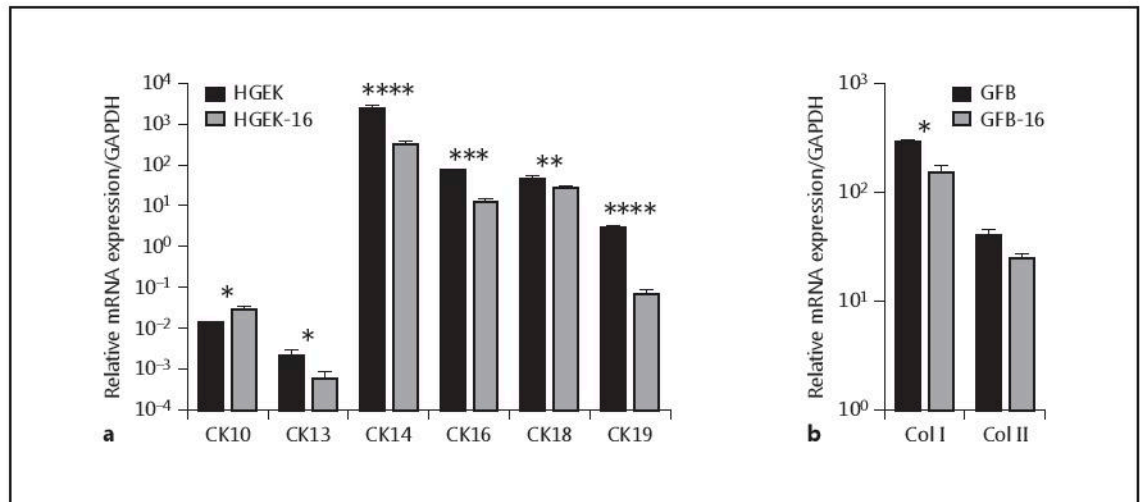


**Fig. 3.** Expression of differentiation markers in primary and immortalized cells from different passages. **a** The values of CK10, CK13, CK14, CK16, CK18 and CK19 represent values of 3 or 18 passages, respectively, for primary (HGEK) or immortalized epithelial cells (HGEK-16; means  $\pm$  SD) as described in Materials and Methods. **b** The expression levels of Col I and II were compared between primary (GFB) and immortalized cells (GFB-16). Values (means  $\pm$  SD) of 4 and 10 passages for GFB and GFB-16,

respectively (online suppl. table S1; for all online suppl. material, see [www.karger.com/doi/10.1159/000363694](http://www.karger.com/doi/10.1159/000363694)) as described in Materials and Methods. For a better understanding of the data, results are presented on a logarithmic scale. For each marker, mRNA levels were normalized with a housekeeping gene (GAPDH). \*  $p < 0.05$ , \*\*  $p < 0.001$ , \*\*\*  $p < 0.0001$ , \*\*\*\*  $p < 0.00001$ , primary cells vs. immortalized cells.

showed morphologies similar to their parental cells at early passages, although primary cells were more heterogeneous in their morphology.

The subculture time of primary gingival keratinocytes and fibroblasts remained similar in early passages, but cells proliferated more slowly and became senescent at 4 and 18 population doublings, respectively. In comparison, immortalized cells showed continuous proliferation and expansion over 30 population doublings whilst retaining a similar cobblestone or spindle-shape phenotype. The growth behavior of the immortalized cell lines remained constant over time and required subcultivation every 4–5 days (fig. 1e).

#### Immortalized Cell Lines Express Stable Levels of HPV16-E6/E7

To test for the presence and expression levels of the HPV16-E6/E7, mRNAs of HGEK-16 and GFB-16 were extracted from the cells in different passages and examined by qRT-PCR (fig. 2). The analysis confirmed oncogene expression in all HPV16-E6/E7-transduced cells at all detected passages at a similar level. No oncogene expression was detected in the corresponding parental primary cells (data not shown).

#### Immortalized Cell Lines in Monolayer Cultures Express Similar Levels of Cell-Specific Markers when Compared with Their Parental Cells

Since CK are the main intermediate filaments of gingival epithelia, mRNA levels of selected CK were examined as differentiation markers. Therefore, CK10, CK13, CK14, CK16, CK18 and CK19 were tested in primary HGEK and HGEK-16 cells by qRT-PCR (fig. 3a). Essentially, HGEK and HGEK-16 cells all expressed these CK, although slight effects on CK expression by HPV16-E6/E7 were noted. Both cell types expressed low levels of CK10 and CK13 and high levels of CK14, CK16, CK18 and CK19 (fig. 3a). Immunohistochemical analysis also confirmed strong expression of CK14 in HGEK-16 monolayer cultures (fig. 4c). As a marker of cornifying epithelium, CK10 was expressed at low level when compared to CK14, the marker of stratifying epithelium, which was expressed at highest levels. The marker of non-cornified epithelium, CK13, was present but at lower levels. Magnitudes of gene expression of the selected CK were compared between HGEK and HGEK-16. CK10 and CK13 were expressed at slightly higher levels in HGEK-16 (0.45-fold,  $p = 0.0237$ , and 3.60-fold,  $p = 0.0399$ , respectively) compared with HGEK. In contrast, HGEK-16 expressed lower levels of CK14, CK16, CK18 and CK19 (7.44-fold,



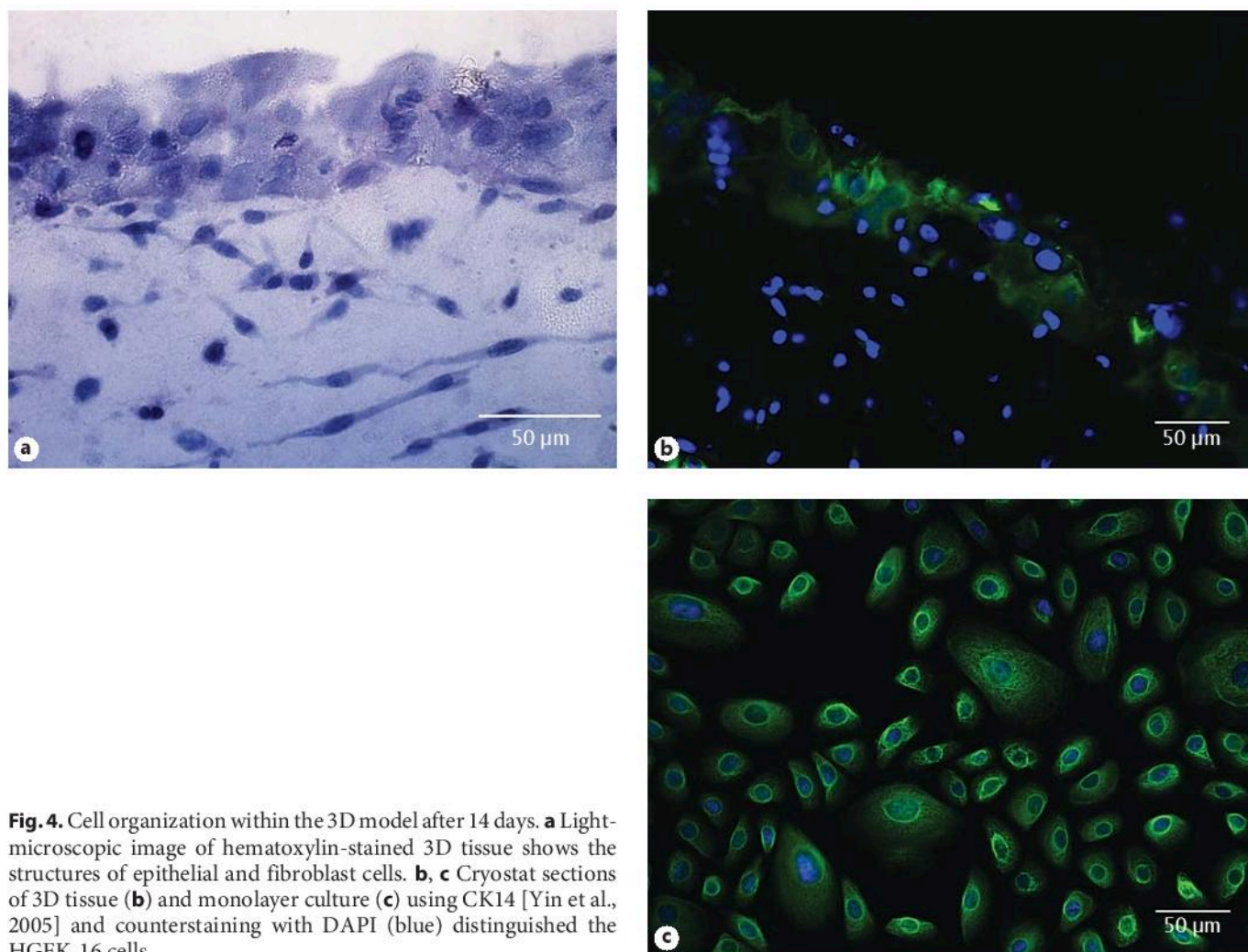


**Fig. 4.** Cell organization within the 3D model after 14 days. **a** Light-microscopic image of hematoxylin-stained 3D tissue shows the structures of epithelial and fibroblast cells. **b, c** Cryostat sections of 3D tissue (**b**) and monolayer culture (**c**) using CK14 [Yin et al., 2005] and counterstaining with DAPI (blue) distinguished the HGEK-16 cells.

$p < 0.00001$ ; 5.62-fold,  $p = 0.0002$ ; 1.58-fold,  $p = 0.0087$ , and 40.13-fold,  $p < 0.00001$ , respectively) compared with HGEK.

In addition, expression levels of extracellular matrix-related genes (i.e. Col I and Col II) were examined for GFB and GFB-16. Both fibroblast cell types demonstrated strong expression of Col I and Col II (fig. 3b), with Col I expression in GFB-16 being slightly lower (1.62-fold,  $p = 0.024$ ) than in GFB.

#### *Behavior of Immortalized Human Gingival Epithelial and Fibroblastic Cells in 3D Organotypic Cultures* 3D Organotypic Cell Cultures Showed a Multilayer Structure

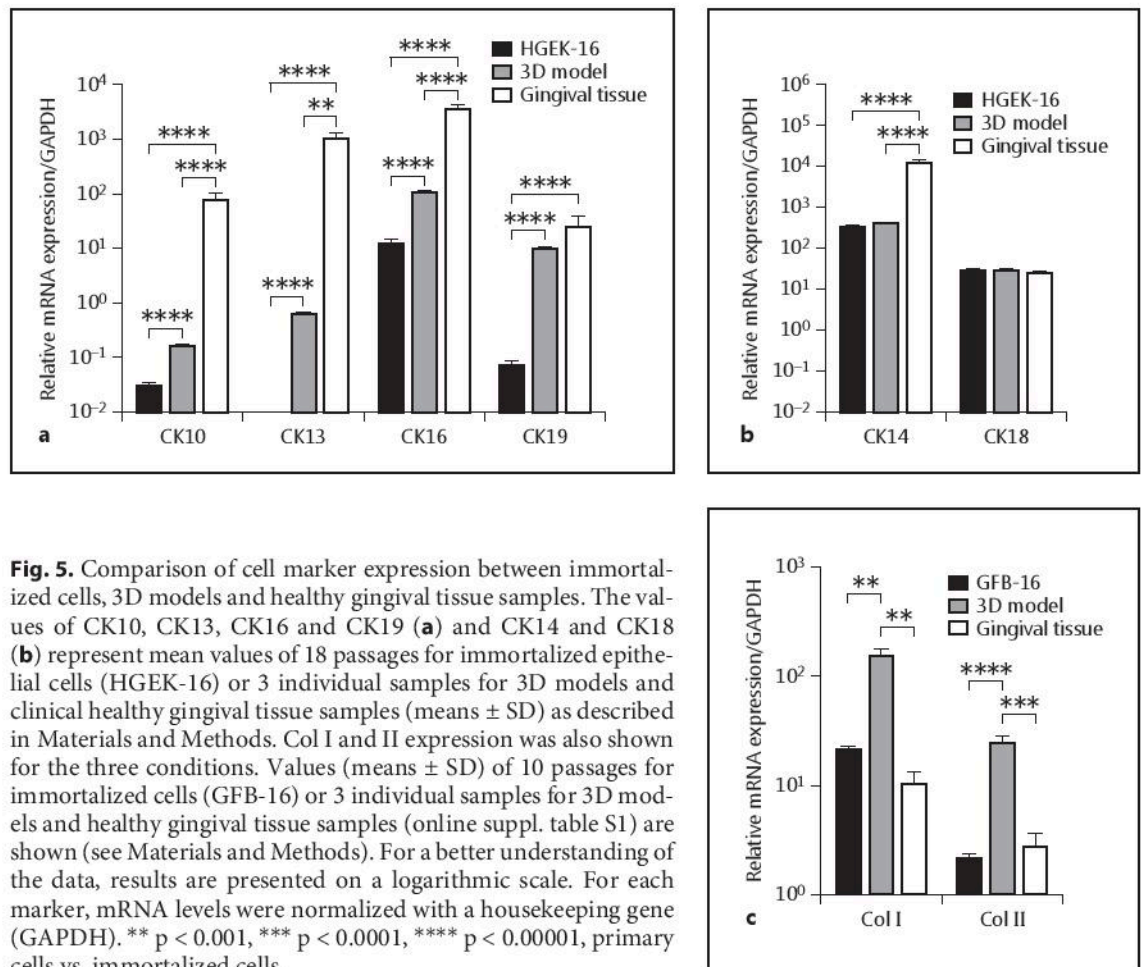
GFB-16 and HGEK-16 cells were grown to confluence in monolayer cultures and then used to construct 3D or-

ganotypic cultures. Figure 4a shows a representative section of this model stained with hematoxylin. HGEK-16 cells formed a multilayered regenerated epithelium with no obvious keratinizing superficial layer on the surface, which is similar to the non-keratinized oral epithelia such as junctional epithelium in vivo. The HGEK-16 cells formed multilayers of epithelia and GFB-16 fibroblasts were evenly distributed in the Col gel matrix. Like in monolayer cultures (fig. 4c), HGEK-16 epithelium in 3D organotypic cultures revealed strong CK14 staining (fig. 4b).

#### Gene Expression Levels of CK and Col in 3D Organotypic Cultures Were Closer to the Levels in Healthy Gingiva than in 2D Monolayer Cultures

One of the key differences between in vitro and in vivo epithelia is that they express epithelial markers different-





ly [Locke et al., 2008]. We expected the CK expression levels in organotypic cultures to be closer to the levels found in vivo in human tissue than in monolayer culture. Therefore, CK expression in organotypic cultures, healthy gingival tissue and monolayer cultures of HGEK-16 were compared using qRT-PCR. In addition, mRNA expression levels of Col I and Col II were compared between organotypic cultures, clinical samples and GFB-16 cells grown as monolayers.

qRT-PCR analysis showed that the expression levels of CK in HGEK-16 organotypic cultures are closer to those in gingival tissue than to monolayer cell cultures (fig. 5a, b). Especially for CK19, 3D model expression is 135.91-fold higher than in the immortalized cells, with no significant difference to the level in gingival tissue models (2.50-fold,  $p > 0.05$ ). The levels of CK10, CK13 and CK16 in gingival tissue were significantly higher (465.21-fold,  $p < 0.00001$ ; 1,658.49-fold,  $p < 0.0001$ , and 32.07-fold,

$p < 0.00001$ , respectively) than the levels in the 3D models. However, these values are significantly less than the difference between gingival tissue (2,674.31-fold,  $p < 0.00001$ ; 1,785,091.51-fold,  $p < 0.00001$ , and 287.61-fold,  $p < 0.00001$ , for CK10, CK13 and CK16, respectively) and HGEK-16 grown as monolayers.

CK14 and CK18 expression in 3D models showed no significant differences with monolayer parallel cultures (fig. 5b). Both 3D models and HGEK-16 monolayers expressed significantly lower levels of CK14 compared with gingival tissue (0.027-fold,  $p < 0.00001$ , and 0.032-fold,  $p < 0.00001$ , for HGEK-16 and 3D models compared with gingival tissue, respectively), while for CK18, HGEK-16 monolayer cells, 3D cultures and gingival tissue showed no significant difference in expression. Col I and Col II expression was found to be significantly higher in GFB-16 monolayer (14.49-fold,  $p < 0.000$ , and 8.29-fold,  $p < 0.00001$ , respectively) than the levels in gingival tissue



(fig. 5c). However, expression of both Col genes showed no significant differences between gingival tissue and the 3D model.

## Discussion

To decipher the pathologies of periodontal diseases, it is important to establish *in vitro* models that mimic the mechanisms taking place within the gingival tissue. In the present study, we established epithelial and fibroblastic cell lines from human gingiva. Both epithelial and fibroblastic cell lines demonstrated a stable infinite growth with epithelium-like and spindle fibroblastic-shape morphology, respectively. Additionally, 3D multilayered organotypic culture was formed by use of embedded fibroblasts in a Col gel.

It has long been known that connective tissue underlying epithelia not only supports growth but also regulates differentiation of the epithelia [Karring et al., 1975]. Therefore, such organotypic cultures should consist of both epithelium and connective tissue. For the purpose of generating such a model, we developed and characterized immortalized cell lines (HGEK-16 and GFB-16) through the expression of HPV16-E6/E7 oncogenes. Stable expression levels of E6 and E7 throughout many passages confirmed successful immortalization. In our study, no morphology difference was observed between primary cultures and immortalized cell lines even after 50 (HGEK-16) and 35 passages (GFB-16). Earlier studies have reported immortalized human gingival fibroblasts by gene transfection of human telomerase reverse transcriptase [Kamata et al., 2004; Illeperuma et al., 2012], although other studies have shown that co-expression of human telomerase reverse transcriptase with other immortalizing genes, i.e. HPV16-E6/E7, was required for efficient immortalization of oral epithelial cells [Kamata et al., 2004].

The HGEK-16 cells had characteristic ‘cobblestone’ appearance of oral epithelial cells, while GFB-16 cells exhibited spindle-shaped morphology as their primary counterparts. qRT-PCR analysis showed that, like primary gingival fibroblasts, GFB-16 cells express highly abundant levels of Col I. Regarding the expression of Col II in the present experimental system, while its expression is not a typical feature of the gingival mucosa, there is evidence that under certain conditions GFB can express this and have potential to differentiate into chondrocyte-like cells [Yeh et al., 2013].

During periodontal infection, the junctional epithelium is exposed to a biofilm, and this tissue is therefore the subject of intense study into this disease [Bosshardt and Lang, 2005]. Several earlier studies have reported that gingival epithelial cells can form a multilayered epithelium when co-cultured with fibroblastic cells within 3D matrices allowing more direct comparisons to *in vivo* models [Dongari-Bagtzoglou and Kashleva, 2006; Roesch-Ely et al., 2006]. Indeed, when the transformed HGEK cells were co-cultured in a Col matrix along with human gingival fibroblasts, their characteristics were qualitatively and quantitatively closer to those in human gingival tissue than to monolayer cultures. One of the drawbacks of utilizing immortalized cell lines in organotypic cultures is that these cells may show carcinoma-like invasion patterns into the underlying connective tissue, especially in the presence of fibroblast/Col matrices [Costea et al., 2006]. Fortunately, in our model, HGEK-16 showed no invasive trend into the fibroblast/Col matrix when both cell lines were used to concomitantly construct organotypic tissue.

Within the gingiva, the expression patterns of various CK have been used as molecular indicators for different oral gingival epithelium regions. Previous studies showed varying expression levels between the keratinized region, the non-keratinized oral junctional epithelium and sulcular epithelium [Bragulla and Homberger, 2009; Hsieh et al., 2010]. Therefore, CK10, CK13, CK14, CK16, CK18 and CK19 were chosen as cell-specific markers [Locke et al., 2008]. CK19 is considered a marker for early differentiation stages of stratified epithelia [Groger et al., 2008] and is mostly found in simple epithelia, such as the junctional epithelium [Mackenzie and Gao, 1993]. Therefore, increased expression of CK19 in the present 3D organotypic tissue model is a common feature of junctional epithelium. CK10 and CK16 are known to be largely expressed in cornifying stratified epithelia [Coulombe and Omary, 2002] as well as in proliferating epithelia [Freedberg et al., 2001]. Thus, healthy gingival tissue samples, which contain mainly keratinized epithelia, expressed very high levels of these keratins. In contrast, the expression of these two CK was significantly lower in the present organotypic tissue compared to patient tissue. As these are considered essential for terminal differentiation of keratinized epithelia, low expression of CK10 and CK16 in our model confirms that the formed multilayered epithelium is rather non-keratinized.

In conclusion, the immortalized cell lines generally inherited the characteristics of their parental primary tissue cells. When cultured in 3D Col matrix, these immortal-



ized cell lines resembled their in vivo counterpart more closely than the corresponding monolayer cultures. These results indicate that our new cell lines may be useful tools for studying the physiology and pathobiology of gingival tissue in vitro. Moreover, this could present a practical model for studies of biofilm-gingival tissue interactions in vitro [Belibasakis et al., 2014; Belibasakis and Thurnheer, 2014]. The development of this model is not necessarily restricted to the gingiva, but could potentially be

expanded with adequate modifications for applications on the respiratory or gastrointestinal tract mucosa, or the skin.

## Acknowledgments

The authors would like to thank Dr. Andrew F. Irvine for English corrections.

## References

- Akgul, B., N. Bostanci, K. Westphal, I. Nindl, H. Navsaria, A. Storey, H. Pfister (2010) Human papillomavirus 5 and 8 E6 downregulate interleukin-8 secretion in primary human keratinocytes. *J Gen Virol* 91(Pt 4): 888–892.
- Albandar, J.M. (2011) Underestimation of periodontitis in NHANES surveys. *J Periodontol* 82: 337–341.
- Belibasakis, G.N., A. Johansson, Y. Wang, C. Chen, S. Kalfas, U.H. Lerner (2005) The cytolethal distending toxin induces receptor activator of NF- $\kappa$ B ligand expression in human gingival fibroblasts and periodontal ligament cells. *Infect Immun* 73: 342–351.
- Belibasakis, G.N., A. Meier, B. Guggenheim, N. Bostanci (2011) The RANKL-OPG system is differentially regulated by supragingival and subgingival biofilm supernatants. *Cytokine* 55: 98–103.
- Belibasakis, G.N., K. Bao, N. Bostanci (2014) Transcriptional profiling of human gingival fibroblasts in response to multi-species in vitro subgingival biofilms. *Mol Oral Microbiol* 29: 174–183.
- Belibasakis, G.N., T. Thurnheer (2014) Validation of antibiotic efficacy on in vitro subgingival biofilms. *J Periodontol* 85: 343–348.
- Bosshardt, D.D., N.P. Lang (2005) The junctional epithelium: from health to disease. *J Dent Res* 84: 9–20.
- Bostanci, N., G. Emingil, B. Saygan, O. Turkoglu, G. Atilla, M.A. Curtis, G.N. Belibasakis (2009) Expression and regulation of the NALP3 inflammasome complex in periodontal diseases. *Clin Exp Immunol* 157: 415–422.
- Bragulla, H.H., D.G. Homberger (2009) Structure and functions of keratin proteins in simple, stratified, keratinized and cornified epithelia. *J Anat* 214: 516–559.
- Costea, D.E., K. Kulasekara, E. Neppelberg, A.C. Johannessen, O.K. Vintermyr (2006) Species-specific fibroblasts required for triggering invasiveness of partially transformed oral keratinocytes. *Am J Pathol* 168: 1889–1897.
- Coulombe, P.A., M.B. Omary (2002) 'Hard' and 'soft' principles defining the structure, function and regulation of keratin intermediate filaments. *Curr Opin Cell Biol* 14: 110–122.
- Dongari-Bagtzoglou, A., H. Kashleva (2006) Development of a highly reproducible three-dimensional organotypic model of the oral mucosa. *Nat Protoc* 1: 2012–2018.
- Freedberg, I.M., M. Tomic-Canic, M. Komine, M. Blumenberg (2001) Keratins and the keratinocyte activation cycle. *J Invest Dermatol* 116: 633–640.
- Groger, S., J. Michel, J. Meyle (2008) Establishment and characterization of immortalized human gingival keratinocyte cell lines. *J Periodontol* 43: 604–614.
- Guggenheim, B., R. Gmür, J.C. Galicia, P.G. Stathopoulou, M.R. Benakanakere, A. Meier, T. Thurnheer, D.F. Kinane (2009) In vitro modeling of host-parasite interactions: the 'subgingival' biofilm challenge of primary human epithelial cells. *BMC Microbiol* 9: 280.
- Hsieh, P.C., Y.T. Jin, C.W. Chang, C.C. Huang, S.C. Liao, K. Yuan (2010) Elastin in oral connective tissue modulates the keratinization of overlying epithelium. *J Clin Periodontol* 37: 705–711.
- Illeperuma, R.P., Y.J. Park, J.M. Kim, J.Y. Bae, Z.M. Che, H.K. Son, M.R. Han, K.M. Kim, J. Kim (2012) Immortalized gingival fibroblasts as a cytotoxicity test model for dental materials. *J Mater Sci Mater Med* 23: 753–762.
- Kamata, N., R. Fujimoto, M. Tomonari, M. Taki, M. Nagayama, S. Yasumoto (2004) Immortalization of human dental papilla, dental pulp, periodontal ligament cells and gingival fibroblasts by telomerase reverse transcriptase. *J Oral Pathol Med* 33: 417–423.
- Karring, T., N.P. Lang, H. Loe (1975) The role of gingival connective tissue in determining epithelial differentiation. *J Periodontol* 10: 1–11.
- Locke, M., P.L. Hyland, C.R. Irwin, I.C. Mackenzie (2008) Modulation of gingival epithelial phenotypes by interactions with regionally defined populations of fibroblasts. *J Periodontol* 43: 279–289.
- Mackenzie, I.C., Z. Gao (1993) Patterns of cytokeratin expression in the epithelia of inflamed human gingiva and periodontal pockets. *J Periodontol* 28: 49–59.
- MacNeil, S. (2007) Progress and opportunities for tissue-engineered skin. *Nature* 445: 874–880.
- Nanci, A., D.D. Bosshardt (2006) Structure of periodontal tissues in health and disease. *Periodontol* 2000 40: 11–28.
- Pi, S.H., S.K. Lee, Y.S. Hwang, M.G. Choi, S.K. Lee, E.C. Kim (2007) Differential expression of periodontal ligament-specific markers and osteogenic differentiation in human papilloma virus 16-immortalized human gingival fibroblasts and periodontal ligament cells. *J Periodontol* 42: 104–113.
- Radyuk, S.N., P.A. Mericko, T.G. Popova, E. Grene, K. Alibek (2003) In vitro-generated respiratory mucosa: a new tool to study inhalational anthrax. *Biochem Biophys Res Commun* 305: 624–632.
- Roesch-Ely, M., T. Steinberg, F.X. Bosch, E. Musig, N. Whitaker, T. Wiest, A. Kohl, G. Komposch, P. Tomakidi (2006) Organotypic cocultures allow for immortalized human gingival keratinocytes to reconstitute a gingival epithelial phenotype in vitro. *Differentiation* 74: 622–637.
- Sacks, P.G. (1996) Cell, tissue and organ culture as in vitro models to study the biology of squamous cell carcinomas of the head and neck. *Cancer Metastasis Rev* 15: 27–51.
- Sandros, J., P.N. Papapanou, U. Nannmark, G. Dahlen (1994) *Porphyromonas gingivalis* invades human pocket epithelium in vitro. *J Periodontol* 29: 62–69.
- Smola, H., H.J. Stark, G. Thiekotter, N. Mirancea, T. Krieg, N.E. Fusenig (1998) Dynamics of basement membrane formation by keratinocyte-fibroblast interactions in organotypic skin culture. *Exp Cell Res* 239: 399–410.
- Yeh, H.Y., T.Y. Lin, C.H. Lin, B.L. Yen, C.L. Tsai, S.H. Hsu (2013) Neocartilage formation from mesenchymal stem cells grown in type II collagen-hyaluronan composite scaffolds. *Differentiation* 86: 171–183.
- Yin, T., S. Getsios, R. Caldelari, L.M. Godsel, A.P. Kowalczyk, E.J. Muller, K.J. Green (2005) Mechanisms of plakoglobin-dependent adhesion: desmosome-specific functions in assembly and regulation by epidermal growth factor receptor. *J Biol Chem* 280: 40355–40363.

# Paper 4





[Click for updates](#)

## Virulence

Publication details, including instructions for authors and subscription information:

<http://www.tandfonline.com/loi/kvir20>

### Establishment of an oral infection model resembling the periodontal pocket in a perfusion bioreactor system

Kai Bao<sup>a</sup>, Adam Papadimitropoulos<sup>b</sup>, Baki Akgül<sup>c</sup>, Georgios N Belibasakis<sup>d</sup> & Nagihan Bostanci<sup>a</sup>

<sup>a</sup> Oral Translational Research; Institute of Oral Biology; Center of Dental Medicine; University of Zürich; Zürich, Switzerland

<sup>b</sup> Cellec Biotek AG; Basel, Switzerland

<sup>c</sup> Institute of Virology; University of Cologne; Cologne, Germany

<sup>d</sup> Oral Microbiology and Immunology; Institute of Oral Biology; Center of Dental Medicine; University of Zürich; Zürich, Switzerland

Accepted author version posted online: 14 Jan 2015. Published online: 14 Jan 2015.

**To cite this article:** Kai Bao, Adam Papadimitropoulos, Baki Akgül, Georgios N Belibasakis & Nagihan Bostanci (2015) Establishment of an oral infection model resembling the periodontal pocket in a perfusion bioreactor system, *Virulence*, 6:3, 265-273, DOI: [10.4161/21505594.2014.978721](https://doi.org/10.4161/21505594.2014.978721)

**To link to this article:** <http://dx.doi.org/10.4161/21505594.2014.978721>

PLEASE SCROLL DOWN FOR ARTICLE

Taylor & Francis makes every effort to ensure the accuracy of all the information (the "Content") contained in the publications on our platform. Taylor & Francis, our agents, and our licensors make no representations or warranties whatsoever as to the accuracy, completeness, or suitability for any purpose of the Content. Versions of published Taylor & Francis and Routledge Open articles and Taylor & Francis and Routledge Open Select articles posted to institutional or subject repositories or any other third-party website are without warranty from Taylor & Francis of any kind, either expressed or implied, including, but not limited to, warranties of merchantability, fitness for a particular purpose, or non-infringement. Any opinions and views expressed in this article are the opinions and views of the authors, and are not the views of or endorsed by Taylor & Francis. The accuracy of the Content should not be relied upon and should be independently verified with primary sources of information. Taylor & Francis shall not be liable for any losses, actions, claims, proceedings, demands, costs, expenses, damages, and other liabilities whatsoever or howsoever caused arising directly or indirectly in connection with, in relation to or arising out of the use of the Content.

This article may be used for research, teaching, and private study purposes. Terms & Conditions of access and use can be found at <http://www.tandfonline.com/page/terms-and-conditions>

**It is essential that you check the license status of any given Open and Open Select article to confirm conditions of access and use.**



# Establishment of an oral infection model resembling the periodontal pocket in a perfusion bioreactor system

Kai Bao<sup>1</sup>, Adam Papadimitropoulos<sup>2</sup>, Baki Akgül<sup>3</sup>, Georgios N Belibasakis<sup>4</sup>, and Nagihan Bostanci<sup>1,\*</sup>

<sup>1</sup>Oral Translational Research; Institute of Oral Biology; Center of Dental Medicine; University of Zürich; Zürich, Switzerland; <sup>2</sup>Celtec Biotech AG; Basel, Switzerland;

<sup>3</sup>Institute of Virology; University of Cologne; Cologne, Germany; <sup>4</sup>Oral Microbiology and Immunology; Institute of Oral Biology; Center of Dental Medicine; University of Zürich; Zürich, Switzerland

**Keywords:** biofilm, collagen, cytokines, gingival epithelium, gingival fibroblasts, in vitro model, monocytic, multiplex immunoassay, organotypic culture, perfusion bioreactor, periodontal pocket

Periodontal infection involves a complex interplay between oral biofilms, gingival tissues and cells of the immune system in a dynamic microenvironment. A humanized in vitro model that reduces the need for experimental animal models, while recapitulating key biological events in a periodontal pocket, would constitute a technical advancement in the study of periodontal disease. The aim of this study was to use a dynamic perfusion bioreactor in order to develop a gingival epithelial-fibroblast-monocyte organotypic co-culture on collagen sponges. An 11 species subgingival biofilm was used to challenge the generated tissue in the bioreactor for a period of 24 h. The histological and scanning electron microscopy analysis displayed an epithelial-like layer on the surface of the collagen sponge, supported by the underlying ingrowth of gingival fibroblasts, while monocytic cells were also found within the sponge mass. Bacterial quantification of the biofilm showed that in the presence of the organotypic tissue, the growth of selected biofilm species, especially *Campylobacter rectus*, *Actinomyces oris*, *Streptococcus anginosus*, *Veillonella dispar*, and *Porphyromonas gingivalis*, was suppressed, indicating a potential antimicrobial effect by the tissue. Multiplex immunoassay analysis of cytokine secretion showed that interleukin (IL)-1  $\beta$ , IL-2, IL-4, and tumor necrosis factor (TNF)- $\alpha$  levels in cell culture supernatants were significantly up-regulated in presence of the biofilm, indicating a positive inflammatory response of the organotypic tissue to the biofilm challenge. In conclusion, this novel host-biofilm interaction organotypic model might resemble the periodontal pocket and have an important impact on the study of periodontal infections, by minimizing the need for the use of experimental animal models.

## Introduction

The two major forms of periodontal diseases are gingivitis and periodontitis. Approximately 80% of the world population exhibit gingivitis,<sup>1</sup> while 15% may exhibit severe destructive periodontitis.<sup>2</sup> Periodontitis is the primary cause of adult tooth loss due to its destructive effect on the periodontal connective tissues and underlying alveolar bone.<sup>3</sup> Besides, recent evidence shows that the effects of periodontal infections may well expand beyond the oral cavity, to be implicated in systemic diseases, such as diabetes mellitus and cardiovascular diseases.<sup>4,5</sup>

The causation of these infections involves the complex interaction between biofilm communities forming on the tooth surface, and the neighboring host periodontal tissues.<sup>6</sup> Biofilms are polymicrobial communities embedded in a dense extracellular matrix

produced by the different constituent species.<sup>6</sup> More than 700 species<sup>7–9</sup> have already identified in the oral cavity that may colonize the biofilms, but the actual number could be even higher, due to the limitations in detection by the contemporary technologies.<sup>10</sup> As constituents of the biofilm, bacteria can better withstand environmental stresses and receive metabolic benefits from each other.<sup>6</sup> The health-associated biofilms do not trigger a strong inflammatory response. In fact, some studies indicate that these biofilms actually benefit gingival health, by locally boosting the immune systems.<sup>9</sup> However, a biofilm could start to trigger inflammation when the composition of bacterial community shifts to a more pathogenic one.<sup>11,12</sup>

In response to the biofilm accumulation, the host tissue produces an inflammatory response for the recruitment of immune cells (e.g. polymorphonuclear leukocytes, monocytes),<sup>3</sup> and

© Kai Bao, Adam Papadimitropoulos, Baki Akgül, Georgios N Belibasakis, and Nagihan Bostanci

\*Correspondence to: Nagihan Bostanci; Email: nagihan.bostanci@zzm.uzh.ch

Submitted: 08/14/2014; Revised: 09/22/2014; Accepted: 10/16/2014

<http://dx.doi.org/10.4161/21505594.2014.978721>

This is an Open Access article distributed under the terms of the Creative Commons Attribution-Non-Commercial License (<http://creativecommons.org/licenses/by-nc/3.0/>), which permits unrestricted non-commercial use, distribution, and reproduction in any medium, provided the original work is properly cited. The moral rights of the named author(s) have been asserted.



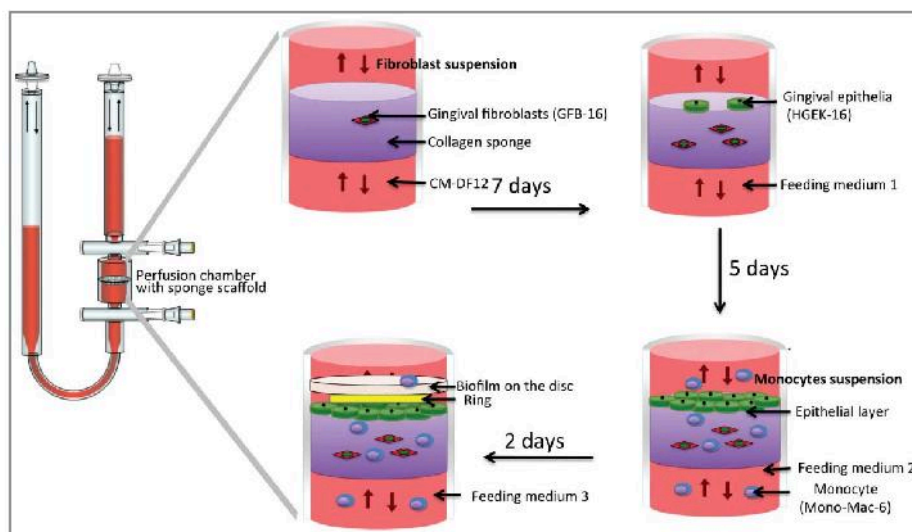


**Figure 1.** Schematic representation of the procedure used to establish the biofilm-3D gingival organotypic tissue co-culture model.

It is technically very challenging to reconstitute multi-tissue structures, such as gingiva, in *in vitro* cultures. Bioreactors, including perfusion systems, have been developed and used for *in vitro* modeling of various other infections including the lung,<sup>38</sup> the intestine,<sup>39,40</sup> and the colon.<sup>41,42</sup> Such a system could mimic the natural environment at local sites (e.g., temperature, atmosphere, shear stress), allowing for the study of biofilm-related mucosal disease under more realistic conditions. Yet, such a system has not been so far implemented in the field of periodontal infections. Apart from structural cells (i.e. fibroblasts and epithelial cells), cells of the immune system, such as monocytes can be readily incorporated into a perfusion bioreactor system, for the study of the biofilm challenge in an environment simulating the established periodontal pocket.

secretes a number of small compounds of the immune system (e.g. antibodies, cytokines and prostaglandins). If the inflammation tends to become chronic and the biofilm fails to be eliminated, the network of inflammatory molecules that has been established can cause connective tissue damage and bone destruction.<sup>3,13</sup> In some severe periodontitis cases, this may eventually lead to tooth loss if the inflammation remains unresolved.<sup>14</sup>

Several models have been used to understand mechanisms underlying periodontal infections, however, none of them appears to be reliable and reproducible. Experimental animals models of oral infection cannot efficiently represent human oral pathogenic bacteria,<sup>15,16</sup> whereas human experimental studies may answer questions regarding the initiation of these diseases,<sup>17</sup> but difficult to identify mechanisms that convert protective inflammation to tissue destructive lesion, due to ethical considerations. Most studies using *in vitro* models have only employed single oral bacterial species to challenge 2-dimensional monolayer cells,<sup>18,19</sup> or cells in suspension,<sup>20-22</sup> despite that periodontal infections are biofilm-related.<sup>23</sup> Moreover, monolayer cell culture systems do not adequately mimic the morphological and functional features of primary gingival tissues.<sup>24</sup>

Previous studies have shown 3D organotypic culture systems to mimic the *in vivo* situation better than 2D monolayer cultures.<sup>25,26</sup> It is known that epithelial cells differentiate to their nature state in primary tissue with the support of underlying fibroblasts in the connective tissue.<sup>25,27</sup> Therefore, 3D models using both epithelial cells and fibroblasts are preferable for the study of gingival tissues.<sup>28-32</sup> Besides, during chronic periodontal inflammation, it is possible that part of the epithelial layer of the tissue is degraded and the underlying fibroblast-comprised connective tissue may directly confront the oral biofilm. Indeed, fibroblasts are also actively participating in bacterially-induced inflammation,<sup>33,34</sup> and there are studies available that investigate their interaction with biofilms *in vitro*.<sup>35-37</sup>

The aim of this study was to develop a gingival organotypic tissue consisting of gingival epithelial cells, fibroblasts and monocytic cells, in a dynamic environment, which was achieved with the use of a perfusion bioreactor system. An 11-oral (subgingival) species biofilm grown on hydroxyapatite discs, which was established in our laboratory based on the previous models,<sup>36,43-46</sup> provides a model closer to the *in vivo* situation than single or few bacterial species. This was used to challenge the generated organotypic gingival tissue within the bioreactor, in a low oxygen environment, thus validating the usability of this organotypic tissue. It is anticipated that this novel dynamic tissue-biofilm interaction model may mimic the periodontal pocket environment and thus provide a more accurate *in vitro* experimental platform for the study of periodontal infections.

## Results

### Histological analysis of the organotypic tissue on the collagen sponge

The GFB-16, HGEK-16, and Mono-Mac-6 cells were seeded on the collagen sponges under the U-CUP perfusion bioreactor to construct 3D *in vitro* gingival tissue as described in materials and methods. The biofilm challenge was later introduced to the system for 24 h, to mimic periodontal infection. The morphology of the 3D model was evaluated by Masson's Trichrome stain (Fig. 2). In the control group whereby the biofilm was absent (Fig. 2a), there was a consistent epithelial-like layer of cells formed on the surface of the collagen, while inside the collagen structure, cells with long protrusions spread along the collagen fibers were observed. In the presence of biofilms (Fig. 2b), the epithelial-like layer was disrupted, with the appearance of many rounded big cells next to the collagen surface, that were not detectable in the control group.



### Scanning electron microscopy (SEM) analysis of the organotypic tissue surface

SEM was used to analyze the structure of the collagen sponge surfaces in contact with the biofilms. As seen from this analysis, the collagen sponge that served as a scaffold displayed a regular mesh of layers (Fig. 3a). When seeded onto the collagen sponge, cells filled most gaps between collagen fibers and formed a dense structure (Fig. 3b). In the collagen sponge, on which the biofilm was seeded (in the absence of host cells), clumps of predominately coccoid bacteria were observed in conjunction to the collagen fibers, and all over the mass of the sponge (Fig. 3c; Fig. S1). Such clumps of bacterial colonies were not found when the biofilms were co-cultured in the presence of the 3D gingival tissue, despite the presence of many large, monocyte-like cells (Fig. 3d), rather than the layered cells that were previously observed when the cells were seeded alone (Fig. 3b).

### Quantification of biofilms

After 24 h in co-culture with the organotypic gingival tissue, the bacterial composition of the biofilm was evaluated and compared to that of the biofilm in culture with the collagen sponge alone (Fig. 4). Significantly different numbers between the two groups were detected for *C. rectus*, *A. oris*, *S. anginosus*, *V. dispar*, and *P. gingivalis* (33.28-fold,  $P = 0.0002$ ; 11.09-fold,  $P = 0.0067$ ; 16.65-fold,  $P = 0.0036$ ; 17.46-fold,  $P = 0.0266$ ; and 19.28-fold,  $P = 0.0014$ ; respectively). Other differences did not prove to be statistically significant, hence the numbers of the remaining species were not affected.

### Quantification of cytokines secretion

Finally, the level of cytokines in the culture medium was investigated by the use of a 10-plex immunoassay platform (Fig. 5). After 24 h of challenge, the biofilm caused a significant increase in the production of IL-1 $\beta$ , IL-2, IL-4, and TFN- $\alpha$  by the organotypic gingival tissue, compared to the unchallenged control tissue alone (56.01-fold,  $P = 0.0011$ ; 6.94-fold,  $P < 0.0001$ ; 1.70-fold,  $P < 0.0001$ ; and 45.63-fold,  $P = 0.0006$ ; respectively). This finding confirms the inflammatory-

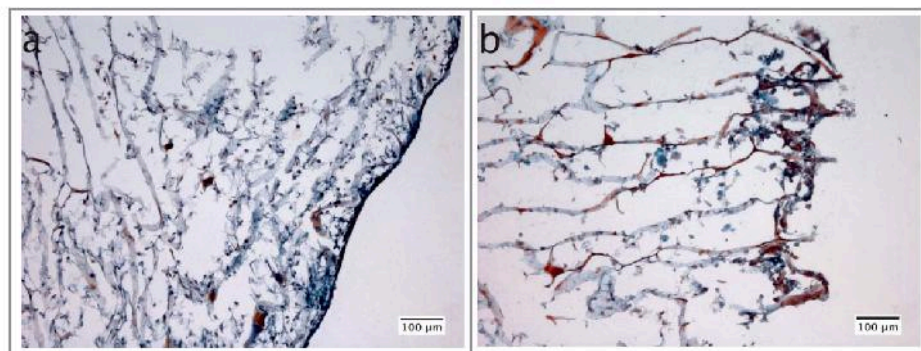


**Figure 2.** Masson's trichrome staining used for histological analysis of the collagen sponges, in which the 3D gingival tissue had been reconstructed in vitro. The tissue was co-cultured for 24 h with hydroxyapatite discs without (a) or with the biofilm (b).

inducing capacity of the biofilm on the organotypic gingival tissue.

## Discussion

In this study, we developed an organotypic co-culture system for the study of interactions between gingival tissues and subgingival biofilms in a U-CUP perfusion bioreactor device. The model shows compatible histological features to a periodontal

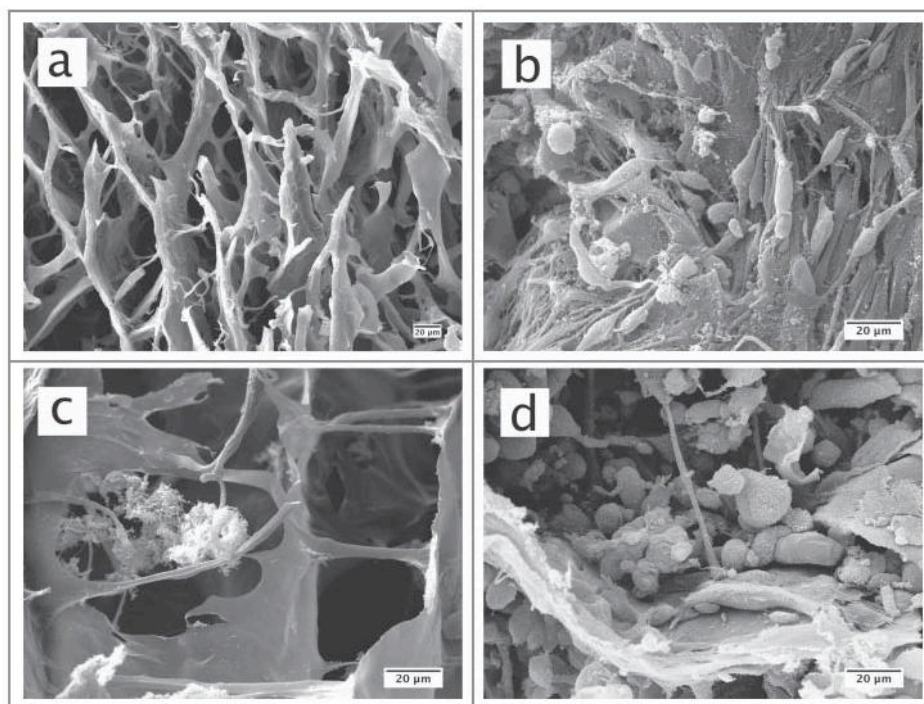


**Figure 3.** SEM images of original collagen sponge structures (a), collagen sponges on which the 3D in vitro gingival tissue had been reconstructed (b), collagen sponges in the presence of biofilms only (c), or collagen sponges on which the 3D in vitro gingival tissue had been reconstructed and challenged with the biofilms for 24 h (d).



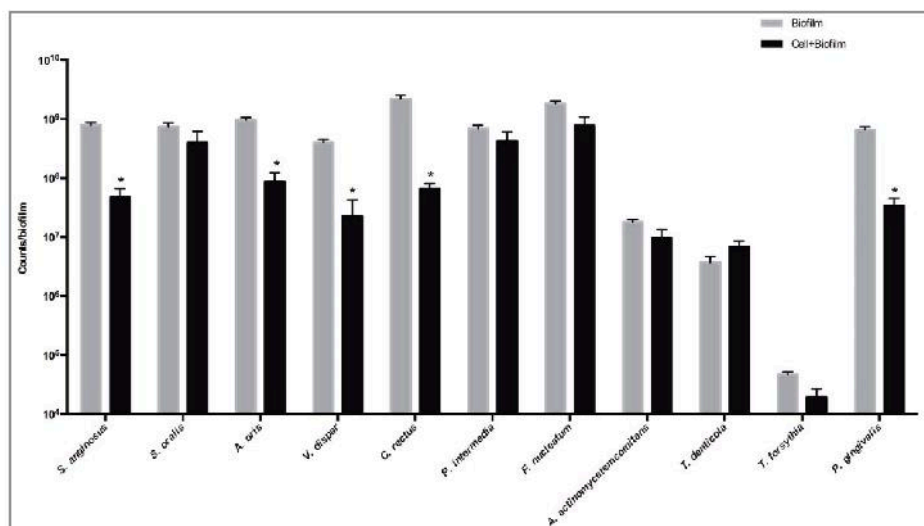


**Figure 4.** Quantification of bacterial numbers in biofilms. The biofilms were either cultured on blank collagen sponges (biofilm), or co-cultured with the 3D in vitro gingival tissue for 24 h (biofilm + cell). These values represent mean values of triplicate experiments  $\pm$  standard deviation (SD). The results are presented on a logarithmic scale. Asterisk (\*) represents the significance of differences ( $P \leq 0.05$ ) between the 2 groups.

pocket in vivo and utilizes a biofilm in order to challenge a multi-layered epithelial-fibroblast tissue, constructed using previously established immortalized human gingival cells,<sup>32</sup> and enriched further with monocytic cells.

As first line of the host defense, gingival tissue provides an epithelial layer firmly aligned onto the tooth surface.<sup>47</sup> Many approaches have been applied to create such an epithelial structure in vitro, for the study of the mechanisms of periodontal diseases. Moreover, the gingival epithelium is supported by the gingival connective tissue,<sup>47</sup> which consist of fibroblasts that produce a firm collagen network and produce important growth

established over time.

In our model, collagen sponges were used to create such a space while allowing gingival fibroblast and epithelial cells to attach onto them. Thus, a 3-phase seeding protocol was developed, ensuring that an epithelial layering and underlying connective tissue is formed, while maintaining constant flow of culture medium and cells of the immune cell. This system was microbially-challenged with an in vitro generated subgingival biofilm, grown onto hydroxyapatite surface (analogous to the tooth surface). Previous experimental models have already used single bacteria species, including *A. actinomycetemcomitans*, *F. nucleatum*, to challenge an epithelial-fibroblasts co-cultured model.<sup>55-57</sup>

Earlier works in our group have used this subgingival biofilm model in static co-culture either with gingival fibroblasts<sup>36</sup> or with multilayer gingival organotypic epithelium, in order to study various aspects of host tissue-oral biofilm interaction.<sup>58,59</sup>

As most subgingival species are strict anaerobes,<sup>6</sup> they were grown separately under anaerobic conditions, prior to being introduced into the bioreactor environment along with the organotypic tissue. It should be noted that, in vivo, diseased human gingival tissues present in 2 % oxygen and are exposed to shear forces by saliva and gingival exudate at flow rate of 0.4–2.0 ml/min.<sup>60</sup> These microenvironment conditions were also mimicked within the present bioreactor model, demonstrating that both the

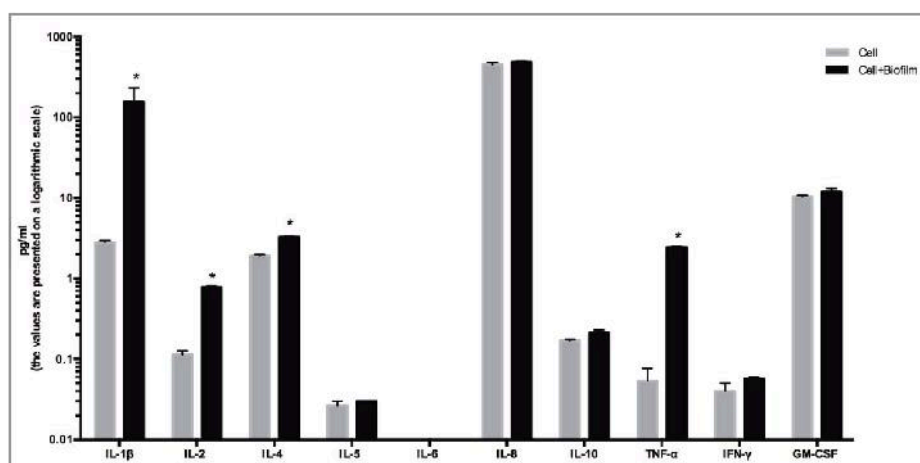


**Figure 5.** Quantification of cytokine secretion. The 3D in vitro gingival tissue were cultured either in the presence of only pellicle coated hydroxyapatite discs (cell) or co-cultured with biofilm-grown hydroxyapatite discs (biofilm + cell) for 24 h. These values represent mean values of triplicate experiments  $\pm$  standard deviation (SD). The results are presented on a logarithmic scale. Asterisk (\*) represents the significance of differences ( $P \leq 0.05$ ) between the 2 groups.



organotypic tissue and the bacterial biofilm are able to survive, co-exist and interact during the given experimental period of 24 h. The numbers of some bacterial species (namely *S. anginosus*, *A. oris*, *V. dispar*, *C. rectus* and *P. gingivalis*) were suppressed in the presence of the organotypic tissue, compared to the collagen sponge alone. Accordingly, bacterial aggregates were sparsely detectable on cells-seeded collagen surfaces. This potentially indicates the antimicrobial capacity of the tissue cells and/or the involvement of the immune cells in controlling bacterial colonization in the present experimental model.

To further evaluate the *in vivo* relevance of this model, selected secreted cytokines were measured by multiplex immunoassay technology. We detected the up-regulation of the pro-inflammatory cytokines IL-1 $\beta$ , IL-2, IL-6, and TNF- $\alpha$  on the secreted bioreactor medium (analogous to GCF), after 24 h of challenge of the tissue with the biofilm. Indeed, several studies have demonstrated that patients with periodontitis also display higher concentrations of IL-1 $\beta$ ,<sup>61,62</sup> IL-2,<sup>61</sup> IL-6,<sup>63,64</sup> and TNF- $\alpha$ <sup>62</sup> in GCF, compared to healthy gingiva. The regulation of cytokines or chemokines in gingival tissues is a complex process that involves many cells of the immune system,<sup>20,65-67</sup> or structural tissue cells.<sup>68,69</sup> To further enhance this model, additional elements could be introduced into this system, such as neutrophils and B- or T-lymphocytes, following the same protocol as with the Mono-Mac-6 cell lines.

In clinical studies,<sup>70</sup> increasing number of *T. forsythia*, *P. gingivalis*, *P. intermedia*, and *F. nucleatum* correlated with an up-regulation of IL-1 $\beta$ , while increasing number of *S. oralis*, and *S. anginosus* correlated with up-regulation the TNF- $\alpha$ , which may be in line with our observations in this *in vitro* experimental system. With regards to *in vitro* studies, the effects of periodontal bacteria are more representative when part of biofilm communities. Hence, the comparison of the effects of 2 biofilms with slightly altered bacterial composition can be useful for evaluating the relative involvement of different species in tissue cytokine responses.<sup>59</sup>

In conclusion, we have developed a novel model system to resemble the periodontal pocket, which allows for the simultaneous study of the interaction between oral biofilms, gingival tissues and cells of the immune system, in a biologically relevant environment. To our knowledge, this is the first model that utilized a perfusion bioreactor to study periodontal infection *in vitro*, and its establishment could also have an impact in the study of other biofilm-related diseases. Moreover, this *in vitro* system may reduce the need for usage of experimental animal models in periodontal research.

## Materials and Methods

### Cell culture

The development of the present 3D cell culture model required a combination of gingival epithelial keratinocytes, gingival fibroblasts and monocytic cells. Immortalized human gingival epithelial keratinocytes (HGEK-16) and immortalized human gingival fibroblasts (GFB-16) were established by transducing

E6/E7 oncoproteins from human papillomavirus type 16 (HPV16-E6/E7) to primary cells.<sup>32</sup> HGEK-16s were maintained in complete epithelial medium (CM-DKSFM) consisting of defined keratinocyte serum free medium (Gibco, 10744-019), supplemented with 100 U/ml penicillin (Sigma, 15140-122), 100  $\mu$ g/ml streptomycin (Sigma, 15140-122), 2 mM L-glutamine (Sigma, G7513), and 0.25  $\mu$ g/ml fungizone (Sigma, 15290-018). GFB-16s were maintained in complete fibroblasts medium (CM-DF12) Dulbecco's modified Eagle medium consisting of nutrient mixture F-12 media (Sigma-Aldrich, D8900-10L), supplemented with 1.2 g/ml of Na-Bicarbonate (Sigma-Aldrich, S5761), 10 % PAN Sera FBS special designed for ES cells (FBS, Bioswisstec AG, 2602), 100 U/ml penicillin, 100  $\mu$ g/ml streptomycin, 2 mM L-glutamine, and 0.05  $\mu$ g/ml fungizone.

The human myelomonocytic cell line Mono-Mac-6 obtained from the German Collection of Microorganisms and Cell Cultures (Mascheroder, Braunschweig, Germany) was maintained in complete myelomonocytic medium (CM-RPMI) consisting of RPMI-glutamax (Gibco, 72400-021), supplemented with 10% fetal bovine serum, 1% non-essential amino acids (Gibco, 11140-035), 1% sodium pyruvate (Gibco, 11360-039) and 9  $\mu$ g/ml bovine insulin (Sigma, 8418) 100 U/ml penicillin, 100  $\mu$ g/ml streptomycin, and 0.05  $\mu$ g/ml fungizone.

### *In vitro* biofilm formation

An 11 species biofilm was established based on a previously developed Zürich 10 species subgingival biofilm model.<sup>43,71</sup> The following strains were used included in this model: *Prevotella intermedia* ATCC 25611T (OMZ 278), *Aggregatibacter actinomycetemcomitans* JP2 (OMZ 295), *Campylobacter rectus* (OMZ 398), *Veillonella dispar* ATCC 17748T (OMZ 493), *Fusobacterium nucleatum* subsp. *nucleatum* (OMZ 598), *Streptococcus oralis* SK248 (OMZ 607), *Treponema denticola* ATCC 35405T (OMZ 661), *Actinomyces oris* (OMZ 745), *Streptococcus anginosus* ATCC 9895 (OMZ 871), *Tannerella forsythia* (OMZ 1047) and *Porphyromonas gingivalis* W50 (OMZ 308). Briefly, 200  $\mu$ l of bacterial cell suspensions containing equal densities ( $OD_{550} = 1.0$ ) of each strain were mixed with 1.6 ml of growth medium consisting 60% saliva,<sup>72</sup> 10% human serum, 30% mFUM,<sup>73</sup> and 0.5% hemin to initiate biofilm formation on hydroxyapatite discs (diameter 13 mm) (Clarkson Chromatography Products, custom made), pre-coated for 4 h with saliva, which was diluted 1:2 in a mixture of 0.9% NaCl and distilled water. A ring that is slightly larger than hydroxyapatite disc was sheathed around the veneer of the disc. The diameter of inner core at one end of the ring is smaller than 13 mm, therefore able to seal the hydroxyapatite disc inside. This end of the ring is around 1 mm longer than the surface of the hydroxyapatite disc, creating a gap between the biofilm surface and the bottom of the well. The discs were incubated for 64 h in anaerobic conditions, with medium renewed at 16 h and 40 h. During the first medium renewal, additional 40  $\mu$ l of *T. denticola* ( $OD_{550} = 1.0$ ) were further added to each well. The discs were dip-washed in saline at 16 h, 20 h, 24 h, 40 h, 44 h, 48 h and 64 h.



### Development of the 3D organotypic culture system in bioreactor

The 3D organotypic culture was established using 3D collagen sponge (porcine collagen, type I) scaffolds (Optimaix, Matricel GmbH, O3D304030) cut into a disc shape with 8 mm in diameter and 3 mm thick in a perfusion bioreactor (UCUP, Cellec Biotek AG, [www.cellectbiotech.com](http://www.cellectbiotech.com), UCUP001) based on a previously developed bioreactor system.<sup>74,75</sup> Briefly, the scaffold was embedded within a pair of provided adaptors and placed inside the bioreactor chamber, in order to constrain the cell/medium suspension passing through its pores, avoiding thus convectional flow (Fig. 1). The flow rate was controlled by the PHD Ultra Syringe Pump (included in the U-CUP bioreactor package).

The protocol for the development of the 3D co-culture in the bioreactor is schematically shown in Fig. 1. Initially,  $2 \times 10^6$  GFB-16 cells suspended in CM-DF12 were perfused through each  $8 \times 3$  mm 3D collagen sponge scaffold, at a superficial velocity of 1000  $\mu\text{m}/\text{sec}$  for 15 h, followed by 100  $\mu\text{m}/\text{sec}$ , as previously has been demonstrated to maximize the seeding efficiency of porous scaffold materials and allow subsequent tissue development.<sup>75,76</sup> After 7 days, the bioreactor chambers were opened under sterile hood and  $1 \times 10^6$  HGEK-16 cells were statically seeded on the top of same 3D collagen sponge in order to form an epithelial layer on its surface. Cells were incubated in feeding medium 1 (CM-DKSF: CM-DF12 = 1:1) for 3 h to allow cell attachment before initiating again the perfusion at a velocity of 100  $\mu\text{m}/\text{sec}$ . After 5 days,  $2 \times 10^6$  Mono-Mac-6 cells were injected into the bioreactor system and continued the perfusion at a velocity of 100  $\mu\text{m}/\text{sec}$ , in feeding medium 2 (CM-DMEM: CM-DF12: CM-RPMI = 1:1:1). After 2 days, the sponge was washed 3 times with feeding medium 3 (antibiotic free CM-DMEM: CM-DF12: CM-RPMI = 1:1:1) to remove any remaining antibiotic, prior to the addition of the biofilm in the system (description in the next section). The removed medium was also retained in order to collect the Mono-Mac-6 cells by centrifugation, and thereafter added back to the system with feeding medium 3. The cultures were fed every 2 d during this process, before being brought in co-culture with the biofilm.

In order to mimic the conditions of periodontal infection, hydroxyapatite discs with or without (control) the biofilms were introduced into the bioreactor chambers. Briefly, the bioreactor chambers were opened under sterile conditions in tissue culture, and the hydroxyapatite discs were placed by press-fit within the provided adaptors, facing the epithelial surface of the generated 3D organotypic tissue, or the collagen sponge alone (control). The chambers were closed again and perfusion flow continued at a flow rate of 135  $\mu\text{m}/\text{sec}$  in feeding medium 3 for additional 24 h. The culture temperature was 37°C and the atmospheric conditions 2% O<sub>2</sub> and 5% CO<sub>2</sub>.

### Biofilm harvesting and quantification by real-time quantitative polymerase chain reaction (qPCR)

For the evaluation of the bacterial composition of the biofilm after 24 h of co-cultured, the discs were removed from the bioreactor and vigorously vortexed for 3 min with 1 ml 0.9 % NaCl,

and sonicated at 25 W for 5 seconds. The bacterial suspensions were stored at 20°C before being processed for real-time quantitative PCR (qPCR) analysis. The DNA was extracted from bacterial suspensions using the GenElute™ bacterial genomic DNA kit (Sigma-Aldrich, NA2110) following the gram-positive lysis protocol of manufacturer's guideline with expanded lysis steps from 30 min to 1 h (lysozyme/mutanolysin step), and from 10 min to 30 min (proteinase K step). All primers were designed using online NCBI/ Primer-BLAST tool (<http://www.ncbi.nlm.nih.gov/tools/primer-blast>) targeted 16S rRNA gene (Table 1). The qPCR runs were performed using SYBR® Green PCR Master Mix (Life Technologies, 4309155) in a StepOnePlus™ Real-Time PCR Systems (Applied Biosystems) at 95°C for 10 min, 40 cycles of 95°C for 15 s and 60°C for 1 min. Standard curves were generated using DNA extracted from planktonic cultures of each of the 11 species used in biofilm, and the abundances were calculated using the theoretical genome weight of each organism from each strain according to the NCBI database, as previously described.<sup>44</sup>

### Quantification of cytokine secretion

Upon completion of the experiments, the flow culture medium was collected from bioreactors, and centrifuged at 1500 rpm for 5 min before being filtered through 0.2  $\mu\text{m}$  pore size, and stored at -80°C for further uses. The Cytokine Human Ultrasensitive 10-Plex Panel (Novex®, ThermoScientific, LHC6004) was used to quantify cytokines in the collected medium, according to the manufacturer's instructions. The following cytokines were tested in this assay: Interleukin (IL)-1 $\beta$ , IL-2, IL-4, IL-8, IL-5, IL-6, IL-10, Interferon gamma (IFN- $\gamma$ ), Tumor necrosis factor  $\alpha$  (TNF- $\alpha$ ), and granulocyte-macrophage colony-stimulating factor (GM-CSF) with sensitivities more than 0.05, 0.05, 0.1, 0.05, 0.1, 0.5, 0.05, 0.1, 0.5, and 0.1 pg/ml, respectively. These cytokines were detected with premixed antibody beads, read on a Luminex® 200 system, and analyzed by xPONENT® software (ThermoScientific).

### Harvesting of organotypic culture and histological analysis by Masson's Trichrome staining

The collagen sponges containing the generated 3D organotypic gingival tissue were removed from the bioreactor once the experiment was completed. They were then fixed with 3% paraformaldehyde in 2% sucrose/PBS buffer for 2 h, washed 3  $\times$  20 min in PBS, dehydrated in 15% sucrose/PBS for 2 h, and kept in 30% sucrose/PBS overnight at 4°C.

Slices of harvested sponges were introduced into aluminum foil molds filled with 5% gelatin and 5% sucrose solution, before snap frozen in cold 2-methylbutane (around -40°C by dry ice). The frozen blocks were sectioned into 16  $\mu\text{m}$  and transferred to Superfrost® Plus slides (ThermoScientific, 10143352). The slides were dried in room temperature overnight. They were stained with Weigert's iron hematoxylin (Sigma-Aldrich, 03979) for 20 sec, washed in tap water for 2 min, and rinsed in distilled water, stained with solution A (0.5 g acid fuchsin (Sigma-Aldrich, 857343), 0.5 g ponceau syldine (Sigma-Aldrich, 81465), 1 ml glacial acetic acid (Sigma-Aldrich, 537020), and 99 ml distilled



**Table 1** Primer sequences and properties

Organism	Sequence (5' → 3')	Strand on template	Size of amplicon (bases)	T <sub>m</sub> (°C)	Ref #
Streptococcus anginosus	ACCAGGTCTTGACATCCCGATGCTA CCATGCACCACTGTACCCGA	+ —	76	59.25 59.04	44
Streptococcus oralis	ACCAGGTCTTGACATCCCTCTGACC ACCACCTGTACCTCTGTCCCG	+ —	70	59.42 59.85	44
Actinomyces oris	GCCTGTCCCTTTGTGGGTGGG GCGGCTGCTGGCACGTAGTT	+ —	71	59.57 60.32	44
Veillonella dispar	CCCGGGCCTGTACACACCG CCCACCGGCTTTGGGCACTT	+ —	62	59.7 59.83	44
Fusobacterium nucleatum	CGCCCCGCACACACGAGA ACACCTCGGAACATCCCTCCTTAC	+ —	75	59.04 59.48	44
Campylobacter rectus	TCACGCCCCGTACACCATG CCGGTTTGGTATTTGGGCTTCGAGT	+ —	57	59.35 59.5	44
Prevotella intermedia	GCGTGCAGATTGACGGCCCTAT GGCACACGTGCCCGCTTTACT	+ —	68	59.61 60.24	44
Porphyromonas gingivalis	GCGAGAGCCTGAACACGCA ACTCGTATCGCCCGTTATCCCGTA	+ —	90	59.07 59.44	44
Treponema denticola	TAAGGGACAGCTTGCTACCCCTA CACCCACGCTTACTCACCAGTC	+ —	55	58.84 59.76	44
Tannerella forsythia	CGATGATACGCGAGGAACCTTACCC CCGAAGGGAAGAAAGCTCTCACTCT	+ —	72	59.07 58.01	44
Aggregatibacter actinomycetemcomitans	GTGGGGAGCAAACAGGATTAG CCTAAGGCACAAACCCATCTC	+ —	260	58.63 58.63	77
T <sub>m</sub> , melting temperature					

water) for 15 min, rinsed with distilled water, stained with solution B (1 g phosphomolybdic acid (Sigma-Aldrich, 79560) in 100 ml distilled water) for 5 min, rinsed with distilled water, stained with solution C (2 g light green SF yellowish (Sigma-Aldrich, 62110) and 2 ml glacial acetic acid in distilled water to a final volume of 100 ml) for 1 min, rinsed with distilled water, and dehydrated with 100% ethanol.

### Scanning electron microscopy

For SEM analysis of the 3D culture, slices of harvested collagen sponges were introduced into 0.185 M Sodium cacodylate buffer for one day, dissected and left for 1 day in cacodylate before being immersed in 2.5% glutaraldehyde in cacodylate for 45 min, washed in cacodylate for 1 h, 5 min in H<sub>2</sub>O, and then stored at 4°C overnight in 50% acetone. The samples were later dehydrated in a graded series of acetone, dried in CO<sub>2</sub>, and thereafter mounted on aluminum stubs and sputter-coated with 4 nm of platinum. The samples were imaged using a TESCAN VEGA TS 5136 XM scanning electron microscope (Tescan) at 25 KV.

### Statistical evaluation

All data present in the experiment derives from triplicate bio-film cultures. For the bacterial determination by qPCR, the values were logarithmically transformed, and then inserted to Prism v.6 software (GraphPad, La Jolla California USA). The statistical differences ( $P \leq 0.05$ ) between the groups were calculated by student t-test. For the determination of cytokine concentrations, the statistical differences ( $P \leq 0.05$ ) between the groups were calculated by student t-test.

### Disclosure of Potential Conflicts of Interest

No potential conflicts of interest were disclosed.

### Supplemental Material

Supplemental data for this article can be accessed on the publisher's website.

### References

- Albandar JM. Underestimation of periodontitis in NHANES surveys. J Periodontol 2011; 82:337-41; PMID:21214340; <http://dx.doi.org/10.1902/jop.2011.100638>
- Brown LJ, Loe H. Prevalence, extent, severity and progression of periodontal disease. Periodontol 2000 1993; 2:57-71; PMID:9673181; <http://dx.doi.org/10.1111/j.1600-0757.1993.tb00220.x>
- Ohlrich EJ, Cullinan MP, Seymour GJ. The immunopathogenesis of periodontal disease. Aust Dental J 2009; 54 Suppl 1:S2-10; PMID:19737265; <http://dx.doi.org/10.1111/j.1834-7819.2009.01139.x>
- Kebschull M, Demmer RT, Papapanou PN. "Gum bug, leave my heart alone!"—epidemiologic and mechanistic evidence linking periodontal infections and atherosclerosis. J Dent Res 2010; 89:879-902; PMID:20639510
- Belibasakis GN, Bostanci N. Inflammatory and bone remodeling responses to the cytolethal distending toxins. Cells 2014; 3:236-46; PMID:24709959; <http://dx.doi.org/10.3390/cells3020236>
- Socransky SS, Haffajee AD. Periodontal microbial ecology. Periodontol 2000 2005; 38:135-87; PMID:NOT\_FOUND; <http://dx.doi.org/10.1111/j.1600-0757.2005.00107.x>
- Kuramitsu HK, He X, Lux R, Anderson MH, Shi W. Interspecies interactions within oral microbial communities. Microbiol Mol Biol Rev 2007; 71:653-70; PMID:18063722; <http://dx.doi.org/10.1128/MMBR.00024-07>
- Rosan B, Lamont RJ. Dental plaque formation. Microbes Infect 2000; 2:1599-607; PMID:11113379
- Jenkinson HF, Lamont RJ. Oral microbial communities in sickness and in health. Trends Microbiol 2005; 13:589-95; PMID:16214341; <http://dx.doi.org/10.1016/j.tim.2005.09.006>
- Aas JA, Paster BJ, Stokes LN, Olsen I, Dewhirst FE. Defining the normal bacterial flora of the oral cavity. J Clin Microbiol 2005; 43:5721-32; PMID:16272510; <http://dx.doi.org/10.1128/JCM.43.11.5721-5732.2005>
- Sbordone L, Bortolaia C. Oral microbial biofilms and plaque-related diseases: microbial communities and their role in the shift from oral health to disease. Clin Oral Investig 2003; 7:181-8; PMID:14598129; <http://dx.doi.org/10.1007/s00784-003-0236-1>
- Darveau RP. Periodontitis: a polymicrobial disruption of host homeostasis. Nature Rev Microbiol 2010;

- 8:481-90; PMID:20514045; <http://dx.doi.org/10.1038/nrmicro2337>
13. Graves D. Cytokines that promote periodontal tissue destruction. *J Periodontol* 2008; 79:1585-91; PMID:18673014
14. Hirschfeld L, Wasserman B. A long-term survey of tooth loss in 600 treated periodontal patients. *J Periodontol* 1978; 49:225-37; PMID:277674; <http://dx.doi.org/10.1902/jop.1978.49.5.225>
15. Graves DT, Fine D, Teng YT, Van Dyke TE, Hajishengallis G. The use of rodent models to investigate host-bacteria interactions related to periodontal diseases. *J Clin Periodontol* 2008; 35:89-105; PMID:18199146; <http://dx.doi.org/10.1111/j.1600-051X.2007.01172.x>
16. McMahon KT, Wasfy MO, Yonushonis WP, Minah GE, Falkler WA, Jr. Comparative microbiological and immunological studies of subgingival dental plaque from man and baboons. *J Dent Res* 1990; 69:55-9; PMID:2303597; <http://dx.doi.org/10.1177/00220345900690010901>
17. Syed SA, Loesche WJ. Bacteriology of human experimental gingivitis: effect of plaque age. *Infect Immun* 1978; 21:821-9; PMID:711336
18. Reddi D, Bostanci N, Hashim A, Aduse-Opoku J, Curtis MA, Hughes FJ, Belibasakis GN. Porphyromonas gingivalis regulates the RANKL-OPG system in bone marrow stromal cells. *Microbes Infect* 2008; 10:1459-68; PMID:18789397; <http://dx.doi.org/10.1016/j.micinf.2008.08.007>
19. Reddi D, Brown SJ, Belibasakis GN. Porphyromonas gingivalis induces RANKL in bone marrow stromal cells: involvement of the p38 MAPK. *Microb Pathog* 2011; 51:415-20; PMID:21939752; <http://dx.doi.org/10.1016/j.micpath.2011.09.001>
20. Hamed M, Belibasakis GN, Cruchley AT, Rangarajan M, Curtis MA, Bostanci N. Porphyromonas gingivalis culture supernatants differentially regulate interleukin-1beta and interleukin-18 in human monocytic cells. *Cytokine* 2009; 45:99-104; PMID:19091595; <http://dx.doi.org/10.1016/j.cyt.2008.11.005>
21. Bostanci N, Reddi D, Rangarajan M, Curtis MA, Belibasakis GN. Porphyromonas gingivalis stimulates TACE production by T cells. *Oral Microbiology Immunol* 2009; 24:146-51; PMID:19239642; <http://dx.doi.org/10.1111/j.1399-302X.2008.00488.x>
22. Belibasakis GN, Reddi D, Bostanci N. Porphyromonas gingivalis induces RANKL in T-cells. *Inflammation* 2011; 34:133-8; PMID:20446027; <http://dx.doi.org/10.1007/s10753-010-9216-1>
23. Jenkinson HF. Beyond the oral microbiome. *Environ Microbiol* 2011; 13:3077-87; PMID:21906224; <http://dx.doi.org/10.1111/j.1462-2920.2011.02573.x>
24. Radyuk SN, Mericko PA, Popova TG, Grene E, Alibek K. In vitro-generated respiratory mucosa: a new tool to study inhalational anthrax. *Biochem Biophys Res Commun* 2003; 305:624-32; PMID:12763040; [http://dx.doi.org/10.1016/S0006-291X\(03\)00830-1](http://dx.doi.org/10.1016/S0006-291X(03)00830-1)
25. Mussig E, Tomakidi P, Steinberg T. Gingival fibroblasts established on microstructured model surfaces: their influence on epithelial morphogenesis and other tissue-specific cell functions in a co-cultured epithelium: an in-vitro model. *J Orolfac Orthop* 2009; 70:351-62; PMID:19997994
26. Bragulla HH, Homberger DG. Structure and functions of keratin proteins in simple, stratified, keratinized and cornified epithelia. *J Aesthet* 2009; 214:516-59; PMID:19422428; <http://dx.doi.org/10.1111/j.1469-7580.2009.01066.x>
27. Karring T, Lang NP, Loe H. The role of gingival connective tissue in determining epithelial differentiation. *J Periodontol Res* 1975; 10:1-11; PMID:124329; <http://dx.doi.org/10.1111/j.1600-0765.1975.tb00001.x>
28. Dongari-Bagtzoglou A, Kashleva H. Development of a highly reproducible three-dimensional organotypic model of the oral mucosa. *Nature protocols* 2006; 1:2012-8; PMID:17487190; <http://dx.doi.org/10.1038/nprot.2006.323>
29. Igarashi M, Irwin CR, Locke M, Mackenzie IC. Construction of large area organotypic cultures of oral mucosa and skin. *J Oral Pathol Med* 2003; 32:422-30; PMID:12846789
30. Choe MM, Tomei AA, Swartz MA. Physiological 3D tissue model of the airway wall and mucosa. *Nature protocols* 2006; 1:357-62; PMID:17406256; <http://dx.doi.org/10.1038/nprot.2006.54>
31. Chai WL, Moharamzadeh K, Brook IM, Emanuelsson L, Palmquist A, van Noort R. Development of a novel model for the investigation of implant-soft tissue interface. *J Periodontol* 2010; 81:1187-95; PMID:20450401; <http://dx.doi.org/10.1902/jop.2010.090648>
32. Bao K, Akgül B, Bostanci N. Establishment and characterization of immortalized gingival epithelial and fibroblastic cell lines for development of organotypic cultures. *Cells, tissues, organs* in press; PMID:25471635
33. Locke M, Hyland PL, Irwin CR, Mackenzie IC. Modulation of gingival epithelial phenotypes by interactions with regionally defined populations of fibroblasts. *J Periodontol Res* 2008; 43:279-89; PMID:18447855; <http://dx.doi.org/10.1111/j.1600-0765.2007.01028.x>
34. Leki PC, Pender N, McCulloch CA. Is fibroblast heterogeneity relevant to the health, diseases, and treatments of periodontal tissues? *Crit Rev Oral Biol Med* 1997; 8:253-68; PMID:9260043; <http://dx.doi.org/10.1177/10454411970080030201>
35. Belibasakis GN, Bostanci N, Reddi D. Regulation of protease-activated receptor-2 expression in gingival fibroblasts and Jurkat T cells by Porphyromonas gingivalis. *Cell Biology Int* 2010; 34:287-92; PMID:19947912; <http://dx.doi.org/10.1042/CBI20090290>
36. Belibasakis GN, Bao K, Bostanci N. Transcriptional profiling of human gingival fibroblasts in response to multi-species in vitro subgingival biofilms. *Mol Oral Microbiol* 2014; 29:174-83; PMID:24758474; <http://dx.doi.org/10.1111/omi.12053>
37. Belibasakis GN, Johansson A, Wang Y, Chen C, Kalfas S, Lemer UH. The cytolysin distending toxin induces receptor activator of NF-kappaB ligand expression in human gingival fibroblasts and periodontal ligament cells. *Infect Immun* 2005; 73:342-51; PMID:15618171; <http://dx.doi.org/10.1128/IAI73.1.342-351.2005>
38. Carterson AJ, Honer zu Bentrop K, Ott CM, Clarke MS, Pierson DL, Vanderburg C, Buchanan KL, Nickerson CA, Schurr MJ. A549 lung epithelial cells grown as three-dimensional aggregates: alternative tissue culture model for Pseudomonas aeruginosa pathogenesis. *Infect Immun* 2005; 73:1129-40; PMID:15664956; <http://dx.doi.org/10.1128/IAI73.2.1129-1140.2005>
39. Timmins NE, Scherberich A, Fruh JA, Heberer M, Martin I, Jakob M. Three-dimensional cell culture and tissue engineering in a T-CUP (tissue culture under perfusion). *Tissue Eng* 2007; 13:2021-8; PMID:17590148; <http://dx.doi.org/10.1089/ten.2006.0158>
40. Voisard D, Meuwly F, Ruffieux PA, Baer G, Kadouri A. Potential of cell retention techniques for large-scale high-density perfusion culture of suspended mammalian cells. *Biotechnol Bioeng* 2003; 82:751-65; PMID:12701141; <http://dx.doi.org/10.1002/bit.10629>
41. McCoy RJ, O'Brien FJ. Influence of shear stress in perfusion bioreactor cultures for the development of three-dimensional bone tissue constructs: a review. *Tissue Eng Part B, Rev* 2010; 16:587-601; PMID:20799909; <http://dx.doi.org/10.1089/ten.teb.2010.0370>
42. Yeats AB, Fisher JP. Tubular perfusion system for the long-term dynamic culture of human mesenchymal stem cells. *Tissue Eng Part C, Methods* 2011; 17:337-48; PMID:20929287; <http://dx.doi.org/10.1089/ten.tec.2010.0172>
43. Ammann TW, Belibasakis GN, Thurnheer T. Impact of early colonizers on in vitro subgingival biofilm formation. *PLoS One* 2013; 8:e83090; PMID:24340084; <http://dx.doi.org/10.1371/journal.pone.0083090>
44. Ammann TW, Bostanci N, Belibasakis GN, Thurnheer T. Validation of a quantitative real-time PCR assay and comparison with fluorescence microscopy and selective agar plate counting for species-specific quantification of an in vitro subgingival biofilm model. *J Periodontol Res* 2013; 48:517-26; PMID:23278531; <http://dx.doi.org/10.1111/jre.12034>
45. Ammann TW, Gmur R, Thurnheer T. Advancement of the 10-species subgingival Zurich Biofilm model by examining different nutritional conditions and defining the structure of the in vitro biofilms. *BMC Microbiol* 2012; 12:227; PMID:23040057; <http://dx.doi.org/10.1186/1471-2180-12-227>
46. Belibasakis GN, Guggenheim B, Bostanci N. Down-regulation of NLRP3 inflammasome in gingival fibroblasts by subgingival biofilms: involvement of Porphyromonas gingivalis. *Innate Immun* 2013; 19:3-9; PMID:22522430; <http://dx.doi.org/10.1177/1753425912444767>
47. Schroeder HE, Listgarten MA. The gingival tissues: the architecture of periodontal protection. *Periodontol* 2000 1997; 13:91-120; PMID:9567925; <http://dx.doi.org/10.1111/j.1600-0757.1997.tb00097.x>
48. Coste DE, Kulasekara K, Neppelberg E, Johannessen AC, Vintermyr OK. Species-specific fibroblasts required for triggering invasiveness of partially transformed oral keratinocytes. *Am J Pathol* 2006; 168:1889-97; PMID:16723704; <http://dx.doi.org/10.2353/ajpath.2006.050843>
49. Tomakidi P, Fusenig NE, Kohl A, Komposch G. Histomorphological and biochemical differentiation capacity in organotypic co-cultures of primary gingival cells. *J Periodontol Res* 1997; 32:388-400; PMID:9210093; <http://dx.doi.org/10.1111/j.1600-0765.1997.tb00549.x>
50. Rouabiah M, Deslauriers N. Production and characterization of an in vitro engineered human oral mucosa. *Biochem Cell Biol* 2002; 80:189-95; PMID:11898714; <http://dx.doi.org/10.1139/o01-237>
51. Tomakidi P, Breikreutz D, Fusenig NE, Zoller J, Kohl A, Komposch G. Establishment of oral mucosa phenotype in vitro in correlation to epithelial anchorage. *Cell Tissue Res* 1998; 292:355-66; PMID:9560478; <http://dx.doi.org/10.1007/s004410051066>
52. Schroeder HE, Munzel-Pedrazzoli S. Morphometric analysis comparing junctional and oral epithelium of normal human gingiva. *Helv Odontol Acta* 1970; 14:53-66; PMID:5486280
53. Schroeder HE. Quantitative parameters of early human gingival inflammation. *Arch Oral Biol* 1970; 15:383-400; PMID:5270171
54. Schroeder HE. Transmigration and infiltration of leucocytes in human junctional epithelium. *Helv Odontol Acta* 1973; 17:6-18; PMID:4699377
55. Pollanen MT, Gursay UK, Kononen E, Uitto VJ. Fusobacterium nucleatum biofilm induces epithelial migration in an organotypic model of dento-gingival junction. *J Periodontol* 2012; 83:1329-35; PMID:22248219; <http://dx.doi.org/10.1902/jop.2012.110535>
56. Paino A, Lohemaa E, Somunen R, Tuominen H, Korhonen J, Pollanen MT, Ihälin R. Interleukin-1beta is internalised by viable Aggregatibacter actinomycetemcomitans biofilm and localizes to the outer edges of nucleoids. *Cytokine* 2012; 60:565-74; PMID:22898394; <http://dx.doi.org/10.1016/j.cyt.2012.07.024>
57. Dabija-Wolter G, Sapkota D, Cimpan MR, Neppelberg E, Bakken V, Coste DE. Limited in-depth invasion of Fusobacterium nucleatum into in vitro reconstructed human gingiva. *Arch Oral Biol* 2012; 57:344-51; PMID:22024403; <http://dx.doi.org/10.1016/j.archoralbio.2011.09.015>



58. Thurnheer T, Belibasakis GN, Bostanci N. Colonisation of gingival epithelia by subgingival biofilms in vitro: Role of "red complex" bacteria. *Arch Oral Biol* 2014; 59:977-86; PMID:24949828
59. Belibasakis GN, Thurnheer T, Bostanci N. Interleukin-8 responses of multi-layer gingival epithelia to subgingival biofilms: role of the "red complex" species. *PLoS One* 2013; 8:e81581; PMID:24339946; <http://dx.doi.org/10.1371/journal.pone.0081581>
60. Loesche WJ, Gusberti F, Mettraux G, Higgins T, Syed S. Relationship between oxygen tension and subgingival bacterial flora in untreated human periodontal pockets. *Infect Immun* 1983; 42:659-67; PMID:6642647
61. Shaddox LM, Wiedey J, Calderon NL, Magnusson I, Bimstein E, Bidwell JA, Zapert EF, Aukhil I, Waller SM. Local inflammatory markers and systemic endotoxin in aggressive periodontitis. *J Dent Res* 2011; 90:1140-4; PMID:21730256; <http://dx.doi.org/10.1177/0022034511413928>
62. Navarro-Sanchez AB, Faria-Almeida R, Bascones-Martinez A. Effect of non-surgical periodontal therapy on clinical and immunological response and glycaemic control in type 2 diabetic patients with moderate periodontitis. *Journal of clinical periodontology* 2007; 34:835-43; PMID:17850602; <http://dx.doi.org/10.1111/j.1600-051X.2007.01127.x>
63. Kardesler L, Buduneli N, Cetinkalp S, Lappin D, Kinane DF. Gingival crevicular fluid IL-6, tPA, PAI-2, albumin levels following initial periodontal treatment in chronic periodontitis patients with or without type 2 diabetes. *Inflamm Res* 2011; 60:143-51
64. Duarte PM, de Oliveira MC, Tambeli CH, Parada CA, Casati MZ, Nociti FH, Jr. Overexpression of interleukin-1beta and interleukin-6 may play an important role in periodontal breakdown in type 2 diabetic patients. *J Periodontol* 2007; 42:377-81; PMID:17559636; <http://dx.doi.org/10.1111/j.1600-0765.2006.00961.x>
65. Bostanci N, Allaker RP, Belibasakis GN, Rangarajan M, Curtis MA, Hughes FJ, McKay IJ. Porphyromonas gingivalis antagonises Campylobacter rectus induced cytokine production by human monocytes. *Cytokine* 2007; 39:147-56; PMID:17709256; <http://dx.doi.org/10.1016/j.cyt.2007.07.002>
66. Bostanci N, Akgul B, Tsakanika V, Allaker RP, Hughes FJ, McKay IJ. Effects of low-dose doxycycline on cytokine secretion in human monocytes stimulated with Aggregatibacter actinomycetemcomitans. *Cytokine* 2011; 56:656-61; PMID:21962932; <http://dx.doi.org/10.1016/j.cyt.2011.08.039>
67. Bostanci N, Allaker R, Johansson U, Rangarajan M, Curtis MA, Hughes FJ, McKay IJ. Interleukin-1alpha stimulation in monocytes by periodontal bacteria: antagonistic effects of Porphyromonas gingivalis. *Oral Microbiol Immun* 2007; 22:52-60; PMID:17241171; <http://dx.doi.org/10.1111/j.1399-302X.2007.00322.x>
68. Belibasakis GN, Johansson A, Wang Y, Chen C, Lagergard T, Kalfas S, Lerner UH. Cytokine responses of human gingival fibroblasts to Actinobacillus actinomycetemcomitans cytolysin distending toxin. *Cytokine* 2005; 30:56-63; PMID:15804596; <http://dx.doi.org/10.1016/j.cyt.2004.11.008>
69. Belibasakis GN, Guggenheim B. Induction of prostaglandin E(2) and interleukin-6 in gingival fibroblasts by oral biofilms. *FEMS Immunol Med Microbiol* 2011; 63:381-6; PMID:22092565; <http://dx.doi.org/10.1111/j.1574-695X.2011.00863.x>
70. Teles RP, Gursky LC, Faveri M, Rosa EA, Teles FR, Feres M, Socransky SS, Haffajee AD. Relationships between subgingival microbiota and GCF biomarkers in generalized aggressive periodontitis. *J Clin Periodontol* 2010; 37:313-23; PMID:20447254; <http://dx.doi.org/10.1111/j.1600-051X.2010.01534.x>
71. Guggenheim B, Gmur R, Galicia JC, Stathopoulou PG, Benakanakere MR, Meier A, Thumheer T, Kinane DF. In vitro modeling of host-parasite interactions: the 'subgingival' biofilm challenge of primary human epithelial cells. *BMC Microbiol* 2009; 9:280; PMID:20043840; <http://dx.doi.org/10.1186/1471-2180-9-280>
72. Guggenheim B, Giertsen E, Schupbach P, Shapiro S. Validation of an in vitro Biofilm Model of Supragingival Plaque. *J Dent Res* 2001; 80:363-70; PMID:11269730; <http://dx.doi.org/10.1177/00220345010800011201>
73. Gmur R, Guggenheim B. Antigenic heterogeneity of Bacteroides intermedius as recognized by monoclonal antibodies. *Infect Immun* 1983; 42:459-70; PMID:6196291
74. Braccini A, Wendt D, Jaquiere C, Jakob M, Heberer M, Kenins L, Wodnar-Filipowicz A, Quarto R, Martin I. Three-dimensional perfusion culture of human bone marrow cells and generation of osteoinductive grafts. *Stem Cells* 2005; 23:1066-72; PMID:16002780; <http://dx.doi.org/10.1634/stemcells.2005-0002>
75. Wendt D, Marsano A, Jakob M, Heberer M, Martin I. Oscillating perfusion of cell suspensions through three-dimensional scaffolds enhances cell seeding efficiency and uniformity. *Biotechnol Bioeng* 2003; 84:205-14; PMID:12966577; <http://dx.doi.org/10.1002/bit.10759>
76. Wendt D, Stroebel S, Jakob M, John GT, Martin I. Uniform tissues engineered by seeding and culturing cells in 3D scaffolds under perfusion at defined oxygen tensions. *Biorheology* 2006; 43:481-8; PMID:16912419
77. Belibasakis GN, Ozturk VO, Emingil G, Bostanci N. Soluble triggering receptor expressed on myeloid cells 1 (sTREM-1) in gingival crevicular fluid: association with clinical and microbiologic parameters. *J Periodontol* 2014; 85:204-10; PMID:23659423; <http://dx.doi.org/10.1902/jop.2013.130144>

# Paper 5

# SCIENTIFIC REPORTS

OPEN

## Proteomic profiling of host-biofilm interactions in an oral infection model resembling the periodontal pocket

Received: 03 July 2015

Accepted: 07 October 2015

Published: 03 November 2015

Kai Bao<sup>1</sup>, Georgios N. Belibasakis<sup>2</sup>, Nathalie Selevsek<sup>3</sup>, Jonas Grossmann<sup>3</sup> & Nagihan Bostanci<sup>1</sup>

Periodontal infections cause inflammatory destruction of the tooth supporting tissues. We recently developed a dynamic, *in vitro* periodontal organotypic tissue model in a perfusion bioreactor system, in co-culture with an 11-species subgingival biofilm, which may recapitulate early events during the establishment of periodontal infections. This study aimed to characterize the global proteome regulations in this host-biofilm interaction model. Semi-quantitative shotgun proteomics were applied for protein identification and quantification in the co-culture supernatants (human and bacterial) and the biofilm lysates (bacterial). A total of 896 and 3363 proteins were identified as secreted in the supernatant and expressed in the biofilm lysate, respectively. Enriched gene ontology analysis revealed that the regulated secreted human tissue proteins were related to processes of cytoskeletal rearrangement, stress responses, apoptosis, and antigen presentation, all of which are commensurate with deregulated host responses. Most secreted bacterial biofilm proteins derived from their cytoplasmic domain. In the presence of the tissue, the levels of *Fusobacterium nucleatum*, *Actinomyces oris* and *Campylobacter rectus* proteins were significantly regulated. The functions of the up-regulated intracellular (biofilm lysate) proteins were associated with cytokinesis. In conclusion, the proteomic overview of regulated pathways in this host-biofilm interaction model provides insights to the early events of periodontal pathogenesis.

Periodontal infections are the primary reasons for adult tooth loss, due to the destruction of tooth-supporting (periodontal) tissues<sup>1</sup>. While environmental pressures and genetic variations may exert different susceptibilities among individuals on the development of the diseases<sup>2</sup>, these diseases are of inflammatory pathogenesis and initiated by the formation of a microbial biofilm (commonly known as “dental plaque”) which accumulates on the tooth surface<sup>2</sup>. Biofilms are complex polymicrobial communities of endogenous oral species, with more than 700 microbial species already having been identified in the oral cavity potentially constituting part of each biofilm<sup>3</sup>. When in the dense yet dynamic structure of a biofilm, oral microorganisms display increased resistance to environmental stresses<sup>3</sup>. There are structural and functional relationships between the constituent species of the biofilm and the attached surface<sup>4</sup>, which may be symbiotic<sup>5</sup> or antagonistic<sup>6</sup>. Biofilms consisting of commensal species may actually provide a health benefit to the gingival tissue, by positively priming the immune system<sup>7</sup>. Under certain environmental pressures, a shift of the flora may be favoured towards a more to pathogenic one, triggering disease<sup>1,8,9</sup>. These concepts are accepted today as a model of polymicrobial synergy and dysbiosis<sup>9</sup>.

<sup>1</sup>Oral Translational Research, Institute for Oral Biology, Center of Dental Medicine, University of Zürich, Zürich, Switzerland. <sup>2</sup>Oral Microbiology and Immunology, Institute for Oral Biology, Center of Dental Medicine, University of Zürich, Zürich, Switzerland. <sup>3</sup>Functional Genomics Center Zürich, University of Zürich, Zürich, Switzerland. Correspondence and requests for materials should be addressed to N.B. (email: Nagihan.Bostanci@zzm.uzh.ch)



The periodontium is a syncytium of specialised tissues that surround and support the teeth. Gingival epithelia line the surfaces of the periodontium and are the first layers that encounter the tooth. They act as physical barriers against infection and aid the immune response with their enzyme-rich lysosomes and semi-permeability that allows the trafficking of immune cells to the site of infection<sup>10</sup>. The underlying connective tissues supports and regulates the function of the epithelium<sup>11</sup>, while protecting the underlying alveolar bones and periodontal ligament that hold the tooth in place. The epithelium and connective tissue are collectively known as the gingival tissue. Periodontal inflammation in response to the causative biofilm is initiated in the gingival tissue<sup>2</sup>. As a result, immune cells, such as polymorphonuclear leukocytes, macrophages and lymphocytes are recruited to the region in order to tackle the establishing bacterial infection. Nevertheless, an excessive and deregulated inflammatory reaction will eventually cause connective tissue breakdown and alveolar bone loss, manifesting as periodontitis<sup>12</sup>.

Periodontal infections are complicated processes that require the understanding of both the microbial and host component, as well as their interaction. Therefore, we recently developed a complex periodontal infection model<sup>13</sup> that includes an 11-species biofilm used to challenge a generated organotypic tissue consisting of gingival epithelial, gingival fibroblast and monocytic cells grown on collagen sponges. The whole co-culture was performed in a closed dynamic perfusion bioreactor system that ensured the establishment of continuous shear forces. During that study we also characterized the model morphologically, in terms of cytokine production and bacterial profiling, and concluded that it closely resembles the *in vivo* environment.

The study of periodontal disease on the proteomic level has become increasingly popular in recent years, as a result of improvements in mass spectrometry-based technologies<sup>14</sup>. This has enabled high-throughput clinical studies of protein expression in gingival cervical fluid (GCF), for example<sup>14</sup>. *In vitro* studies on the proteome of cells<sup>15</sup> and multispecies biofilms<sup>16,17</sup> or host-biofilm interaction infection models<sup>15</sup> are also available, all of which broaden our knowledge of periodontal infections. Hence, the present study utilised semi-quantitative proteomics with the aim to characterise changes in the proteome that take place in our recently established *in vitro* periodontal infection model<sup>13</sup>. This approach aspires to unravel in more detail the intricate interactions between the gingival tissue and subgingival biofilms during the early stages of the establishment of periodontal inflammation.

## Results

**Qualitative and semi-quantitative proteomic experiments.** After 24 h of co-culture of the *in vitro* multispecies biofilm with the organotypic gingival tissue in a perfusion bioreactor<sup>13</sup>, the culture supernatants were collected and processed for proteomic analysis. The following groups were included: a) biofilm-challenged organotypic tissue (tissue + biofilm) b) organotypic tissue alone (tissue) and c) biofilm alone (biofilm). The detailed structural characterization of this multispecies biofilm and organotypic tissue was reported recently<sup>13</sup>. In brief, histology and electron microscopy revealed that the tissue consisted of a superficial epithelial-like layer and an underlying collagen-supported connective tissue rich in gingival fibroblasts and monocytic cells. In presence of the tissue, the growth of selected biofilm species (*Campylobacter rectus*, *Actinomyces oris*, *Streptococcus anginosus*, *Veillonella dispar*, and *Porphyromonas gingivalis*) was suppressed, potentially demonstrating an antimicrobial effect by the tissue.

For the proteomic analyses performed in this study, proteins were accepted if at least two peptides were present, with peptide false discovery rate (pepFDR) set to less than 1%, and protein false discovery rate (proFDR) to less than 3%. In this experiment, actual pepFDR and proFDR were 0.65% and 2.4%, respectively. The overlaps of detected human and bacterial proteins in pair-wise comparisons of these three groups are shown in Fig. 1, whereas lists of identified human and bacterial proteins are presented in supplementary Table S1 and supplementary Table S2, respectively. In all, a total of 620 human proteins and 276 bacterial proteins were identified. When human proteins were taken into account, 37 proteins were exclusively identified in the tissue + biofilm group, whereas 215 proteins were exclusively identified in the tissue group alone. There was also a considerable protein overlap between the two groups ( $n = 368$ ), as shown by the intersection sets of the Venn diagrams (Fig. 1). Of 276 secreted bacterial proteins, 179 were derived uniquely from *F. nucleatum*. Numerically, more proteins belonging to *S. oralis*, *S. anginosus*, and *V. dispar* were identified in the biofilm group, while more proteins belonging to *P. intermedia* were present in the tissue + biofilm group. The species-specific taxonomy of the all identified bacterial proteins numbers is provided in Table 1.

Quantitative differences in protein expression were assessed by spectral counting, as detailed in the methods section. The quantitative comparison was based on proteins identified with  $p$  value of  $\log_2$  Fold Change (logFC) smaller than 0.05 for the statistical test. With these criteria, a total of 228 proteins of either human ( $n = 76$ ) or bacterial ( $n = 152$ ) origin were filtered as significantly regulated ones. For the regulated secreted human proteins, the down-regulated proteins outnumbered the up-regulated ones by approximately 20%. For the regulated secreted bacterial proteins, the up-regulated proteins outnumbered the down-regulated ones by approximately 18%. For the regulated biofilm lysate proteins, the down-regulated ones outnumbered the up-regulated ones by approximately 92%. To graphically represent these data, a volcano plot was used (Supplementary Fig. S1a and Supplementary Fig. S1b).

**Secreted proteins of human origin.** Out of 76 human proteins, 4 and 54 proteins were uniquely quantified in the tissue + biofilm and tissue groups, respectively, while in the remaining proteins, 18 were

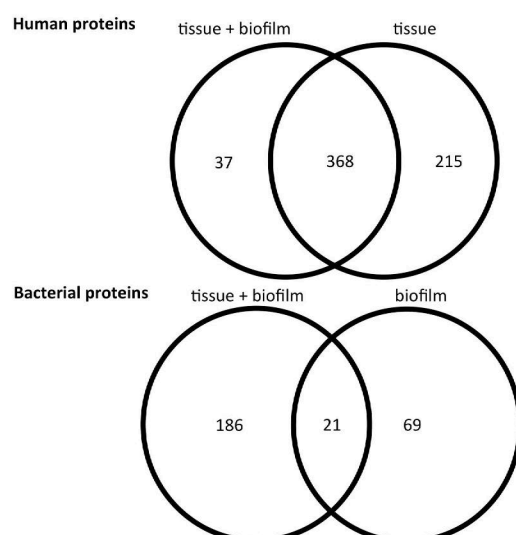


**Figure 1. Venn diagram of identified protein numbers in culture supernatants.** Protein numbers for each category is depicted. Details of human and bacterial proteins in each group are listed in Supplementary Information Table S1 and Table S2, respectively.

	tissue + biofilm	overlap	biofilm
<i>A. oris</i>	1	0	0
<i>A. actinomycetemcomitans</i>	1	0	0
<i>C. rectus</i>	0	0	1
<i>F. nucleatum</i>	168	5	6
<i>P. gingivalis</i>	1	0	0
<i>P. intermedia</i>	11	3	2
<i>S. anginosus</i>	1	4	8
<i>S. oralis</i>	3	8	37
<i>T. forsythia</i>	0	0	0
<i>T. denticola</i>	0	1	0
<i>V. dispar</i>	0	0	15

**Table 1. Number of identified secreted bacterial proteins in culture supernatants by each species.**

Number of proteins identified from culture supernatants were grouped and listed on the table based on whether they were identified in tissue + biofilm, biofilm alone, or overlap group (identified in both groups).

jointly quantified in both groups. Of those 18 proteins, 9 were up-regulated and 9 down-regulated in the tissue + biofilm group according to the regulation criteria. The relative enrichment pattern for human proteins is also shown as a heatmap (Fig. 2).

These differentially expressed human proteins (combining both up-regulated and down-regulated ones) were further enriched using the MetaCore software (<https://portal.genego.com>, Thomson Reuters) following enrichment analysis as described in the methods<sup>18</sup>. The lists of top 10 GO processes and process networks for these proteins in the tissue + biofilm, compared to the tissue group alone are provided in Table 2 and 3, respectively. Regulated proteins in each category are shown in supplementary Table S3. The results were ranked according to increasing *P* value. With respect to GO processes, the most regulated ones involved epidermis and skin development, and also antigen presentation and processing (Table 2). Subsequently, the most over-represented process networks were *cytoskeleton—intermediate filaments* (7 out of 81 proteins, *P* value 1.433E-06), *protein folding* (5 out of 69 proteins, *P* value 1.207E-04), and *immune response—phagosome in antigen presentation* (7 out of 243 proteins, *P* value 1.555E-03) (Table 3).

A network built using the “analyse network” algorithm to connect the proteins in this process. The top 10 most predominant potential protein interaction networks among these regulated human proteins associated with all involved GO processes and given *P* value are listed in Table S4, while the regulation relations of the top 3 groups are highlighted in Figs 3–5. The first top regulated network named *Calreticulin*, *AP-2 alpha subunits*, *AHNAK*, *LTBP2*, *SPRR1A* revealed activation of damage-associated



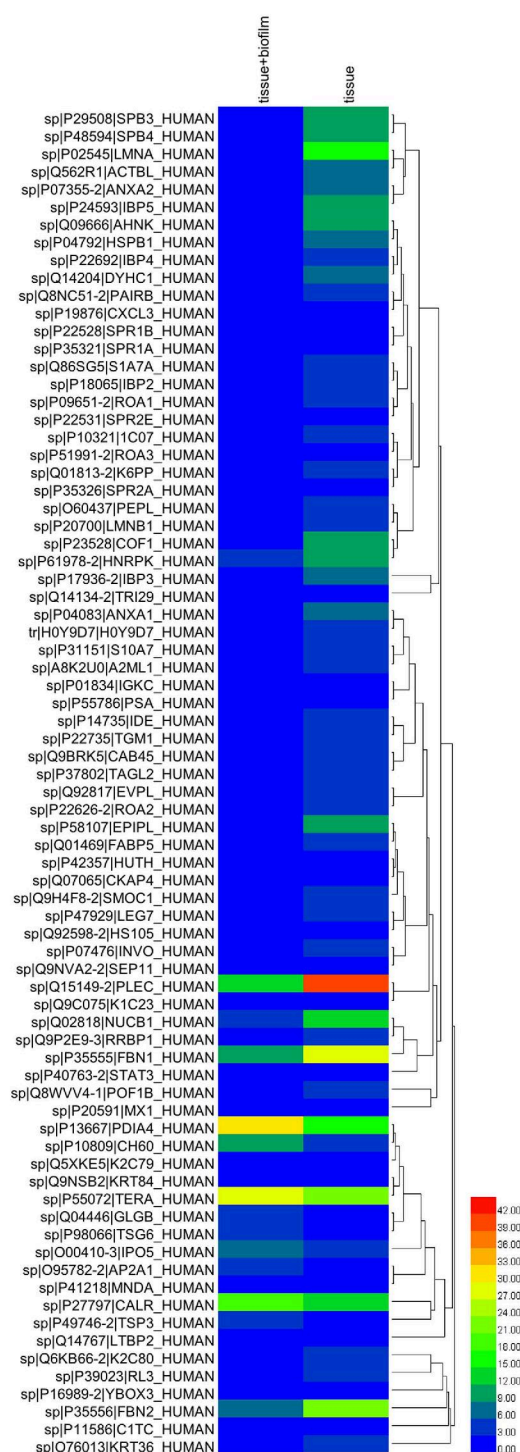


**Figure 2. Heat map of differentially regulated human proteins in culture supernatants.** Hierarchical clustering of significantly altered proteins (LogFC  $P < 0.05$ ) were performed by the average linkage method using the Heml software. The colours in the map display the mean value for individual proteins (represented by a single row) within each experimental group (represented by a single column). Expression values are shown as a colour scale, with higher values represented by red and lower represented by blue. The colour scale bar gradient is shown at the right corner of the figure.

molecular patterns, including calreticulin and down regulation of cell-adhesion molecules such as latent transforming growth factor beta binding protein 2 (Fig. 3). This network has a total of 51 proteins including 14 of them from our regulated list. The  $P$  value of the network is  $8.89 \times 10^{-32}$ , which indicated that the probability of assembly from a random set of nodes (proteins) was very low (see supplementary Table S4). *Regulation of response to stress, cellular response to chemical stimulus, regulation of defence response,*

No.	Processes	Regulated	p-value	FDR
1	epidermis development	15/405	2.081E-11	3.965E-08
2	antigen processing and presentation of endogenous peptide antigen via MHC class I via ER pathway, TAP-independent	6/19	5.517E-11	5.255E-08
3	skin development	15/468	1.575E-10	7.548E-08
4	keratinocyte differentiation	10/146	1.585E-10	7.548E-08
5	antigen processing and presentation of exogenous peptide antigen via MHC class I, TAP-independent	6/25	3.538E-10	1.025E-07
6	antigen processing and presentation of endogenous peptide antigen via MHC class I via ER pathway	6/25	3.538E-10	1.025E-07
7	keratinization	8/76	3.765E-10	1.025E-07
8	antigen processing and presentation of endogenous peptide antigen via MHC class I	6/29	9.379E-10	2.233E-07
9	antigen processing and presentation of endogenous peptide antigen	6/32	1.774E-09	3.754E-07
10	antigen processing and presentation of endogenous antigen	6/34	2.617E-09	4.985E-07

**Table 2. Top 10 enriched GO processes of regulated human proteins in culture supernatants.**

No.	Processes	Regulated	p-value	FDR
1	Cytoskeleton_Intermediate filaments	7/81	1.433E-06	1.218E-04
2	Protein folding_Response to unfolded proteins	5/69	1.207E-04	5.129E-03
3	Immune response_Phagosome in antigen presentation	7/243	1.555E-03	4.405E-02
4	Apoptosis_Apoptotic nucleus	5/159	5.271E-03	1.021E-01
5	Inflammation_NK cell cytotoxicity	5/164	6.003E-03	1.021E-01
6	Proliferation_Negative regulation of cell proliferation	5/184	9.658E-03	1.352E-01
7	Signal transduction_Androgen receptor nuclear signaling	4/126	1.216E-02	1.352E-01
8	Immune response_Antigen presentation	5/197	1.272E-02	1.352E-01
9	Cell adhesion_Cell-matrix interactions	5/211	1.671E-02	1.578E-01
10	Inflammation_IL-13 signaling pathway	3/91	2.680E-02	2.278E-01

**Table 3. Top 10 enriched process networks of regulated proteins in culture supernatants.**

and *immune system process* were among the most associated GO terms suggesting that these proteins may be involved in the initiation of periodontal infection. Notably, within this network, a chemokine pathway- GRO-3-IL8RB-Actin cytoskeletal—including GRO-3, and interleukin (IL)-8 receptor was present (canonical pathway, cyan colored interaction arrows). While IL-8 has been extensively studied in periodontal infection, little is known about GRO-3 although it has capacity to activate neutrophils.

The second top regulated network named *Plectin 1, hnRNP K, Envoplakin, TGM1, SPRR1B* (Fig. 4) constituted 50 proteins, including 13 proteins from our regulated list with a *P* value of 4.3E-29. Further analysis of the proteins in the network suggested that disease associated biofilm challenge caused highly coordinated activation of several proteins associated with toll-like receptor pathways. The third most affected network named *IDE, Kappa chain (Ig light chain), Cofilin, MNDA, MHC class I* featured activation of antigen processing and presenting pathways (Fig. 5).

Furthermore, mapping of the regulated proteins onto canonical pathway maps revealed that most altered pathways including *cytoskeleton remodelling-filaments, regulation of degradation of deltaF508-CFTR in CF* and *IL-13 signaling via JAK-STAT*. Intracellular filaments including epithelial keratins are mainly located in the cytoplasm and nucleus and are cross-linked by binding proteins like plectin, envoplakin, periplakin, epiplakin. These proteins are involved in maintaining cell and tissue integrity. IL-13 is known to play an important role in the regulation of immune responses and is also implicated in other pathological conditions, but not yet in periodontal infection. This indicates alterations in cellular integrity and immunity, in response to disease-associated biofilms.

**Secreted proteins of bacterial biofilm origin.** For secreted bacterial proteins, the regulated trends are shown in Table 4. Among the significantly regulated proteins, 128 were increased (up-regulated, positive Log FC value), whereas 24 were decreased (down-regulated, negative Log FC value) in the biofilm-challenged tissue group versus the un-challenged tissue group. The functions of the significantly altered bacterial proteins were manually enriched by GO process terms, according to Uniprot (Fig. 6). In general, a total of 259, 105, and 58 GO terms were generated for molecular function, biological process,

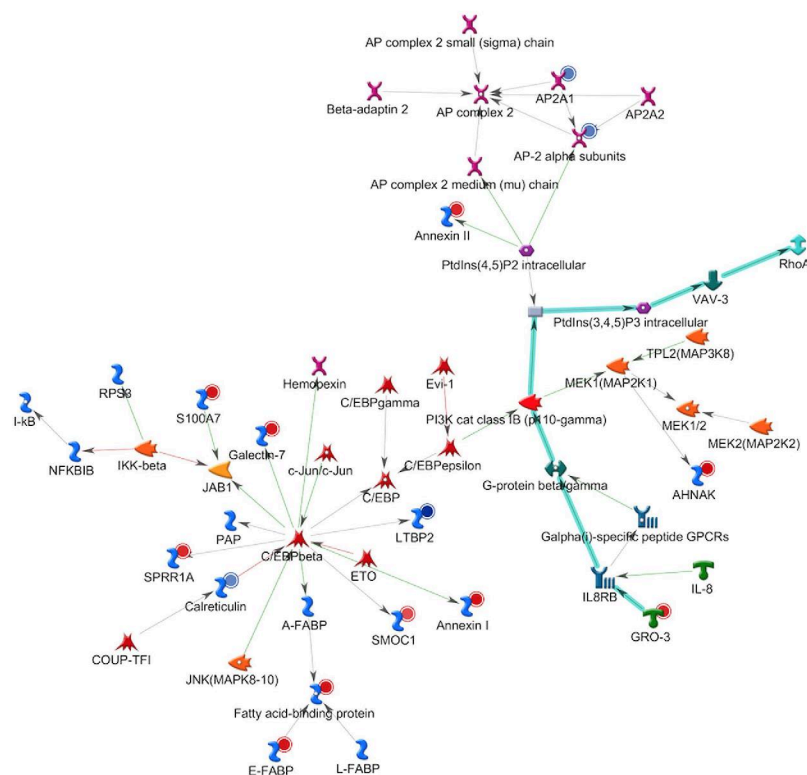


**Figure 3. Analysis of the most significantly regulated network: relationships of the regulated human proteins.** Networks of protein interactions in regulated human proteins (including Calreticulin, AP-2 alpha subunits, AHNAK, LTBP2, SPRR1A) using MetaCore. The networks between the regulated proteins were calculated based on the “analyse network” algorithm value, then the network maps of their putative protein interactions and related proteins were predicated accordingly from MetaCore database. The regulated human proteins from the list (Table S3) are denoted in smaller circles. Smaller red and blue circles indicated up-regulated and down-regulated proteins, respectively. Green arrows indicate activation of the corresponding proteins; red arrows, inhibition; and gray arrows, unspecified. The cyan highlighted edges in the legend represent the canonical pathways, as recorded by MetaCore. For detailed network symbol legend, see supplementary Figure S4 for full annotations of nodes.

and cellular component, respectively, based upon the up-regulated proteins in the tissue + biofilm group, compared to the biofilm group alone. Among the down-regulated proteins, 98, 41, and 35 enriched GO terms corresponded to molecular function, biological process, and cellular component, respectively. In general, less GO terms appeared for up-regulated, compared to down-regulated proteins. Besides, *cytoplasm* was the most common enriched cellular component GO term, in both down regulated and up-regulated proteins (37% and 55% of all terms, respectively). Finally, 17% of the cell component GO terms in down-regulated proteins came from extracellular region, and this percentage was not matched in the up-regulated proteins.

**Intracellular protein changes of biofilms in response to the host tissue.** As also described earlier<sup>13</sup>, upon completion of the experimental period, the biofilms were able to survive, although most of the bacterial species were suppressed in the presence of the organotypic host tissue. To evaluate such proteomic changes within the subgingival biofilms their cell lysates were collected and processed for further proteomic analysis. In this experiment, the actual pepFDR and proFDR were 0.2% and 1%, respectively.

In the tissue + biofilm group, a total of 2594 proteins were identified (302 human, and 2292 bacterial proteins). In the biofilm alone group, a total of 2655 proteins were identified (88 human and 2567 bacterial). The overlaps of detected proteins between these two groups are shown in Fig. 7. The species-specific taxonomy of the identified protein numbers are provided in Table 5, whereas Supplementary Table S5 presents the detailed information of total unique peptide counts and the annotation of proteins identified the biofilm lysates. Interestingly, 202 proteins of *S. oralis* were uniquely identified in the organotypic tissue group, while only 3 such proteins were uniquely identified in the biofilm group. Conversely, only 1 protein of *V. dispar* was uniquely identified in the tissue + biofilm group compared with 371 proteins in the biofilm group. Of note, only 2 proteins from *T. forsythia* were identified in total. Given the numerically low amount of *T. forsythia* in the biofilm<sup>13</sup>, this might give an underrepresentation of proteins in the biofilm.



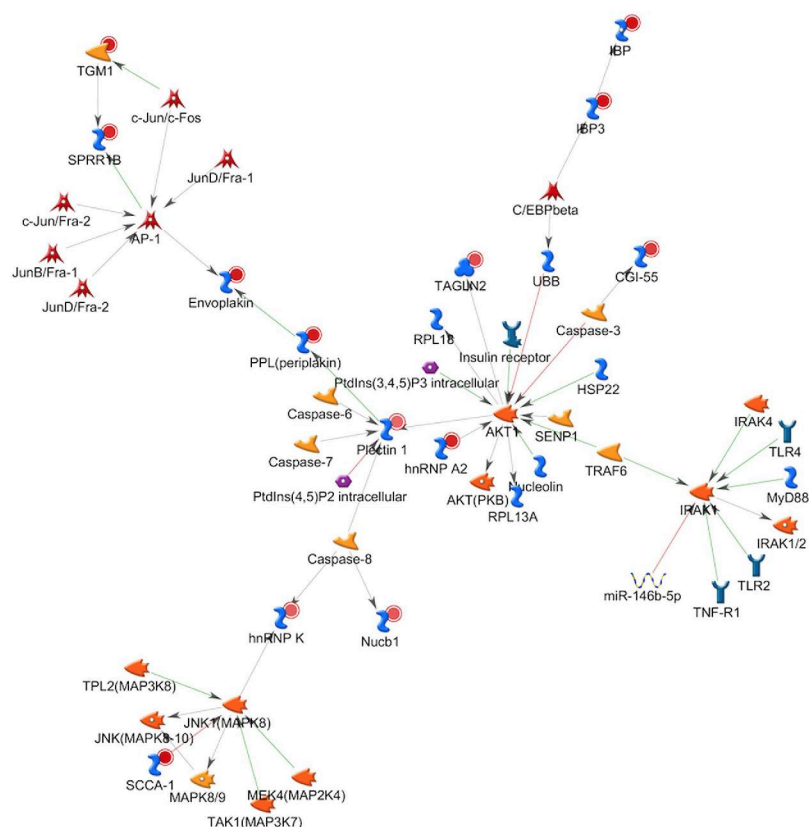


**Figure 4. Analysis of the second most significantly regulated network: relationships of the regulated human proteins.** Networks of protein interactions in regulated proteins (including Plectin 1, hnRNP K, Envoplakin, TGM1, SPRR1B) using MetaCore. The networks between regulated proteins were calculated based on the “analyze network” algorithm value, then the network maps of their putative protein interactions and related proteins were predicated accordingly from the MetaCore database. The regulated human proteins from our list (Table S3) are denoted in smaller circles. Smaller red and blue circles indicated up-regulated and down-regulated proteins, respectively. Green arrows indicate activation of the corresponding proteins; red arrows, inhibition; and gray arrows, unspecified. For detailed network symbol legend, see Supplementary Figure S4 for full annotations of nodes.

To further evaluate the abundance of the identified proteins, spectral counting was used to further compare the proteomic expression profiles in the biofilm lysates. The list of identified proteins is presented in Supplementary Table S5. The human proteins identified in these lysates could be due to false discovery, or constitute remnants of the biofilm growth medium (which contained human serum), or of the hydroxyapatite-coating salivary pellicle on which the biofilms were grown. Nevertheless, these were not further considered, in order to maintain the focus on the regulated bacterial proteins. A visualized result of regulated proteins among all proteins is shown in a volcano plot (Supplementary Fig. S1c), using the  $-1 \times \log_{10}$  (P value) vs.  $\log_2$  (fold-change ratio). Hence, a total of 1081 proteins were classified as regulated proteins. Of those, 518 proteins were up-regulated, whereas 563 proteins were down-regulated (Table 6) in the tissue + biofilm group, compared to the biofilm alone. Interestingly, proteins from each species showed different tendencies of regulation. For example, all regulated proteins of *V. dispar* in the tissue + biofilm group were down-regulated compared to the biofilm group alone whilst *A. oris* and *T. denticola* only had up-regulated proteins. When the *V. dispar* proteins were ranked according to their relative significant abundance, among the top five regulated ones were carboxylase domain protein, phosphoglycerate kinase, pyruvate synthase, methylmalonyl-CoA mutase and formate C-acetyltransferase. The top five up-regulated *T. denticola* proteins were oligopeptide/dipeptide ABC transporter periplasmic peptide-binding protein, filament protein A, lipoprotein, OppA protein and major outer sheath protein.

The GO term enrichment from regulated bacterial proteins is shown as a pie chart (Fig. 8). A total of 837, 453, and 259 GO terms were generated for molecular function, biological process, and cellular component, respectively, based upon the up-regulated proteins in the tissue + biofilm, compared to the biofilm alone. For the down-regulated proteins, a total of 935, 489, and 252 GO terms were generated. Among the enriched GO terms of molecular function, “ATP binding” was the most common one in both up-regulated (13%) and down-regulated (11%) groups. “Translation”, constituted 16% and 13% of the most common enriched up-regulated and down-regulated GO term for biological processes, respectively,

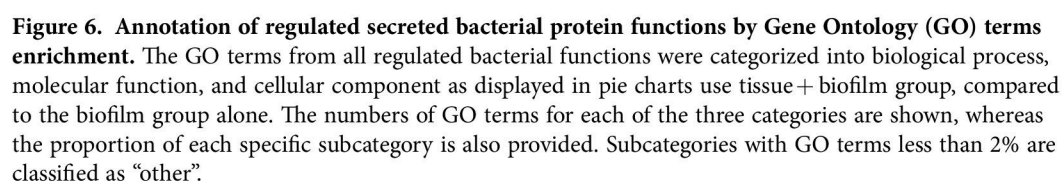


**Figure 5. Analysis of the third most significantly regulated network: relationships of the regulated human proteins.** Networks of protein interactions in regulated human proteins (including IDE, Kappa chain (Ig light chain), Cofilin, MNDA, MHC class I proteins) using MetaCore. The networks between regulated proteins were calculated based on the “analyze network” algorithm value, then the network maps of their putative protein interactions and related proteins were predicated accordingly from the MetaCore database. The regulated human proteins from our list (Table S3) are denoted in smaller circles. Smaller red and blue circles indicated up-regulated and down-regulated proteins, respectively. Green arrows indicate activation of the corresponding proteins; red arrows, inhibition; and gray arrows, unspecified. For detailed network symbol legend, see Supplementary Figure S4 for full annotations of nodes.

Species	tissue + biofilm	overlap (up)	overlap (down)	biofilm
<i>A. oris</i>	0	0	0	0
<i>A. actinomycetemcomitans</i>	0	0	0	0
<i>C. rectus</i>	0	0	0	0
<i>E. nucleatum</i>	115	1	0	0
<i>P. gingivalis</i>	0	0	0	0
<i>P. intermedia</i>	8	1	0	0
<i>S. anginosus</i>	1	0	3	0
<i>S. oralis</i>	2	0	6	5
<i>T. forsythia</i>	0	0	0	0
<i>T. denticola</i>	0	0	0	2
<i>V. dispar</i>	0	0	0	8

**Table 4. Number of differentially regulated secreted bacterial proteins in culture supernatants by each species.** Regulation trends of the quantified proteins from culture supernatants are listed in the table based on whether they were uniquely identified in tissue + biofilm, biofilm alone, or based on their up- or down-regulation trend in the overlap group. The regulation trends were considered using peptide counting methods compare tissue + biofilm group to the biofilm group alone.





## Discussion

Considering the biological resemblance to the *in vivo* environment, its feasibility to culture and its relatively low cost compared to other *in vivo* models, the mucosal organotypic models<sup>19,20</sup> in conjunction with a multispecies biofilm<sup>13,15,21,22</sup> are becoming increasingly utilised for studying the interactions between host tissues and oral biofilms. However, few of them combine both these elements together for studying infection processes of periodontal disease<sup>15</sup>. Our recently developed organotypic model, cultivating an epithelial-fibroblast and monocyte containing tissue in a three dimensional conformation, which was

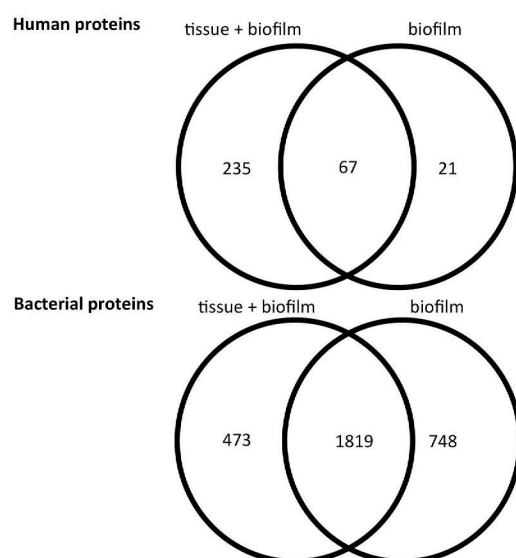


**Figure 7. Venn diagram of identified protein numbers in biofilm lysates.** Protein numbers for each category is depicted. Details of proteins in each group are listed in Supplementary Information Table S5.

Species	tissue + biofilm	Overlap	biofilm
<i>A. oris</i>	58	5	1
<i>A. actinomycetemcomitans</i>	8	13	2
<i>C. rectus</i>	45	79	3
<i>F. nucleatum</i>	41	791	125
<i>P. gingivitis</i>	5	172	55
<i>P. intermedia</i>	12	341	176
<i>S. anginosus</i>	25	88	10
<i>S. oralis</i>	202	252	3
<i>T. forsythia</i>	1	1	0
<i>T. denticola</i>	75	9	2
<i>V. dispar</i>	1	68	371
<i>H. sapiens</i>	235	67	21
sum	708	1886	769

**Table 5. Number identified biofilm lysates proteins from each species.** Proteins identified from biofilm lysates were listed on the table based on whether they were uniquely identified in tissue + biofilm, biofilm alone, or overlapping proteins groups (identified in both groups).

thereafter challenged by a multi-species biofilm in a perfusion bioreactor, is one of the most complex infection systems currently available<sup>13</sup>. In the present study, we characterized the full secreted proteome ('periodontal exudate') of this recently described model, which includes the integrated analysis of both host tissue and biofilm bacteria secreted proteins. We also characterized the proteomic changes occurring in the biofilm itself when in contact with the tissue, by analysing lysates of its cell-associated content. First, we used label-free bottom-up proteomic technology to screen and identify target proteins that were regulated in the gingival extracellular milieu upon interaction with disease associated biofilms. Second, we generated functional gene networks and pathway maps using the Metacore tool in order to integrate the interactions of the identified human proteins. The combination of mass-spectrometry based label-free quantitative proteomics with bioinformatics analysis provided extensive insights into understanding the host-biofilm interaction dynamics in a given microenvironment. This approach provides a holistic view of the early events that may take place in the gingival tissue as the associated biofilms, during the initiation of periodontal inflammation.

One of the first qualitative observations in this study was that more secreted human proteins were detectable in the tissue when biofilms were absent. On the contrary, under biofilm challenge, fewer proteins were detectable and the most were down-regulated compared to the control. This supports the notion



Species	tissue + biofilm	overlap (up)	overlap (down)	biofilm
<i>A. oris</i>	39	5	0	0
<i>A. actinomycetemcomitans</i>	2	7	0	2
<i>C. rectus</i>	15	19	1	1
<i>F. nucleatum</i>	20	30	44	32
<i>P. gingivalis</i>	2	7	12	13
<i>P. intermedia</i>	5	27	79	66
<i>S. anginosus</i>	16	19	3	5
<i>S. oralis</i>	121	117	1	0
<i>T. forsythia</i>	1	0	0	0
<i>T. denticola</i>	58	8	0	0
<i>V. dispar</i>	0	0	49	255

**Table 6. Number of differentially regulated proteins in biofilm lysate by each species.** Regulation trends of quantified proteins from biofilm lysates were listed on the table based on whether they were uniquely identified in tissue + biofilm, biofilm alone, or based on their up- or down-regulation trend in the overlap group. The regulation trends were considered using peptide counting methods compare tissue + biofilm group to the biofilm group alone.

that biofilm challenge can dampen the host responses to favour microbial survival and establishment in the tissue<sup>23</sup>. It is also supported by previous reports in gingival organotypic epithelial cultures studying either the whole secretome<sup>15</sup> or individual cytokines<sup>24</sup>, and reports in gingival fibroblasts demonstrating that biofilms down-regulate key intracellular components of the inflammatory response<sup>25,26</sup>. The present organotypic tissue model contains both the epithelial and connective tissue component of gingiva, as well as cells of the immune system, and further reinforces these earlier works.

The collected supernatant of the bioreactor culture was used to analyse the ‘periodontal exudome’ in this model. The content of this supernatant may share some similarities to the gingival cervical fluid (GCF) *in vivo*. Indeed, some of the identified proteins, especially those associated with immune responses, including annexin A1, calgranulin B, cathepsin G, were also found in previous proteomics analysis performed in GCF<sup>27</sup>. Although the other identified proteins, like HSP60, HLA-C were not readily identified in the proteomic studies of GCF, earlier evidence has shown that these proteins can exist in periodontal tissues<sup>28</sup>.

In our recent work we reported the morphological disruption of the epithelium-like surfaces on this organotypic tissue when co-cultured with biofilms<sup>13</sup>. The bioinformatics analysis of the regulated proteins performed here identified that cytoskeletal remodelling, keratinisation and deregulations in protein unfolding were among the most affected process networks, whereas epidermis development and skin development were among the most affected GO processes. Hence, the morphological observations of epithelial disruption concur with the regulated process on the proteomic level. While healthy and minimally challenged, the oral epithelium exhibits a rapid turn-over in order to maintain a tolerable host-bacterial equilibrium<sup>29</sup>, a process that is impaired in the course of periodontal infection.

Disruption of epithelial integrity could also be explained by regulation of lamin A/C and lamin B1 as found in this experimental model. Lamins are components of the inner nuclear member, believed to play an important role for nuclear assembly and chromatin organisation. They are also related to the many apoptosis signalling pathways<sup>30</sup>, which also ranked among the top regulated process networks in response to the biofilm challenge. Considering that lamins are mainly found in cytoplasm, increasing their presence in the bioreactor supernatant probably originates from lysed epithelial cells, which could also be interpreted as cell death. In line with apoptosis, negative regulation of cell proliferation was also one of the enriched process networks. Interestingly, lamin A/C is known to effect osteogenesis<sup>31</sup>, which could potentially be involved in alveolar bone resorption occurring at later stages of periodontal infection. Together, all these processes indicate that the presence of the biofilm affected tissue growth, induced apoptosis and consequently led to it structural disruption, as previously observed microscopically<sup>13</sup>.

Apart from the physical barrier to pathogens, epithelium is known to mediate the innate immune responses by recruiting cells of the immune system, such as neutrophils and antigen presentation to the T-helper cell<sup>32</sup>. The bioinformatic enrichment of GO processes revealed the regulation of *antigen processing and presentation* of endogenous and exogenous peptide antigens via MHC class I. Normally, MHC class I are considered to be regulated by viral peptides, although bacteria are also found to manipulate these pathways<sup>33</sup>. Immune IL-13 signalling was also one of the top 10 regulated process networks. As part of its role in inflammation roles, IL-13 induces the production of matrix metalloproteinases (MMPs)<sup>34</sup>. Since MMPs are important molecules to degrade primarily the connective tissues<sup>35</sup>, this finding could be well in line with the disruptions of gingival fibroblast attachment, described in our previous report<sup>13</sup>.

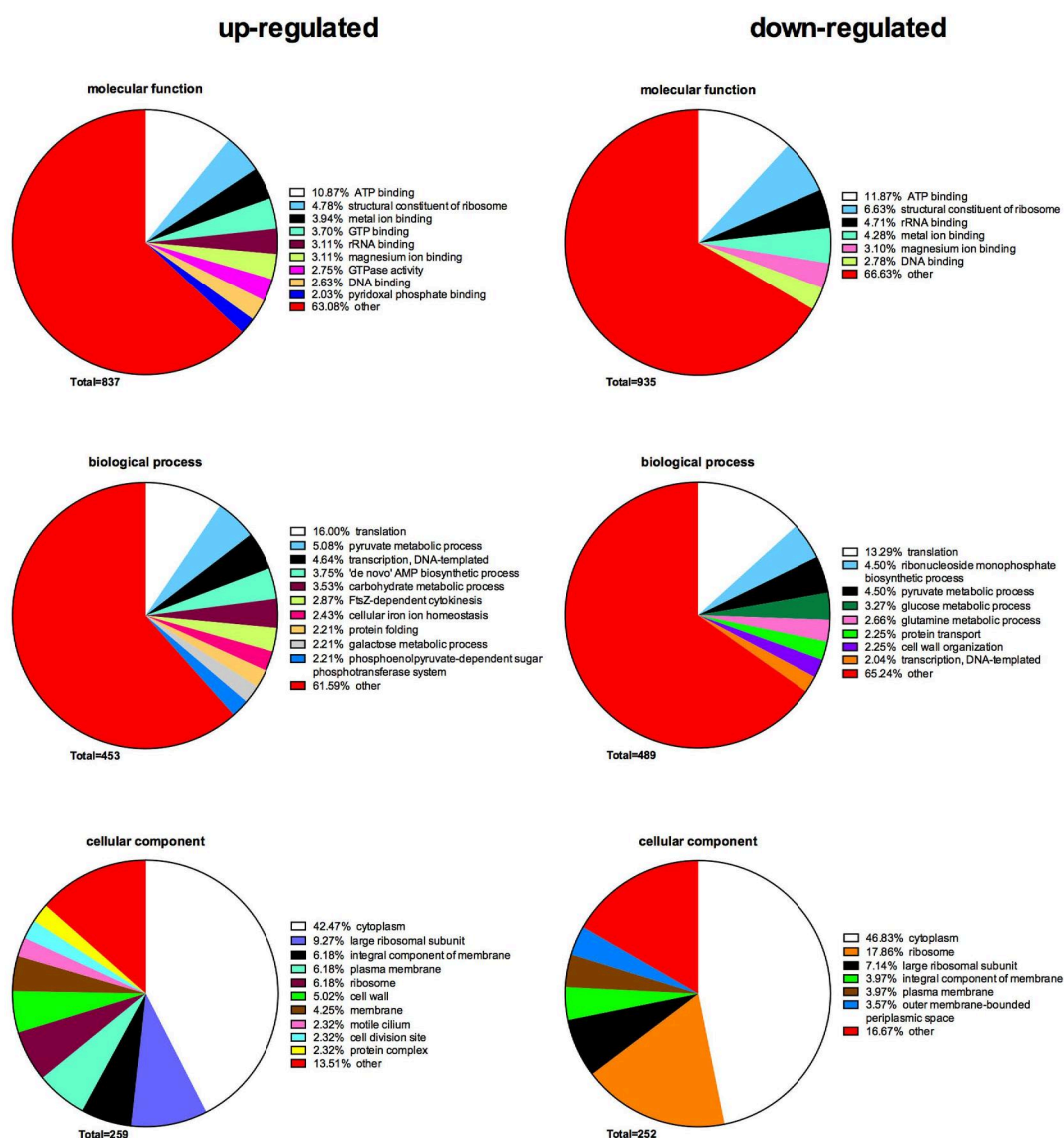


**Figure 8. Annotation of regulated bacterial protein functions in biofilm lysates by enrichment of Gene Ontology (GO) terms.** The GO terms from all regulated bacterial functions were categorized into biological process, molecular function, and cellular component as displayed in pie charts use tissue + biofilm group, compared to the biofilm group alone. The numbers of GO terms for each of the three categories are shown, whereas the proportion of each specific subcategory is also provided. Subcategories with GO terms less than 2% are classified as “other”.

Finally, GO processes related to toll-like receptors (TLRs) appeared in 3 out of top 10 enriched network links of regulated proteins in bioreactor supernatant (Table S4). Although TLRs are potentially expressed in all three host cell types represented in our models, they might have different functions during the processes of periodontal infections. For epithelial cells, TLR is important to recognise different bacterial Pathogen-Associated Molecular Patterns (PAMPs)<sup>36</sup>, and maintain the balance between commensal bacteria and epithelial integrity through a well-controlled innate immune response. *P. gingivalis*, a constituent species of the present biofilm model, may avoid the activation of TLRs through its cell surface fimbriae (FimA), which may however not evade detection by monocytes<sup>37</sup>. In the case of fibroblasts, following epithelial layer degradation, increasing TLR stimulation may result in the expression of inflammatory factors that further stimulate tissue degradation<sup>38</sup>. Activating these TLR pathways is also well in line with the increased cytokine expression, as previously reported<sup>13</sup>.

Biofilms are the initiating factor of periodontal infections. Secreted bacterial proteins from the biofilms may regulate host tissue functions in a manner that is detrimental for the pathogenesis of periodontal disease<sup>39,40</sup>. Conversely, dynamic changes are also imposed on the microbiological profile of the biofilms during their interaction with host tissues, a concept well summarized by the ‘ecological plaque hypothesis’<sup>41,42</sup>. In the present biofilm model we hold the technical advantage of knowing in advance the



specific constituent species, and therefore we could manually enrich the GO terms of all the bacterial proteins ascribed to the function of the whole biofilm<sup>17</sup> to avoid the low consistency in *in vivo*. The number of identified secreted bacterial proteins was less than half (44%) the number of human proteins. However, only 7% of these proteins were identified in biofilm lysates under both tissue challenged and biofilm alone conditions. This left a large amount of them to be considered as “regulated proteins”, as they were absent from the occasional comparison group. Interestingly, *F. nucleatum* expressed more than half of both identified and regulated proteins. Moreover, these numbers in the biofilm-challenged tissue group were higher than the biofilm alone group, despite the lower (but not significantly) bacterial cell numbers. In terms of biofilm formation, *F. nucleatum* plays an important role in connecting early colonizes with late colonizes due to its ability that co-aggregated with many different species<sup>43</sup>. Besides, it is also reported that *F. nucleatum* can invade oral epithelial<sup>44</sup> and fibroblastic cells<sup>45</sup>, and its culture filtrates strongly induced apoptosis of monocytic cell lines<sup>46</sup>. All these functions may explain the relatively stable numbers of *F. nucleatum* proteins in the presence of the organotypic tissue. Moreover, this bacterium has also been reported to increase the virulence<sup>47</sup> and attachment to the host cells<sup>48</sup> of *P. gingivalis*. Therefore, as one of the most abundant gram-negative species<sup>43</sup>, *F. nucleatum* may have a mechanistic advantage in surviving the host challenge, while maintaining a relatively stable bacterial number.

For further bioinformatics analysis of bacterial proteins in the bioreactor supernatant, the biofilm was considered as a whole unit, rather than by its individual species. Hence, the pie charts of enriched GO terms of all the bacterial proteins were divided into three separate ontologies: 1) molecular function, 2) biological process, 3) cell component. The most popular enriched GO term from molecular function category among up-regulated bacterial proteins in the tissue + biofilm group was *nucleotide binding*. This result is consistent with the observation that some of the most popular enriched GO term in the biological process category were *translation* and *protein folding*. Another interesting finding is that the second popular GO term among the down-regulated bacterial proteins in the cell component category is the *extracellular region*, which was not prevalent among the up-regulated proteins. This may indicate the presence of more intact bacteria in the biofilm alone group.

Intracellular proteins of the biofilm lysate were further considered. More proteins were identified in biofilm lysates compared to the secreted bioreactor supernatants. More interestingly, although the tissue-encountered biofilms synthesized significantly less intracellular bacterial proteins, most of them were regulated, reflecting an adaptational response to the tissue. In fact, different patterns of proteome adaptation were observed for the individual bacterial species. Unlike in the bioreactor supernatant, intracellular *F. nucleatum* proteins did not show a strong regulation in the presence of the organotypic tissue. Instead, although present at lower cell numbers, *Actinomyces oris* and *Campylobacter rectus* displayed more identified and regulated proteins in the biofilm lysates, in the presence of the organotypic tissue. Considering that the numbers of these two species was also lower in the tissue + biofilm group, this trend was less likely caused by different protein input. *A. oris* is an early colonizer, reported to have a mutualistic growth with *P. gingivalis*<sup>49</sup>. In the biofilm, relationships between *A. oris* and *Streptococcus spp.* are associated to co-aggregation<sup>43</sup> and possible the regulation of *Streptococci spp.* through digestion of quorum sensing molecule autoinducer 2<sup>50</sup>. Lack of *A. oris* and *Streptococcus spp.* from this “subgingival” biofilm model is clearly shown to impose a number for structural and compositional changes in the rest of the biofilm species<sup>51</sup>. *C. rectus*, appears in relative late stage of biofilm formation<sup>52</sup> and is clinically associated with periodontal infections. In *in vivo* studies, *C. rectus* was found to increase the TLR-4 expression in mice<sup>53</sup>, or cause alveolar bone loss in the capuchin monkey<sup>54</sup>. Both of the streptococci, *A. oris* and *C. rectus* appear to increase their cytoplasmic protein expression in the present of the tissue. One prime example of *T. denticola* up-regulated proteins was its major outer sheath protein. This primary virulence determinant in *Treponema denticola*, known to induce cytotoxic responses, inflammatory pathways and inhibit chemotactic events in host cells<sup>55</sup>. These results indicate that, under tissue challenge, the virulence of specific pathogenic bacteria may be enhanced.

The enriched GO terms among regulated proteins showed a trend of cytokinesis of the bacteria in the biofilm, when in presence of the organotypic tissue. Among the categories of biological process, one of the unique GO terms appearing in up-regulated proteins was *filamenting temperature-sensitive mutant Z (FtsZ)-depend cytokinesis*. FtsZ is an essential and highly conserved bacterial cytokinesis protein<sup>56</sup>. Using their C-terminal GTPase-activating domain, FtsZ constructs a Z-ring structure at the site of spectrum formation<sup>57</sup>. This could also explain the appearance of the unique GO term of *GTP binding* and *GTPase activity* among up-regulated proteins in the category of molecular function. Moreover, the cell component category displayed a unique group of proteins identified as *cell division site*. According to the enriched proteins, these may result in thicker cell bacterial walls rendering the bacteria more mobile.

## Conclusion

This study dissected the protein cross-talk between oral biofilms and organotypic gingival tissue, in a dynamic, complex *in vitro* experimental model of periodontal infection. In the presence of the biofilm, less secreted proteins of the organotypic tissue are detectable, implying a down-play of the host responses. Proteomic profiling of the secreted host proteins revealed a tendency for cytoskeletal rearrangement, stress responses, apoptosis and antigen presentation. These are commensurate with disruption of the tissue barrier and activation of immune recognition responses. On the biofilm side, most of the secreted bacterial proteins derived from the cytoplasmic domain, whereas the functions of the



up-regulated intracellular proteins were associated with cell division and cytokinesis. These affected host and biofilm pathways may represent early events of periodontal pathogenesis, and should be further investigated in translational studies for their role in the establishment of periodontitis.

## Methods

**Biofilms and bioreactor medium collection.** Biofilms and bioreactor medium used in this work were collected from our previous study<sup>13</sup>. Briefly, in this *in vitro* model we co-cultured an 11-species biofilm with gingival organotypic tissue in a perfusion bioreactor system (UCUP, Celtec Biotek AG, www.celtecbiotek.com, UCUP001) to evaluate the effects of biofilm on the tissue. The 11-species biofilm used in this study included the following species: *Prevotella intermedia* ATCC 25611T (OMZ 278), *Aggregatibacter actinomycetemcomitans* JP2 (OMZ 295), *Campylobacter rectus* (OMZ 398), *Veillonella dispar* ATCC 17748T (OMZ 493), *Fusobacterium nucleatum subsp. nucleatum* (OMZ 598), *Streptococcus oralis* SK248 (OMZ 607), *Treponema denticola* ATCC 35405T (OMZ 661), *Actinomyces oris* (OMZ 745), *Streptococcus anginosus* ATCC 9895 (OMZ 871), *Tannerella forsythia* (OMZ 1047) and *Porphyromonas gingivalis* W50 (OMZ 308). Immortalized gingival epithelial cells and gingival fibroblasts, as well as a monocytic cell line<sup>20</sup> were perfused through 3D collagen sponge (porcine collagen, type I) scaffolds (Optimaix, Matricel GmbH, O3D304030) into the bioreactor to create organotypic tissue. Later, the 11-species biofilm models were co-cultured with the generated organotypic tissues in the bioreactor for 24 h, in order to mimic *in vitro* the gingival tissue-biofilm interface. In parallel, organotypic tissues or biofilms alone, each represented in biological triplicates, were also cultured under the same conditions, serving as controls. The individual bacterial species in the biofilms were quantified as previously described<sup>13</sup>. The medium collected from the bioreactor under each of the 3 different experimental conditions after 24 h, was centrifuged at 1500 rpm for 5 min, and filtered through 0.2 µm pore size. Both medium and biofilm were stored at −80 °C, for the further usage.

**Sample preparations.** The collected bioreactor media (i.e. culture supernatants) were subjected to Amicon Ultra-4 cut off 3 kDa (millipore) to concentrate and processed with ProteoMiner Protein Enrichment Kits (Bio-Rad) following the manufacturer's guidelines to increase the abilities to detect the low-abundance proteins. Proteins lysates of the biofilm were extracted as described previously<sup>17</sup>. Briefly, the biofilms were collected by centrifugation, lysed in medium with 4% w/v Sodium Dodecyl Sulfate (SDS), 0.1 mM dithiothreitol (DTT) and 100 mM Tris-HCl pH 8.2, then sonicated using high intensity focused ultrasound (UTR2000, Hielscher).

**Protein digestion and C18 clean up.** After sample preparation, the collected bioreactor media or processed biofilm lysates were measured with Qubit® Protein Assay Kit (Life Technologies). Solutions of 20 µg of proteins per each sample were subjected on the filter device with relative molecular mass cut-offs of 30,000 (30 k filter), for the digestion and detergent remove as described previously<sup>17</sup>. Briefly, the samples were denatured with 8 M urea in 100 mM Tris/HCl buffer (addition 0.1 mM DTT to the bioreactor medium), alkylated with 0.05 M iodoacetamide, and washed by 0.5 M NaCl. They were then digested by trypsin (Promega) at an enzyme to protein ratio of 1:40 in 0.05 M triethylammonium bicarbonate (TEAB) medium in wet-cell chamber overnight. The digested peptides were collected by centrifugation and the reactions were stopped by adding trifluoroacetic acid (TFA) to a final concentration of 0.5%. Digested solutions were desalted using reverse phase cartridges Finissterre SPE C18 (Wicom International AG) as described previously<sup>17</sup>. Briefly, SPE C18 cartridges were first wet with 100% methanol, followed with 60% of acetonitrile (ACN) in 0.1% TFA, equilibrated with 3% of ACN in 0.1% TFA. Then, the digested solutions were loaded onto cartridges, washed with 3% ACN in 0.1% TFA, eluted with 0.5 ml of 60% ACN in 0.1% TFA, dried in vacuum centrifuge, and solubilized with 30 µl 3% ACN in 0.1% formic acid. The desalted samples were stored at −20 °C until further use.

**LC-MS/MS analysis and database search.** 3 µl desalted samples were then injected into a Q-Exactive mass spectrometer (Thermo Fisher Scientific) for proteomic analysis. The peptides were separated on an Easy nano-flow HPLC system (Thermo Fisher Scientific) coupled to a fused silica emitter (15 cm long, 75 µm diameter) packed with a ReproSil-Pur C18-AQ 120 A and 1.9 µm resin (Dr. Maisch HPLC GmbH). The linear gradient of acetonitrile/water (acetonitrile gradient from 2 to 35% in 120 minutes) with 0.1% formic acid was used to separate peptide at a flow rate of 300 nl/min. A data-dependent method that automatically switches between MS and MS/MS using a top-12 method was used to acquire mass spectrum. These spectra were then acquired in the Orbitrap analyzer at a mass range of 300–1700 *m/z*. The higher energy collisional dissociation (HCD) peptide fragments acquired at 28 normalized collision energy were analyzed at high resolution.

**Protein Identification.** Database searches were approached as described previously<sup>17</sup>. Briefly, mass spectrum files were generated using Proteome Discoverer (Thermo) v. 1.4, and then analyzed with Mascot (version 2.4.1) using a customized database consisting of *Homo sapiens* database from Uniprot (release date 22 May 2014, including isoforms) and 11 bacterial species database from NCBI database

(release date 28 February 2014). The human database includes 88,708 sequences; the bacterial database includes 228,240 sequences; while known MS contaminants database includes 260 sequences. Same numbers of reverse sequences (ie: 88,708, 228,240, and 260, for human, bacterial, and MS contaminants database) are also included in database as decoy. The precursor and fragment ion tolerance were 10 ppm and  $\pm 0.05$  Da, respectively. For tryptic digestion options, up to two missed cleavages per peptide were allowed. Both carbamidomethylation and oxidation option were selected as variable modification parameters. The Mascot research results were imported into Scaffold (version Scaffold\_4.2.1, Proteome software) to validate MS/MS-based peptides and protein identifications. The protein list was filtered at a 3.0% protein false discovery rate (protFDR) with 2 minimal peptides, and 1.0% peptide false discovery rate (pepFDR) threshold.

**Spectral count-based label-free quantitation.** Spectrum counting was applied to quantify relative protein content. The quantitative values assigned to each identified protein by Scaffold (version scaffold\_4.40) and used for calculation of relative protein abundance. The quantitative values were normalised for individual protein expression between different samples by correcting the raw spectral counts by the total number of spectra observed in a given sample. Further calculations were done with R using the EdgeR package<sup>58</sup>. We reported data as log<sub>2</sub> Fold Change (logFC), log-counts-per-million (logCPM), and related *p* value for each protein between the compared conditions. Proteins were considered to be significantly different in terms of abundance if the *p* value was  $\leq 0.05$ . Furthermore, volcano plots were generated with R to visualize different expression.

**Data visualization by heat map and cluster analysis.** The regulated trends of secreted human proteins were visualised by use of heat-map made by Heml (version 1.0.1)<sup>59</sup>. Hierarchical clustering analysis was done with the average linkage method using the Heml software. Quantitative heat map displays the mean quantitative value for each protein, previously calculated with Scaffold software.

**Gene Ontology (GO) analysis of differentially expressed human proteins.** To annotate the protein functions at the gene level, differentially expressed human proteins were extrapolated to MetaCore database (released on 14<sup>th</sup> May 2015) for “enrichment analysis” and “built network”. Through the “enrichment analysis”, Metacore calculated statistically significant enriched “GO processes” and “process networks” based on the probability of GO terms and networks assembly from the regulated proteins among the human protein information in their database as a *p* value. Accordingly, MetaCore is able to provide a quantitative analysis of the top 10 relevant biological functions. To show these proteins in the context of their interacting network, these proteins were further processed to “built network”, using the “analyze network” algorithm, one of the nine network building-algorithms in MetaCore. The *P* values of the resulting network are the possibility of the potential networks according to the curated human protein interaction database within the MetaCore.

**Gene Ontology (GO) analysis of differentially expressed bacterial proteins.** We also analysed how the bacterial proteome changes in the bioreactor culture supernatants, as well as in the biofilm lysates<sup>17</sup>, in the presence or absence of the organotypic tissue. Briefly, GO terms from all the regulated bacterial proteins were assembled from the UniProt Knowledgebase release date 14<sup>th</sup> April 2015) enriched by REVIGO (release date 21<sup>th</sup> April 2015)<sup>60</sup>, and manually summarized into pie charts. The enriched GO terms were listed from the highest to the lowest according to their proportions among all the terms. The terms that show less than two per cent were clustered into the “other” category.

## References

1. Darveau, R. P. Periodontitis: a polymicrobial disruption of host homeostasis. *Nat Rev Microbiol* **8**, 481–490, doi: 10.1038/nrmicro2337 (2010).
2. Page, R. C. & Kornman, K. S. The pathogenesis of human periodontitis: an introduction. *Periodontol* **2000** **14**, 9–11 (1997).
3. Aas, J. A., Paster, B. J., Stokes, L. N., Olsen, I. & Dewhirst, F. E. Defining the normal bacterial flora of the oral cavity. *J Clin Microbiol* **43**, 5721–5732, doi: 10.1128/JCM.43.11.5721-5732.2005 (2005).
4. Berezow, A. B. & Darveau, R. P. Microbial shift and periodontitis. *Periodontol* **2000** **55**, 36–47, doi: 10.1111/j.1600-0757.2010.00350.x (2011).
5. Ramsey, M. M., Rumbaugh, K. P. & Whiteley, M. Metabolite cross-feeding enhances virulence in a model polymicrobial infection. *PLoS pathog* **7**, e1002012, doi: 10.1371/journal.ppat.1002012 (2011).
6. Bachtar, E. W. *et al.* AI-2 of *Aggregatibacter actinomycetemcomitans* inhibits *Candida albicans* biofilm formation. *Front Cellul Infect Microbiol* **4**, 94, doi: 10.3389/fcimb.2014.00094 (2014).
7. Jenkinson, H. F. & Lamont, R. J. Oral microbial communities in sickness and in health. *Trends microbiol* **13**, 589–595, doi: 10.1016/j.tim.2005.09.006 (2005).
8. Hajishengallis, G. Immunomicrobial pathogenesis of periodontitis: keystones, pathobionts, and host response. *Trends immunol* **35**, 3–11, doi: 10.1016/j.it.2013.09.001 (2014).
9. Hajishengallis, G. & Lamont, R. J. Beyond the red complex and into more complexity: the polymicrobial synergy and dysbiosis (PSD) model of periodontal disease etiology. *Mol Oral Microbiol* **27**, 409–419, doi: 10.1111/j.2041-1014.2012.00663.x (2012).
10. Segui, S., Godeau, G. & Brousse, N. Immunohistological and morphometric analysis of intra-epithelial lymphocytes and Langerhans cells in healthy and diseased human gingival tissues. *Arch Oral Biol* **45**, 441–452 (2000).
11. Locke, M., Hyland, P. L., Irwin, C. R. & Mackenzie, I. C. Modulation of gingival epithelial phenotypes by interactions with regionally defined populations of fibroblasts. *J Periodontal Res* **43**, 279–289, doi: 10.1111/j.1600-0765.2007.01028.x (2008).



12. Belibasakis, G. N. & Bostanci, N. The RANKL-OPG system in clinical periodontology. *J Clin Periodontol* **39**, 239–248, doi: 10.1111/j.1600-051X.2011.01810.x (2012).
13. Bao, K., Papadimitropoulos, A., Akgul, B., Belibasakis, G. N. & Bostanci, N. Establishment of an oral infection model resembling the periodontal pocket in a perfusion bioreactor system. *Virulence*, **0**, doi: 10.4161/21505594.2014.978721 (2015).
14. Bostanci, N. *et al.* Label-free quantitative proteomics reveals differentially regulated proteins in experimental gingivitis. *J Proteome Res*, doi: 10.1021/pr300761e (2012).
15. Bostanci, N. *et al.* Secretome of gingival epithelium in response to subgingival biofilms. *Mol Oral Microbiol*, doi: 10.1111/omi.12096 (2015).
16. Hendrickson, E. L. *et al.* Proteomics of *Fusobacterium nucleatum* within a model developing oral microbial community. *MicrobiologyOpen* **3**, 729–751, doi: 10.1002/mbo3.204 (2014).
17. Bao, K., Bostanci, N., Selevsek, N., Thurnheer, T. & Belibasakis, G. N. Quantitative proteomics reveal distinct protein regulations caused by *Aggregatibacter actinomycetemcomitans* within subgingival biofilms. *PLoS One* **10**, e0119222, doi: 10.1371/journal.pone.0119222 (2015).
18. Bessarabova, M., Ishkin, A., JeBailey, L., Nikolskaya, T. & Nikolsky, Y. Knowledge-based analysis of proteomics data. *BMC Bioinformatics* **13** Suppl 16, S13, doi: 10.1186/1471-2105-13-S16-S13 (2012).
19. Moharamzadeh, K. *et al.* Tissue-engineered oral mucosa. *J Dent Res* **91**, 642–650, doi: 10.1177/0022034511435702 (2012).
20. Bao, K., Akguel, B. & Bostanci, N. Establishment and Characterization of Immortalized Gingival Epithelial and Fibroblastic Cell Lines for the Development of Organotypic Cultures. *Cells Tissues Organs*, doi: 10.1159/000363694 (2014).
21. Thurnheer, T. & Belibasakis, G. N. Integration of non-oral bacteria into *in vitro* oral biofilms. *Virulence*, **0**, doi: 10.4161/21505594.2014.967608 (2014).
22. Diaz, P. I. *et al.* Synergistic interaction between *Candida albicans* and commensal oral streptococci in a novel *in vitro* mucosal model. *Infect Immun* **80**, 620–632, doi: 10.1128/IAI.05896-11 (2012).
23. Hajishengallis, G. & Lambris, J. D. Microbial manipulation of receptor crosstalk in innate immunity. *Nat. Rev. Immunol.* **11**, 187–200, doi: 10.1038/nri2918 (2011).
24. Belibasakis, G. N., Thurnheer, T. & Bostanci, N. Interleukin-8 responses of multi-layer gingival epithelia to subgingival biofilms: role of the “red complex” species. *PLoS One* **8**, e81581, doi: 10.1371/journal.pone.0081581 (2013).
25. Belibasakis, G. N., Guggenheim, B. & Bostanci, N. Down-regulation of NLRP3 inflammasome in gingival fibroblasts by subgingival biofilms: involvement of *Porphyromonas gingivalis*. *Innate Immun.* **19**, 3–9, doi: 10.1177/1753425912444767 (2013).
26. Bostanci, N., Meier, A., Guggenheim, B. & Belibasakis, G. N. Regulation of NLRP3 and AIM2 inflammasome gene expression levels in gingival fibroblasts by oral biofilms. *Cell Immunol* **270**, 88–93, doi: 10.1016/j.cellimm.2011.04.002 (2011).
27. Bostanci, N. *et al.* Application of label-free absolute quantitative proteomics in human gingival crevicular fluid by LC/MS E (gingival exudatome). *J Proteome Res* **9**, 2191–2199, doi: 10.1021/pr900941z (2010).
28. Belibasakis, G. N., Bao, K. & Bostanci, N. Transcriptional profiling of human gingival fibroblasts in response to multi-species *in vitro* subgingival biofilms. *Mol Oral Microbiol*, doi: 10.1111/omi.12053 (2014).
29. Nanci, A. & Bosshardt, D. D. Structure of periodontal tissues in health and disease. *Periodontol 2000* **40**, 11–28, doi: 10.1111/j.1600-0757.2005.00141.x (2006).
30. Okinaga, T., Kasai, H., Tsujisawa, T. & Nishihara, T. Role of caspases in cleavage of lamin A/C and PARP during apoptosis in macrophages infected with a periodontopathic bacterium. *J Med Microbiol* **56**, 1399–1404, doi: 10.1099/jmm.0.47193-0 (2007).
31. Li, W. *et al.* Decreased bone formation and osteopenia in lamin a/c-deficient mice. *PLoS One* **6**, e19313, doi: 10.1371/journal.pone.0019313 (2011).
32. Ohlrich, E. J., Cullinan, M. P. & Seymour, G. J. The immunopathogenesis of periodontal disease. *Aust Dent J* **54** Suppl 1, S2–10, doi: 10.1111/j.1834-7819.2009.01139.x (2009).
33. Bomberger, J. M. *et al.* *Pseudomonas aeruginosa* Cif protein enhances the ubiquitination and proteasomal degradation of the transporter associated with antigen processing (TAP) and reduces major histocompatibility complex (MHC) class I antigen presentation. *J Biol Chem* **289**, 152–162, doi: 10.1074/jbc.M113.459271 (2014).
34. Van Dyken, S. J. & Locksley, R. M. Interleukin-4- and interleukin-13-mediated alternatively activated macrophages: roles in homeostasis and disease. *Annu Rev Immunol* **31**, 317–343, doi: 10.1146/annurev-immunol-032712-095906 (2013).
35. Sorsa, T. *et al.* Matrix metalloproteinases: contribution to pathogenesis, diagnosis and treatment of periodontal inflammation. *Ann Med* **38**, 306–321, doi: 10.1080/07853890600800103 (2006).
36. Peyret-Lacombe, A., Brunel, G., Watts, M., Charveron, M. & Duplan, H. TLR2 sensing of *F. nucleatum* and *S. sanguinis* distinctly triggered gingival innate response. *Cytokine* **46**, 201–210, doi: 10.1016/j.cyto.2009.01.006 (2009).
37. Eskandari, M. A., Hajishengallis, G. & Kinane, D. F. Differential activation of human gingival epithelial cells and monocytes by *Porphyromonas gingivalis* fimbriae. *Infect Immun* **75**, 892–898, doi: 10.1128/IAI.01604-06 (2007).
38. Hatakeyama, J. *et al.* Contrasting responses of human gingival and periodontal ligament fibroblasts to bacterial cell-surface components through the CD14/Toll-like receptor system. *Oral Microbiol Immunol* **18**, 14–23 (2003).
39. Belibasakis, G. N. & Guggenheim, B. Induction of prostaglandin E(2) and interleukin-6 in gingival fibroblasts by oral biofilms. *FEMS Immunol Med Mic* **63**, 381–386, doi: 10.1111/j.1574-695X.2011.00863.x (2011).
40. Belibasakis, G. N., Meier, A., Guggenheim, B. & Bostanci, N. The RANKL-OPG system is differentially regulated by supragingival and subgingival biofilm supernatants. *Cytokine* **55**, 98–103, doi: 10.1016/j.cyto.2011.03.009 (2011).
41. Marsh, P. D. Are dental diseases examples of ecological catastrophes? *Microbiology* **149**, 279–294 (2003).
42. Takahashi, N. Microbial ecosystem in the oral cavity: Metabolic diversity in an ecological niche and its relationship with oral diseases. *Int Congr Ser* **1284**, 103–112 (2005).
43. Kolenbrander, P. E. *et al.* Bacterial interactions and successions during plaque development. *Periodontol 2000* **42**, 47–79, doi: 10.1111/j.1600-0757.2006.00187.x (2006).
44. Han, Y. W. *et al.* Interactions between periodontal bacteria and human oral epithelial cells: *Fusobacterium nucleatum* adheres to and invades epithelial cells. *Infect Immun* **68**, 3140–3146 (2000).
45. Dabija-Wolter, G. *et al.* *Fusobacterium nucleatum* enters normal human oral fibroblasts *in vitro*. *J Periodontol* **80**, 1174–1183, doi: 10.1902/jop.2009.090051 (2009).
46. Abe, K. Butyric acid induces apoptosis in both human monocytes and lymphocytes equivalently. *J Oral Sci* **54**, 7–14 (2012).
47. Saito, A. *et al.* *Fusobacterium nucleatum* enhances invasion of human gingival epithelial and aortic endothelial cells by *Porphyromonas gingivalis*. *FEMS Immunol Med Microbiol* **54**, 349–355, doi: 10.1111/j.1574-695X.2008.00481.x (2008).
48. Metzger, Z., Blasbalg, J., Dotan, M. & Weiss, E. I. Enhanced attachment of *Porphyromonas gingivalis* to human fibroblasts mediated by *Fusobacterium nucleatum*. *J Endod* **35**, 82–85, doi: 10.1016/j.joen.2008.10.011 (2009).
49. Periasamy, S. & Kolenbrander, P. E. Mutualistic biofilm communities develop with *Porphyromonas gingivalis* and initial, early, and late colonizers of enamel. *J Bacteriol* **191**, 6804–6811, doi: 10.1128/JB.01006-09 (2009).
50. Rickard, A. H. *et al.* Autoinducer 2: a concentration-dependent signal for mutualistic bacterial biofilm growth. *Mol Microbiol* **60**, 1446–1456, doi: 10.1111/j.1365-2958.2006.05202.x (2006).
51. Ammann, T. W., Belibasakis, G. N. & Thurnheer, T. Impact of early colonizers on *in vitro* subgingival biofilm formation. *PLoS One* **8**, e83090, doi: 10.1371/journal.pone.0083090 (2013).